POLITECNICO
MILANO 1863

DIPARTIMENTO DI MECCANICA

Steel metallurgy

Volume II

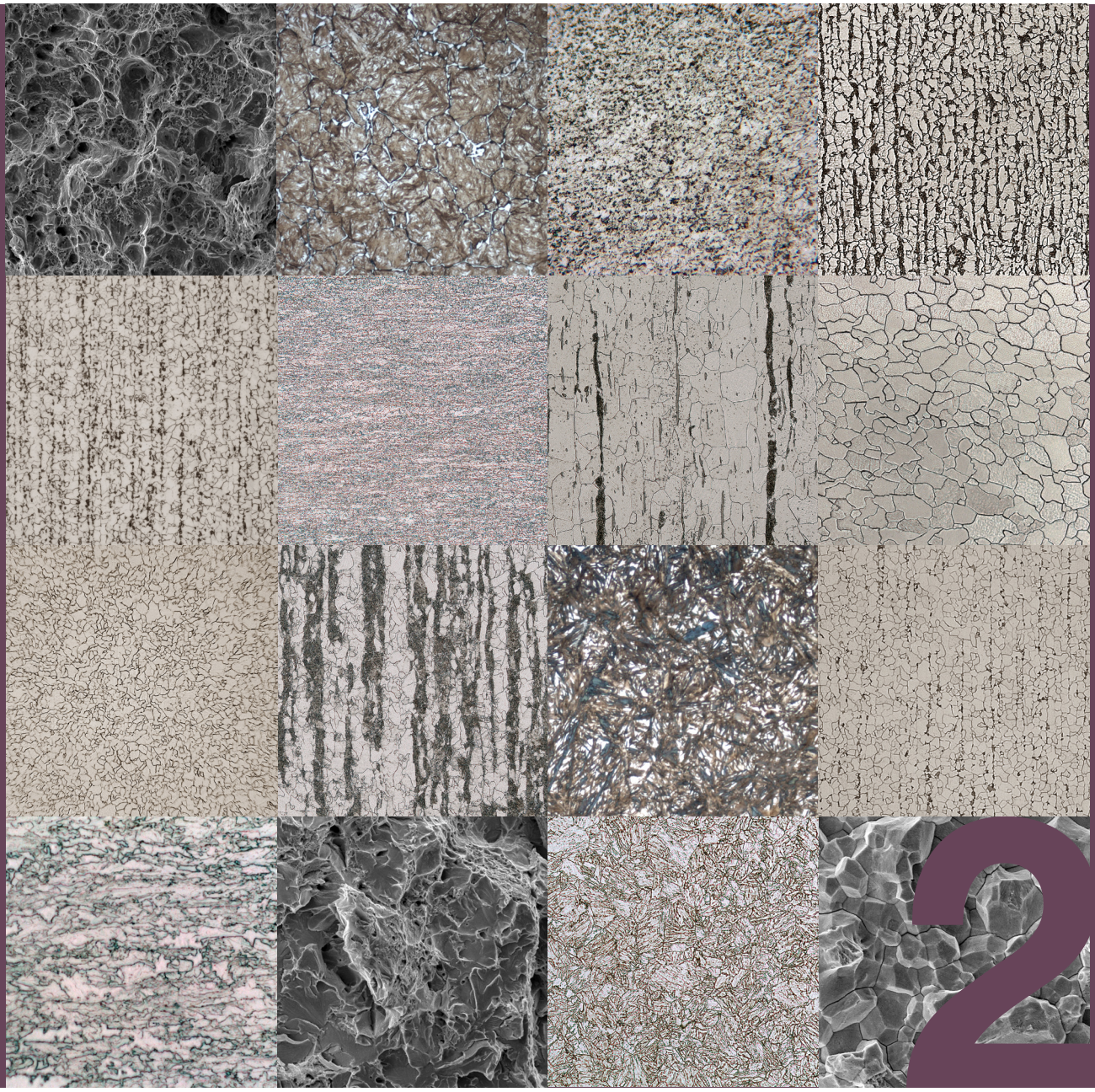

Marco V. Boniardi e Andrea Casaroli

TRAFILIX
INDUSTRIES

(Marco)
This book is dedicated to Marcella
who holds me in her heart every day.

(Andrea)
To my parents and those who, like them, silently work
to improve themselves and the surrounding world.

"Until one is committed, there is hesitancy, the chance to draw back. Concerning all acts of initiative (and creation), there is one elementary truth, the ignorance of which kills countless ideas and splendid plans: that the moment one definitely commits oneself, then Providence moves too. All sorts of things occur to help one that would never otherwise have occurred. A whole stream of events issues from the decision, raising in one's favour all manner of unforeseen incidents and meetings and material assistance, which no man could have dreamed would have come his way. Whatever you can do, or dream you can do, begin it. Boldness has genius, power, and magic in it. Begin it now." [attributed to Johann Wolfgang Goethe (1749 - 1832)]

TABLE OF CONTENTS

PREFACE

This is the last milestone of a journey we started some years ago. This long journey has eventually come to an end with the third volume of the trilogy, the first one being "*Stainless Steels*" followed by "*Steel Metallurgy - Volume 1*" of which this book is the second and conclusive part.

A complicated work that we managed to fully achieve with tenacity, passion and perseverance. When we presented our first volume, we promised to illustrate steel metallurgy from the basics through a linear and simple (yet not simplistic) approach. We kept our word.
We hope we made a good job and that this trilogy will prove useful to students as well as to all those who already work in the metallurgical sector.

Even though from a chronological point of view, things went differently, the scientific and cultural concatenation of our three volumes should be as follows:

- *Steel Metallurgy - Volume 1*, dealing with the physics of metals, phase diagrams, micro-structures and heat treatments;
- *Steel Metallurgy -Volume 2*, examining mechanical tests and the steel grades that are most important at industrial level;
- *Stainless Steels*, specifically describing this important corrosion-resistant steel family.

The credit for this important work goes entirely to the authors, Marco Boniardi and Andrea Casaroli. They not only strongly believed in this project, but also absolutely mastered the "art of communication". Also, I express my praise and appreciation to the Lucefin Group that strongly approved and supported this initiative since the beginning.

Has something been left out? It is likely so, but we trust that our three volumes will provide at least 95% of the knowledge necessary to understand steel metallurgy. Only a few and extremely specific aspects are missing, such as tool steels, steel for wire ropes, bearing steels and steels for high and low temperature applications, which means only a 1 to 2% market share.

Finally, a few words about "sustainability" of steel manufacture and transformation processes, an issue that is growing increasingly important throughout the steelmaking sector. It is also a challenge that only the combined commitment of all those who live our profession passionately every day can win. We really hope that this editorial collection may contribute opening new horizons beyond existing limits.
We shall closely monitor what the future reserves for us in terms of technology and innovation... and willingly share new changes with you.

Giorgio Buzzi, Esine - BS - 3 october 2022

ACKNOWLEDGEMENTS

With *Steel Metallurgy - Part 2* Andrea and I have reached book number three!... and it has to be said, three books is a significant commitment if your goal is to create a work of value and of use to your readers. I have already said this in the past, but I should now say it again: without Andrea, I would never have managed to do all of this. Thank you!
This third volume comes with a challenge: devising credits and thanks without repeating what I wrote in the two previous books.

The only way to say something new is to start from the beginning. I would rather speak in the first person, since at that time my close friendship and professional relationship with Andrea had not yet started.
I learnt the first principles of metallurgy almost forty years ago, when I was attending university lectures at Politecnico di Milano as part of my degree in Mechanical Engineering. There I met Prof. Giuseppe Silva (teaching *Metallurgy*, 1986), Prof. Mario Balbi (teaching *Electrothermics and Electrometallurgy*, 1988) and Prof. Walter Nicodemi (teaching *Iron and Steel Industry and Steelworks*, 1988): they were my teachers and it is fitting for me to thank them. I should also include Prof. Pietro Pedeferri (teaching *Corrosion and the Protection of Metallic Materials*, 1987) in the list of my former professors who got me started as a researcher. It may be a coincidence, but I managed to pass all the above mentioned exams with the highest mark (and also with honours in the case of *Metallurgy*)... and, believe me, this did not happen often during my university studies. This may be because those professors were particularly friendly and cordial (as a matter of fact, I tend to react based on my likes and dislikes) or maybe the subjects they taught were fascinating to me. Who knows? Life is made up of people and those encounters led me on this pathway. Or, as someone said: "Decisions made by the young not only depend on their aptitude, but also on the good fortune of meeting a great teacher."
These men also taught me things that may sound a bit old-fashioned nowadays. They used to say to me: "do not start writing if you don't have something interesting to say" and "you must be fully informed on what you are talking about". They told me the same thing before sending me to give a lesson or attend any meeting: "You must be well prepared or you risk making a bad impression... and bad impressions are not for us". They also taught me to respect all people, whether experienced or still learning.

Andrea and I wish to mention all our mechanical engineering students at Politecnico di Milano (at the Bovisa, Leonardo, Lecco and Piacenza campuses) and at the University of Pavia. Through them we have understood that it is of the utmost importance for explanations to be logical and clear. And that knowledge of a subject should not be conveyed impersonally, but rather in an appealing and suggestive way.
As with the two previous books, many students provided considerable contributions by reviewing the final drafts of this third book. We are extremely grateful to them. We have been lucky to become close friends with some of our former students, but we have lost sight of others. So be it. We carry all of them in our hearts and hope that they too have fond memories of us and our teachings.

Every year, we take comfort in the comments made by our students at the end of their university courses. For example (teaching technique evaluation, anonymous comments, academic year 2020/2021) "The Professor is passionate about his job and knows how to make the dullest subject interesting. Extremely clear explanations; it is impossible not to understand. I do appreciate that he did not take it for granted that a first-year student would already know how machine tools function or how to disassemble a moped (as happened in other courses). It's very inspiring when you meet professors that have other interests in their lives beyond engineering (sometimes, at Politecnico, you feel like you are living a stereotype: engineer = Formula 1). Last but not least; he knows how to speak Italian correctly". What can you say after reading comments like these? Nothing. We are simply happy, perhaps we did a good job. Teachers should be an example to their students. Teaching in a class is not just "one of the many things you have to do". It is much more; it is somewhat of a mission. As Ermanno Ferretti wrote in *Per chi suona la campanella* [For whom the school bell tolls] (2011): "To be good teachers, you should love not only culture, but mainly young people. If you only love your subject you will become disaffected".

In this list Andrea and I wish to mention all of our colleagues in the Materials division of the Department of Mechanical Engineering at Politecnico di Milano, with whom we interact day in day out about metallurgy and its various issues. Maurizio Vedani, Carlo Mapelli, Elisabetta Gariboldi, Barbara Rivolta, Nora Lecis, Fabrizio D'Errico, Silvia Barella, Riccardo Gerosa, Riccardo Casati, Davide Mombelli, Andrea Gruttadauria, Enrique Mariano Castrodeza.
We wish also to mention the lab technicians of the Department of Mechanical Engineering with whom we are (or have been) in close contact. Many thanks to Piero Pellin, Maurizio Pardi, Luca Signorelli, Lorenzo Giudici, Ludovica Rovatti and Michael Ishola Rasheed for your unique assistance. We cannot forget our dearest Cinzia Farina in the administrative office who deserves a big hug.

Talking about metallurgy without involving the world of industry is senseless. In fact, mechanics and metallurgy has been the pillar of small, medium and large Italian enterprises since forever. It would be a big mistake to lose awareness of this essential aspect of engineering.
Many people from the world of industry have consistently helped us throughout these years. Forgive us for not naming them, but we prefer to focus on the companies that had the greatest impact on our efforts, even though some of them do not exist any longer or have changed ownership. Siderurgica Santo Stefano, Trattamenti Termici Nervianesi, Trafilerie Bedini (now Ugitech), Rodacciai, Tenaris Dalmine, Brembo, Forgiatura Vienna, Colmegna, Fomas, Bonfiglioli, De' Longhi, Candy-Hoover, Fedegari Autoclavi, Elettromeccanica Viotto, Sorgenia, Prysmian, Microcontrol, Oric Italiana, OMB, Elli Riduttori and Bodycote. It should be mentioned that some of these companies believed in us at a time when no one else did.

We must also mention the support we received from the laboratory operators involved in steel metallurgy and mechanical testing. Our thanks go to Chiara Tagliabue, Luca Bonvini, Marco Messina, Luca Giudici, Andrea Trombetta, Patrizia Maio, Matteo Borgonovo, Alessandra Marelli, Marco Casaril, Igor Giroletti,

Giovanni Rivolta, Riccardo Fossati, Elena Bresciani, Mauro Ostacoli, Cesare Certini, Gianfranco Zambarbieri, Andrea Capelli, Valentina Ferrari, Federico Bosi, Davide Biffi, Francesco Moretti, Carlo Bonora, Patrizio Brioschi and Ennio Silva.
The book contains many micrographs complete with an indication of the laboratories that produced them. Should you need to get in touch with these laboratories, their contact data are listed below:

- Laboratories of the Department of Mechanical Engineering of Politecnico di Milano, Via La Masa 1, 20156 Milan, Italy;
- Hammer S.r.l. Laboratories, Via Risorgimento 69/22, 20017 Rho (MI), Italy;
- Omeco S.r.l. Laboratories, Via Monviso 56, 20900 Monza (MB), Italy;
- Exova S.r.l. Laboratories (now Element Materials Technology Milan S.r.l.), Via della Pierina 9/11, 26013 Crema (CR), Italy;
- Bonfiglioli S.p.A. Laboratories, Trasmital Division, Via Mattei 12 - Z.I. Selva, 47122 Forlì, Italy

Obviously, the samples were prepared and observed entirely by people, to whom we are extremely grateful, but undoubtedly very little could be done without laboratory instrumentation.

Last, but by no means least, huge thanks go to Giorgio Buzzi, Massimo Sperto and Vittorio Boneschi from the Lucefin group who believed in our work and provided us with this important publishing opportunity.

Our final mention is for the persons who are with us and for us at all times with their daily support.
They are Pinuccia, Francesco, Elena and Pietro for Andrea; Dolores, Piero, Donatella and Marcella for me, with a special thought for my dearest one, my son Davide.

Marco V. Boniardi and Andrea Casaroli, Milano 15 september 2022

Each book - and this is not a flaw - is "alive",
and wishes to continue to live.

For this to occur, your help is needed.
Any suggestions or advice you would like to give us,
and any images or micrographs you would like to send us,
will be well accepted and very appreciated.
You will help us improve the quality of the next edition.

We urge you to write to the following addresses:
marco.boniardi@polimi.it and andrea.casaroli@polimi.it

Thank you everyone in advance... for everything!

1. MECHANICAL STEEL TESTING

The reaction of steel or of any other material to a force applied has always been one of the most interesting issues in the field of engineering. The aim of all mechanical components is to convey static or dynamic loads resulting from operation without being affected by permanent strains changing their dimensions. Also, if you consider an element of a machine or a part of a plant, the need always exists to know which the maximum applicable stress is without the system collapsing.

For all these reasons, steels are subjected to systematic assessment to define their strength and ensure suitability to their intended uses as designed.

The mechanical characteristics of whatever steel type can be measured through a number of tests, all of which can be grouped into three main categories (Figure 1.1):

- *Static or almost-static tests*, such as the tensile test or the hardness tests, where the load is slowly applied over time until reaching a preset value or breakage of the specimen;
- *Impact tests*, such as the impact strength test, where the load is applied impulsively until breakage of the specimen;
- *Cyclic load tests*, such as the fatigue test, where the load is applied cyclically over time, usually following a sinusoidal pattern, until reaching a preset number of loading cycles or breakage of the specimen.

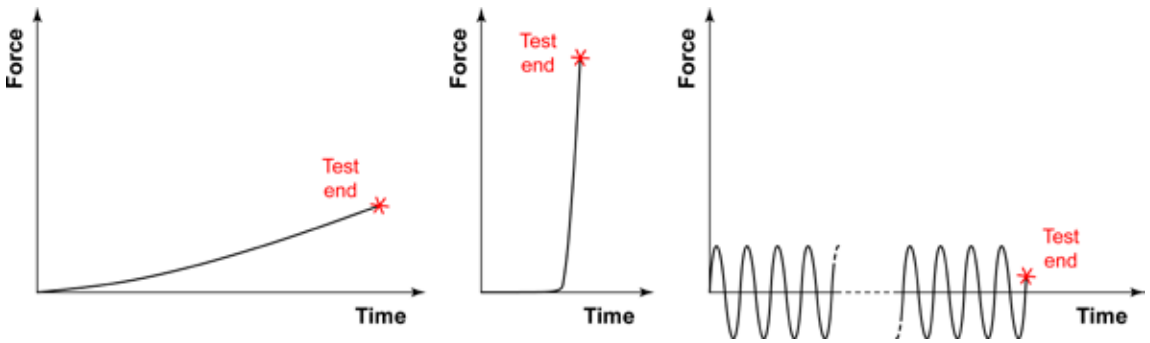

Figure 1.1 – Schematic of force trends as applied over time until specimen breakage for all test types.

Actually, other types of test exist that are suitable to characterize steels and, more generally, metallic and non-metallic materials. Even though they do not fall within the range of this essay, we remind that also *constant load tests* and *technological tests* are of engineering interest. The former include (but not limited to) the creep tests, where the load is kept unchanged in time and specimen elongation or breakage are observed; the latter include (but not limited to) the bending test, the drawing test and the machinability test,

where the material is subjected to complex load systems to characterize its behaviour during certain machining processes (bending, drawing and machinability using machine-tools in the above mentioned cases).
The following chapters illustrate in detail the tensile, hardness, impact strength and fatigue mechanical tests. We provide the main reference standards for each test type together with the parameters that can be obtained. Our aim is to give the reader some basic knowledge of steels, their uses and associated mechanical characterization. Great attention is devoted to the modes with which the tests are conducted, interpretation of results and the metallurgical events that influence them.
Last but not least, the apparent simplicity of the subject "mechanical tests" too often leads to disregard their importance and underrate their delicate experimental implications. This is a great mistake. The tests required to define steel strength are never to be taken for granted. Instead, they are an essential step in metallurgical knowledge and must not be neglected.

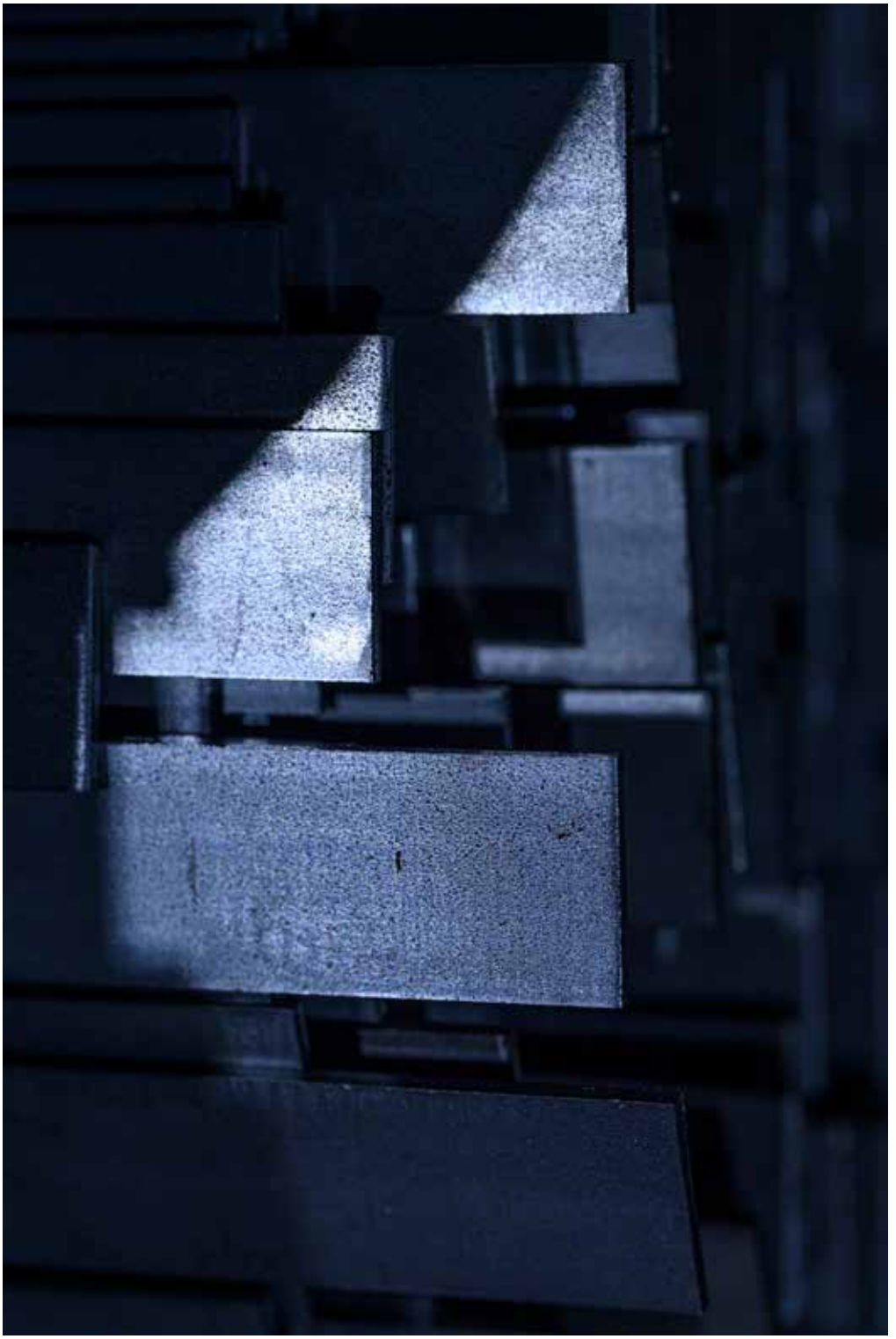

2. STEEL TENSILE TESTING

2.1 Stress and Strain

Tensile testing is the commonest experimental technique that allows determining steel mechanical strength quantitatively. This test is used to ascertain that steel features meet the requirements of a certain reference standard. It is also used to obtain numerical data useful to the designer, such as the Yield Strength or the proof stress (*YS*) and the ultimate tensile stress (*UTS*).

To fully understand the issues associated with tensile testing, you should reflect on two basic magnitudes. They are stress and strain.

Let's take a round bar in length L_0 and with a constant cross-section S_0. A force F is applied at both its ends. This load system is called uniaxial tensile stress. As the round bar has a constant cross-section all along its axis, the external force F is evenly transmitted throughout the cross-section S_0. This means that, if you cut the bar across any plane *A-A* normal to the bar axis, the force F will be balanced by the internal forces of the material that evenly distribute over the shear plane (Figure 2.1). We define stress σ, or *nominal stress* or *conventional stress* or *engineering stress*, the ratio of the force F applied and the bar cross-section S_0, as follows:

$$\sigma = \frac{F}{S_0} \qquad \text{[eq. 2.1]}$$

where σ is a magnitude having the same units of measure of pressure (1 N/m^2 = 1 Pa or, more commonly with metallic materials, 1 N/mm^2 = 1 MPa)[1].

As a result of the force F acting all along the bar axis, the bar is subject to elongation ΔL which causes the cross-section to decrease, thereby guaranteeing volume preservation (Figure 2.2).

We define strain ε, or *nominal strain* or *conventional strain* or *engineering strain*, the ratio between elongation (ΔL) and the initial bar length L_0, as follows (L_f being the final bar length):

$$\varepsilon = \frac{L_f - L_0}{L_0} = \frac{\Delta L}{L_0} \qquad \text{[eq. 2.2]}$$

[1] For example, if the bar cross-section is S_0 = 50 mm^2 and the force applied F is 4000 N (≈ 400 kg_f), the resulting nominal stress will be σ = 80 N/mm^2 = 80 MPa (≈ 8 kg_f/mm^2). In practical terms, stress is the load evenly distributes per unit of area. In the example provided, each mm^2 of steel can stand a load applied of 80 N (≈ 8 kg_f).

where ε is an adimensional magnitude, usually expressed as percentage points or as the ratio of two different units of measure of length[2] (for example mm/m). It should be noticed that strain as defined by [eq. 2.2] is always given by the sum of two contributions, namely elastic strain ε_e and plastic strain ε_p, which means:

$$\varepsilon = \varepsilon_e + \varepsilon_p \qquad \text{[eq. 2.3]}$$

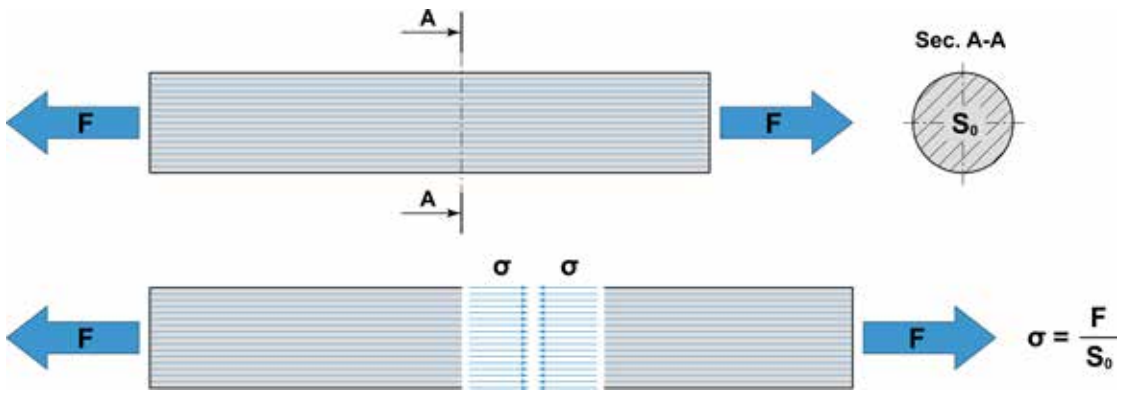

Figure 2.1 – Defining stress in a round bar subject to uniaxial tensile strength. The blue lines show the trend of external actions.

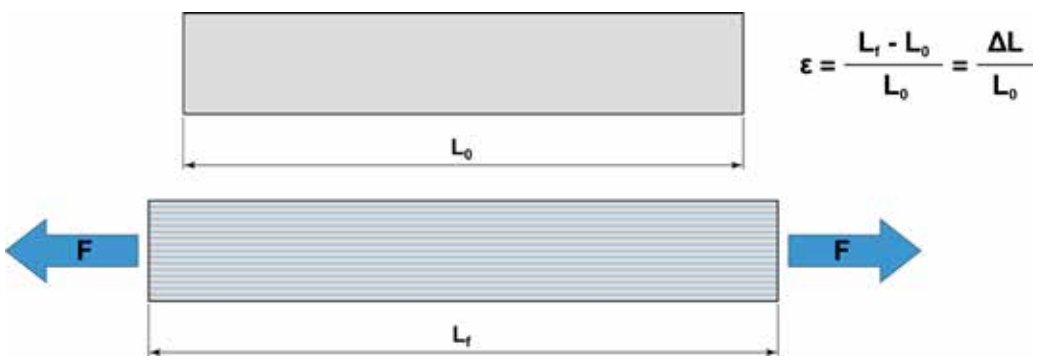

Figure 2.2 – Defining strain in a round bar subject to uniaxial tensile strength.

[2] *This concept can be better explained by means of the following example: presume a round bar with a 1% strain; this means that the bar, under a certain stress, elongates by 1 part every 100 parts of its initial length, i.e. its elongation is equal to 1 mm every 100 mm of its initial length. The same strain can also be expressed as 10 mm per meter (10 mm/m = 10/1000 mm/mm = 1/100 = 1%).*

To calculate the stress and strain values in whatever cross-section of the component, you have to presume that the material is continuous, homogeneous and isotropic. Isotropic means that its mechanical properties are equal at all points and unrelated of the direction along which they are evaluated. Therefore, it should be presumed that steel has no segregations and volume flaws[3] such as cracks, porosity, shrinkage cavities, inclusions, etc.

On the other hand, when observed at a *microscopic* scale, no metal alloy of engineering interest respects the hypotheses of homogeneousness. As all metallic materials, steels are polycrystalline structures where different structural phases or constituents are normally found. Also, even in the case of one-phase alloys, which means characterised by a single structural component, it is common to find micro-segregations and/or minor inclusions, sometimes purposely added to improve material machinability.

From a *macroscopic* point of view, the hypotheses of homogeneousness, isotropy and continuity are normally considered valid because:

- Crystal grains have a reduced average size, typically between 20 μm and 80 μm;
- Crystal grains orientation in the crystal lattice is totally casual;
- No segregations and macroscopic volume flaws are normally found.

Obviously, in the presence of very coarse grains (such as in semi-finished products overheated at high temperature), crystals orientated along a preferential direction (such as in semi-finished products after cold deformation) or segregations and/or macroscopic volume flaws (such as in large castings or forgings), the hypotheses of homogeneousness, isotropy and continuity often do not make sense. In these circumstances, the calculation methods normally used during the design phase are totally unsuitable and can lead to catastrophic failure of the part when in operation.

2.2 Tensile Testing Characteristics

Tensile testing consists in subjecting a specimen, sectioned from the material to be characterised, to an increasing uniaxial tensile load, which causes progressive elongation of the sample until it breaks. The strength applied slowly increases in time and the whole test lasts several minutes. This is called a static or quasi-static load system. The test is normally carried out at room temperature.

The test is aimed at determining steel response in terms of stress applied and strain induced. It also provides some mechanical parameters of engineering interest.

[3] *For an exhaustive study on the crystal lattice, see Chapter 2 of the book "Steel Metallurgy - Volume I" by Boniardi M. and Casaroli A., Lucefin, Esine, 2017.*

The specimen can be round type or sheet/plate type, depending on the type of semi-finished product or material from which it was sectioned[4]. The dimension of the central area, known as gauge length, is of the utmost importance and is characterised by two parameters: its length L_0 and its cross-section S_0 (Figure 2.3). Normally, the following relation between L_0 and S_0 should be respected:

$$L_0 = k \cdot \sqrt{S_0} \qquad \text{[eq. 2.4]}$$

where k is a constant whose most used value is 5.65[5].

This is called a *proportional* type of specimen. Not all samples are this type. In case of metal sheets or strips in thickness lower than 3 mm, the values of L_0 and S_0 are established directly by the standards without respecting the relation [eq. 2.4]. In this case, the specimens are called *non-proportional* specimens.
This is not a merely formal distinction if you consider that specimen strain is heavily affected by the ratio $L_0/\sqrt{S_0}$. Consequently, strain values can be compared exclusively between tests conducted on specimens of the same type.

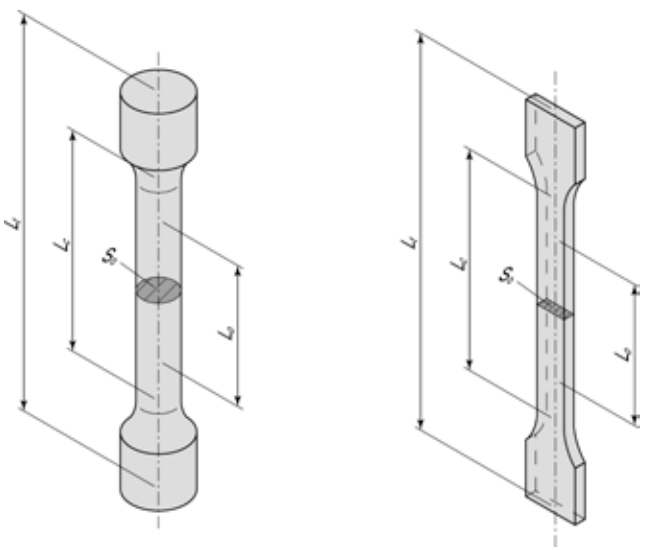

Figure 2.3 – Typical geometry of tensile specimens: (on the left) round-type specimen (on the right) sheet/plate specimen. Note: L_t: total length, L_c: calibrated length with constant cross-section, L_o: gauge length, S_o: gauge length cross-section.

[4] Usually, tensile specimens are round-type; the samples sectioned from forgings, bars, high-thickness rolled products, etc., are always obtained by turning. In the case of thin, flat semi-finished products (such as strips, sheets, etc.), it is more convenient to obtain a plate or sheet type specimen.

[5] In this manner, the following relation applies between the gauge length L_0 and the diameter d_0 of cylindrical specimens: $L_0 = 5.65 \cdot \sqrt{(\pi \cdot d_0^2)/4} = 5 \cdot d_0$ (if L_0 = 50 mm, then d_0 = 10 mm). In the case of sheet/plate type specimens, you have: $L_0 = 5.65 \cdot \sqrt{a_0 \cdot b_0}$ being a_0 and b_0 the two sides of the cross-section. For example, with a 3.2mm thick metal sheet, if L_0 = 50 mm, then S_0 = 25 x 3.2 mm.

The tests are performed using a machine specially designed for uniaxial tensile testing (Figure 2.4). The machine is composed of two columns and two cross beams; the lower cross beam is fixed while the upper cross beam (*crosshead*) is mobile. Two grips are fixed at the beams. They are used to clasp the specimen ends and secure it firmly to the machine.

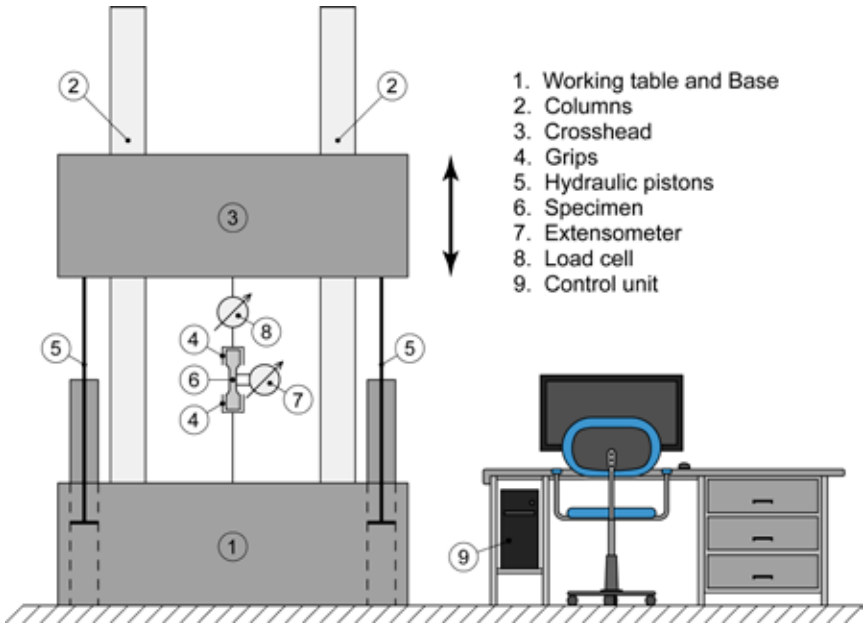

Figure 2.4 – Schematic of an uniaxial tensile testing machine.

During the tensile test, the mobile cross beam gradually lifts. Its motion is driven by mechanical or hydraulic actuators that are electrically controlled by the control unit. The cross beam displacement applies an increasing uniaxial tensile strength onto the specimen, whose value is measured by a load cell. As a consequence of the load F applied, the specimen gradually elongates. The measure of elongation $\Delta L = L_f - L_0$ is obtained from an exstensometer assembled directly to the specimen.

In addition to guaranteeing machine operation, the control unit correlates the values of the load F and of elongation ΔL on an instant-to-instant basis and displays them in a Cartesian diagram as stress σ and strain ε[6]. A typical example of the result obtained at test end is shown in Figure 2.5. The curve σ-ε can be divided into four regions (Figure 2.6).

[6] *Prior to starting the tensile test, the sample should be carefully measured to obtain the values of L_0 and d_0 (or L_0, a_0 and b_0 with sheet/plate type samples) to be entered in the control unit. Once the parameters have been set, the software allows obtaining the values of stress σ and strain ε automatically during the test.*

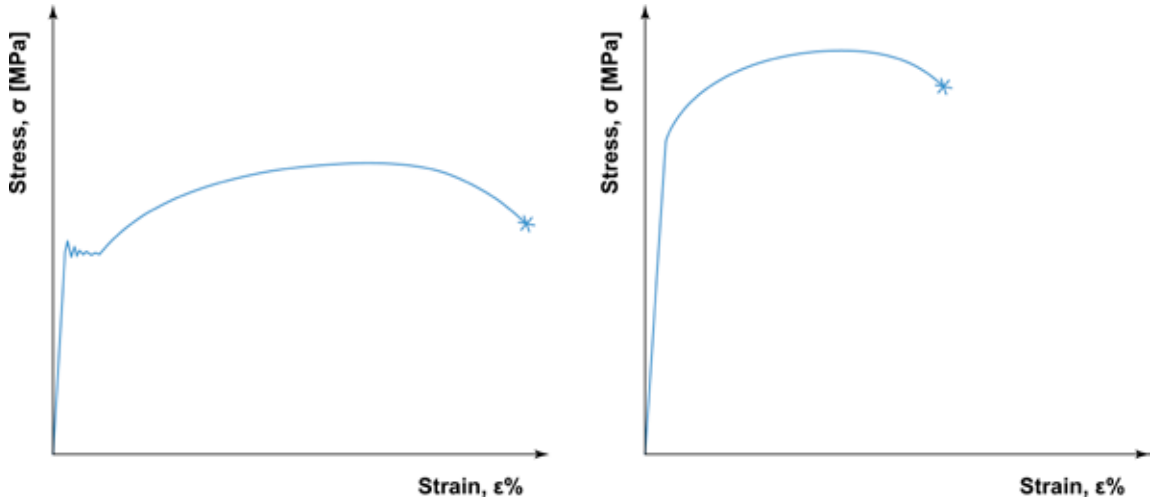

Figure 2.5 – Schematic of the stress-strain curves (σ-ε) for a general-purpose structural steel type EN S275 and for an EN C40 Q&T steel after quenching and tempering at 620°C.

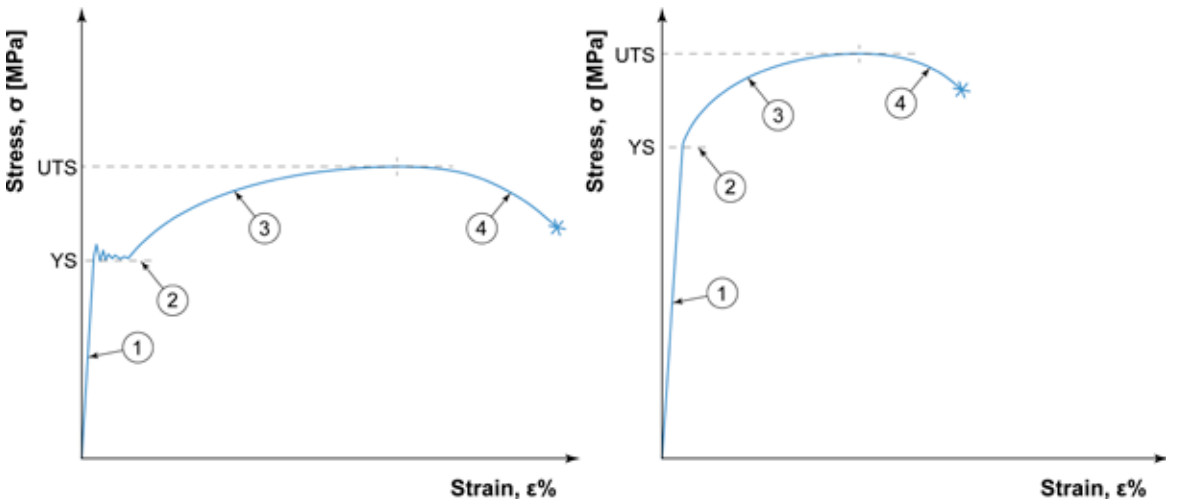

Figure 2.6 – Illustration of the four regions into which you can divide the curves σ-ε for a general-purpose structural steel type EN S275 and for a Q&T steel type EN C40 after quenching and tempering at 620°C.

Region 1 is characterised by a sloping straight line passing through the origin of the axes. Therefore, in this region, the link of stress σ and strain ε is linear. The equation correlating the two magnitudes is:

$$\sigma = E \cdot \varepsilon \qquad \text{[eq. 2.5]}$$

where E is the slope of the straight line and is known as elastic modulus or Young's modulus[7]; its unit of measure is N/mm^2 or MPa.
Region 1 is referred to as the "small deformation region" because ε under load is always below 1% or even as the "elastic deformation region" because if the test is discontinued, the unloading curve overlaps the loading curve[8]. In this length the material behaves exactly as a spring: it gets longer under the effect of the strength applied, and then resumes its original dimensions when the load is removed.

Region 2 marks the end of the elastic strain field and of the linear correlation of σ and ε. In this area you can observe two different situations:

- A significant increase of strain ε at a stress level σ that is almost constant or slightly oscillating between a minimum and a maximum (as it happens with EN S275 steel).
- The presence of a kink in the σ-ε curve highlighting a marked deviation from the linearity typical of the previous elastic length (as it happens with steel EN C40).

These events macroscopically describe that a change is occurring in steel at reticular level. It is from this point that the dislocations responsible for material cold deformation start moving.
The stress level measured in Region 2 is called Yield Strength[9] and is indicated as *YS*. It is an extremely important parameter from the engineering point of view given that it is normally used for static/almost-static design.

With *Regions 3* and *4*, you pass from the field of elastic strain to that of plastic strain, or major strain, that can reach values of tens of percentage points. In Region 3, as the stress applied σ increases, also strain ε remarkably increases. The curve σ-ε reaches the maximum stress value marking the boundary between Region 3 and Region 4. Then, it gradually decreases until the specimen breaks, which is identified by the star at the end of Region 4.

[7] Young's modulus, E, is a physical magnitude, not a mechanical one. The value of E is strictly connected to the properties of the metallic bond between the atoms in the lattice, not to the micro-structure of the material. Therefore, E is independent of the manufacturing process, the strain hardening degree or steel heat treatments. It depends exclusively on the chemical composition of the alloy. Steels possess an elastic modulus between 200,000 and 215,000 MPa (oscillations between 195,000 and 220,000 MPa are typical of stainless steels containing a significant amount of alloying elements in addition to iron and carbon).

[8] The machine can be stopped at any time during the test. Moving the mobile cross beam downwards, you can gradually bring the load applied down to zero. In this manner the control unit records the curve σ-ε during the specimen unloading phase.

[9] If the effort measured in Region 2 oscillates between a minimum and a maximum, consider the minimum value as the Yield Strength that will be indicated as LYS (Lower Yield Strength).

The maximum value of the curve σ-ε is also a very important parameter because it allows defining the Ultimate Tensile Strength of steel, indicated as *UTS*[10].

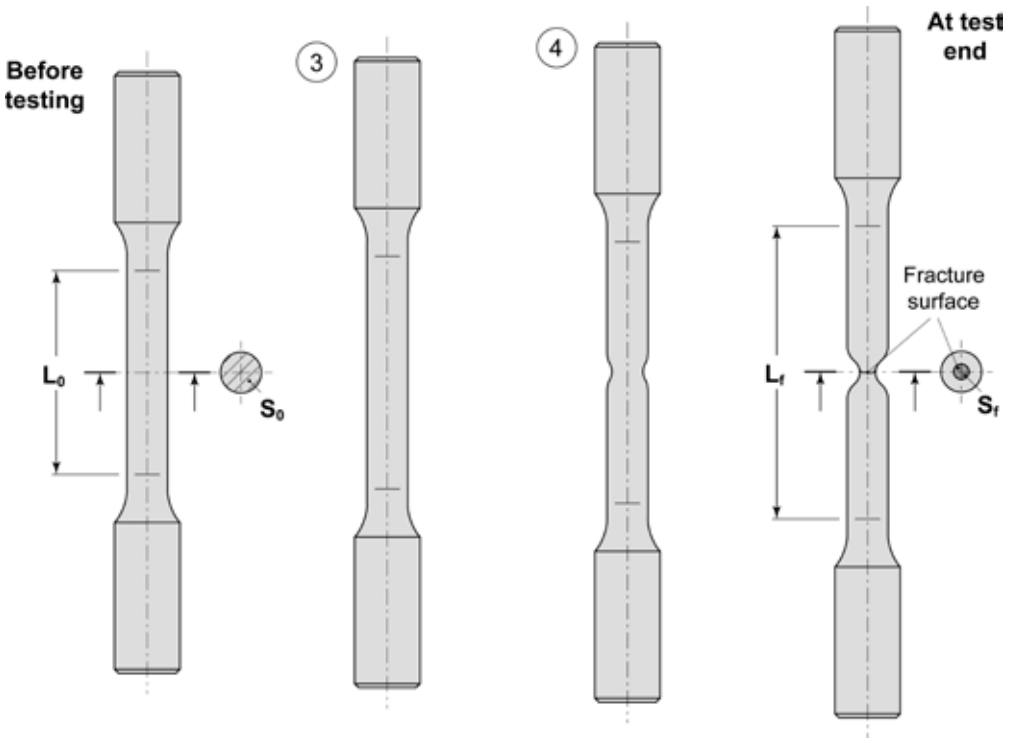

Figure 2.7 – Schematic of the aspect of a tensile specimen before testing, in Region 3, in Region 4 and at test end.

A very special event that distinguishes Region 3 from Region 4 is worth mentioning. While in Regions 1, 2 and 3 strain is consistent, i.e. it spreads evenly all along the calibrated length, in Region 4 strain concentrates in a spot, resulting in a localised reduction of the specimen cross-section that is called *necking* (Figure 2.7). It should also be noticed that strain occurred in Regions 3 and 4 is permanent. This means that steel will exhibit a plastic deformation even when the load it totally removed before the specimen breaks. This concept is clearly illustrated in Figure 2.8, where you can see that the material completely recovers elastic strain ε_e only, while plastic strain ε_p remains unchanged.

[10] *The Ultimate Tensile Strength is not the ultimate load at which the specimen physically breaks, but the maximum stress reached during the test.*

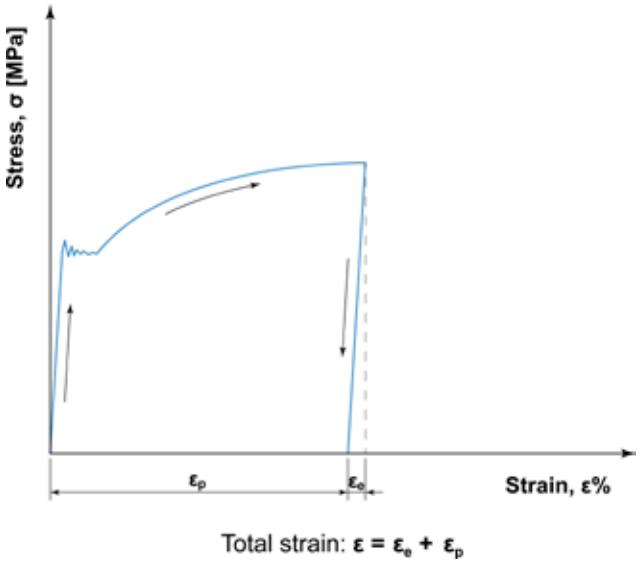

Figure 2.8 – Schematic of the stress-strain curve (σ-ε) for a general-purpose structural steel type EN S275. The tensile test was discontinued and the stress level brought back to zero at the plastic strain region.

At the end of the tensile test, in addition to *E*, *YS* and *UTS*, you can obtain two other parameters of engineering interest, both connected to steel cold formability, namely elongation after fracture (*A%*) and reduction of area (*Z%*).

After recovering the broken specimen, put the two fragments close to one another along the fracture plane, then measure the final gauge length L_f and the diameter d_f of the final cross-section S_f using a sliding gauge. *A%*[11] and *Z%* can be calculated using the following relations[12]:

$$A\% = \frac{L_f - L_0}{L_0} \cdot 100 \qquad \text{[eq. 2.6]}$$

$$Z\% = \frac{S_0 - S_f}{S_0} \cdot 100 \qquad \text{[eq. 2.7]}$$

[11] *If you use proportional specimens where the constant k is equal to a multiple of 5.65, you must indicate its value in a subscript after A% (ex. $A\%_{11.3}$). If you use non-proportional specimens, the identifier A% must be followed by a subscript indicating the gauge length in millimetres (es. $A\%_{80mm}$).*

[12] *Please note that for A% the numerator difference is between initial gauge length and final gauge length. The contrary happens with Z%: initial cross-section less final cross-section at the gauge length.*

For example, if you consider the two cases in Figure 2.5, you obtain the following results for the general-purpose structural steel type EN S275:

$E = 206{,}000\ MPa$
$YS = 310\ MPa$
$UTS = 460\ MPa$
$A\% = 28\%$
$Z\% = 59\%$

and for the Q&T steel type C40 (after quenching and tempering at 620°C):

$E = 206{,}000\ MPa$
$YS = 490\ MPa$
$UTS = 690\ MPa$
$A\% = 19\%$
$Z\% = 46\%$

However, for some steels a weird situation can occur, that is there is no Yield Strength that can be identified with a singularity of the curve σ-ε (Figure 2.9, on the left). To have a numerical information that can be defined as Yield Strength, you should rely on the 0.2% offset Yield Strength.
In these situations, make recourse to an opportune graphic construction (Figure 2.9, on the right).
First of all, measure the value of the longitudinal elastic modulus E considering the initial portion of the curve σ-ε where stress-strain linearity is certainly respected. Take down the value of E and trace both the straight line $\sigma = E \cdot \varepsilon$ passing through the origin of the axes and a line parallel to it but shifted by 0.2% on the abscissae. This is the straight line representing the equation $\sigma = E \cdot (\varepsilon - 0.2)$, where ε is expressed as a percentage. The point of intersection of the second straight line and the curve σ-ε identifies the value of the 0.2% offset Yield Strength also called *Proof Stress* .
For more details concerning tensile testing, we advise reading the EN ISO 6892-1 and ASTM E8 standards[13].

[13] *EN ISO 6892-1 standard "Metallic materials - Tensile testing - Part 1: Method of test at room temperature" and ASTM E8 standard " Tension Testing of Metallic Materials".*

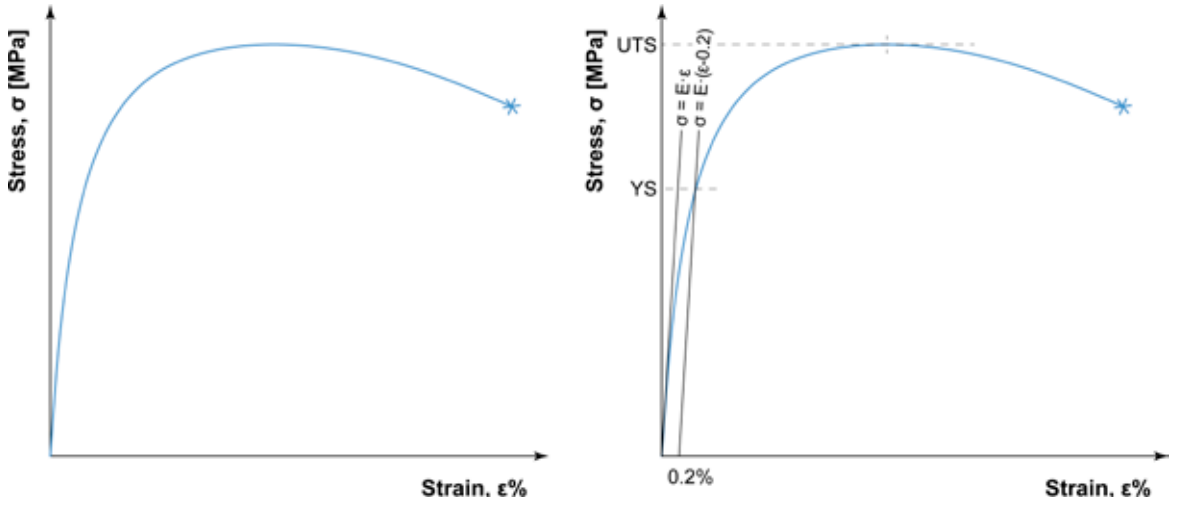

Figure 2.9 – (on the left) Schematic of the stress-strain curve (σ-ε) for a ferritic stainless steel EN X6Cr17 after annealing; (on the right) graphic construction on the same curve as necessary to determine the 0.2% proof stress.

2.3 Steel Ductile or Fragile Behaviour during Tensile Testing

In the previous paragraph we have examined the elastic-plastic behaviour of some steels. The examples provided are typical of ductile steels that reach the breaking point at the end of a phase of more or less marked plastic strain.

This category includes most metals and metal alloys of engineering interest, such as general-purpose structural steels, special structural steels, stainless steels together with aluminium, copper, nickel, titanium and their alloys.

However, not all steels have a ductile behaviour. Some of them exhibit a failure mechanism of fragile type, which means that their plastic strain is very limited or non-existent before reaching the breaking point.

To confirm the above, you can usefully compare the σ-ε graph for an EN C40 Q&T steel quenched in water, with and without tempering at 620°C (Figure 2.10). In the former case, when the elastic limit is exceeded, you observe a large plastic strain before failure (ductile behaviour); in the latter, permanent strains are of an extremely small size (fragile behaviour).

In practice, two indicators allow distinguishing a ductile breakage from a fragile breakage at a macroscopic level:

- *The direction of the fracture plane* that has an inclination of 45° relative to maximum principal stress in ductile materials while in fragile materials its value is 90°;
- *The strain level* that is considerable in ductile materials (above 5%) while it is almost negligible in fragile materials (below 5%).

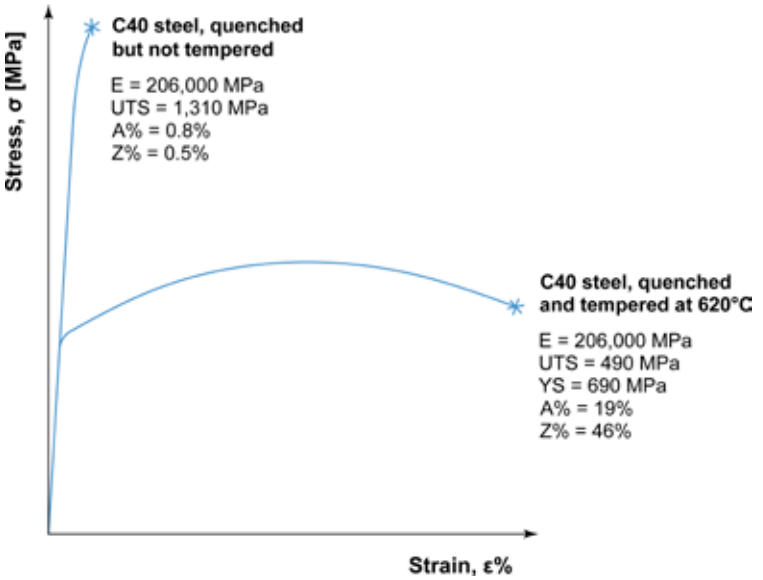

Figure 2.10 – Stress-strain curves (σ-ε) for an EN C40 Q&T steel quenched in water, with and without tempering at 620°C. It should be pointed out that in the case of a fragile behaviour, the indication of the Yield Strength *YS* is senseless [Omeco S.r.l. Laboratories, Monza – Italy].

These differences clearly appear when you compare the fracture surfaces of the two EN C40 steel tensile specimens that were subjected to different heat treatments. The sample quenched and tempered at 620°C exhibits a ductile behaviour (Figure 2.11, on the left), while the quenched-only sample has a fragile behaviour (Figure 2.11, on the right).

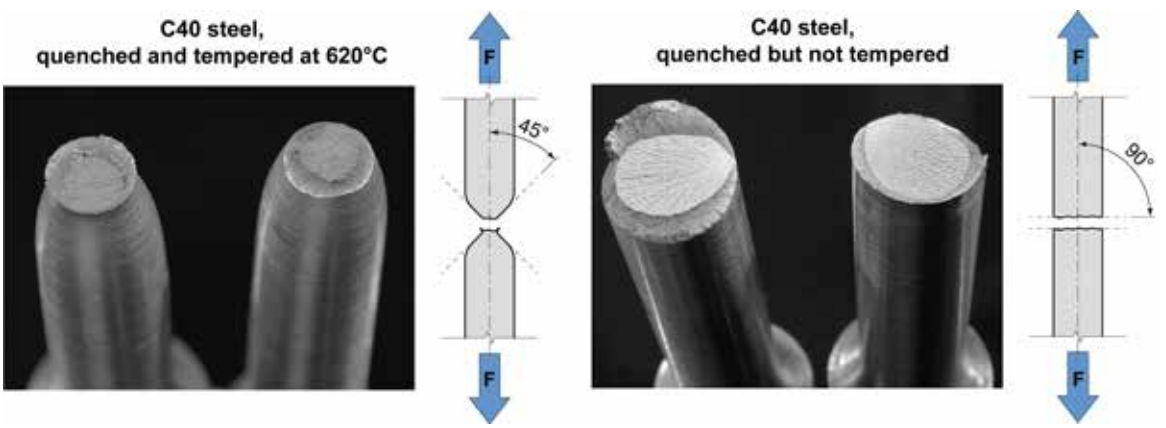

Figure 2.11 – Fracture surfaces of two tensile specimens made from EN C40 steel: (on the left) after quenching and tempering at 620°C and (on the right) after quenching only [Omeco S.r.l. Laboratories, Monza – Italy].

2.4 True Stress and True Strain

Analysing in detail the plastic portion of the stress-strain curve between the Yield Strength and the Ultimate Tensile Strength proves extremely useful when you are going to investigate cold formability of metallic materials.

To this regard, it is necessary to take into account the true stresses and strains (σ^*-ε^*) that affect the specimen during the test, on an instant-by-instant basis, instead of engineering stresses and strains (σ-ε), which are referred to the tensile specimen's original dimensions (S_0 e L_0). After naming S_i and L_i the instant cross-section and the instant gauge length, respectively, you have:

$$\sigma^* = \frac{P}{S_i} \qquad \varepsilon^* = \frac{dL}{L_i} \qquad \text{[eq. 2.8]}$$

You can demonstrate that in the region of consistent straining, i.e. between Yield Strength and maximum stress, the correlation of engineering stresses and strains (σ-ε) with true stresses and strains (σ^*-ε^*) is given by:

$$\sigma^* = \sigma \cdot (\varepsilon + 1) \qquad \varepsilon^* = \ln(1 + \varepsilon) \qquad \text{[eq. 2.9]}$$

Figure 2.12 shows the stress-strain graph in a general tensile test. While in the elastic region, the two curves (σ-ε and σ^*-ε^*) are virtually overlapped, in the plastic region they are significantly apart.

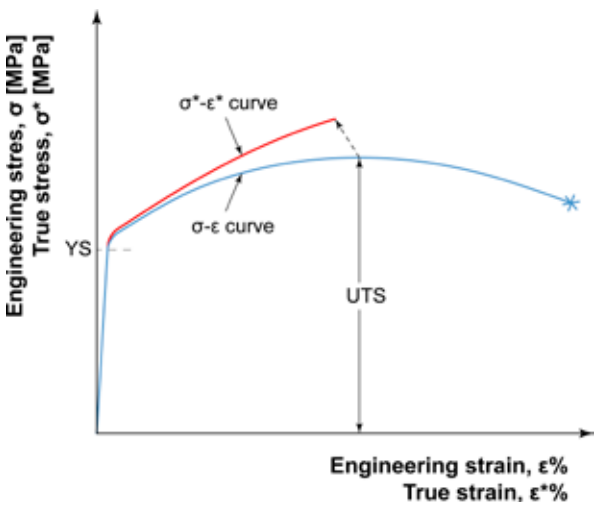

Figure 2.12 – Trend of a general tensile curve in terms of engineering stresses and strains (σ-ε) and of true stresses and strains (σ^*-ε^*) The curve of true stresses and strains is traced to UTS.

In the region of plastic deformation, i.e. between Yield Strength and maximum stress, the curve of true stresses-true strains (σ^*-ε^*) is well represented by Hollomon's equation:

$$\sigma^* = K \cdot (\varepsilon^*)^n \qquad \text{[eq. 2.10]}$$

where K and n are two constants that depend on material and are referred to as strain hardening constant and strain hardening index, respectively. If you re-write the [eq. 2.10] in logarithmic terms to base 10, you have:

$$log_{10}(\sigma^*) = log_{10}(K) + n \cdot log_{10}(\varepsilon^*) \qquad \text{[eq. 2.11]}$$

In a Cartesian reference $log_{10}(\sigma^*)$-$log_{10}(\varepsilon^*)$, this is a straight line with slope n that intercepts $log_{10}(K)$ on the axis $log(\varepsilon^*) = 1$ (Figure 2.13).

The strain hardening index, n, is the aptitude of a steel to plastic deformation by stretching (stretchability) before reaching the necking point. Its value is included between 0 (a perfectly plastic condition) and 1 (a perfectly elastic condition). In practice, in metallic materials, the index n varies from 0.1 to 0.5. A high value of the index n is desirable when the material is to be cold-formed (for steels: $n \geq 0.16$ indicatively), given that this makes it easier to manufacture components with a complex geometry without causing unexpected breakages during straining.

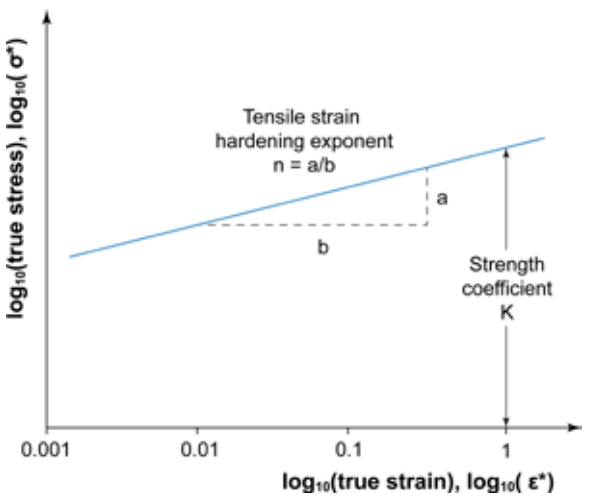

Figure 2.13 – Representation of Hollomon's equation in a bilogarithmic graph $log_{10}(\sigma^*)$-$log_{10}(\varepsilon^*)$.

Always with regard to cold formability, especially in cold-formed flat semi-finished products (strips), it can prove useful to measure the material's plastic strain ratio r [14], also known as Lankford's coefficient and defined by the following formula:

$$r = \frac{\varepsilon_w^*}{\varepsilon_t^*} \quad \text{[eq. 2.12]}$$

where ε^*_w e ε^*_t are the strip's true strain width-wise (w) and thickness-wise (t) during tensile testing (Figure 2.14).

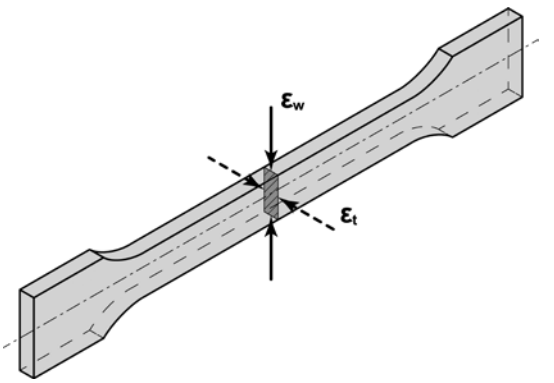

Figure 2.14 – Schematic of strain determination width-wise (w) and thickness-wise (t) in the tensile specimen obtained from a strip [from ASM International 2012].

Due to material anisotropy, in thin cold-finished metal sheets, the plastic strain ratio r changes depending on sampling direction. In steel strips, the index r measured crosswise the rolling axis (r_{90}) is the highest, typically $1.2 < r_{90} < 2$; on the other hand, r taken at 45° (r_{45}) is the lowest, generally $0.6 < r_{45} < 1.2$. As a result, the measures for r are usually taken along three different directions relative to the rolling axis (r_0, r_{45}, r_{90}); then an average value r_m is calculated using the following formula:

$$r_m = \frac{1}{4} \cdot (r_0 + 2r_{45} + r_{90}) \quad \text{[eq. 2.13]}$$

Steels with $r_m \approx 1.4$ exhibit a perfect aptitude to be drawn. Instead, if $r_m \approx 0.7$, their formability characteristics are rather modest.

[14] *The value of r not only depends on the material, but also on the strain level. Normally, r is taken at 20% of the plastic deformation during tensile testing.*

3. STEEL HARDNESS TESTING

3.1 Steel Hardness

Hardness is a magnitude of mechanical nature. In the metallurgical field, it is measured as the resistance opposed by a steel to penetration of a harder material through localised compression.

Hardness is determined by means of mechanical tests that are widely used thanks to both their fast and easy execution and limited cost of the equipment involved. The advantage of this test type is that it can be carried out directly on the part, thereby avoiding damaging it for sampling purposes. Unlike tensile tests, hardness tests do not provide numerical data useful to the designer. They allow evaluating in a simple manner the effectiveness of the manufacturing process to which a component was subjected (such as correct heat treating practices, cold deformation level, etc.) and provide an index of comparison for estimating the quality of multiple steels.

Like tensile tests, hardness tests can be static or quasi-static type. From a practical point of view, the tests are performed by gradually pressing an indenter with known geometrical characteristics against the surface of the part to be examined.

The result is determined by correlating the load F applied to the indenter with the geometrical characteristics of the indentation left in the part or in the specimen (indentation area S or depth h).

Three tests are typically used to measure steel hardness (Figure 3.1), they are:

- The Brinell test;
- The Vickers test; and
- The Rockwell test.

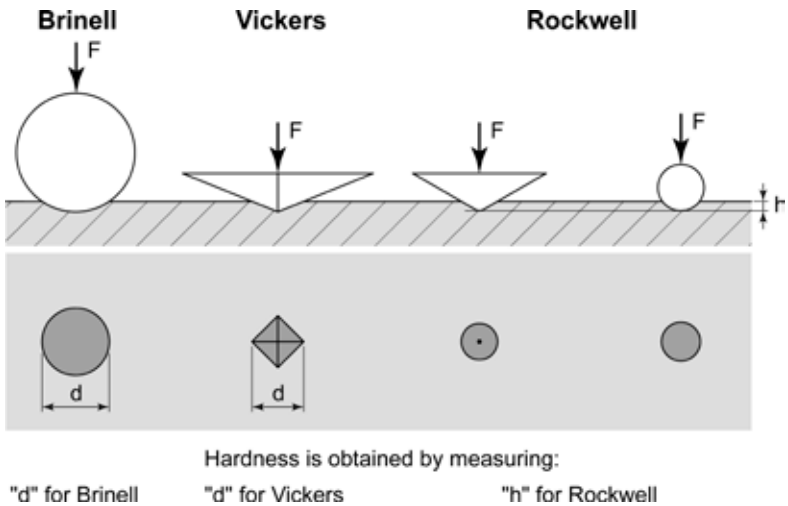

Figure 3.1 – Schematic of the three main hardness tests used in metallurgy.

Hardness tests can be further divided into:

- Macro-hardness tests, where the indentation involves a significant volume of material, in the range of some mm^2. In this case, the load applied to the indenter can vary from 1 kg_f (9.81 N) up to 3000 kg_f (29,800 N) and the indentation obtained can be seen with the naked eye;
- Micro-hardness tests, where the indentation involves a volume of material of less than one mm^2. In this case, the load applied to the indenter is less than 1 kg_f (9.81 N) and you have to make recourse to an optical microscope to observe the indentation.

As hardness tests were developed early in the 20th century, the values of the load applied used to be expressed in kg_f. Therefore, in the continuation of this essay, we deemed it opportune to give up the units of measure of the International System and stick to the original indication in kg_f, that is still in use in most testing machines.

3.2 The Brinell Hardness Test

In the Brinell hardness test, a quenched steel or tungsten carbide spherical indenter is pressed against the surface of the material to be examined, with a certain load and for a preset time. Brinell hardness HB is expressed as the ratio of the force applied F and the indentation area S that exhibits the typical inverted-dome shape. Brinell hardness HB is given by the following relation[1]:

$$HB = \frac{F}{S} = \frac{2 \cdot F}{\pi \cdot D \cdot \left(D - \sqrt{D^2 - d^2}\right)} \qquad \text{[eq. 3.1]}$$

while indentation depth h is expressed by:

$$h = \frac{1}{2} \cdot \left(D - \sqrt{D^2 - d^2}\right) \qquad \text{[eq. 3.2]}$$

where F is the load applied in kg_f, D is the indenter diameter in mm and d is the average diameter of the indentation projection on the sample surface in mm (Figure 3.2).

With annealed or normalized steels, usual testing conditions include using a spherical indenter with a 10mm diameter D, a 3,000 kg_f (29,400 N) load F and an indentation time of 15 seconds. Alternatively, you can use a ball with a smaller diameter matched with a lighter load: for example D = 2.5 mm and F = 187.5 kg_f (1,837 N) or D = 5 mm and F = 750 kg_f (7,350 N).

[1] *If the load applied F is expressed in Newton, the result of the hardness calculation formula should be multiplied by 0.102.*

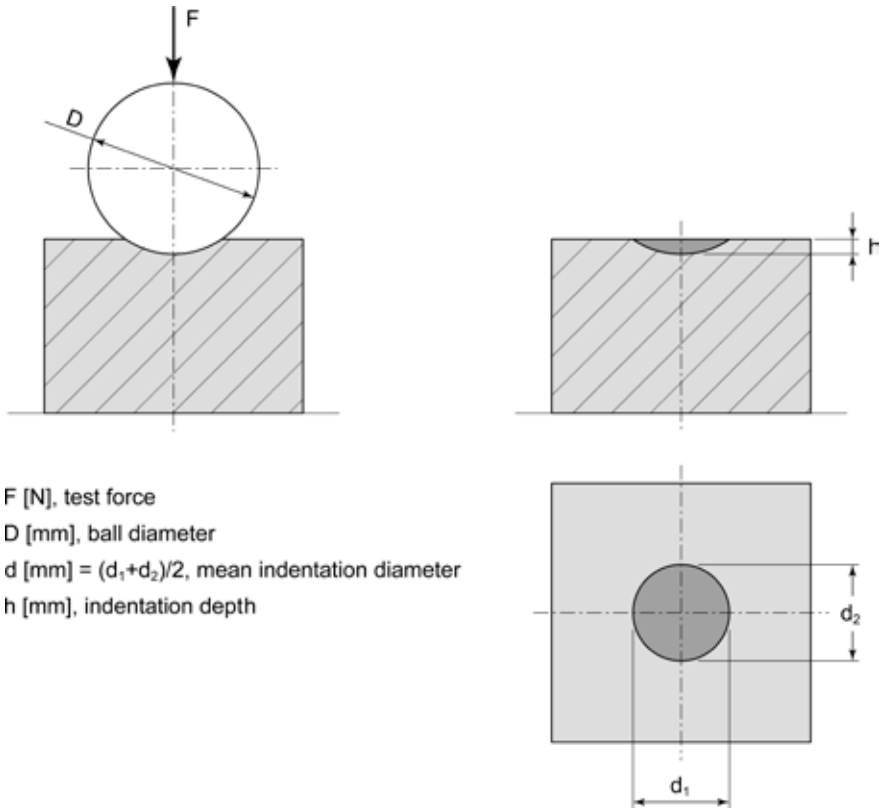

Figure 3.2 – Schematic of the Brinell hardness test and definition of its main test parameters.

For the Brinell test to provide reliable and mutually comparable results, it is necessary to apply some rules. If the ball diameter D and the load applied F are changed, the contact angle β should not exhibit broad variations and oscillate exclusively around a well-defined value of 136° (Figure 3.3). From the practical point of view, this is obtained by strictly limiting the variations of the indentation diameter d-to-ball diameter D ratio, i.e. d/D = 0.25-0.50. You guarantee that this condition is respected by fixing the ratio of the load applied F, in kg_f, and the squared diameter of the ball D, in mm. In the case of steels, this ratio[2] is set at 30, i.e. $F/D^2 = 30$. As you can easily infer, the test conditions set forth in the standards and previously detailed (D= 2.5 mm and F= 187.5 kg_f; D= 5 mm and F= 750 kg_f; D= 10 mm and F= 3,000 kg_f) guarantee exactly the ratio $F/D^2 = 30$.

[2] *If the load applied F is expressed in Newton, the F/D² ratio should be multiplied by 0.102.*

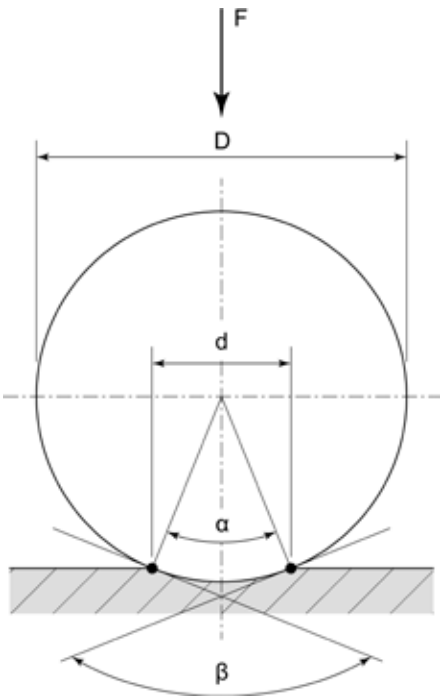

Figure 3.3 – Graphic definition of the contact angle β in a Brinell test in ideal conditions (β = 136°).

With steels, the minimum sample thickness should be at least 8 times the indentation depth *h*. The minimum distance between the centres of two adjacent indentations should be at least 4 times their diameter *d*. The minimum distance between the centre of an indentation and the sample edges should be at least 2.5 times *d*. The support and testing surfaces of the sample should be flat and parallel and accurately finished so that to limit indentation measure errors. Also, before conducting the tests, you should make sure that the specimens are free from oxides, dirt and/or lubricant substances. The diameter *d* is read using an optical microscope assembled to the testing machine. The microscope magnifies the indentation and allows measuring it by means of an opportunely graded scale. Once the test completed, Brinell hardness should be indicated by the index HB, followed by the letter *S* if a quenched steel ball was used or by the letter *W* if a tungsten carbide ball was used. Other indications follow that express testing conditions. For example, 250 HBW 2.5/187.5/20 means that the test was carried out using a tungsten carbide ball and has given a Brinell hardness value of 250. The figures after the HBW index specify that the test was conducted using a 2.5 mm dia. indenter and applying a load of 187.5 kg_f for 20 seconds. Time must be indicated only if different from the standard duration of 15 seconds.

The Brinell test is suitable for steels with maximum hardness 400 HB if using quenched steel balls and 550 HB if using tungsten carbide balls. If hardness exceeds the above mentioned values, the result obtained is not acceptable because ball formability can be compared to that of the material to be examined. It is interesting to point out that, with steels, the Ultimate Tensile Strength expressed in MPa is proportional to Brinell hardness according to the following relation:

$$UTS = 3\text{-}3.3 \cdot HB \qquad \text{[eq. 3.3]}$$

For example, in the case of a steel with Brinell hardness 250 HB, you can estimate an Ultimate Tensile Strength UTS in the range of 750-825 MPa.
For more details on the Brinell test, we advise carefully reading the EN ISO 6506-1 and ASTM E10 standards[3].

3.3 The Vickers Hardness Test

In the Vickers hardness test, the indenter is made of synthetic diamond and shaped as a square base pyramid with a vertex angle of 136°.
As with Brinell hardness, also Vickers hardness is calculated from the ratio between the load applied *F* and the indentation area *S* left in the sample. As indentation projection has almost the shape of a square, Vickers hardness is given by the following relation[4]:

$$HV = \frac{2 \cdot F \cdot sin68°}{d^2} \cong 1.8544 \cdot \frac{F}{d^2} \qquad \text{[eq. 3.4]}$$

while indentation depth *h* is given by:

$$h = \frac{d}{2 \cdot \sqrt{2} \cdot \tan 68°} \cong \frac{d}{7} \qquad \text{[eq. 3.5]}$$

where *F* is the load applied in kg_f and *d* is the average value of the indentation diagonal in mm (Figure 3.4).

[3] *Specifically, EN ISO 6506-1: Metallic materials - Brinell hardness test - Part 1: Test method; ASTM E10: Standard Test Method for Brinell Hardness of Metallic Materials.*

[4] *If the load applied F is expressed in Newton, the result of the hardness calculation formula should be multiplied by 0.102.*

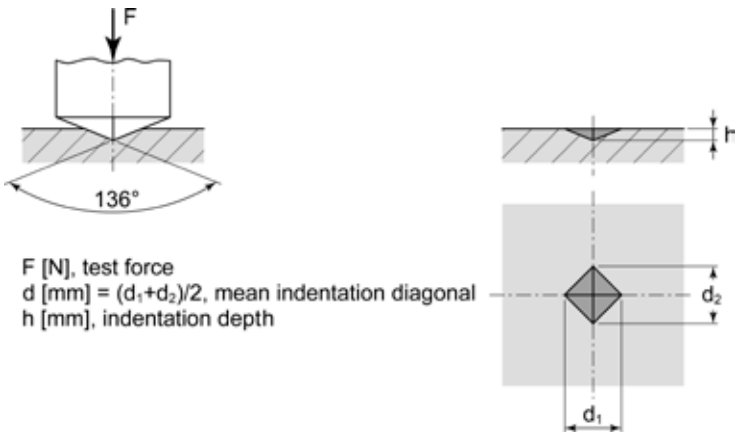

Figure 3.4 – Schematic of the Vickers hardness test and definition of its main testing parameters.

The load applied to the Vickers indenter normally varies from 1 kg_f to 120 kg_f, even if lighter loads are permitted. Application time should be 10 seconds minimum. It is worth mentioning that the tests involving loads of less than 1 kg_f are known as Vickers micro-hardness tests and that in this case result dispersion considerably increases as the load applied decreases.

As it happens with Brinell hardness, also for Vickers hardness it is necessary to apply some rules to obtain reliable and mutually comparable results.

With steels, the minimum sample thickness should be at least 1.5 times the indentation diagonal *d*. The minimum distance between the centres of two adjacent indentations should be at least 3 times *d*. The minimum distance between the indentation centre and the specimen edges should be at least 2.5 times *d*. The sample support and testing surfaces should meet the same requirements as for Brinell hardness (flat and parallel surfaces, accurate finishing, no oxides, dirt and/or lubricant substances), but with even stricter tolerances. Vickers indentations are definitely smaller than Brinell's and even minor flaws in the sample can result in unacceptable reading errors.

Compared to the Brinell test, the Vickers test offers the great advantage of using a synthetic diamond indenter with a vertex angle of 136°. Therefore, the contact angle remains constant and you can carry out hardness tests involving different loads without changing the indenter.

Thanks to these characteristics, the Vickers test allows examining a range of steels with widely different hardness values. For example, you can go from 150-200 HV of annealed or normalized low carbon steels to 1,800-2,200 HV that are typical of the carbides found in tool steels.

Indentation limited depth and small size enable using the Vickers test also for measuring hardness in surface-treated components. Using loads equal to or less than 0.5 kg_f (in which cases you talk about Vickers micro-hardness), you can measure hardness trend in the case-hardened, nitrited or surface quenched layer.

Furthermore, the possibility to use extremely light loads, down to a minimum of 10 g_f, allows measuring hardness of the single phases inside the structural constituents, such as the Fe_3C phase of lamellae in carbon steels or the σ phase in stainless steels.

Also in the case of Vickers and micro-Vickers hardness, the indentation average diagonal is read using the optical microscope assembled to the testing machine. Given the minuscule size of indentations, higher magnifications (from 100x to 1,000x) than in the Brinell test (8x-10x) are required.

Vickers hardness should be indicated using the HV index followed by the values expressing the testing conditions. For example, 550 HV 5/20 means that the test has given a Vickers hardness value of 550 and was performed using a 5 kg_f load applied for 20 seconds. Also in this case, indentation time must be indicated only if different from the standard value of 15 seconds.

Given that the same physics principle is applied to measure Vickers and Brinell hardness[5] (namely, the ratio between the load F applied to the indenter and the area S of the indentation left in the sample), also Vickers hardness can be used to estimate the Ultimate Tensile Strength of steels in accordance with the following relation:

$$UTS = 3\text{-}3.3 \cdot HV \qquad \text{[eq. 3.6]}$$

For more details on the Vickers hardness test, we advise carefully reading the EN ISO 6507-1, ASTM E92 and ASTM E384 standards[6].

3.4 The Rockwell Hardness Test

Two different types of indenter are normally used for the Rockwell hardness test, as follows:

- A tungsten carbide ball with diameter 1/16 of an inch (about 1.587 mm) and a total applied load of 100 kg_f for the measure scale type *B*, or
- A synthetic diamond cone with a vertex angle of 120° and a total applied load of 150 kg_f for the measure scale type *C*[7].

To evaluate steel hardness, the Rockwell test takes into consideration the indentation depth h and not the indentation area S, as it happens with the Brinell and Vickers tests (Figure 3.5). This peculiarity makes the Rockwell test the fastest and simplest to automate.

---

[5] *The Brinell and Vickers hardness scales can be correlated to one another using the formula $HB \cong 0.95 \cdot HV$.*

[6] *Specifically, EN ISO 6507-1: Metallic materials - Vickers hardness test - Part 1: Test method; ASTM E92: Standard Test Methods for Vickers Hardness and Knoop Hardness of Metallic Materials, and ASTM E384: Standard Test Method for Microindentation Hardness of Materials.*

[7] *Many other scales exist for measuring Rockwell hardness in addition to scales B and C. To this regard, we advise carefully perusing the reference standards (see note 10).*

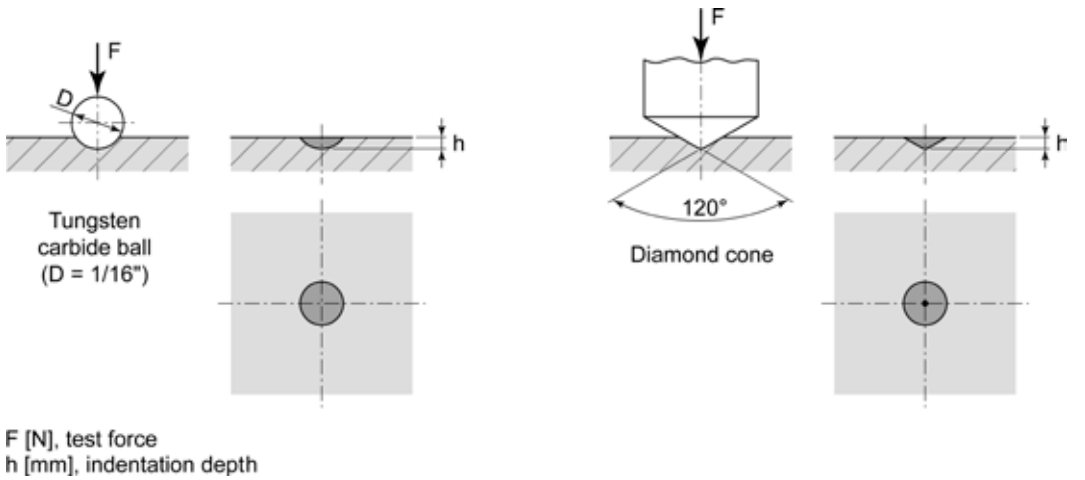

Figure 3.5 – Definition of the main parameters for the Rockwell hardness scales *B* and *C* (on the left and on the right, respectively).

The Rockwell hardness test consists in a well-defined sequence of operations to be performed one after the other (Figure 3.6).

1. First, the indenter is placed onto the part/sample and a 10 kg_f pre-load F_0 is applied. The testing machine defines this position of the indenter as the initial level "*i*" from which to measure the indentation depth.
2. Then, a load F_1 is added to the indenter in the amount of 90 kg_f for scale *B* ($F_0 + F_1 = 100\ kg_f$) or 140 kg_f for scale *C* ($F_0 + F_1 = 150 kg_f$). The total load is kept for a preset time. From the previous level "*i*" the indenter reaches the maximum indentation depth "*m*".
3. Finally, when the preset time has elapsed, the load F_1 (90 kg_f for scale *B* or 140 kg_f for scale *C*) is removed from the indenter. As a consequence, the indenter moves to the final level "*f*"[8] and the testing machine measures the indentation depth *h* as the difference between level "*i*" and level "*f*".

Rockwell hardness is calculated on the basis of the following relations (HRB for measure scale *B*; HRC for measure scale *C*):

$$HRB = 130 - \frac{h}{0.002} \quad \text{[eq. 3.7]}$$

$$HRC = 100 - \frac{h}{0.002} \quad \text{[eq. 3.8]}$$

where the indentation depth[9] *h* is measured in millimetres.

[8] *When the load F_1 is removed, the material exhibits an elastic recovery of limited extent. This is why the indenter actually climbs from level "m" to level "f".*

[9] *All Rockwell hardness points, both B and C, correspond to an indentation depth of 2 μm.*

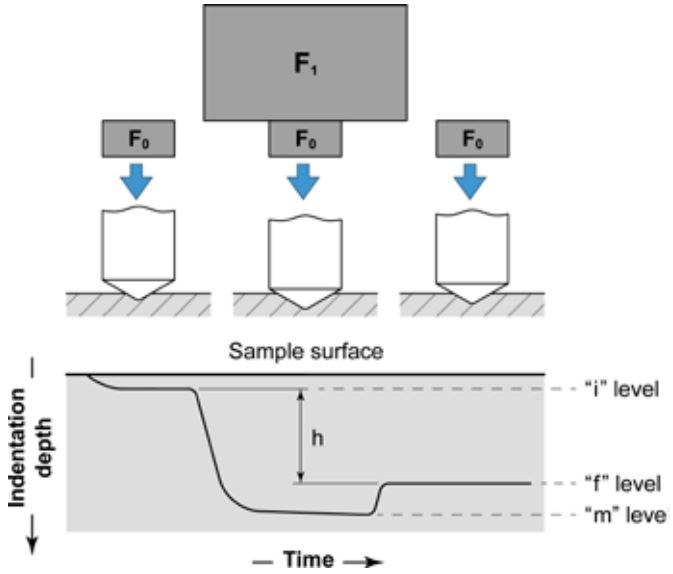

Figure 3.6 – Schematic of the operations to be performed to carry out the Rockwell hardness test.

To measure Rockwell hardness correctly, it is necessary to apply some rules so that to obtain reliable and mutually comparable results.

With steels, the minimum sample thickness should be at least 15 times the indentation depth *h* for scale *B* and 10 times for scale *C*. The minimum distance between the centres of two adjacent indentations should be at least 3 times their diameter *d*. The minimum distance between the centre of an indentation and the sample edge should be at least 2.5 times *d*.

The sample support and testing surfaces should meet the same requirements as for the Brinell and Vickers tests (flat and parallel surfaces, accurate finishing, no oxides, dirt and/or lubricant substances) with tolerances similar to those required by the Brinell test.

The Rockwell test requires extreme care when preparing the specimen support plane and in its positioning. Actually, the test is very sensitive to sample failures, which would introduce an unacceptable error in the measure of the indentation depth *h*. During the execution of the Rockwell test (*B* or *C*), the testing machine calculates *h* and gives the operator the value of material hardness. It is not necessary to measure the indentation directly. Thanks to is practicality and immediate reading feature, Rockwell hardness is used in both labs and workshops.

The Rockwell test B has validity in the measure range 35 to 100 HRB and is suitable for fully annealed or normalized steels and for austenitic, ferritic or duplex stainless steels. The Rockwell test *C* has validity in the measure range 20 to 70 HRC and is used for quenched and tempered steels with UTS > 600 MPa.

Rockwell hardness is expressed by the index HR, followed by the letter associated with indenter used, as in the following example: 60 HRC means that the test has given a value for Rockwell hardness type C equal to 60 points.

As already observed, the principle upon which Rockwell hardness is calculated is different from Brinell and Vickers hardnesses, specifically the indentation depth h in the first case, the indentation area *S* in the second case. Therefore, it is not possible to establish correlations between the two scales on the basis of the physical analogy of the phenomenon. However, you can always define empirical equivalences between the scales (*HRB/HRC and HB/HV*) by measuring hardness of the same steel type with the different testing methods. An example in this sense is provided in Table 3.1, taken from the ASTM E140 standard[10]. For more details on the Rockwell test, we advise carefully reading the UNI EN ISO 6508 and ASTM E18 standards[11].

Rockwell B [HRB]	Vickers [HV]	Brinell [HBS/HBW]	Rockwell C [HRC]	Vickers [HV]	Brinell [HBS]	Brinell [HBW]
100	240	240	60	697	…	…
98	228	228	58	653	…	615
96	216	216	56	613	…	577
94	205	205	54	577	…	543
92	195	195	52	544	…	512
90	185	185	50	513	…	481
88	176	176	48	484	451	455
86	169	169	46	458	432	432
84	162	162	44	434	409	409
82	156	156	42	412	390	390
80	150	150	40	392	371	371
78	144	144	38	372	353	353
76	139	139	36	354	336	336
74	135	135	34	336	319	319
72	130	130	32	318	301	301
70	125	125	30	302	286	286
68	121	121	28	286	271	271
66	117	117	26	272	258	258
64	114	114	24	260	247	247
62	110	110	22	248	237	237
60	107	107	20	238	226	226

Table 3.1 – Equivalence table of *HRB, HRC, HB*, and *HV* hardness tests for non-austenitic steels [from ASTM E140].

[10] *Specifically, ASTM E140: Standard Hardness Conversion Tables for Metals Relationship Among Brinell Hardness, Vickers Hardness, Rockwell Hardness, Superficial Hardness, Knoop Hardness, Scleroscope Hardness, and Leeb Hardness. A similar standard is the EN ISO 18265 standard: Metallic materials - Conversion of hardness values.*

[11] *Specifically, EN ISO 6508-1: Metallic materials - Rockwell hardness test - Part 1: Test method and ASTM E18: Standard Test Methods for Rockwell Hardness of Metallic Materials.*

4. STEEL IMPACT TEST

4.1 Fracture Toughness and Brittleness

Whatever their end-use, all steels must have a tough behaviour. If so, component fracture can only occur after heavy plastic deformation of the metallic mass, which is a premonitory sign of possible failure.

If steel had a brittle behaviour, failure would occur fully unannouncedly. Brittle fracture occurs suddenly, with no plastic deformation. Fracture propagation is extremely fast, at a speed equal to sound speed in that medium (about 5000 m/s in steel). In many cases, in addition to the main brittle fracture plane, you observe also fragmentation phenomena with projections of metal parts in the environment.

As regards ductile or brittle fractures, there is another important, yet often overlooked, aspect to be mentioned: using an intrinsically tough material does not guarantee component ductile failure. Don't forget that brittle fractures occur also in steels with a tough behaviour. In these cases, however, the failure does not depend on the material used, but on other factors, such as:

- Low working temperature,
- High load application speed,
- Cracks and/or metallurgical or geometrical discontinuities with a notch radius close to zero being present in the component, or
- Combined action of the causes listed above.

The impact test was developed exactly to quantify resistance to brittle fracture in all steels grades and is now the commonest and cheapest mechanical test available to this aim. Actually, this experimental test, together with the tensile test, is the most used to establish whether a steel matches the applicable reference standards[1].

4.2 The Impact Test

The impact test or Charpy test[2] consists in applying an impulsive load to a notched specimen under three point bending stress. To this aim, a special testing machine is used fitted with pendulum hammer. Depending on steel grade and reference standards, the test can be run either at room temperature or at lower temperatures.

---

[1] In English sector terminology this property is called impact strength. The English term resilience has a different meaning compared to Italian. It refers to the ability of a mechanically stressed material to absorb energy and give it back after unloading. Also, the English term resilience is commonly used in psychology, much more than in mechanics, where it defines the aptitude of a person to rapidly recover from difficulties.

[2] The test is named after Georges Augustin Albert Charpy (1865-1945), a French engineer, who first presented this test to the scientific community during the 7th international meeting of the Association for Testing of Materials, held in Budapest from the 8th to the 13th of September 1901.

The EN ISO 148-1 and ASTM E23 standards specify two standardised types of impact test specimens[3]: the Charpy V-notch specimen and the Charpy U-notch specimen. Both are 55 mm long prism-shaped samples with a 10x10 mm square section, characterised by the presence of a notch in the middle of the longer axis. In the former case, the notch is V-shaped with a 45° angle, 2 mm depth and radius of 0.25 mm; in the latter, the notch is U-shaped with depth equal to 5 mm and radius of 1 mm[4] (Figure 4.1).

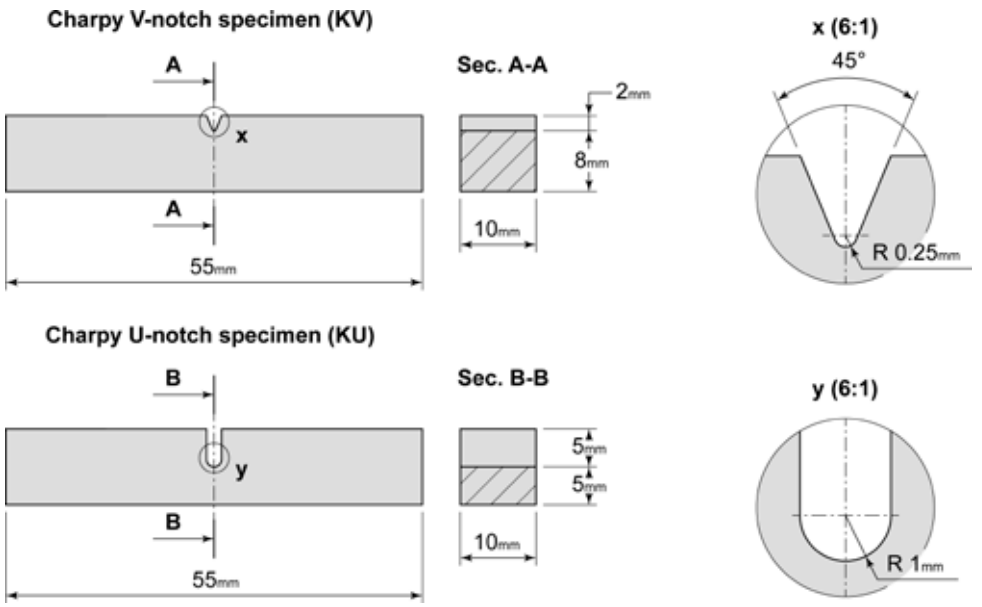

Figure 4.1 – Geometrical characteristics of *V*-notch and *U*-notch impact test specimens

First, the sample to be tested is left at room temperature or pre-cooled down to the temperature required; then it is placed horizontally along its longer axis with its ends resting onto the two test machine supports that are called anvils.

The impulsive load is provided by the pendulum hammer dropping from a pre-fixed height. The hammer hits the specimen at its middle plane, on the surface opposite to the notched one. Due to high impact speed, estimated around 4-5 m/s, the specimen suddenly bends and breaks. The deformation speed induced in the material is also very high, around 10^3 s^{-1} (Figure 4.2).

[3] Specifically, the EN ISO 148-1 standard "Metallic materials - Charpy pendulum impact test - Part 1: Test method" that governs the impact test according to European criteria and the ASTM E23 standard "Standard Test Methods for Notched Bar Impact Testing of Metallic Materials" that makes reference to American criteria.

[4] The presence of the notch (either V- or U-shaped) promotes specimen fracture by inducing an equitriaxial stress close to the notch apex. This limits dislocation motion locally, consequently limiting also steel plastic strain.

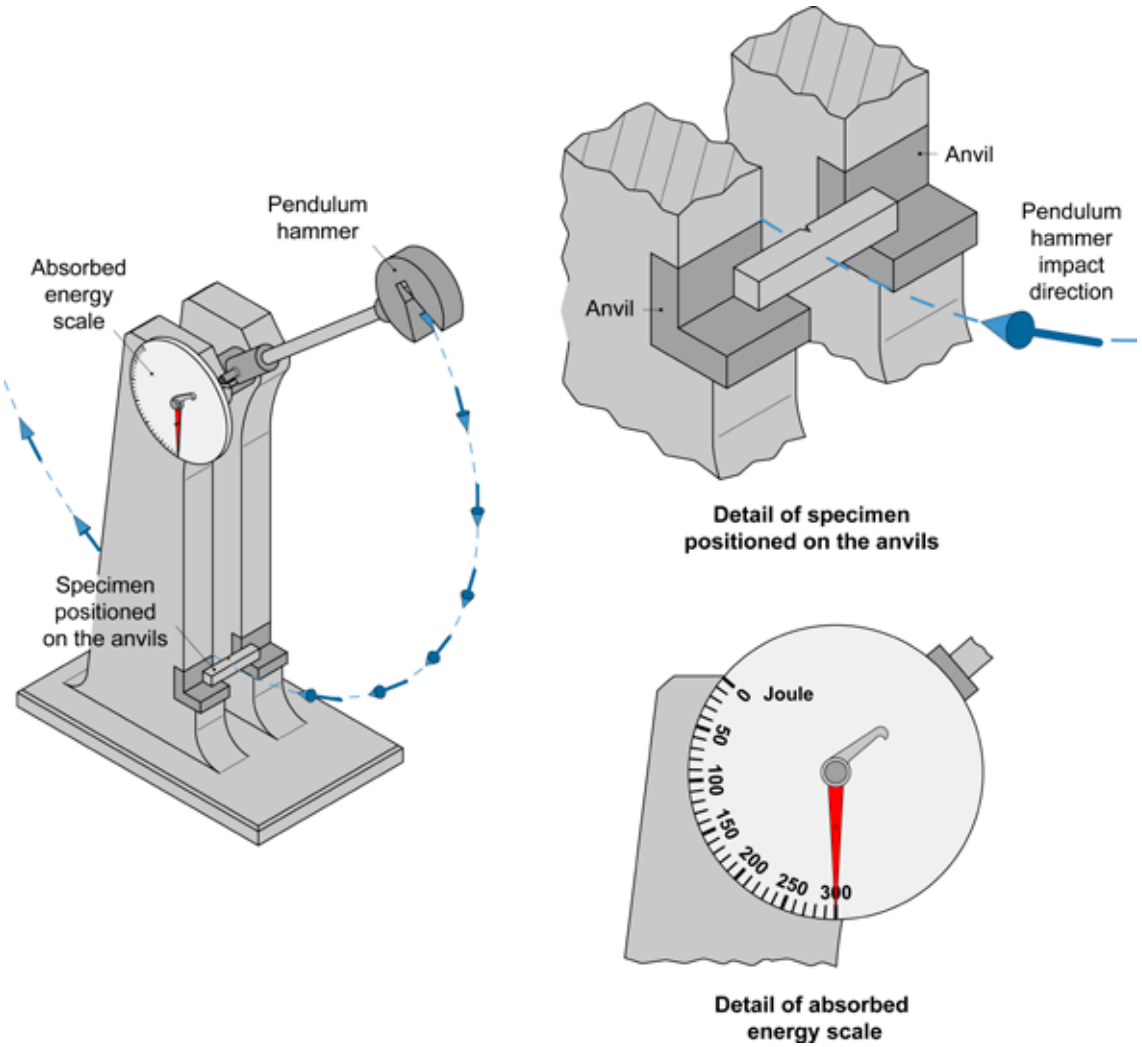

Figure 4.2 – Schematic of the impact testing machine with specimen positioning; the falling direction of the pendulum hammer is also indicated.

The Charpy test result is the amount of energy used to break the specimen at a certain test temperature. The value is automatically provided by the machine that calculates the difference between the initial potential energy ($m \cdot g \cdot h_1$) of the pendulum hammer and its final one ($m \cdot g \cdot h_2$). Notice that these magnitudes are proportional to initial height (h_1) and maximum final height (h_2) that the pendulum hammer attains after hitting the sample.

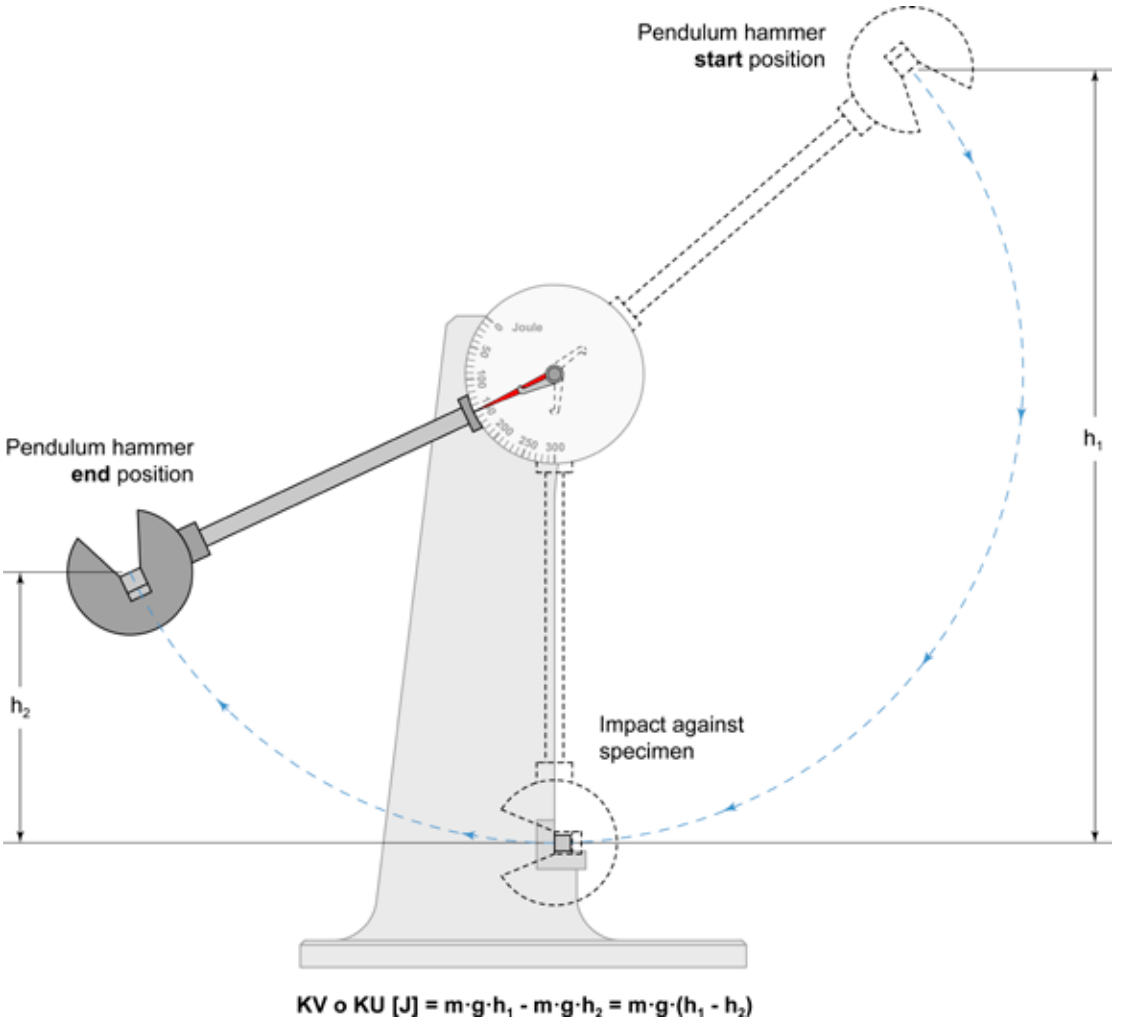

Figure 4.3 – Schematic calculation of the energy absorbed to break the Charpy specimen.

At test end, the result is expressed using the letters KV or KU (depending on whether Charpy *V*-notch or *U*-notch specimens are used) followed by the energy value in Joule (Figure 4.3).

Due to scatter of results, impact strength is always measured as the average of three tests conducted at the same temperature. For example, if three Charpy *V*-notch specimens tested at -20°C, give the results of 65 J, 57 J and 60 J, impact strength is indicated as $KV_{mean, -20°C} = 60.7$ J.

The extent of result scatter is often connected not only with correct test procedure, but also with the specimen fabrication method. Notch geometry, depth and, above all, finish accuracy are critical parameters that must be complied with (Figure 4.4). The result can be significantly affected also by wrong positioning of the specimen on the anvils.

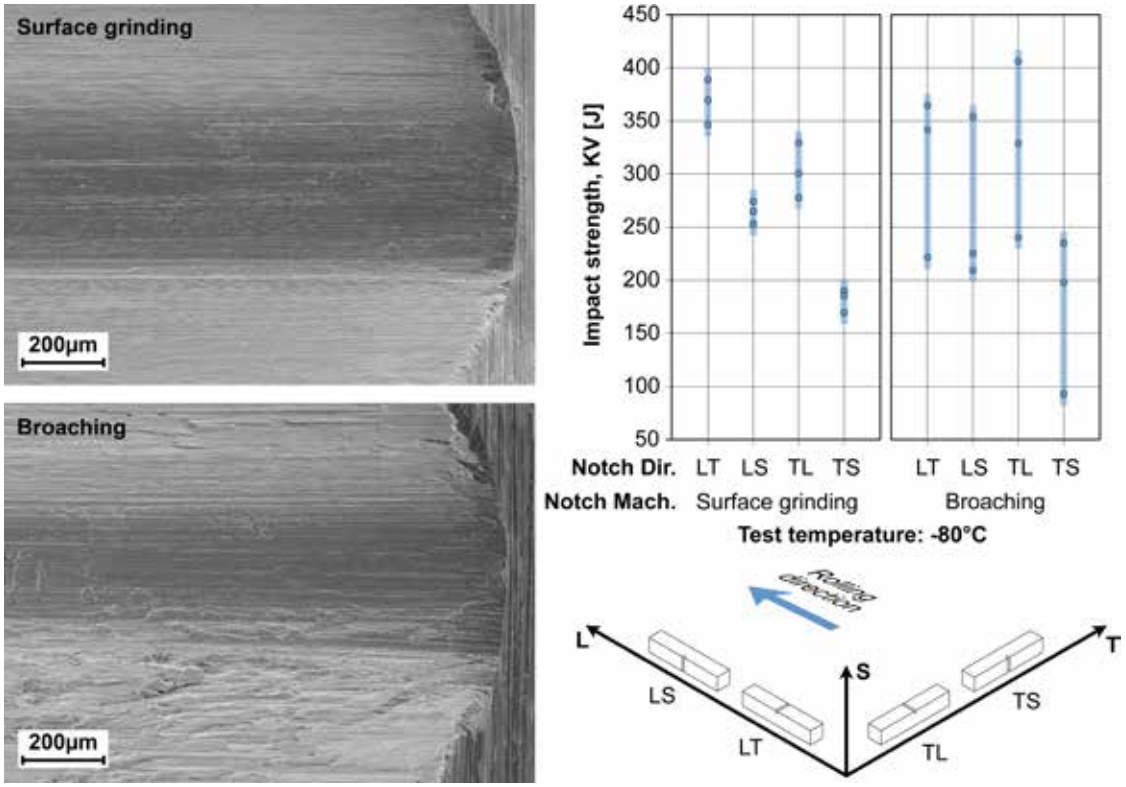

Figure 4.4 – Effect of specimen fabrication methods on scatter of impact test results: (on the left) microscopic appearance of the notch bottom obtained by grinding or broaching; (on the right) trend of impact test results with reference to notch finish accuracy and sampling direction (dual-phase stainless steel grade EN X2CrNiMoN22-5-3, test temperature: -80°C) [Laboratories of the Department of Mechanical Engineering of Politecnico di Milano – Milan, Italy].

Another important parameter that you can evaluate is the macroscopic appearance of the fracture surface. Specimen visual inspection allows establishing if the fracture occurred in a fully tough, fully brittle or mixed tough/brittle manner. The different fracture types are clearly visible with the naked eye. Brittle fractures are brightly reflective while ductile fractures are dull and with a fibrous appearance. In the case of mixed fractures, the brittle failure is always located in the middle of the fracture surface under the notch while the ductile area is positioned at the outer perimeter (Figure 4.5).

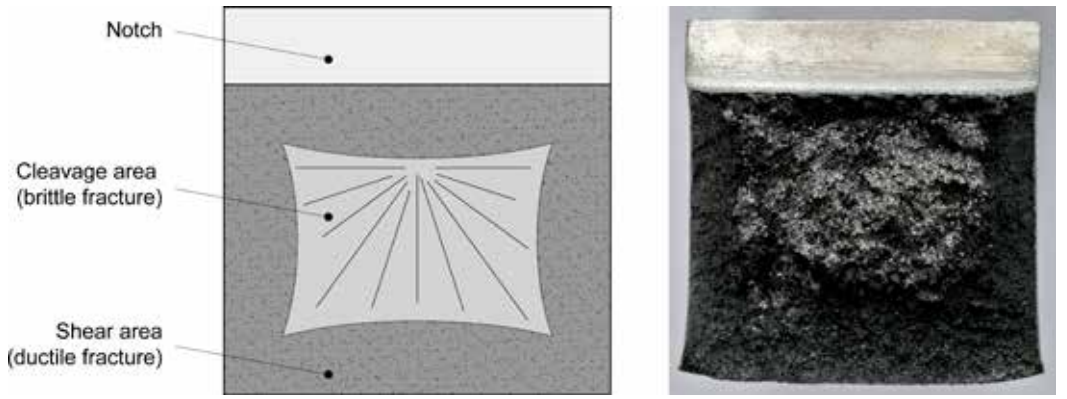

Figure 4.5 – Schematic and real-life example of an impact test specimen fracture surface with indication of the ductile and brittle failure areas (free-cutting steel grade EN 11SMnPb37, test temperature: 20°C, KV 21 J; brittle fracture percentage: 35%). [Hammer S.r.l. Laboratories - Rho, Italy].

The impact test is essential to categorise steels on the basis of their fracture toughness/brittleness following working temperature changes. This is an essential condition to correctly select the materials with which to build mechanical structures or components. The Charpy test allows evaluating steel sensitivity to brittle fracture simply and rapidly and is more suitable to test this property than tensile testing.
However, *the value of the energy absorbed during the impact test cannot be used for engineering purposes*[5] because if you change the notch shape and/or the specimen size, the results you obtain cannot be compared to one another, even if the tests were conducted using the same steel and at the same temperature. It should also be pointed out that the load condition imposed upon the sample (impact at very high speed) is exceedingly severe and does not represent in the least the design solutions usually implemented for mechanical components.

4.3 The Impact Energy Transition Curve

If you are looking for a practical indication of steel resistance to brittle fracture, the value to be considered is not the maximum level of energy absorbed to break the specimen (i.e., impact strength), but rather the ability of the material to go on absorbing energy at increasingly colder temperatures.

[5] *The main reason for which the discipline of fracture mechanics developed early in the Seventies of the last century was the need to measure a parameter (known as "fracture toughness, K_{IC}") to be used at design level that would keep into account steel brittle fracture resistance following temperature changes. For more details on this subject, see, for example, Broek D., The Practical Use of Fracture Mechanics, Kluwer, Dordrecht, NL, 1988.*

This information can be obtained only after completing a series of impact tests at temperatures below room temperature. By so doing, you can determine the temperature at which a tough failure mechanism (high energy absorption, low brittle fracture percentage) turns into a fragile failure mechanism (low energy absorption, high brittle fracture percentage). This temperature is called *ductile-brittle transition temperature*, *DBTT*, and is the level below which the risk of brittle fracture actually exists (Figure 4.6).

Test temperature [°C]	20	-30	-60	-90	-120	-150	-196
Impact strength, KV [J]	84 - 77 - 80	74 - 79 - 82	64 - 69 - 59	33 - 40 - 36	15 - 13 - 17	8 - 4 - 6	3 - 4 - 1
Brittle fracture [%]	0 - 0 - 0	2 - 0 - 0	20 - 25 - 28	64 - 56 - 61	86 - 80 - 87	95 - 100 - 97	100 - 100 - 100

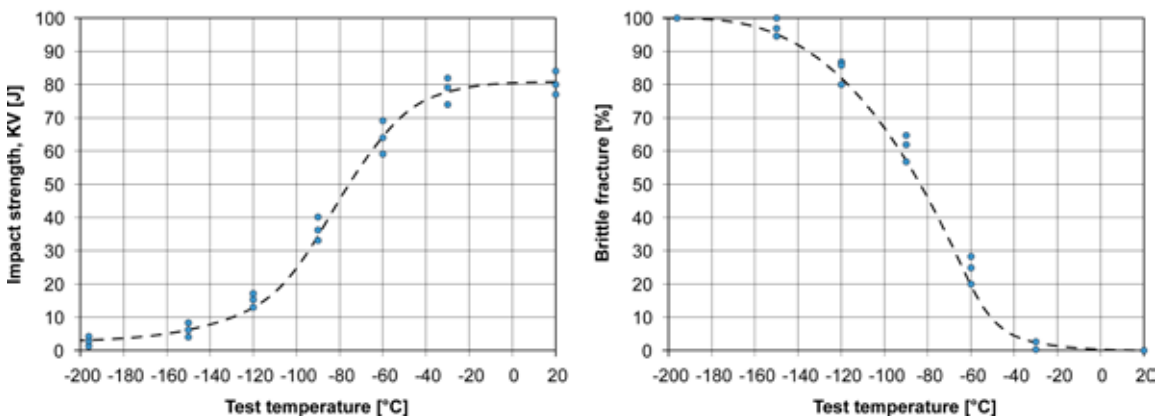

Figure 4.6 – Impact energy transition curves for steel grade EN 36CrNiMo4, oil quenched and tempered at 620°C. The graphs were obtained by interpolating impact strength values measured at increasingly colder temperatures compared to room temperature (on the left: energy absorbed - test temperature; on the right: brittle fracture percentage - test temperature) [Hammer S.r.l. Laboratories - Rho, Italy].

The ductile-brittle transition temperature cannot be defined exactly given that both energy decrease and brittle fracture area increase occur gradually. Therefore, a convention is adopted to identify this parameter[6] (Figure 4.7):

- The ductile-brittle transition temperature, *DBTT*, is determined at the average energy value between the maximum and minimum levels on the impact energy transition curve;
- The *Fracture Appearance Transition Temperature*, *FATT*, is defined at the surface that generates 50% of brittle fracture.

[6] *In this text we describe the commonest criteria to define steel ductile-brittle transition temperature. For more details, see Dieter G. E., Mechanical Metallurgy, McGraw Hill - London, UK, 1988.*

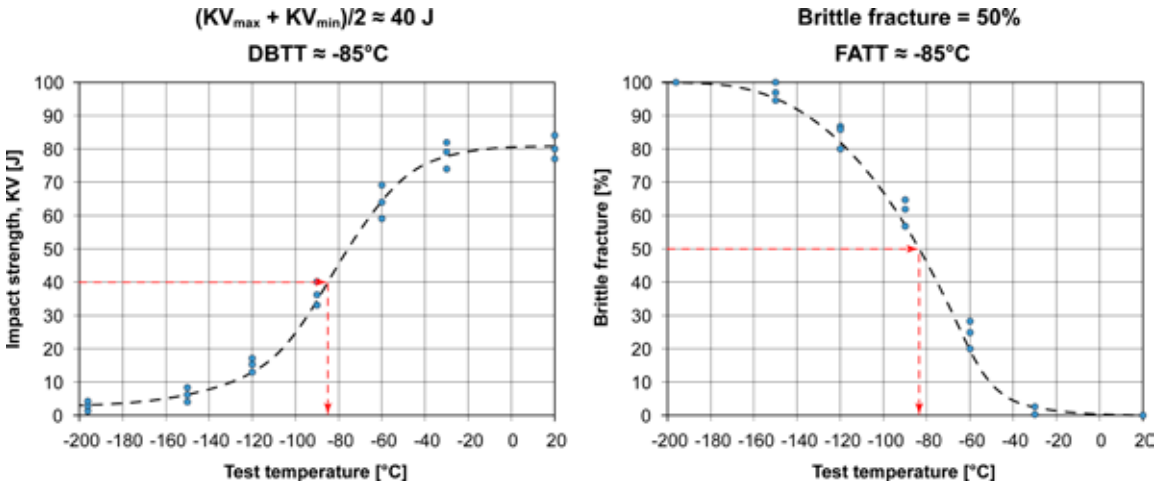

Figure 4.7 – Ductile-brittle transition temperature identification starting from the experimental curves shown in Figure 4.6.

Another recurrent criterion, mainly found in product standards, identifies the ductile-brittle transition temperature on the basis of an arbitrary value of absorbed energy that, for structural carbon steels, is 27 J. Notice that the value of 27 J used to determine the ductile-brittle transition temperature is taken from experimental tests; therefore, it should not be considered the sole reference value for all steel grades[7].

4.4 Steel Metallurgy and Impact Strength

Impact strength, or resistance to brittle fracture, is strictly connected with steel metallurgical characteristics. For example, steels with very high resistance are intrinsically more brittle than mild carbon steels or austenitic stainless steels. Besides, in some cases, material brittleness can originate from embrittlement phenomena, such as hydrogen embrittlement, temper brittleness, ageing in mild carbon steels, etc.

To increase steel impact strength, you can act on some metallurgical characteristics, among which steel chemical composition, average grain size, micro-structure and inclusion content.

[7] *"27 J" is obtained by converting the English numerical indication "20 ft · lb$_f$" (foot x pound force) into units of measure of the international system. Established in the United States early in the 20th century as the acceptability threshold of impact strength for carbon steels, this indication is still in use in the ASTM (American Society for Testing and Materials) and ASME (American Society of Mechanical Engineers) standards.*

The most significant improvement is obtained by controlling steel carbon content because this chemical element negatively affects steel resistance to brittle fracture. Decreasing the amount of carbon makes steel tougher and the *DBTT* moves by approximately 14°C towards colder temperatures with every 0.1% reduction of the carbon content. Remember, however, that reducing the carbon content brings about a gradual decrease of both steel hardness and Ultimate Tensile Strength (Figure 4.8).

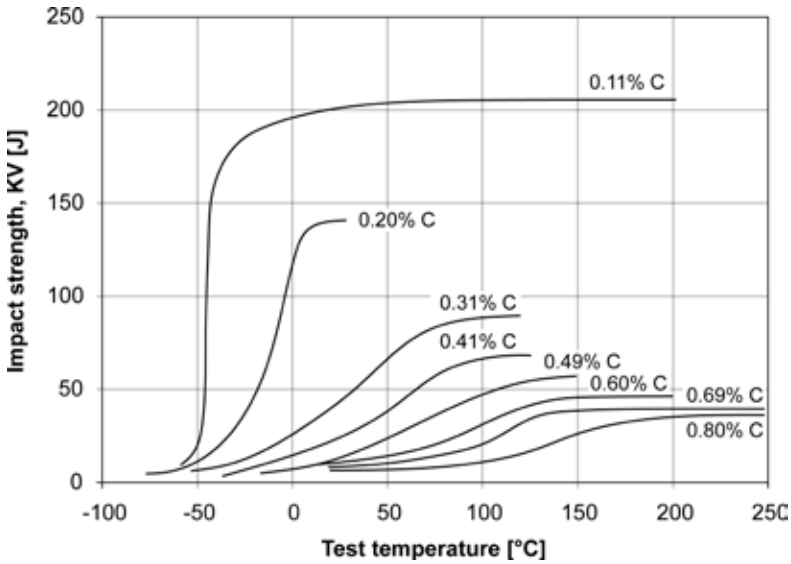

Figure 4.8 – Carbon effect on the *DBTT* for non-alloyed steels after normalizing (ferritic-pearlitic micro-structure) [from Burns and Pickering 1964].

Manganese and nickel have beneficial effects. Adding manganese causes the *DBTT* to move towards colder temperatures in the amount of 5°C with each 0.1% increase in the manganese content. To guarantee a suitable level of brittle fracture resistance, the manganese/carbon ratio should normally range between 3 and 7. In this manner, you can lower the *DBTT* down to about -50°C, as it is typical for most structural carbon steels (Figure 4.9).

Nickel exerts an even more beneficial effect than manganese. With nickel contents between 3% and 8%[8] the *DBTT* moves towards temperatures close to -150°C. Larger amounts would completely eliminate the ductile-brittle transition temperature with the associated curve becoming almost horizontal. In these conditions the material is tough at all application temperatures (Figure 4.10)[9].

[8] Steels with nickel contents above 5% are identified as high alloy steels and cannot be considered as structural special or carbon steels.

[9] All metals and alloys that, at room temperature, have a face-centred cubic (F.C.C.) crystal lattice like copper, aluminium, silver, gold, nickel, lead and platinum do not exhibit the ductile-brittle transition. Steels can also acquire this property thanks to the addition of a nickel content exceeding 8%. This happens because nickel is an austenising element that stabilises austenite at room temperature.

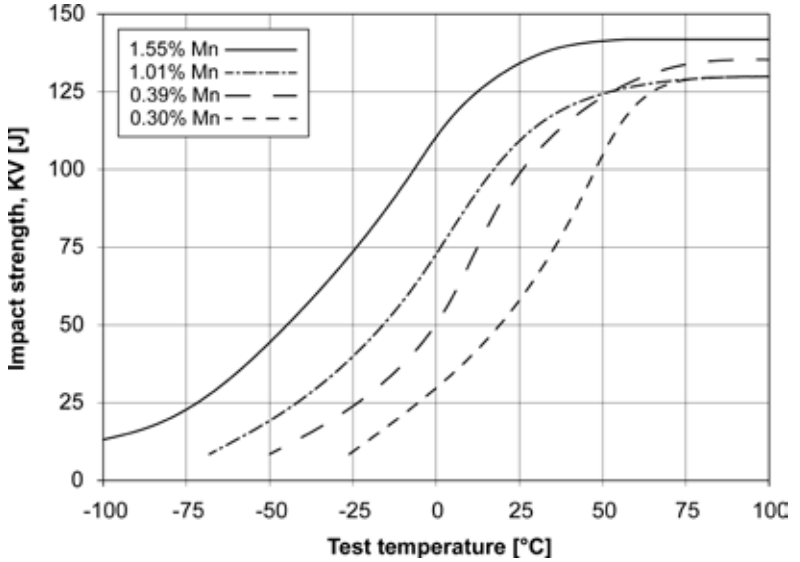

Figure 4.9 – Manganese effect on the impact energy transition curve for medium-low carbon steel (C = 0.30%; normalizing treatment; ferritic-pearlitic structure) [from Rineholt and Harris 1951].

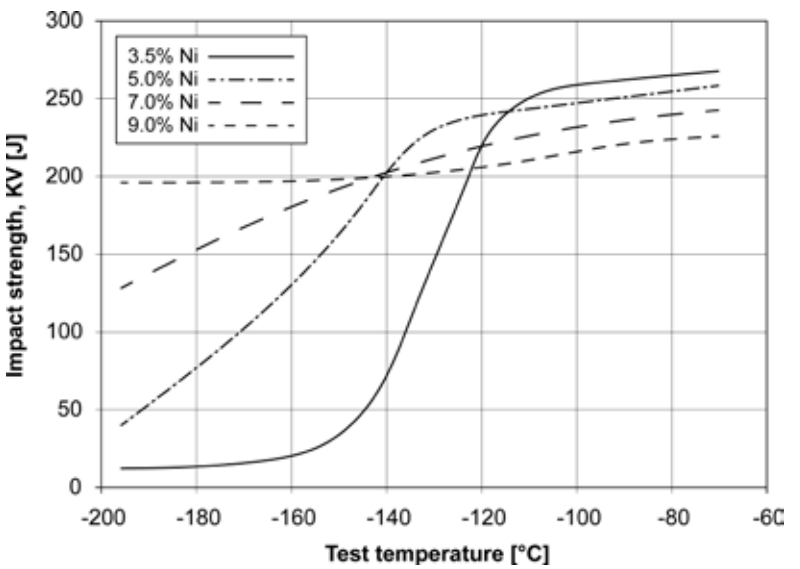

Figure 4.10 – Nickel effect on impact strength transition curves for low carbon steels (C = 0.055 to 0.062%; Mn = 0.71 to 0.73%; Si = 0.18 to 0.23%) [from Wang et al. 2017].

The other alloying elements that steel may contain, such as chromium, molybdenum, silicon, aluminium, vanadium and niobium, produce variable effects.
Chromium and molybdenum improve absorbed energy values even if they involve a minor displacement of the *DBTT* towards higher temperatures. To this regard, it should be opportunely reminded that chromium is normally added to increase steel hardenability while molybdenum is meant to inhibit temper embrittlement.
Silicon, in contents typical of steel manufacture (0.15 to 0.30%), has beneficial effects because it decreases steel inclusion content. Silicon higher percentages (0.75 to 2.00%), as in spring steel, cause impact strength to worsen a bit.
Aluminium, used for steel deoxidation, contributes improving impact strength because it promotes the reduction of average grain size (Figure 4.11).

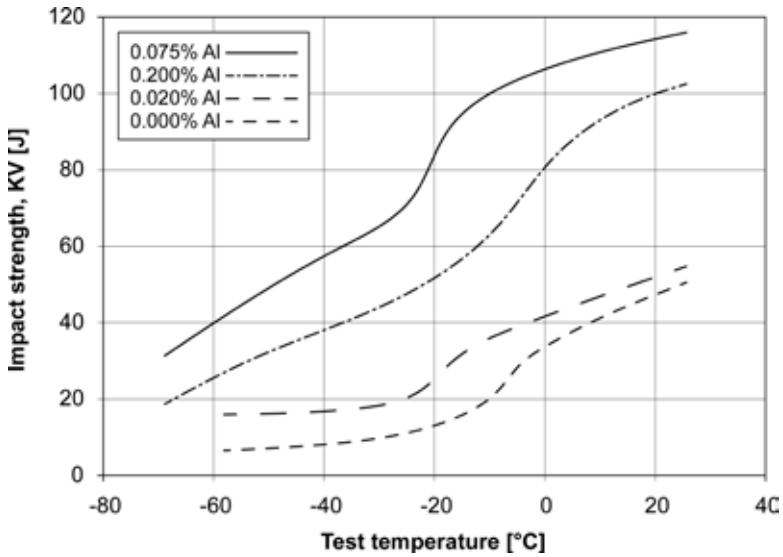

Figure 4.11 – Aluminium effect on impact energy transition curves for medium carbon steels after normalizing [from ASM-H.1 1991].

Vanadium and niobium are used as micro-alloying elements in low carbon steels; usually, their maximum contents range around 0.10 to 0.15%. These elements not only induce steel reinforcement by precipitation (*HSLA* steels), but also tend to inhibit grain growth during the thermo-mechanical processes for the manufacture of semi-finished products. Thus, vanadium and niobium improve impact strength both in terms of energy absorbed and as regards *DBTT* displacement towards colder temperatures (Figure 4.12).

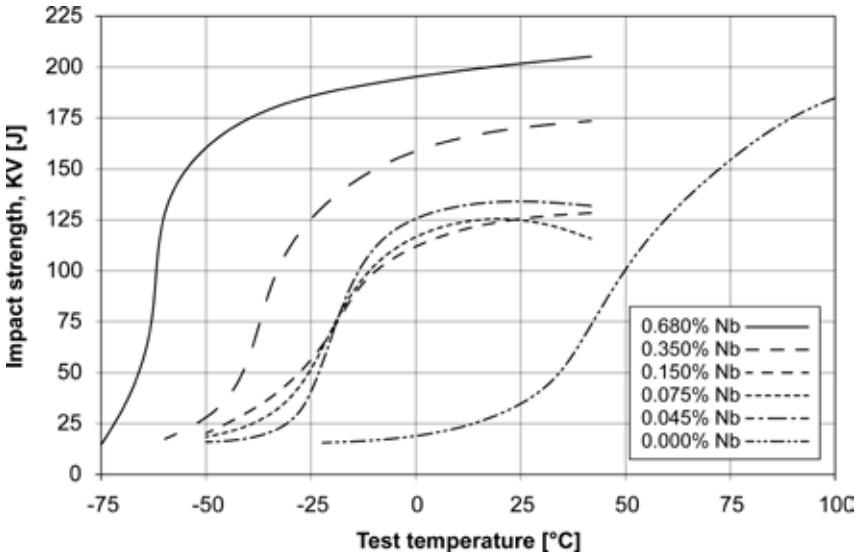

Figure 4.12 – Niobium effect on impact energy transition curves for low carbon steels after normalizing at 955°C [from Phillips et al. 1964].

Phosphor, sulphur and oxygen are detrimental elements because they drastically deteriorate steel resistance to brittle fracture. The *DBTT* moves towards higher temperatures by approximately 5° to 7°C with every 0.01% of phosphor or sulphur and by approximately 6°C with every 0.001% of oxygen (Figure 4.13).

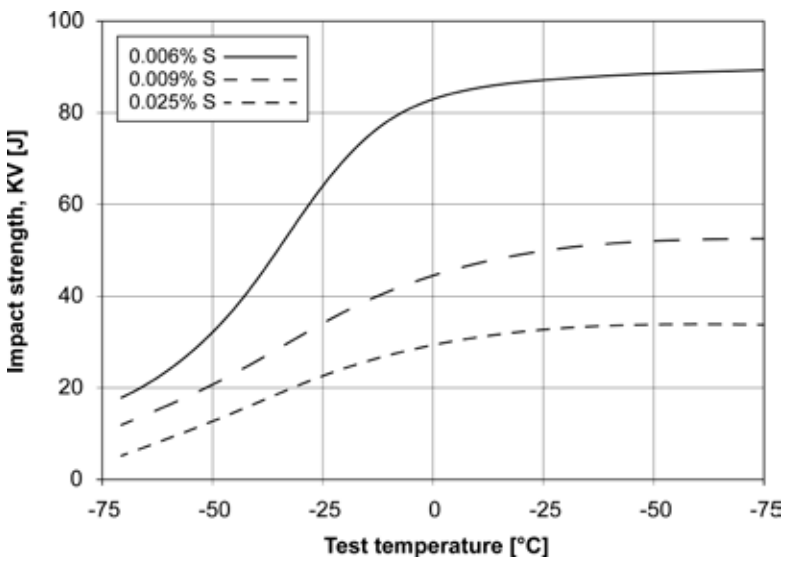

Figure 4.13 – Sulphur effect on impact energy transition curves for HSLA steels [from ASM-H.1, 1991].

With the same chemical composition, also average grain size plays an important role in this context because as grain size decreases, the *DBTT* moves towards increasingly colder values. In structural carbon steels, for example, the *DBTT* decreases by approximately 16°C with each one-point increase in the ASTM10 grain size measure scale. For this reason, structural carbon steels with the same chemical composition exhibit higher impact strength after being normalized (fine ferrite and pearlite structure) than after being annealed (coarse ferrite and pearlite structure).

Another important element is steel micro-structure (Figure 4.14). Tempered martensite is the toughest micro-structure in special structural steels, followed by bainite and pearlite.

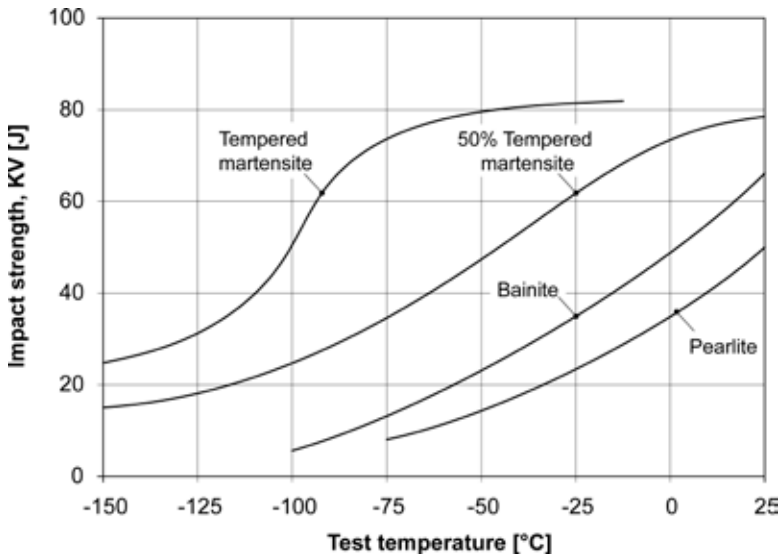

Figure 4.14 – Micro-structure effect on brittle fracture resistance for Q&T steel with a medium carbon content (C = 0.40%; Cr = 0.70%, Mo = 0.32%). Note: The pearlitic structure is obtained by isothermal cooling at 650°C; the bainitic structure is obtained by cooling in a molten lead bath at 450°C; the 50% martensite structure is obtained by quenching in a molten lead bath at a 450°C for 35 seconds; the 100% martensite structure is obtained by quenching in oil; in all cases, tempering was performed to attain the same final hardness [from ASM-H.1 1991].

---

[10] According the ASTM E112 standard "Standard Test Methods for Determining Average Grain Size" (to which reference should be made for more details), the average austenitic grain size is determined using optical microscopy after sample preparation and etching in accordance with specific procedures (such as the McQuaid-Ehn method). Average grain size, indicated as G, is given by the number of grains n that can be observed in a sample area measuring one square inch (25.4 x 25.4 mm^2) under 100x magnification. The formula used to calculate G is: $n = 2^{G-1}$. Notice that G increases at the average grain size decreases. A crystal micro-structure with G = 12 corresponds to an average grain size of 5.6 µm, to 11 µm if G = 10, to 22 µm if G = 8, to 45 µm if G = 6, to 90 µm if G = 4 and to 180 µm if G = 2. Good quality steel has a typical average grain size ranging from G = 6 to G = 10. In any case, the finer the steel grain, the better the steel mechanical properties, i.e., Ultimate Tensile Strength, hardness and impact strength.

The inclusion content is very also important. Very clean steels with few small-sized inclusions, behave definitely better than dirty steels. This trend is made manifest by comparing the ductile-brittle behaviour of structural carbon steel grade EN S275 with that of free-cutting steel grade EN 11SMn37 (Figure 4.15).

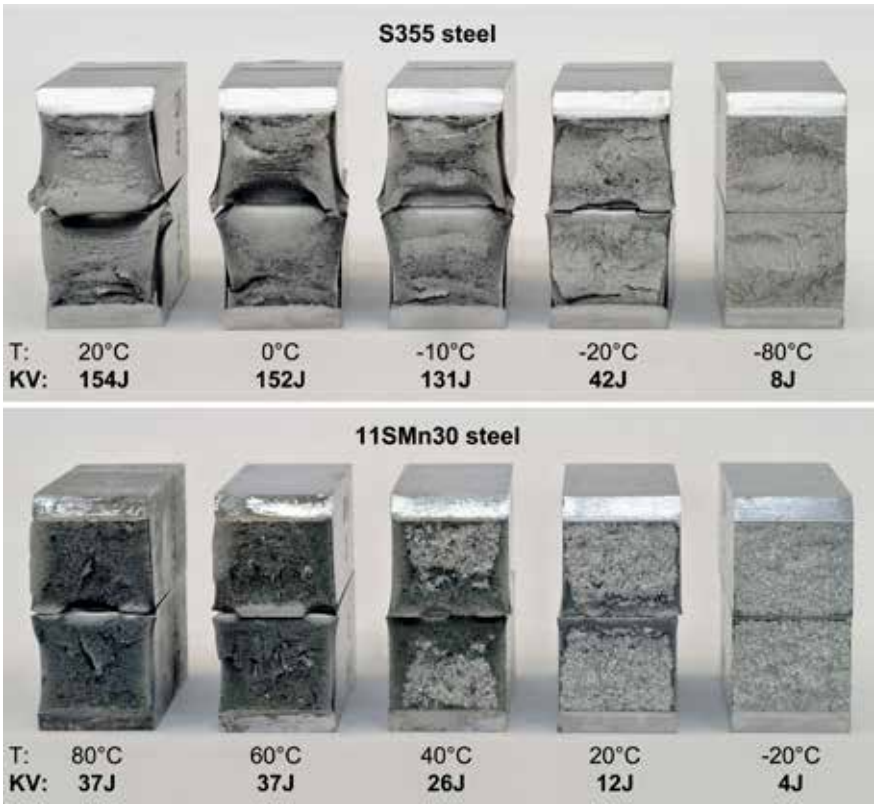

Figure 4.15 – Fracture surface appearance of impact test specimens (top) for structural carbon steel grade EN S275 and (bottom) for free-cutting steel grade EN 11SMn37 [Hammer S.r.l. Laboratories - Rho, Italy].

A last essential aspect to understand steel fracture toughness/brittleness issues is connected with banding (or banded structure), which refers to the pattern of arrangement of material fibres after casting and hot deformation. Every time a semi-finished product is made, no matter if it is obtained by rolling, forging or drawing, the material takes on a fibrous structure - totally similar to wood structure - that is orientated along the direction of the prevailing plastic strain.
Due to banding, a strange phenomenon takes place, namely the mechanical properties measured along the direction of the fibres are systematically higher than the ones taken crosswise.

To this regard, Figure 4.16 shows the transition curves for specimens sectioned in parallel or crosswise the axis of a steel plate after hot deformation. Specimens *A* and *B* are taken in the direction parallel to the rolling direction. In the *A* case, the notch lies along the thickness while in the *B* case it is orientated square to the axis. The *C* specimens were taken crosswise of the rolling direction and the notch is positioned along the thickness.

As you can easily infer, in specimens orientated parallel to the rolling direction (*A* and *B*), all fibres cooperate to steel resistance and their pattern opposes fracture propagation, while in the samples arranged crosswise the axis (*C*), the failure runs across the adjacent fibres that hinder fracture development only marginally. Therefore, energy absorbed by specimens *C* is definitely lower than in the cases of specimens *A* and *B*.

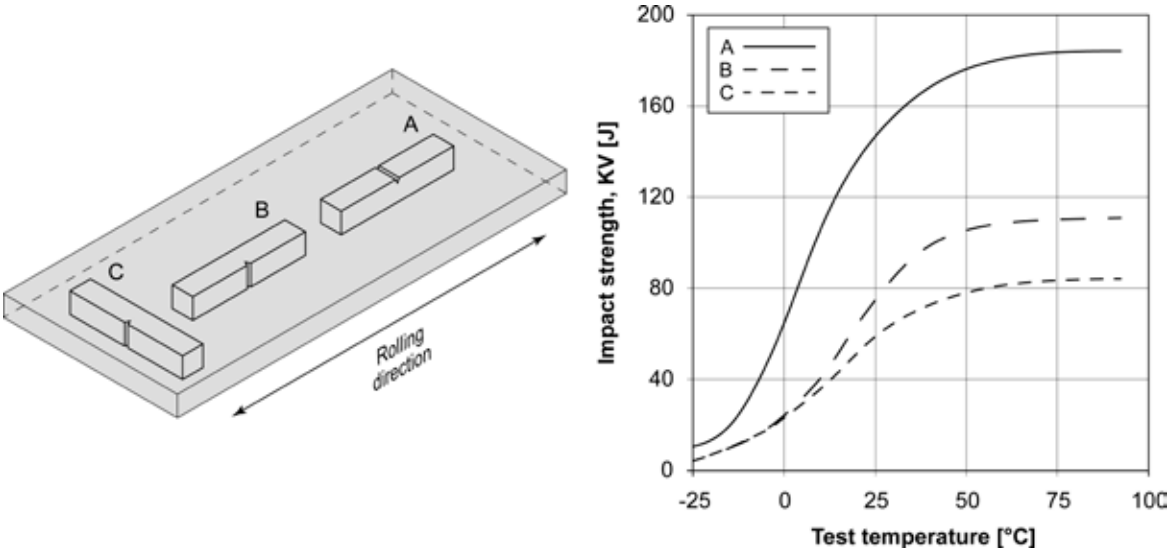

Figure 4.16 – Impact energy transition curves for steel with C = 0.012%. Effect of the fibre pattern in a plate after hot deformation depending on specimen sectioning direction [from Puzak et al. 1952].

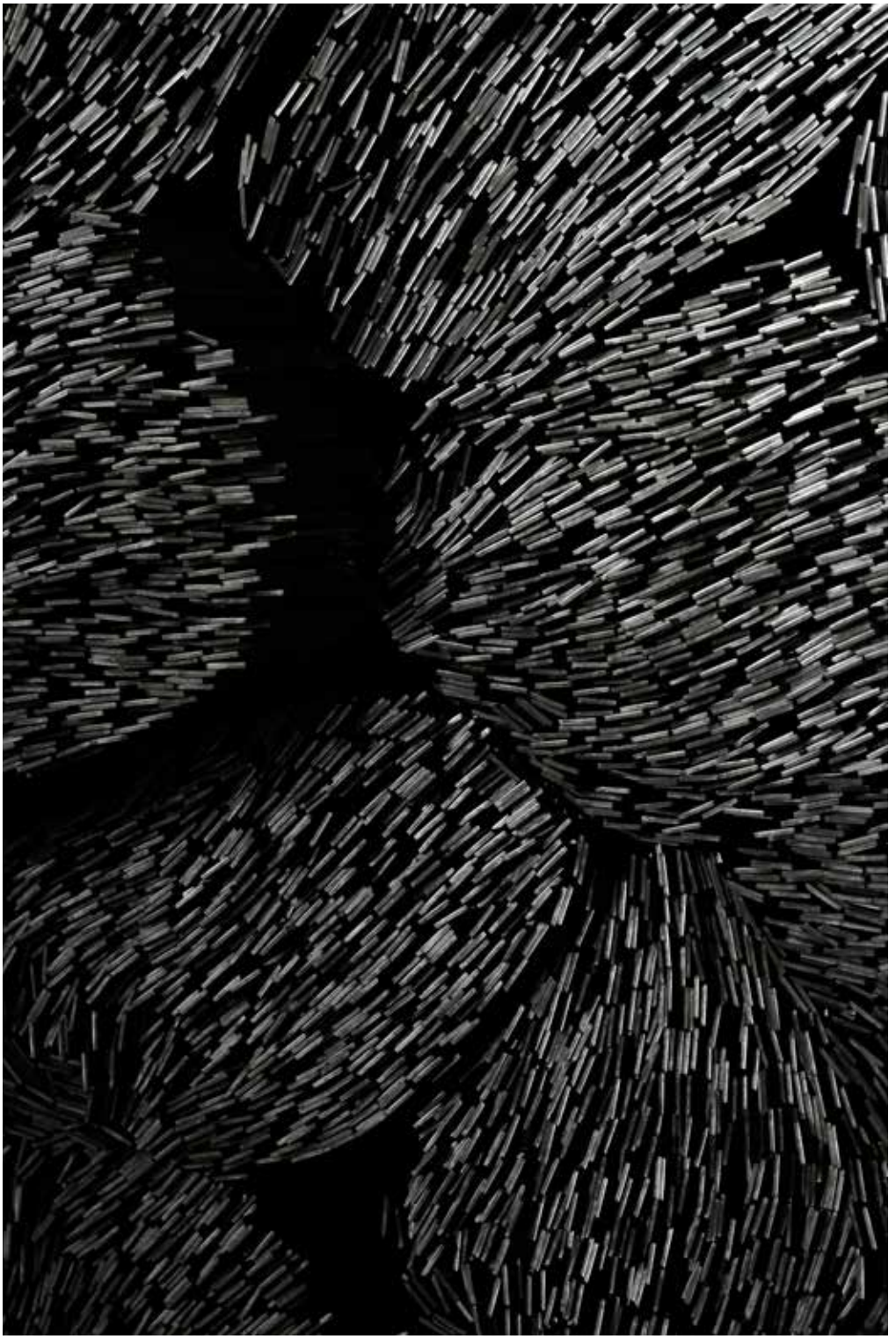

5. DUCTILE AND BRITTLE FAILURE IN STEELS

5.1 Failure Mechanisms

The macroscopically ductile or brittle behaviours in steels find their origin in the deformation and fracture mechanisms that occur in crystal lattices at microscopic level.

In the case of plastic deformation, the predominant physical event is slippage of crystallographic planes, i.e., the relative displacement of two or more areas in a crystal lattice under shear stress τ. This deformation mechanism is promoted by dislocations, without which the shear stress τ would exceed the value measured experimentally by several orders of magnitude[1]. However, what we have described so far does not enable understanding why a mechanical component bends when it is stressed by external tensile, compressive, bending and torsional forces, individually or in combination.

To better understand this issue, you can usefully make reference to Schmid model that allows determining the value of shear stress τ on the assumption that the metallic mass is subjected to uniaxial tensile stress and consists of one cylindrical grain.

According to this model, average stresses τ and σ, which respectively act tangentially and perpendicularly to a generic plane A in the crystal grain, are connected to the applied force F and to the area A_0 normal to the axis by the following relations:

$$\tau = \frac{F}{A_0} \cdot \cos\theta \cdot \cos\varphi \qquad \text{[eq. 5.1]}$$

$$\sigma = \frac{F}{A_0} \cdot \cos\theta \cdot \text{sen}\,\varphi \qquad \text{[eq. 5.2]}$$

being θ and φ the angles formed by the axis and, respectively, the lines parallel and normal to plane A. If you change the inclination of this plane, you can determine the angle φ raising τ and σ to their highest level. Maximum shear stress τ_{max} is reached with $\varphi = 45°$ while maximum tensile stress σ_{max} is reached with $\varphi = 90°$ (Figure 5.1).

Plastic deformation does not occur at all levels of τ. For slippage of the metallic mass to take place, it is necessary that maximum shear stress τ_{max} exceeds a critical value, known as τ_{cr} (*critical resolved shear stress*), that suffices to set the dislocations in motion.

As simple at it may sound, Schmid model allows understanding why in steels exhibiting a macroscopically ductile behaviour, the fracture plane is always inclined by 45° relative to the principal stress direction. Necking in tensile specimens is a typical example of this phenomenon.

[1] *For a detailed study on dislocations and, more generally, on crystal lattice flaws, see Chapter 2 of the book "Steel Metallurgy - Volume I" by M. Boniardi and A. Casaroli, Lucefin - Esine, Italy, 2017.*

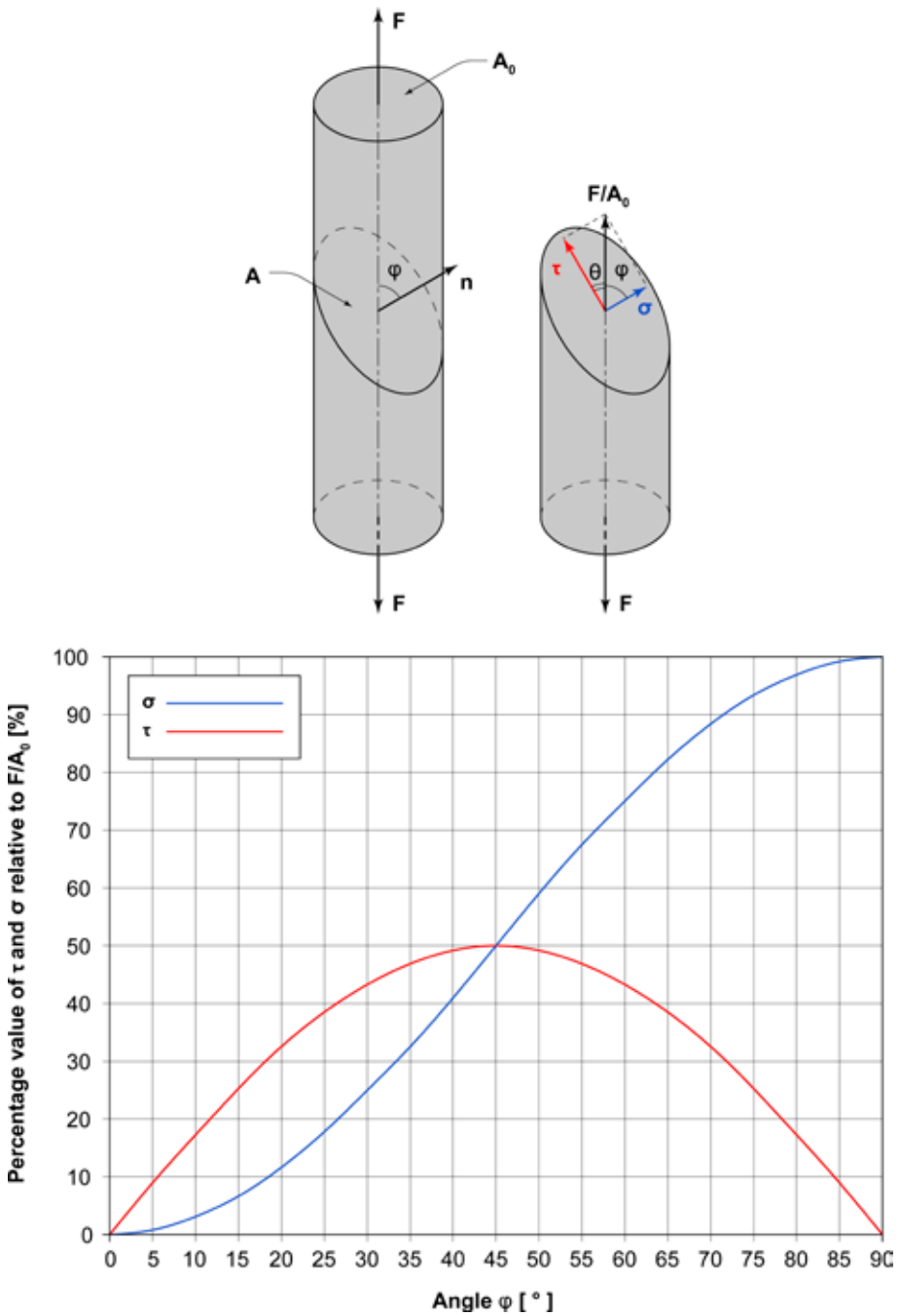

Figure 5.1 – Trend of average stresses that are tangential (τ) and normal (σ) to plane *A* inclined relative to the axis in accordance with angles θ and φ. The values of τ and σ are expressed as percentages of the average stress generated by the force *F* on the surface A_0, this being normal to the grain axis [from Brooks et al. 1993]

To extend Schmid model to crystal lattices, two other concepts should be introduced. In a generic crystal lattice, plastic deformation preferably involves crystallographic planes that have:

- Higher atomic density, and
- Greater interplanar distance,

which means along planes where a minimum amount of energy E is required to trigger the slipping movement (Figure 5.2).

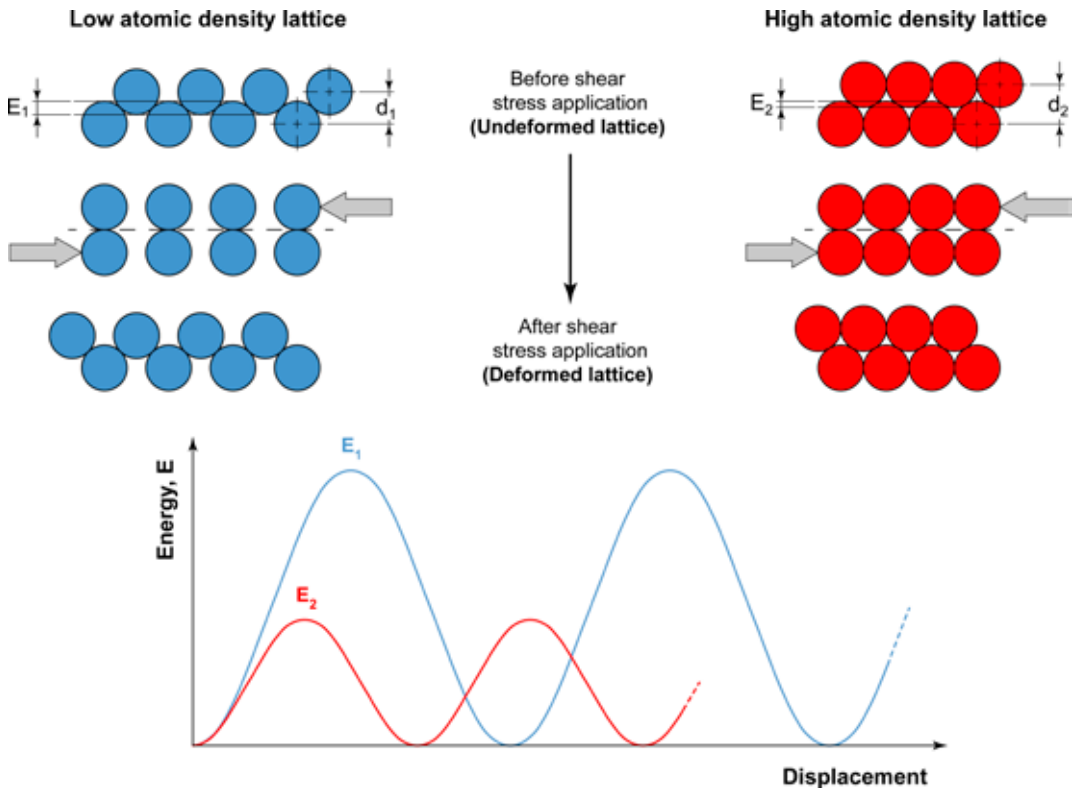

Figure 5.2 – Slippage mode of two adjacent lattice planes: (on the left) the case of a plane with low atomic density; (on the right) the case of a plane with high atomic density. Notice that E is the energy required to trigger slippage (proportional to τ_{cr}) and d is the interplanar distance.

Now, let's examine the case of steels and identify the planes with higher atomic density and greater interplanar distance.

In a body-centred cubic (B.C.C.) lattice, as in α-iron, there are 6 slip planes and 2 preferential slip directions per plane; in this case, we talk about a 6 x 2 = 12 plastic deformation systems. Similarly, in a face-centred cubic (F.C.C.) lattice as in γ-iron, you find 4 slip planes along 3 slip directions for a total of 4 x 3 = 12 plastic deformation systems (Figures 5.3 and 5.4).

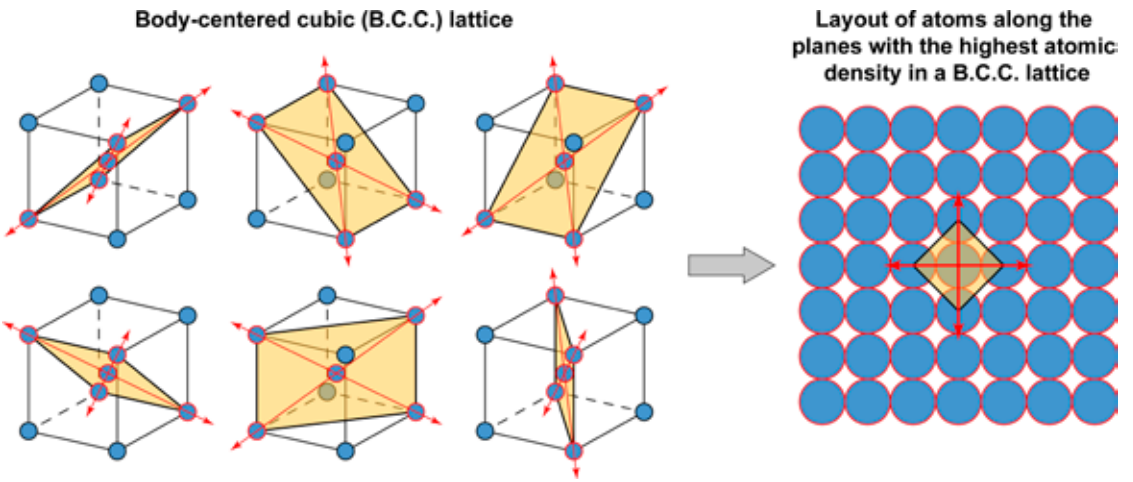

Figure 5.3 – Slip planes and slip directions in elementary cells of a B.C.C. lattice.

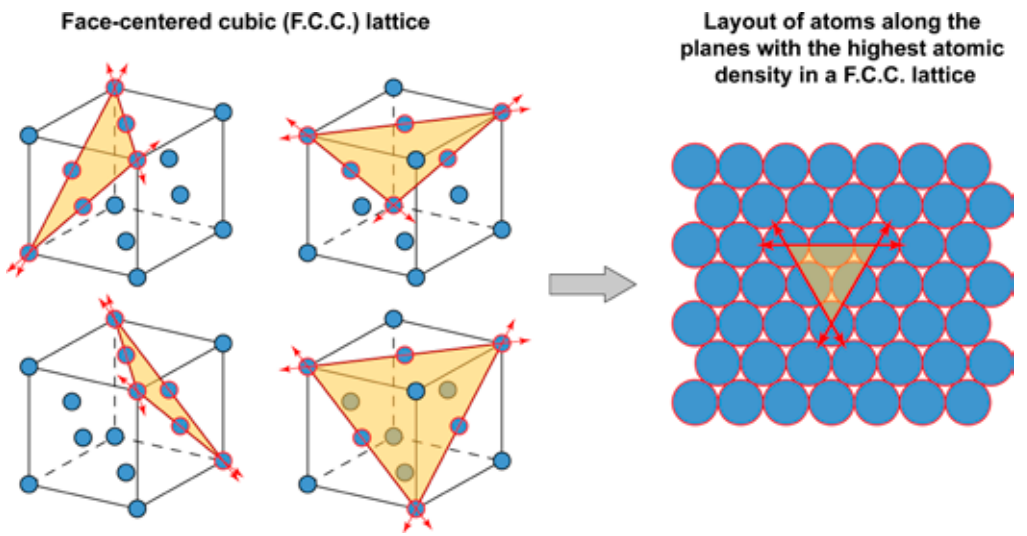

Figure 5.4 – Slip planes and slip directions in elementary cells of an F.C.C. lattice.

Now, let's extend this issue to polycrystalline materials that are characterised by myriads of grains with different crystallographic orientation.

If you apply an uniaxial tensile stress, plastic deformation does not occur in all grains at the same time and to the same extent , but first activates in crystals where at least one preferential slip direction (among those with higher atomic density and greater interplanar distance) lies exactly on the plane under maximum shear stress τ . When τ_{max} matches τ_{cr} , plastic strain will start.

Obviously, as the applied force F increases, also shear stress τ increases until even possibly exceeding the critical value τ_{cr} also for the grains that are orientated unfavourably to shear stress. In the end, this causes a condition of generalised strain with plastic deformation of the entire metallic mass (Figure 5.5).

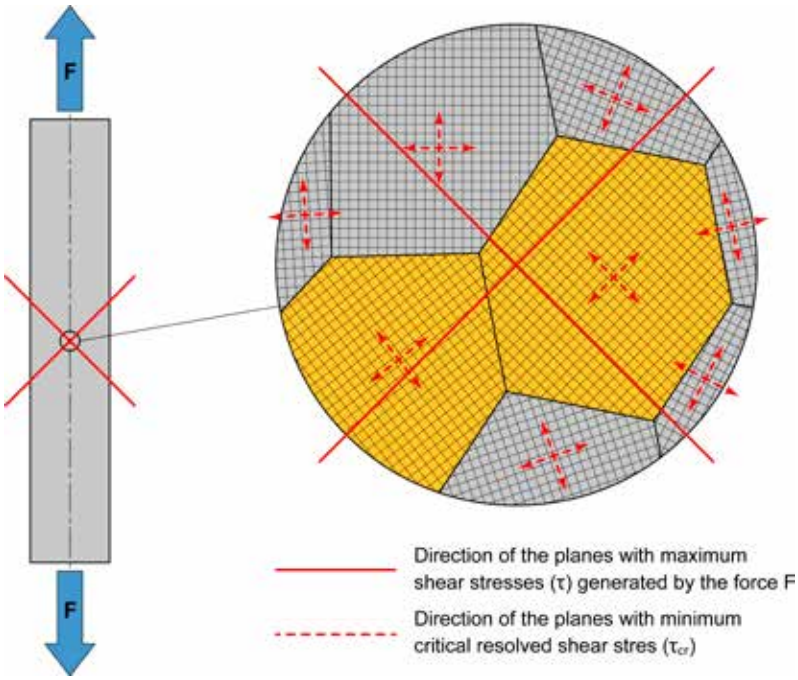

Figure 5.5 – Schematisation of crystal grain strain mechanism in a cylindrical bar under uniaxial tensile stress. Solid red lines indicate the planes where the shear stresses (τ) generated by the load F reach their highest value; the dashed red lines show the planes along which the critical resolved shear stress (τ_{cr}) is minimum. The grains most favourably orientated to slipping are highlighted in orange.

Similarly to tangential stresses τ, also normal stresses σ relative to the generic plane A in Figure 5.1 can exceed a critical value σ_{cr}. When this occurs, the material fails by *cleavage* and all atomic links in a certain crystal lattice plane, known as a cleavage plane, suddenly break. Once the critical stress for cleavage fracture, σ_{cr}, is exceeded, the grain splits without plastic deformation.
In reality, plastic deformation and cleavage are two competitive mechanisms whose activation depends on the type of stress applied to the component, amount of the stresses that develop inside the component and the values of critical resolved shear (τ_{cr}) and cleavage stresses (σ_{cr}).
If in a certain section of the part, the shear component τ of the inner actions increases faster than the normal component σ (dashed black line in Figure 5.6), dislocation motion activates and failure will be characterised

by plastic deformation. If the contrary occurs, dislocation motion is inhibited and fracture occurs by cleavage (solid black line in Figure 5.6).

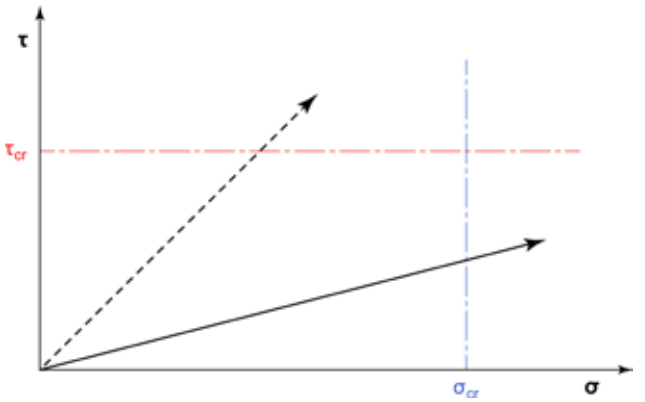

Figure 5.6 – Load conditions resulting in failure by plastic deformation (dashed black line) or failure by cleavage (solid black line) [from Brooks et al. 1993].

Failure modes are also influenced by the value of the critical stress that should be reached for failure activation (τ_{cr} or σ_{cr}), which basically depends on the four following factors.

1. *Nature of material.* As already said, plastic deformation occurs as a consequence of the relative movement of the planes with higher atomic density and greater interplanar distance, illustrated in Figures 5.3 and 5.4. To this regard, notice that the interplanar distance between the planes with the highest atomic density is greater in the case of a F.C.C. lattice than in the case of a BCC lattice[2]. Besides, the slip planes in an F.C.C. lattice have higher atomic density than those in a B.C.C. lattice.[3]. Consequently, plastic deformation in an F.C.C. lattice is always definitely more elevated than in a B.C.C. lattice.
2. *Temperature*. Normally, critical stresses from plastic deformation, τ_{cr}, and from cleavage, σ_{cr}, decrease as temperature increases because the interatomic forces in the metallic link depend on temperature. In B.C.C. lattice steels, plastic deformation is promoted by temperatures that are equal to or higher than ductile-brittle transition temperature, *DBTT*, while cleavage is promoted by colder temperatures (Figure 5.7).

---

[2] In a B.C.C. lattice, interplanar distance d is equal to $\sqrt{6}/3$ R (being R the atomic radius). In the case of α-iron, given R = 0.125 nm, d $\cong$ 0.102 nm. In an F.C.C. lattice, the interplanar distance d is equal to $2 \cdot \sqrt{6}/3$ R. In the case of γ-iron, given R = 0.126 nm, d $\cong$ 0.206 nm (for the values of the atomic radii R of α-iron and γ-iron, see the book "Steel Metallurgy - Volume I" by M. Boniardi and A. Casaroli A., Lucefin - Esine, Italy, 2017).

[3] In the elementary cell of a B.C.C. lattice, the surface area of the plane with the highest atomic density is equal to $16 \cdot \sqrt{2}/3 \cdot R^2$ (being R the atomic radius) while in the case of an F.C.C. lattice, the surface area measures $4 \cdot \sqrt{3} \cdot R^2$. In both cases, given that in the planes with the highest atomic density you have two atoms (the surface area of the atoms in the plane is equal to $2 \cdot \pi \cdot R^2$), atomic density (the surface area of the atoms in the plane relative to the plane surface area) is ~83.3% in a B.C.C. lattice and ~90.7% in an F.C.C. lattice.

This reversed behaviour does not occur in F.C.C. lattice steels where plastic deformation is promoted in all cases. The energy required to trigger slipping in F.C.C. lattices is much lower than in B.C.C. lattices.

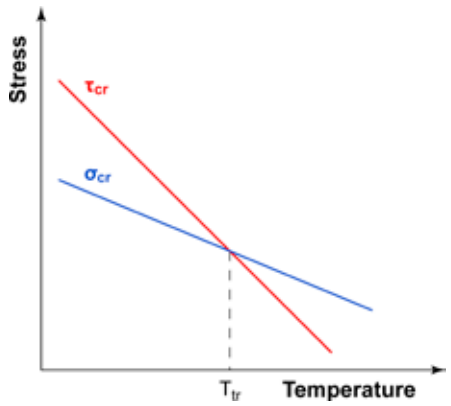

Figure 5.7 – Trend of critical resolved shear stress (τ_{cr}) and critical stress for cleavage fracture (σ_{cr}) as a function of temperature in a B.C.C. lattice steel [from Brooks et al. 1993].

3. *Load Application Speed.* At room temperature, load application speed has a significant influence only when it is approximately one thousandth of a second or less, which is typical in explosions or high-speed ballistic impacts. In these conditions, the impulse of the forces in question is not long enough to start dislocation motion. This being inhibited, the failure mode will be brittle type (Figure 5.8).

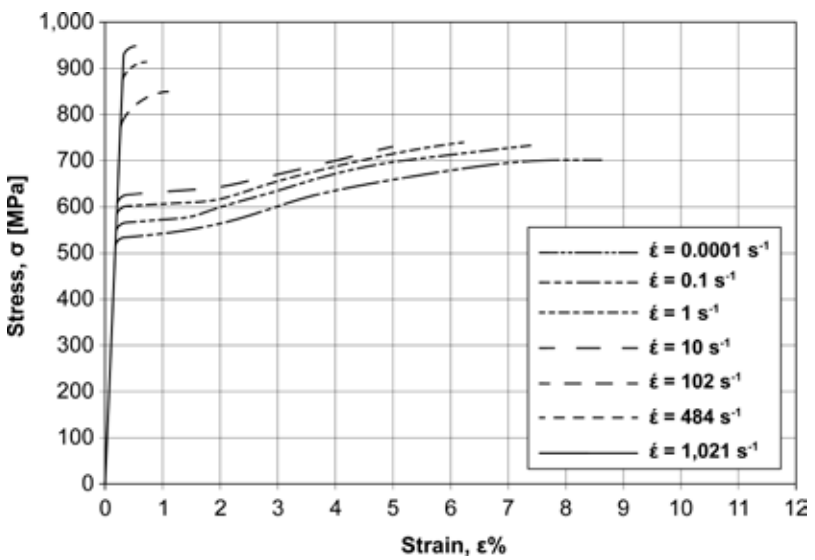

Figure 5.8 – Trend of the stress-strain curve for steel grade EN 20MnMoNi5-5 after quenching and tempering as strain speed increases at room temperature [from Davis et al. 1982].

4. *Presence of geometrical notches, metallurgical discontinuities with an extremely sharp notch radius and/or cracks.* Mechanical components often exhibit stress intensification areas (such as notches, holes, section changes, metallurgical discontinuities, cracks, porosity, inclusions, and so on) where actual stress exceeds nominal stress by far, thereby promoting local fracture of the component. A triaxial state of stress always develops in those areas, where the three principal stresses are almost equal. In this situation, shear stresses tend to zero (Figure 5.9) and the material finds it hard to slip as it becomes prone to brittle fracture. This possibility increases with higher component thickness and/or longer notch length. Both these factors make plastic deformation increasingly difficult as they promote brittle fracture by cleavage.

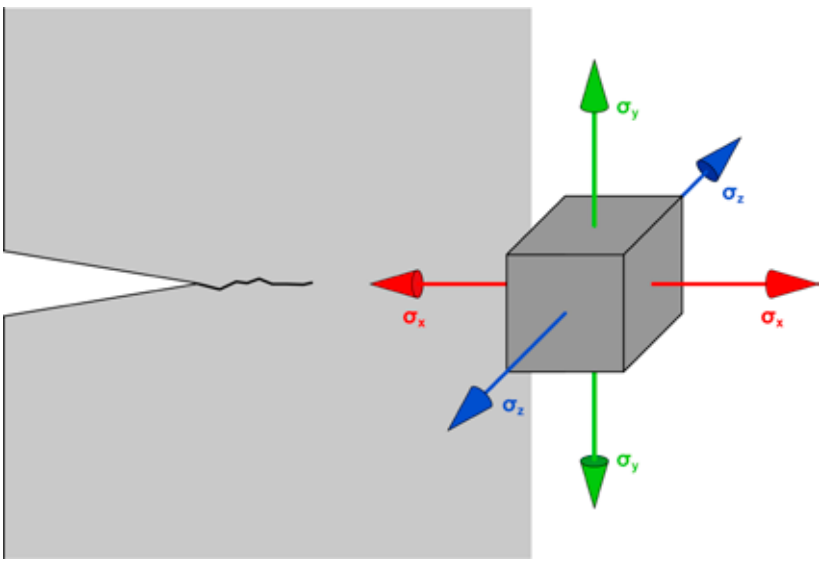

Figure 5.9 – Triaxial stress state at the crack tip in a generic very thick mechanical component.

5.2 Micro-Void Coalescence Fracture

In steels with a ductile behaviour, the fracture surface is generated by coalescence of the micro-voids (dimples) generated by plastic deformation at small discontinuities in the metallic mass, such as second-phase particles, inclusions and/or grain boundaries. Later on, as deformation increases, the micro-voids become larger and coalesce until forming a continuous surface. This failure mechanism, which is strictly connected to dislocation motion in the metallic mass, leads to the formation of a fracture surface characterised by micrometric *dimples* (Figure 5.10).

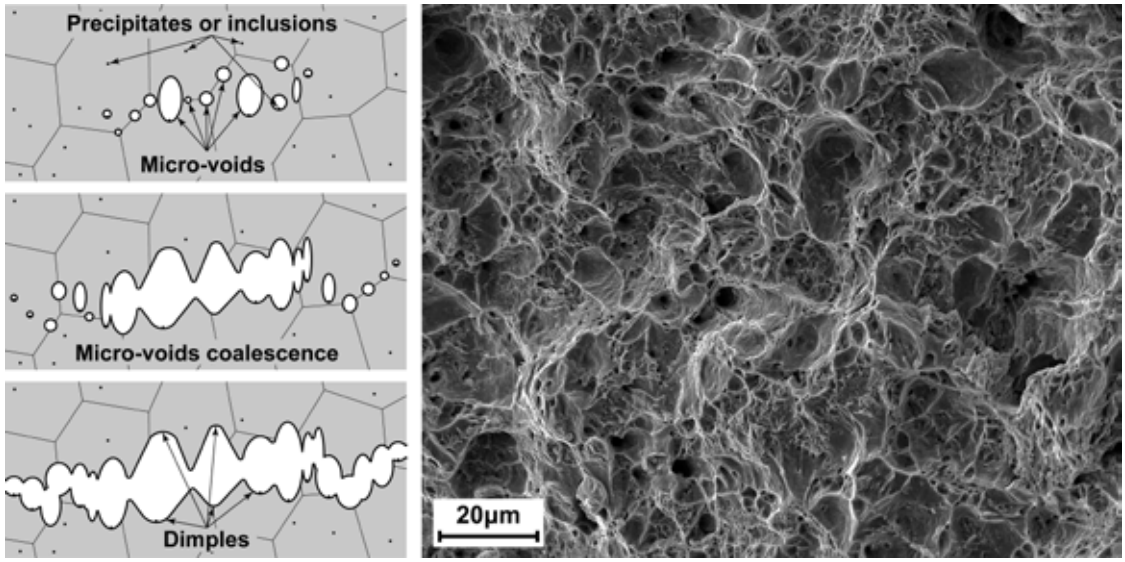

Figure 5.10 – *Dimple* formation mechanism and appearance of a fracture surface generated by micro-void coalescence as seen through an electronic scanning microscope [Laboratories of the Department of Mechanical Engineering of Politecnico di Milano – Milan, Italy].

Dimple size basically depends on the number and distribution of the micro-voids that nucleated during plastic deformation. *Dimple* shape varies in accordance with the type of load applied. Tensile stresses produce *dimples* with roundish equiaxial geometry while shear, torsion or tear stresses generate elongated *dimples* stretching along the fracture plane. In these cases, you should observe both faces of the fracture surface. If the load is shear or torsion type, *dimples* are arranged in the opposite direction whereas the direction is the same if tear stress is applied (Figure 5.11).

5.3 Transgranular Cleavage Fracture

Transgranular cleavage is the failure mode typical of steels affected by brittle fracture. It is characterised by the grains neatly splitting in two with no evidence of plastic deformation. This is the reason why these fractures are called transgranular, which means fractures that run across the crystal grains. The fracture plane is always perpendicular to the direction of maximum principal stress.

In theory, transgranular cleavage in a polycrystalline metal material should produce a fracture characterised by highly reflective flat surfaces. In reality, the crystal lattice always has flaws causing the nucleation of many micro-cracks that propagate at different levels and then join to one another by means of sudden plane changes. In practice, the resulting fracture surface appears as shown in Figure 5.12, which is the typical appearance of fractures due to transgranular cleavage.

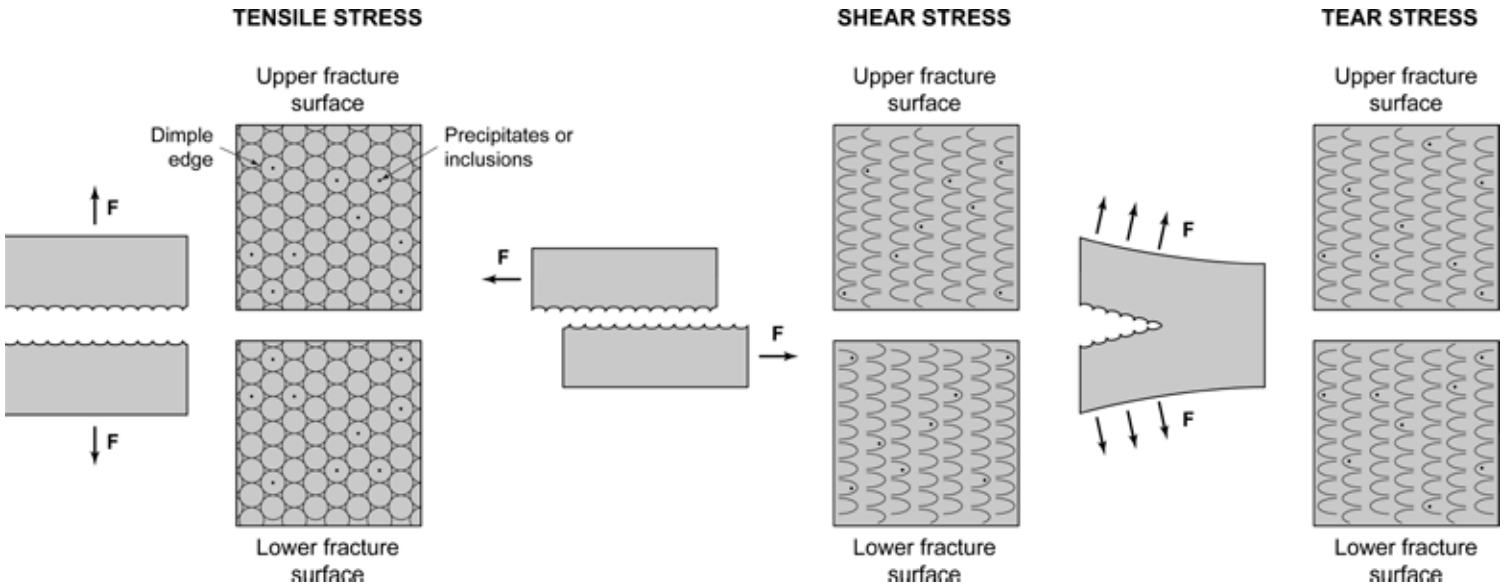

Figure 5.11 – Influence of load conditions on shape/geometry of *dimples* typical of micro-void coalescence fractures.

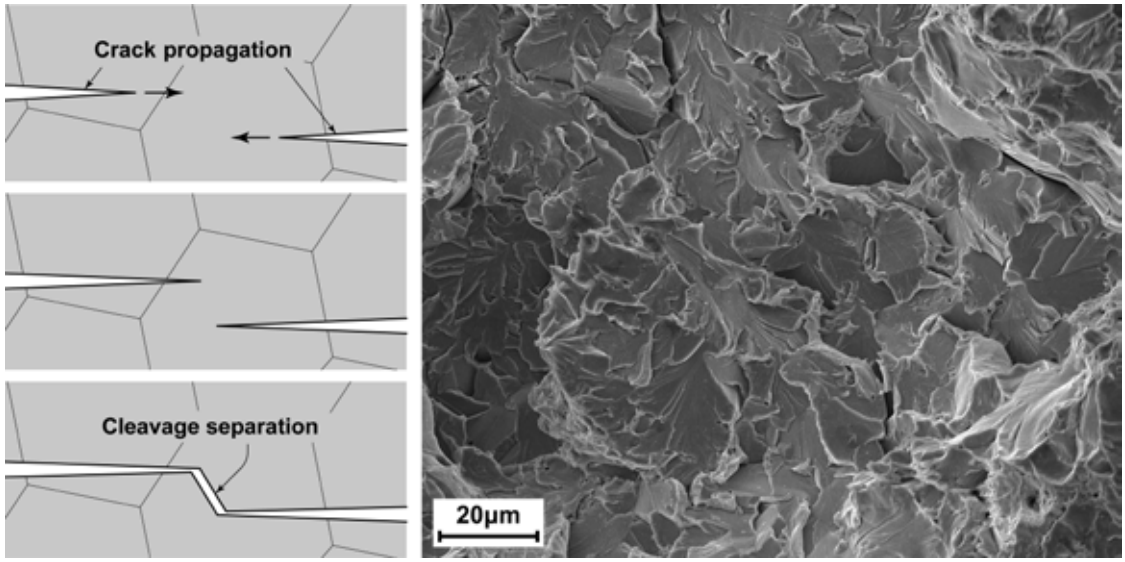

Figure 5.12 – Schematised illustration of cleavage separation of residual links between the transgranular cleavage planes and appearance of the fracture surface as seen through an electronic scanning microscope [Laboratories of the Department of Mechanical Engineering of Politecnico di Milano – Milan, Italy].

Cleavage fractures show a distinctive *river pattern* morphology. These traces form when fracture propagates through grains with a different crystallographic orientation. In this phase, the original micro-crack divides into several sections set on slightly different planes. The resulting morphology is similar to that of a river with its branches. River patterns allow identifying the local direction of propagation of a micro-crack that, like a river, runs from upstream to downstream (Figure 5.13).

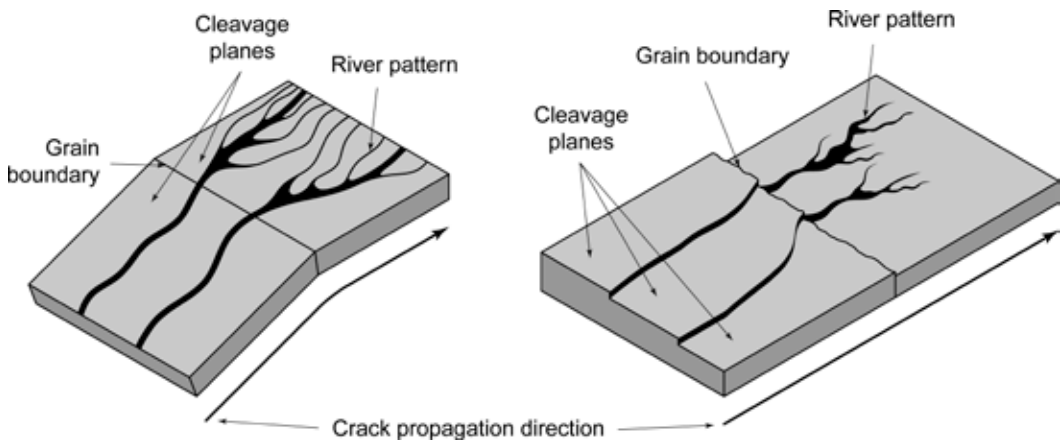

Figure 5.13 – Grain boundary effect in a fracture surface generated by transgranular cleavage [from da ASM-H.12 1987].

Transgranular brittle fractures occur when the dislocation motion in the crystal lattice is inhibited. They are typical in brittle events caused by conditions unrelated to steel. Should such external conditions be removed, steel would resume a ductile behaviour. These failures occur at temperatures colder than transition temperature or when loads are applied at extremely high strain speeds or in the presence of flaws with a notch radius close to zero (sharp-edged geometrical discontinuities, metallurgical defects, cracks, etc.).

5.4 Mixed Type Fracture

The mechanisms triggering mixed type fractures activate whenever a fracture does not totally develop either due to plastic deformation or transgranular cleavage.

A typical example is provided by metallic materials with a B.C.C. lattice, which includes most steels when they are at the ductile-brittle transition temperature. In these cases the fracture surface exhibits areas where fracture initiates following transgranular cleavage, but terminates by micro-void coalescence (*dimples*) because residual links are subject to plastic deformation before final fracture. Sometimes, this phenomenon is referred to as a quasi-cleavage fracture (Figure 5.14).

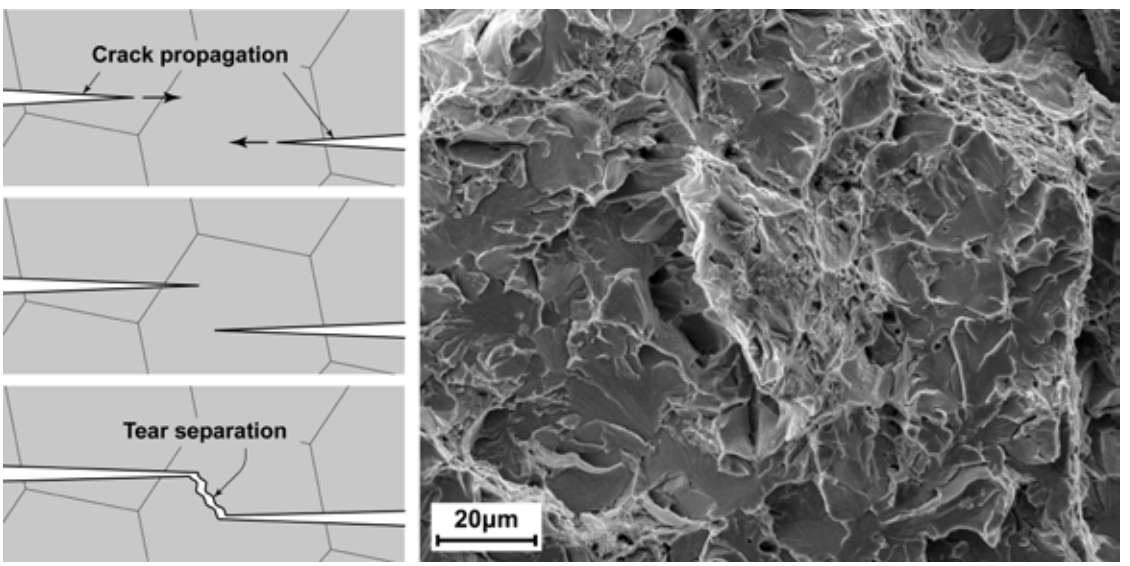

Figure 5.14 – Schematised illustration of tear separation of residual links between transgranular cleavage planes and appearance of a quasi-cleavage fracture as seen through an electronic scanning microscope [Laboratories of the Department of Mechanical Engineering of Politecnico di Milano – Milan, Italy].

5.5 Intergranular Fracture

As previously widely described, the two main failure mechanisms in metallic materials are intimately connected with crystal lattice dislocations. If dislocations are free to move under the action of external forces, you will have plastic deformation; if the dislocation motion is inhibited, you will have transgranular cleavage.

Actually, a third fracture mode does exist. It is brittle type too and characterised by de-cohesion along grain boundaries. It is called intergranular fracture.

This failure type occurs exclusively when tensile strength drastically deteriorates at grain boundaries due to local enrichment of noxious chemical elements or precipitation of a second brittle phase. The fracture plane is always perpendicular to the direction of maximum principal stress but, at microscopic level, it follows the profile of grain boundaries (Figure 5.15).

Intergranular brittle fractures are always a hint of an anomaly occurred during steelmaking and/or steel heat treatment or due to steel being used in a critical environment for which it is not suitable. The causes are always to be found in embrittling events among which, but not limited to, hydrogen embrittlement, temper embrittlement, neutron radiation, liquid metal embrittlement, etc.

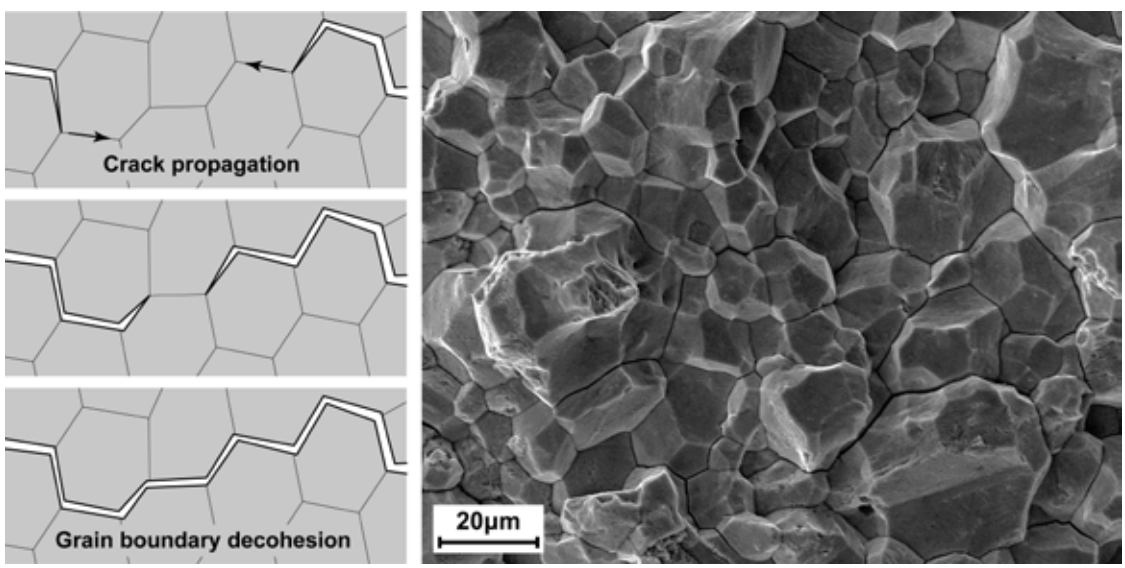

Figure 5.15 – Schematised illustration of grain boundary decohesion mechanisms and appearance of an intergranular fracture surface as seen through an electronic scanning microscope [Laboratories of the Department of Mechanical Engineering of Politecnico di Milano – Milan, Italy].

6. FATIGUE IN STEELS

6.1 What Is Fatigue

Fatigue is the commonest cause of failure in many structural elements, machine parts and industrial components. Fatigue failures typically occur in the mechanical, energy, aerospace, chemical, petrochemical, food, transportation, biomedical and civil industries. The issue is so frequent that about 75% of failures in operation can be blamed on fatigue events. For this reason, we are going to investigate fatigue in depth, also in connection with steel applications in real life.

Unlike brittle fractures, fatigue damage is not sudden and instantaneous. It happens gradually in parts subjected to load applications that are repeated and variable in time with a cyclic and/or oscillatory pattern. Deterioration starts from a small crack that propagates inside the part slowly at first, and then faster and faster. When a critical dimension is reached and the component cross section is considerably reduced, the crack provokes a sudden failure in work conditions deriving from normal operating loads.

Crack formation does not involve macroscopic plastic deformation or necking in the fracture area. To all effects, a fatigue fracture is a morphologically brittle failure. Consequently, you do not have tangible hints of the on-going damaging event until the component suddenly fails.

The issue of fatigue in metallic materials was discovered for the first time early in the 19th century and has been thoroughly studied ever since[1]. The first systematic works are by Wöhler[2] who analysed this phenomenon following the failure of steel railway axles between 1850 and 1860.

Investigations on fatigue intensified after World War II, mainly due to systematic fractures in aircraft, such as the catastrophic failures of the English de Havilland Comet commercial jet planes in the Fifties (Figure 6.1). Given the complexity of this phenomenon, nowadays we are still recording many cases of fatigue fracture in a wide range of industrial products: crankshafts, camshafts, axles, rotors, railway axles, connecting rod-crank systems, tappets, gears, springs and shock absorbers, torsion bars, tubes and pipes, pressure vessels, ropes and cables, turbine and compressor blades, brake callipers, aeronautical structures, off-shore structures, biomedical prostheses and so on.

---

[1] Wilhelm August Julius Albert (1787 - 1846) is generally considered the first to report a fatigue issue. He found this phenomenon in a chain used in a mine. He understood that the failure issue was not connected with overloading, as it was believed at the time, but rather to cyclic repetition of the load applied.

[2] August Wöhler (1819-1914), a German engineer, studied the railways throughout his life. Initially, he dealt with the technical aspects of rail manufacture and locomotive driving and became chief superintendent of all the rolling stock of the German railways. In this period, he made his well-known research works on fatigue failure in railway axles. In 1854 he was appointed director of the Prussian, later German, railways, a post he held until his retirement in 1889.

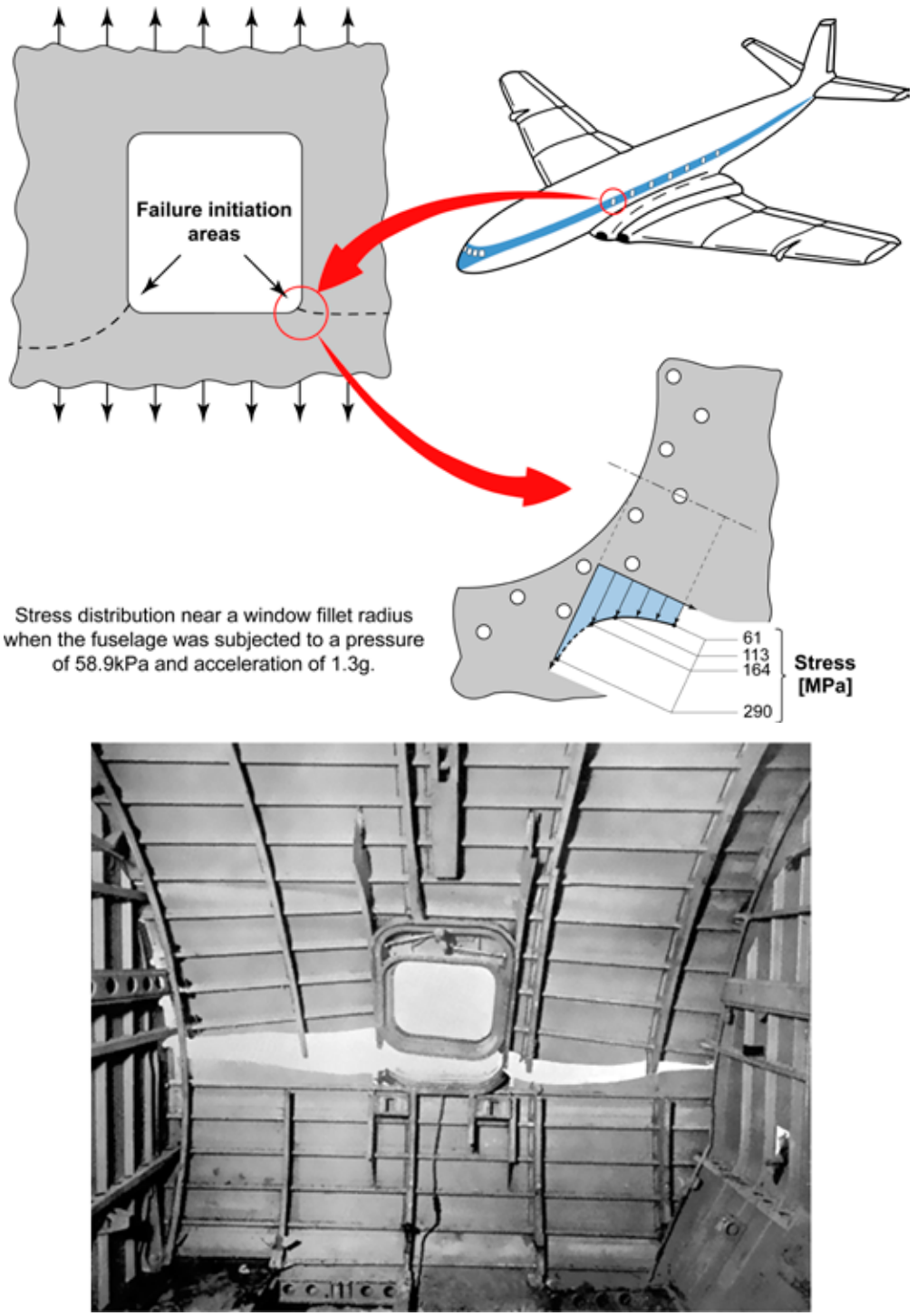

Figure 6.1 – Fatigue failure mechanism in the fuselage of a de Havilland DH. 106 Comet jet plane, near one of the windows – Lab tests on the aircraft marked G-ALYU [from Swift 1987 and Various Authors 1955].

Figure 6.2 – Viareggio railway accident involving the freight train 50325 Trecate-Gricignano. Detail of the fracture surface of the axle broken due to fatigue [pictures by POLFER, Viareggio railway accident, 29 June 2009].

To provide an idea of how topical this problem is today, it suffices to mention two among the most severe train crashes occurred in the last years: the Eschede accident, in Germany in 1998, and the Viareggio accident, in Italy in 2009. In both situations, the root cause for derailing was the fatigue fracture of a rolling stock component, namely the wheel in the German case and the axle in the Italian case (Figure 6.2).
The main reason for which fatigue failures persist is that all structures or mechanical components include areas affected by geometrical discontinuities, surface alterations or flaws that are often hidden and/or not easily quantified. Such local anomalies act as stress intensifiers and, consequently, become the points of origin of most failures.
Another huge problem is connected with poor maintenance of components and deterioration in operation. Corrosion and wear and tear can initiate fatigue cracks even in correctly designed and manufactured components.

6.2 Fatigue Fractures

Fatigue failures occur in normal operating conditions under the action of design nominal stresses. Consequently, the loads applied generate stresses that are below the Yield Strength necessary to start macroscopic plastic deformation in the component.
However, the stresses applied at certain points of the metallic mass can locally exceed the Yield Strength. This can depend on the part surface irregularities, the presence of mechanical or micro-structural discontinuities or component operating damages. Consequently, if you apply an external load to the component cyclically, increasing plastic deformation develops at microscopic level and fatigue cracks are bound to initiate in these points. The root mechanism of this phenomenon is linked to the dislocation motion in the lattice, which is typical of all events relating to mechanical strength in metallic materials.
In a ductile polycrystalline metal alloy, such as steel, cyclic plastic deformation initially occurs in the grains where the slip planes are inclined by 45° relative to the maximum principal stress, i.e. along the crystallographic planes where the shear stress τ is higher. The presence of cyclic tensile stresses leads to the formation of slip bands on the grain surface whose extent increases as the fatigue cycles increase. This causes the material to locally extend outwards (micro-extrusions) or inwards (micro-intrusions) from the surface. Micro-geometric discontinuities allow the development of micro-cracks, in the range of 2 to 3 grains that are orientated by 45° relative to the direction of the maximum principal stress (Figure 6.3). The next propagation phase is governed by the cyclic mechanical stresses with a fracture plane that develops perpendicularly to the maximum principal stress (Figure 6.4).

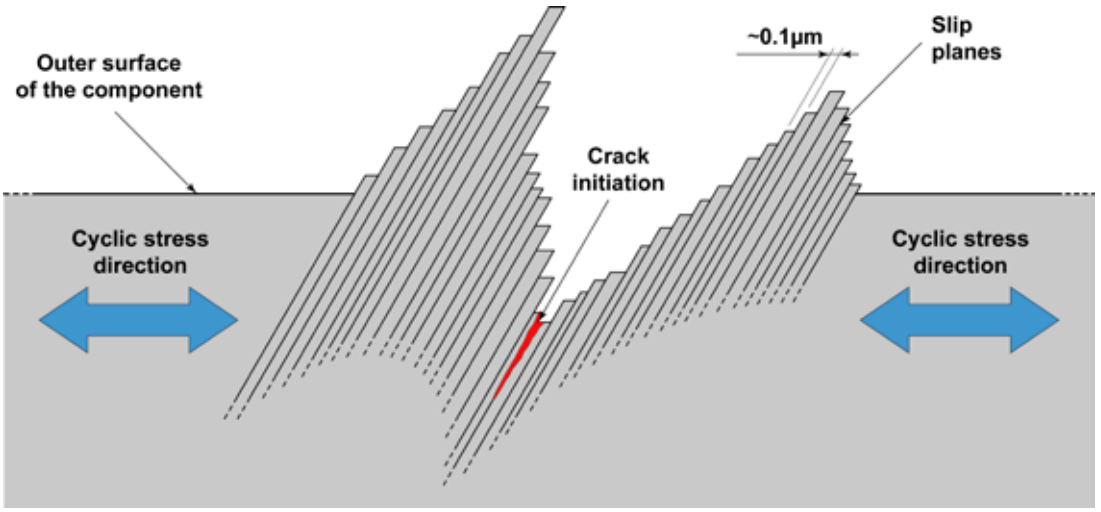

Figure 6.3 – Formation of micro-extrusion and micro-intrusion slip planes in a polycrystalline metallic material and initiation of the fatigue crack.

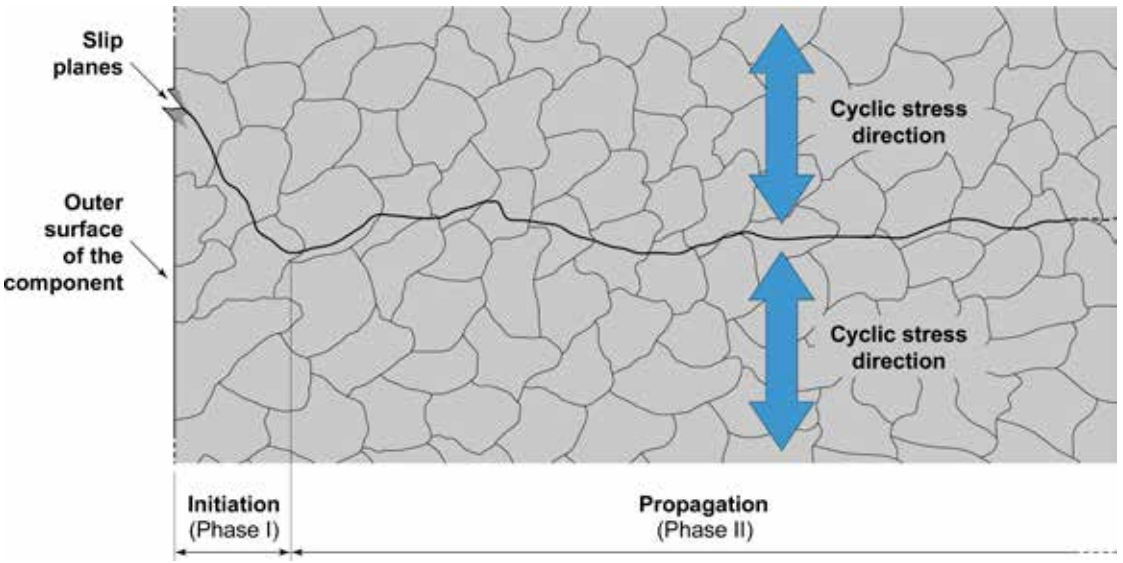

Figure 6.4 – Initiation (phase 1) and propagation (phase 2) of a fatigue crack.

Initiation and propagation of a fatigue failure results from the concurrent action of a cyclic tensile stress repeated in time and local plastic deformation. In the absence of either condition, the fatigue crack cannot nucleate and grow. Cyclic stress enables crack nucleation by starting plastic deformation at local level, and then the tensile component allows the crack to propagate.

With fatigue, it is correct to talk about gradual failure both in the phase before microscopic crack formation and during macroscopic propagation. Fatigue fracture in a component can be divided into three stages that are clearly visible on the fracture surface (Figure 6.4):

I. *Initiation of the fatigue crack*, at surface or sub-surface areas.
II. *Stable growth of the fatigue crack* that gradually runs inside the cross section of the component.
III. *Final fracture due to overloading (or unstable crack growth)* when the component cross section has become so small that it can no longer stand the external load.

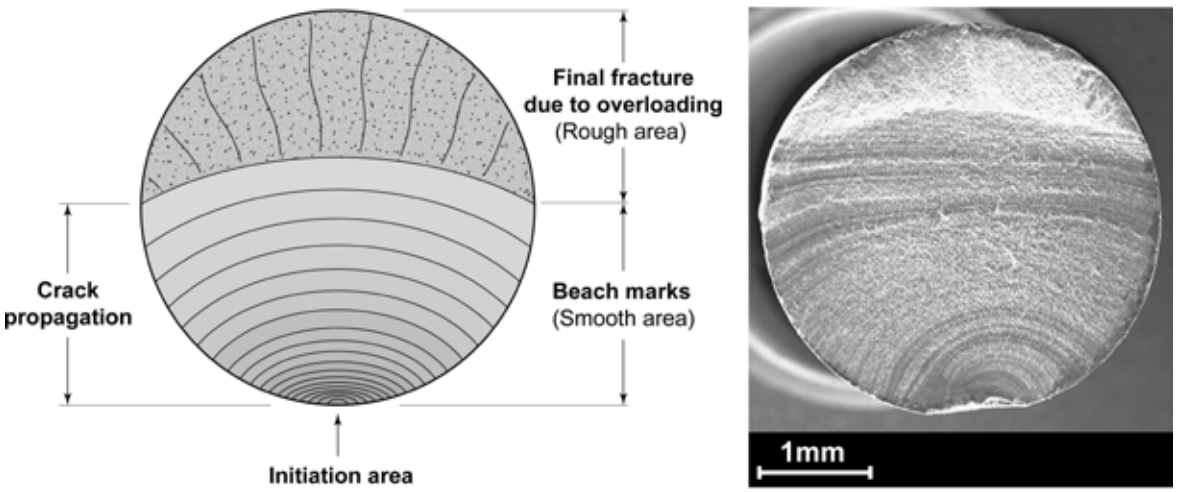

Figure 6.5 – Schematic representation of the three stages of development of fatigue failure and example of a typical fracture surface (aluminium wire in a high voltage lead) [Laboratories of the Department of Mechanical Engineering of Politecnico di Milano - Milan, Italy].

When you examine a mechanical component after fatigue failure, you normally identify two well-defined areas in the fracture surface: the crack initiation and propagation area and the area of the final fracture.
The first area (initiation and propagation) is characterised by concentric lines. These lines are given different names in accordance with their appearance: *oyster-shell marks* or *clamshell marks*, *tide marks*, *ripple marks*, *beach marks*, *stop marks* or *arrest marks*, and *conchoidal marks*. In all cases, they are surface signs showing gradual progressing of the failure and bringing back to the point of origin of the crack. The beach marks or the stop marks (hereafter we are going to use this terminology) appear when the fatigue stress is discontinued for a certain period of time, and then is resumed. If this sequence of events repeats in time, this causes the generation of a fracture surface similar to the one shown in Figure 6.6.

The second area (final fracture) forms when the residual cross section of the component is too small to stand the load applied. The final fracture is a catastrophic and sudden event (unstable crack growth) with no forewarning signs of plastic deformation.

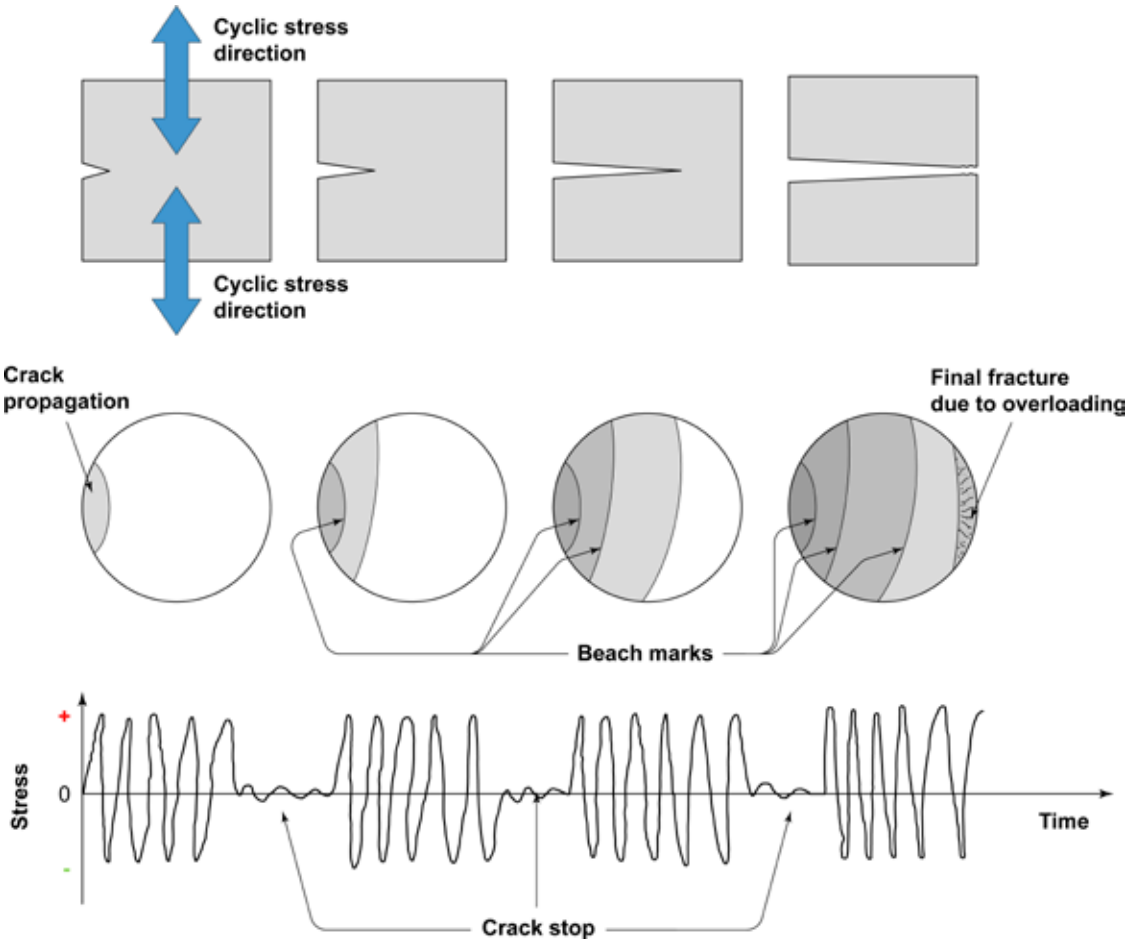

Figure 6.6 – Schematic illustration of a fatigue fracture with formation of beach marks in a real-life component subjected to random cyclic stress [from Brooks C. R., Choudhuri A., Metallurgical Failure Analysis, McGraw-Hill, New York, 1993].

The beach lines are the consequence of local variations in the fracture surface appearance. These changes occur during the stop-and-go phases typical of the intermittent progress of a fatigue crack in a real-life component during operation. Every time the stress is discontinued, the freshly formed fracture surface has the time to oxidize while the portion previously created oxidizes further. Therefore, the beach marks are due

to the different oxide thickness that reflects light in a different manner. In some cases these signs can also appear for the effect of mechanical overloads capable of considerably varying the load cycle amplitude.
Even though the beach marks are a typical element of fatigue failures, their absence does not rule out this type of damage. For example, in lab tests, the cyclic load is never discontinued until the component/specimen breaks. The type of material also plays an important role. The stop marks are conspicuous in ductile materials while they can be missing in brittle materials (such as cast iron).

6.3 Wöhler Curve

The Wöhler curves, also referred to by English authors as *S-N* diagrams, are the commonest method used to describe fatigue resistance of materials (Figure 6.7).
Wöhler curves are Cartesian graphs where the amplitude of the cyclic stress applied is plotted as ordinate (on a linear scale) and the number of cycles leading to breakage or non-breakage of the specimen being tested is plotted as abscissa (on a logarithmic scale on base 10).
This type of curves is used when the specimens are subjected to a high number of cycles, typically above 10^5, i.e. when nominal stress generates strains mostly in the elastic region.
Normally, Wöhler curves exhibit two areas that are typical of the material fatigue behaviour:

- A stress threshold (horizontal segment), that is called fatigue limit, σ_{FA}, and represents the maximum stress below which the specimen does not break; and
- A finite-life fatigue area (sloping segment) where you always observe fatigue failure after a certain number of load cycles.

While the fatigue limit[3], σ_{FA}, is a characteristic typical of virtually all steels (general-purpose structural steels, heat-treated alloy steels, high-strength steels, etc.), in other types of materials (aluminium alloys, copper alloys, austenitic stainless steel, etc.) resistance gradually decreases as the number of cycles increases, but with no lower threshold. Their different behaviour depends on the material crystal lattice that is body-centred cubic (abbreviated B.C.C.) in the former case and face-centred cubic (abbreviated F.C.C.) in the latter case (Figure 6.8).

[3] If not specified otherwise, the considerations expressed in this chapter apply to a general fatigue limit of steel (σ_{FA}). If this is not the case, we always specify the load type: bending fatigue limit (σ_{FAf}), axial fatigue limit (σ_{FAa}) or torsional fatigue limit (σ_{FAt}).

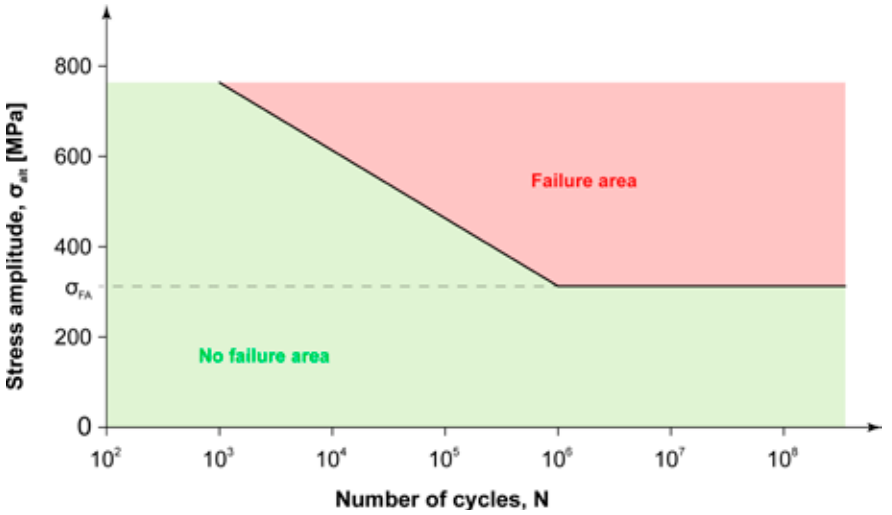

Figure 6.7 – Typical representation of a Wöhler curve (or S-N diagram) for a generic steel; σ_{FA} is the fatigue limit.

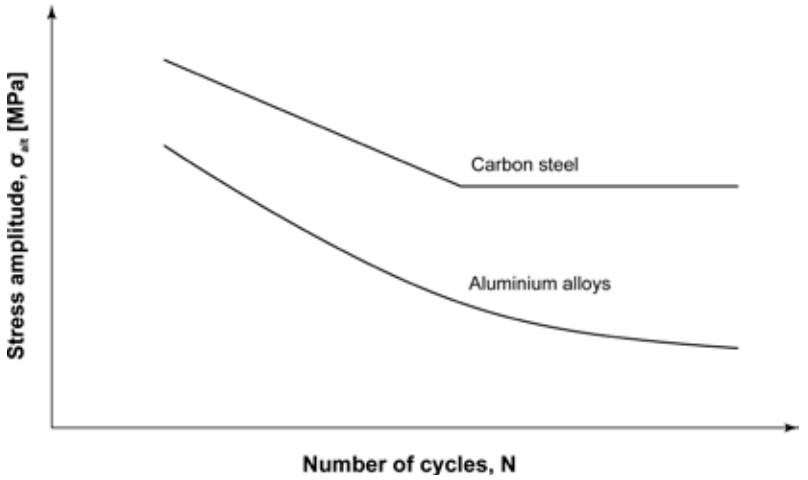

Figure 6.8 – Wöhler curves for a generic carbon steel (or a generic metallic material with B.C.C. lattice) and for a generic aluminium alloy (or a generic metallic material with F.C.C. lattice).

6.4 Wöhler Curve Experimental Determination

To determine the Wöhler curve experimentally, different types of stress can be used ranging from a simple stress pattern (tension-compression, reversed bending, rotating bending and reversed torsion) to more complex situations where simple stress types are combined to simulate the real-life behaviour in operation. For sake of convenience, the cyclic characteristics of fatigue stress are usually described by making reference to a generic stress-time sinusoidal pattern, as shown in Figure 6.9.

In addition to the load application system (reversed bending, rotating bending, tension-compression, reversed torsion, etc.), other significant parameters that should always be recorded during a fatigue test include:

- Maximum stress, σ_{max}
- Minimum stress, σ_{min}
- Average stress, $\sigma_{mean} = (\sigma_{max} + \sigma_{min})/2$
- Stress amplitude, $\sigma_{alt} = (\sigma_{max} - \sigma_{min})/2$
- Stress ratio, $R = \sigma_{min}/\sigma_{max}$

Frequency is another important parameter. Frequency indicates number of load cycle repetitions in the unit of time and is measured in cycles per minute or in Hertz (cycles/sec.).

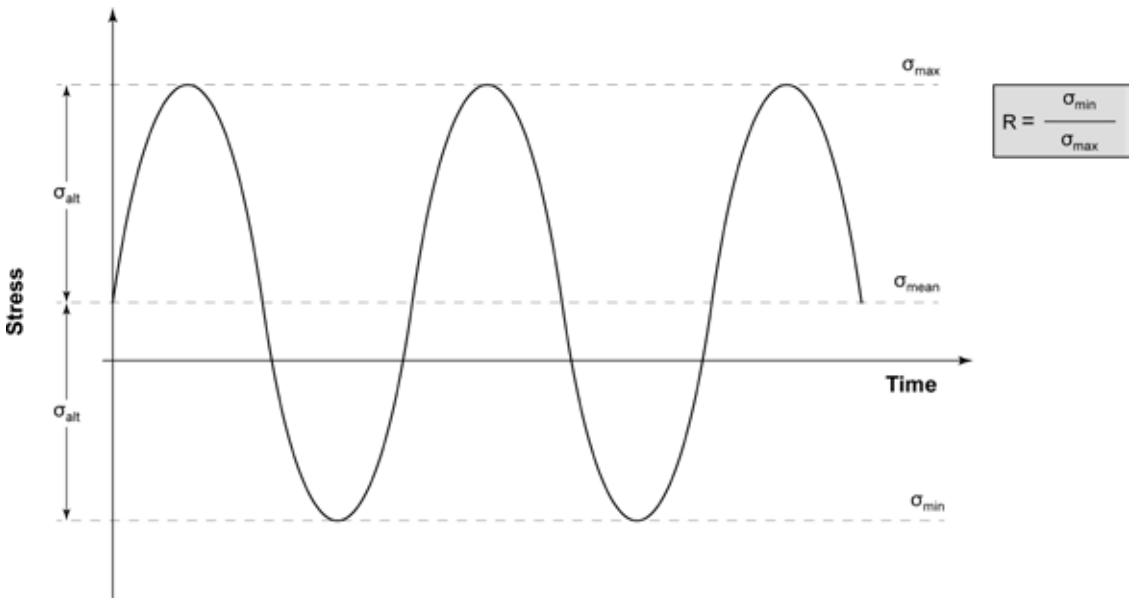

Figure 6.9 – Representation of a generic cyclic stress and its significant reference parameters.

Let's assume that you want to determine the Wöhler curve for a certain material by conducting fatigue tests in rotating bending conditions. The fatigue limit will be indicated by σ_{FAf}, where the subscript *f* refers to the load type (bending, in this case). Usually, the tests are conducted in the air at room temperature.
Let's assume that the material is a Q&T low-alloy chromium molybdenum steel grade, such as EN 25CrMo4, after quenching and tempering, with Ultimate Tensile Strength 760 MPa and Yield Strength 540 MPa.

Your specimen is hourglass type, similar to the cylindrical specimens used for tensile tests. The sample should be mirror-polished (average arithmetic roughness $R_a \leq 0{,}05\mu m$) to avoid that any surface flaws might be the initiation point of early fractures, which would alter test result.

The test consists in applying a rotating bending stress with $R = -1$ (i.e. with $\sigma_{mean} = 0$ and $\sigma_{max} = -\sigma_{min}$) by means of the machine sketched in Figure 6.10 with 3000 rpm mandrel speed (frequency 50 Hertz).

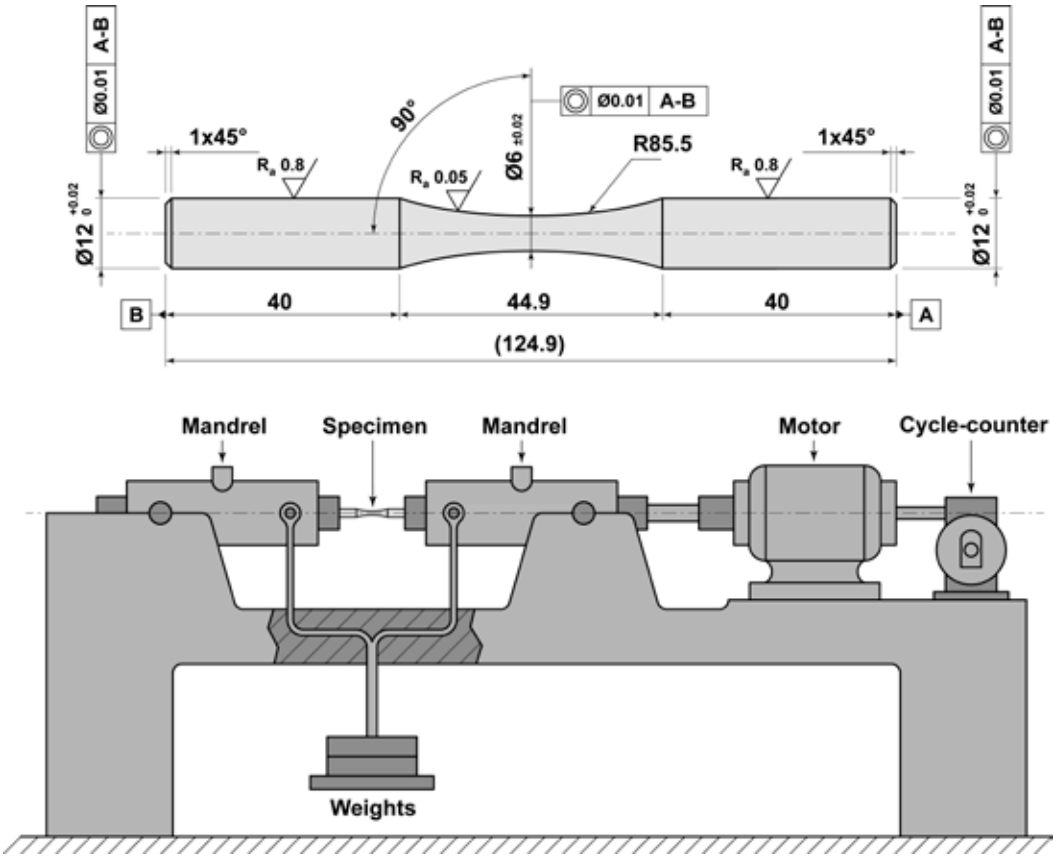

Figure 6.10 – Construction drawing of an hourglass specimen for fatigue testing in rotating bending conditions and schematic of the testing machine used.

After securing the specimen in the grips, bending stress is applied. When the machine mandrel is activated, the sample starts turning on its axis and the points along its circumference are subjected to sinusoidal cyclic stress. This load system is known as rotating bending and is similar, for example, to the load system applied to a railway axle during operation (Figures 6.11 and 6.12).

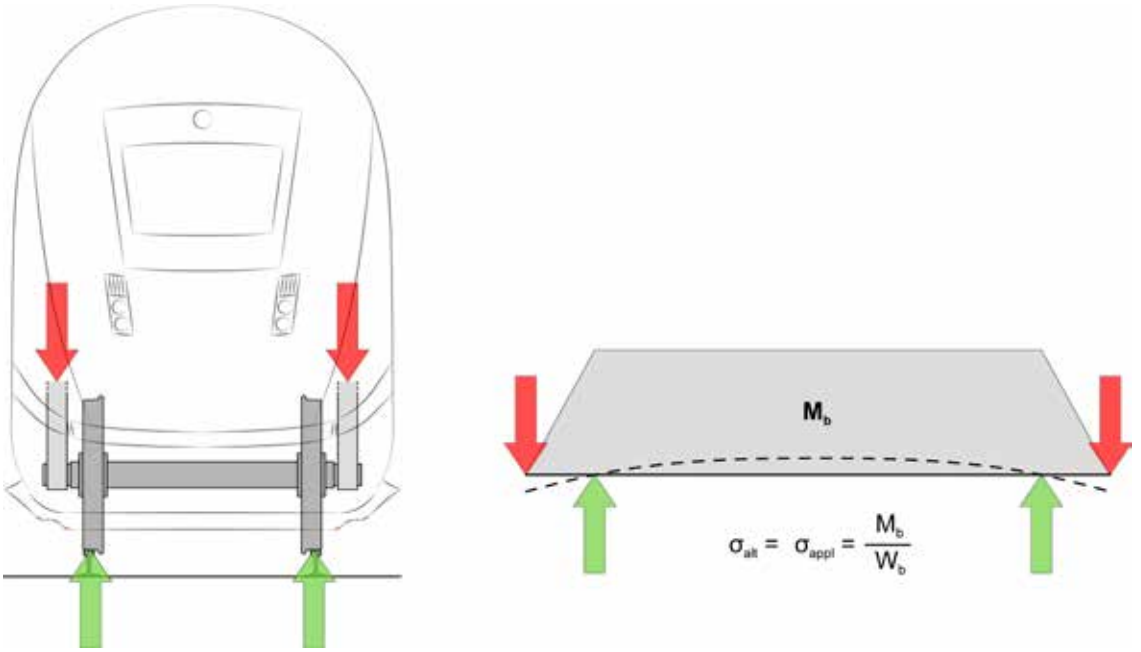

Figure 6.11 – Schematic of a four point bending load as typical in a train axle during operation.

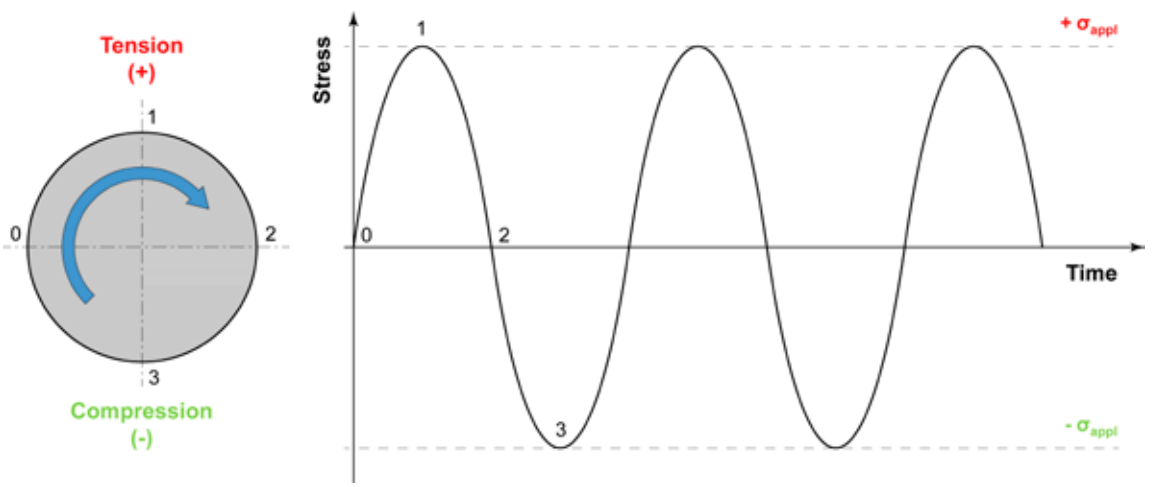

Figure 6.12 – Cyclic stress trend at an unspecified surface point in a train axle during operation.

The test sequence that enables tracing the Wöhler curve is described below. First, we will examine the finite-life fatigue area and then the fatigue limit. See Figure 6.13.

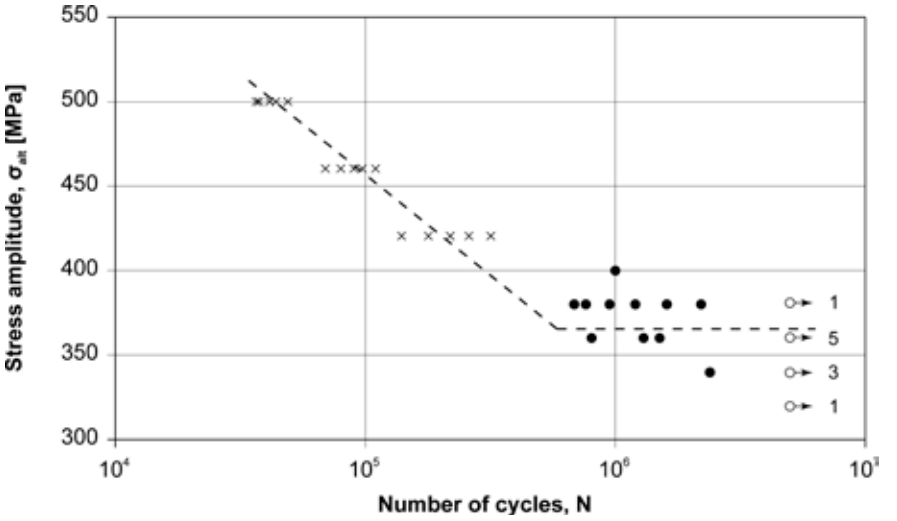

Figure 6.13 – Example of an experimental Wöhler curve obtained in rotating bending conditions (R = -1) for EN 25CrMo4 steel (YS = 540 MPa; UTS = 760 MPa) [Laboratories of the Department of Mechanical Engineering of Politecnico di Milano – Milan, Italy].

Experimental evaluation of finite-life fatigue - Once you know steel mechanical characteristics, in particular its Ultimate Tensile Strength, you can estimate in advance its bending fatigue limit (σ_{FAf})[4] that can be presumed around 380 MPa. With reference to this estimate (σ_{FAf} = 380 MPa) and to the steel Yield Strength (YS = 540 MPa), you can define three equidistant intermediate stress gradients, thereby obtaining 500 MPa, 460 MPa and 420 MPa.

At least 5 tests with constant-amplitude stress are conducted for each of the three levels mentioned above. The number of cycles leading to sample breakage is recorded (indicated by the letter "x" in the diagram). The average deviation and the standard deviation of the cycle number, at each stress level, are the data to be interpolated to trace the finite-life fatigue area in the Wöhler curve (Figure 6.13).

Experimental evaluation of the fatigue limit - Now you determine the bending fatigue limit, σ_{FAf}, that is the horizontal segment of the Wöhler curve using the *staircase* method.

Other specimens are prepared (15 or more, but always in an odd number) fabricated exactly as the previous ones.

[4] *As better detailed in the next paragraph, steel fatigue limit in rotating bending conditions (R = -1) can be estimated approximately as half its Ultimate Tensile Strength* ($\sigma_{FAf} \cong UTS/2$), *at least up to UTS = 1400 MPa.*

The samples are tested in a sequence after defining:

- A constant stress interval, $\Delta\sigma$, between two subsequent test levels (for example 20 MPa)[5];
- A maximum number of load cycles, N_{lim}; when it is reached, the specimen can be considered infinitely resistant at that stress gradient (for example, you can take $5 \cdot 10^6$ cycles for B.C.C.-lattice metallic materials)[6].

The test takes place as follows. The first sample is subjected to a cyclic load close to its estimated fatigue limit (supposedly 380 MPa). When $5 \cdot 10^6$ cycles are completed, the test is considered as passed (reference will be made to an "unbroken specimen" indicated by an empty circle "○"). On the other hand, if the specimen breaks, the test is considered as failed (reference will be made to a "broken specimen" indicated by a filled circle "●").

The next sample will be stressed at a higher level (400 MPa = 380 + 20) or at a lower level (360 MPa = 380 - 20), depending on whether the specimen did not break (○) or broke (●) during the previous test (run at 380 MPa). In brief, if the specimen breaks before $5 \cdot 10^6$ cycles, the next specimen will be tested at a lower level (360 MPa) while if the specimen does not break, the next specimen will be tested at a higher level (400 MPa). And so on until all of the specimens prepared are tested.

An example of results from *staircase* tests is shown in Figure 6.14.

	Tested specimens in numerical order																								
MPa	1	2	3	4	5	6	7	8	9	10	11	12	13	14	15	16	17	18	19	20	21	●	●	i	n_i	$i \cdot n_i$	$i^2 \cdot n_i$
400																●						1	0	4	0	0	0
380	●				●								●		○		●		●		●	6	1	3	1	3	9
360		●		○		●				●		○		○				○		○		3	5	2	5	10	20
340			○				●		○		○											1	3	1	3	3	3
320								○														0	1	0	1	0	0
																			Total (Σ)			11	10		10	16	32
																									N	A	B

Figure 6.14 – Example of staircase fatigue test results for EN 25CrMo4 steel grade, as in previous Figure 6.13.

Selected test levels are indicated in increasing order starting from 0 and are marked with the letter *i*. Given that the stresses applied in this example are 320 MPa, 340 MPa, 360 MPa, 380 MPa and 400 MPa, the five levels are indicated in a numerical sequence from 0 to 4.

[5] *In the staircase method, the stress interval between the test levels depends on many factors; it generally ranges from 5% to 10% of the fatigue limit to be determined. 20 MPa is normally used for steels; for aluminium alloys you can use the same value or 10 MPa.*

[6] *Also the threshold at which to stop the fatigue test depends on the type of material. For carbon or heat treating steels a value between 10^6 and 10^7 is used while for aluminium alloys and austenitic stainless steels a value between 10^7 and 10^8 is more appropriately defined.*

Then, the least frequent event (n_i) is recorded, namely if there are less broken or unbroken specimens (this is why an odd number of samples is used), and the single values of $i \cdot n_i$ and di $i^2 \cdot n_i$ are calculated together with their summations Σ, defining N, A and B as shown in Figure 6.14.
The bending fatigue limit determined experimentally (σ_{FAf}) is the stress threshold where you experience breakage/non breakage of 50% of the samples tested and corresponds to:

$$\sigma_{FAb} = \sigma_0 + \Delta\sigma \cdot \left(\frac{A}{N} \pm 0.5\right) \quad \text{[eq. 6.1]}$$

where σ_0 is the lowest stress gradient used (320 MPa in our case) and $\Delta\sigma$ is the interval between load levels (20 MPa in our case), the sign is "+" if the least frequent event is non-breakage or "-" is the least frequent event is breakage.
Therefore, in the example provided, you have:

$$\sigma_{FAb} = 320 + 20 \cdot \left(\frac{16}{10} + 0.5\right) = 362MPa \quad \text{[eq. 6.2]}$$

The fatigue limit standard deviation, s, corresponds to:

$$s = 1.62 \cdot \Delta\sigma \cdot \left(\frac{NB - A^2}{N^2} + 0.029\right) \; se \; \frac{NB - A^2}{N^2} > 0.3 \quad \text{[eq. 6.3]}$$

$$s = 0.53 \cdot \Delta\sigma \qquad se \; \frac{NB - A^2}{N^2} \leq 0.3 \quad \text{[eq. 6.4]}$$

So, back to our example, you have:

thence:
$$\frac{NB - A^2}{N^2} = 0.64 > 0.3 \quad \text{[eq. 6.5]}$$

$$s = 1.62 \cdot 20 \cdot (0.64 + 0.029) \cong 22MPa \quad \text{[eq. 6.6]}$$

Consequently, for EN 25CrMo4 steel, the bending fatigue limit, σ_{FAf}, where you statistically record breakage/non-breakage of 50% of the samples, is equal to:

$$\sigma_{FAb} = 362 \pm 22MPa \quad \text{[eq. 6.7]}$$

6.5 Estimating Steel Fatigue Limit

Steel fatigue limit, σ_{FA}, is influenced by various factors both intrinsic to steel (i.e. purely metallurgical aspects such as chemical composition, micro-structure, inclusion content, defects, etc.) and extrinsic (in other words unavoidable external conditions such as the load application system, average stress applied, residual stresses, room aggressiveness, etc.).

Intrinsic or Metallurgical Characteristics

The chemical composition affects steel fatigue limit in as much as it increases steel static mechanical strength. Indeed, when the Yield Strength and Ultimate Tensile Strength increase, you always observe a systematic increase of σ_{FA}.

So, not only the fatigue limit increases as the content in carbon, silicon, manganese, chromium, nickel and molybdenum increases, but also for the effect of all other alloying elements that contribute increasing steel static mechanical strength, especially after a suitable heat treatment.

Oxygen, sulphur and nitrogen worsen fatigue resistance in as much as they form non-metallic inclusions (oxides, sulphides, nitrides, etc.). These inclusions originate micro-structural discontinuities in the metallic mass that are preferential points of initiation for fatigue cracks.

Also the shape, size and distribution of discontinuities heavily affect fatigue resistance as they can cause anomalous concentrations of the stresses applied resulting in stress concentration at micro-structural level. The most negative conditions occur in the presence of very hard inclusions and metals characterised by poor ductility.

It should be added that you systematically observe a considerable decrease in fatigue resistance in the presence of porosity, gas porosity, shrinkage cavities (typical casting defects), laps, hydrogen flakes and decarburized areas (more common in forgings and pressed/rolled products) or of micro-cracks (following wrong heat treatments or incorrect welding procedures). The presence of whatever discontinuity, either internal to steel or surfacing, provokes local stress concentration and facilitates the initiation of fatigue fracture.

Also steel micro-structure is a conditioning factor of the crack initiation and propagation process as it determines the modes of development of the initial local plastic deformation mechanisms originating fatigue failure (micro-intrusion and micro-extrusion phenomena). Micro-structures with a high mechanical strength, namely those where the dislocation motion is heavily hindered, oppose the creation of fatigue cracks more effectively. Thus, in steels with the same chemical composition, the finer the micro-structure (small grains), the higher the fatigue resistance of the metallic mass.

If you examine the type of steel micro-structure, tempered martensite (obtainable through quenching and tempering) is always to be preferred to mixed ferrite-pearlite or ferrite-pearlite-bainite structures (resulting from hot deformation processes or annealing/normalizing heat treatments). The worst results, however, are obtained with acicular ferrite, retained austenite, carbide segregation and coarse pearlite.

To conclude, you can assert that as Ultimate Tensile Strength, UTS, increases, also steel fatigue limit gradually increases (Figure 6.15). As already observed[7], steel fatigue limit, σ_{FAf}, in rotating or reversed bending

[7] *See note 4.*

conditions (R = -1) is approximately equal to half its Ultimate Tensile Strength, UTS, as follows:

$$\sigma_{FAb} \cong \frac{UTS}{2} \quad \text{[eq. 6.8]}$$

at least as long as UTS is less than or same as 1400 MPa. If UTS exceeds 1400 MPa, the bending fatigue limit values tend to be very scattered and poorly correlated to UTS; under these conditions it is opportune to presume σ_{FAf} = 700 MPa[8].

If the increase in static mechanical strength derives from cold strain hardening (as it happens, for example, in the drawing, extrusion, cold-rolling and other processes), the resulting fatigue limit increase is much less substantial than shown in Figure 6.15 due to the residual tensile stresses induced in the material during the manufacturing processes. In these conditions, the fatigue limit of the metallic mass should be evaluated on a case-by-case basis through opportune experimental tests[9].

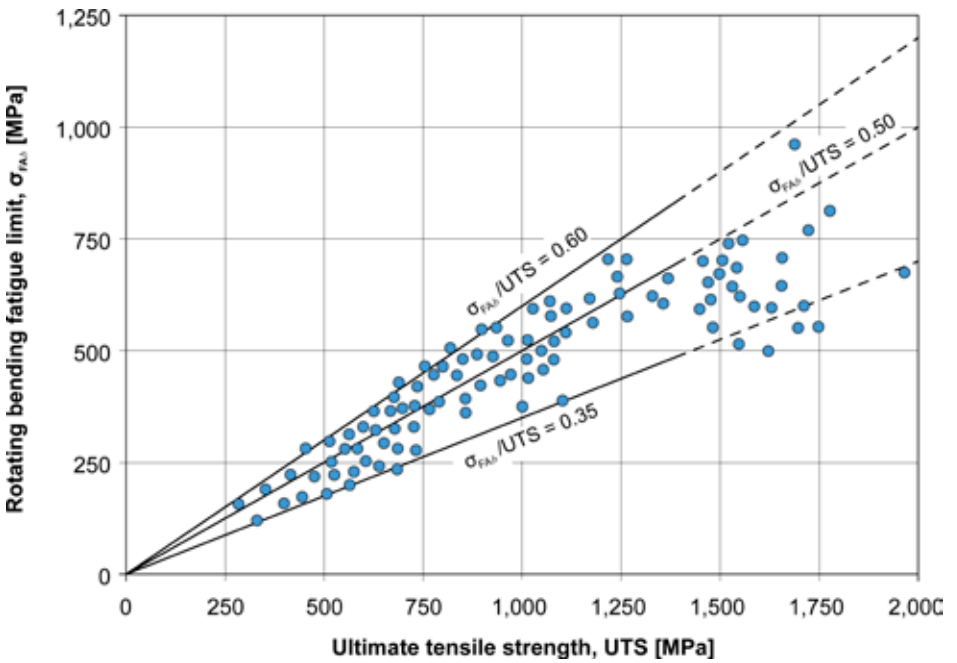

Figure 6.15 – Fatigue limit trend in rotating bending conditions, σ_{FAf}, as a function of the Ultimate Tensile Strength, UTS, for steels with different chemical compositions and micro-structures [from Lee et al. 2005].

[8] *Alternatively, some authors suggest using the following relation (generally more conservative than the one shown in the text and always valid for rotating/reversed bending with R = -1):* $\sigma_{FAb} \cong \frac{1}{4} \cdot (YS + UTS) + 50$

[9] *In the case of strain-hardened steels, the bending fatigue limit (R = -1) usually is in the range of 10 to 40% of Ultimate Tensile Strength after cold plastic deformation. The wide variability of the result depends on the higher or lower strain hardening level induced during the manufacturing process.*

Extrinsic characteristics or imposed from outside

A first aspect that affects steel fatigue limit is connected with the load application modes to the fatigue specimen. If the stress is bending type (rotating or reversed bending), the fatigue limit at room temperature[10] is:

$$\sigma_{FAb} \cong \frac{UTS}{2} \qquad (R = -1) \quad \text{[eq. 6.9]}$$

If the load is applied in tension-compression conditions (reversed axial stress), the axial fatigue limit, σ_{FAa}, is in the range of 0.6 to 0.9 relative to the bending fatigue limit, σ_{FAf}, as follows:

$$\sigma_{FAa} = 0.6\text{-}0.9 \cdot \sigma_{FAf} = 0.6\text{-}0.9 \cdot \frac{UTS}{2} = 0.3\text{-}0.45 \cdot UTS \quad (R = -1) \quad \text{[eq. 6.10]}$$

while in the case of reversed torsional stress, the torsional fatigue limit, σ_{FAt}, is:

$$\sigma_{FA\tau} = 0.5\text{-}0.6 \cdot \sigma_{FAf} = 0.5\text{-}0.6 \cdot \frac{UTS}{2} = 0.25\text{-}0.3 \cdot UTS \quad (R = -1) \quad \text{[eq. 6.11]}$$

Another very important parameter to evaluate steel fatigue limit is the possible presence of average stress (σ_{mean}) other than zero and adding to reversed stress (σ_{alt}) applied to the specimen. You observe that, as average tensile stress (σ_{mean}) increases, the fatigue limit σ_{FA} (bending, axial or torsional) tends to gradually decrease. As an example, Figure 6.16 shows the trend of Wöhler curves obtained by varying the average stress applied, σ_{mean}, for an EN 34CrNiMo6 steel grade subjected to axial fatigue tests.

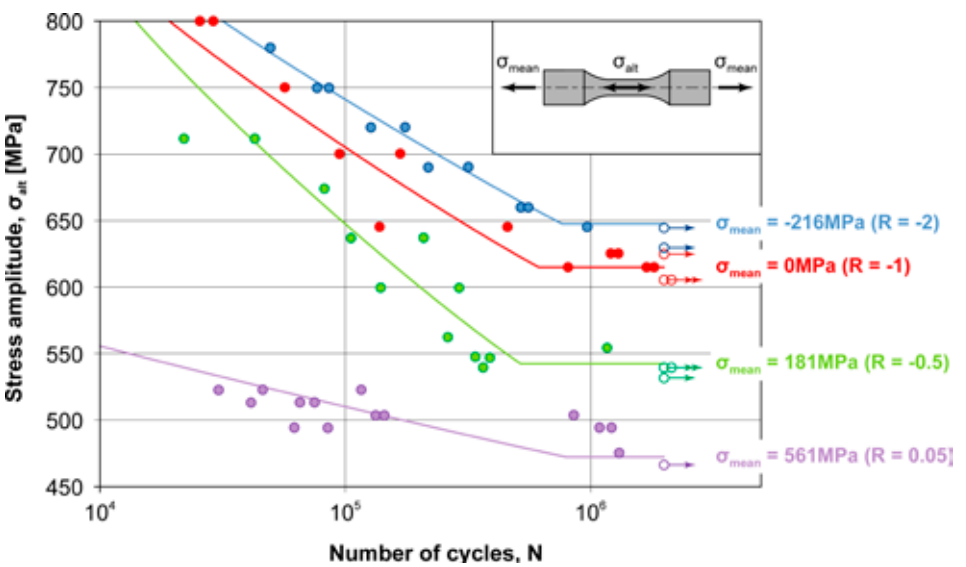

Figure 6.16 – Wöhler curves for EN 34CrNiMo6 steel (YS = 1,084 MPa; UTS = 1,210 MPa) under axial fatigue conditions when the average stress applied is varied [from Pallarés-Santasmartas et al. 2018].

[10] *The considerations set forth herein always refer to steel fatigue behaviour at room temperature. Consult specialised texts for the definition of fatigue limit at high temperature. For the interested reader, it suffices to know that fatigue limit tends to remain constant up to about 250°C, and then it gradually decreases as temperature rises.*

If you examine steels with different chemical compositions and micro-structures and evaluate the different stress types (bending, axial or torsional) experimentally, you observe the possibility of representing the fatigue behaviour using the Haigh diagram that is extensively used for design purposes (Figure 6.17).
In the Haigh diagram, the average stress (σ_{mean}) applied to the specimen is plotted as abscissa and reverse stress (σ_{alt}) as ordinate. To trace the resistance limit curves shown in the diagram, you plot the fatigue limit, σ_{FA}, (either bending, axial or torsional) in the ordinate axis if the average stress applied is equal to zero (R = -1) and steel static strength (to yield, YS, and to fracture, UTS) in the abscissa axis if reversed stress is equal to zero. The curves represent the mathematical correlations most used to interpolate experimental data, thereby defining the resistance limit conditions for the single steel grades in the given conditions of stress applied (σ_{mean} and σ_{alt}).
The equations for the curves shown in Figure 6.17 are as follows (used for $\sigma_{mean} < YS$):

Goodman

$$\frac{\sigma_m}{UTS} + \frac{\sigma_a}{\sigma_{FA}} = 1 \quad \text{[eq. 6.12]}$$

VDI

$$\frac{\sigma_m}{2 \cdot UTS - \sigma_{FA}} + \frac{\sigma_a}{\sigma_{FA}} = 1 \quad \text{[eq. 6.13]}$$

Gerber

$$\left(\frac{\sigma_m}{UTS}\right)^2 + \frac{\sigma_a}{\sigma_{FA}} = 1 \quad \text{[eq. 6.14]}$$

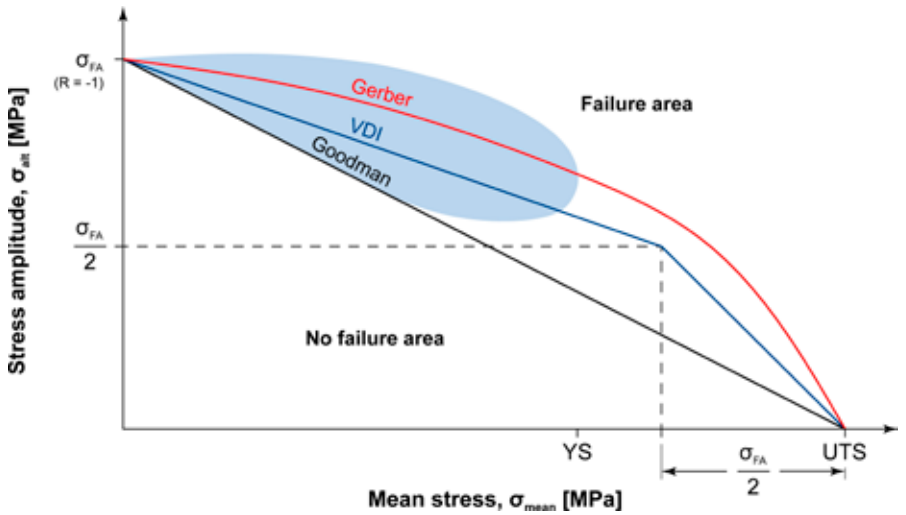

Figure 6.17 – Haigh diagram for a generic steel with the indication of the lines interpolating fatigue test experimental data (according to Goodman, VDI and Gerber). The blue area indicates the field where experimental data are normally located.

The concurrent presence of cyclic stresses and a corrosive environment results in corrosion-fatigue, a phenomenon that considerably affects steel fatigue behaviour.
If you test carbon steels in water (either freshwater or seawater), you commonly observe a significant reduction of the material fatigue limit or, even, that it is totally missing. This latter occurrence highlights that, as the stress applied decreases, you will always experience specimen breakage even if the number of cycles is constantly increased. An example of the above is shown in Figure 6.18 relating to an EN C45 steel grade.

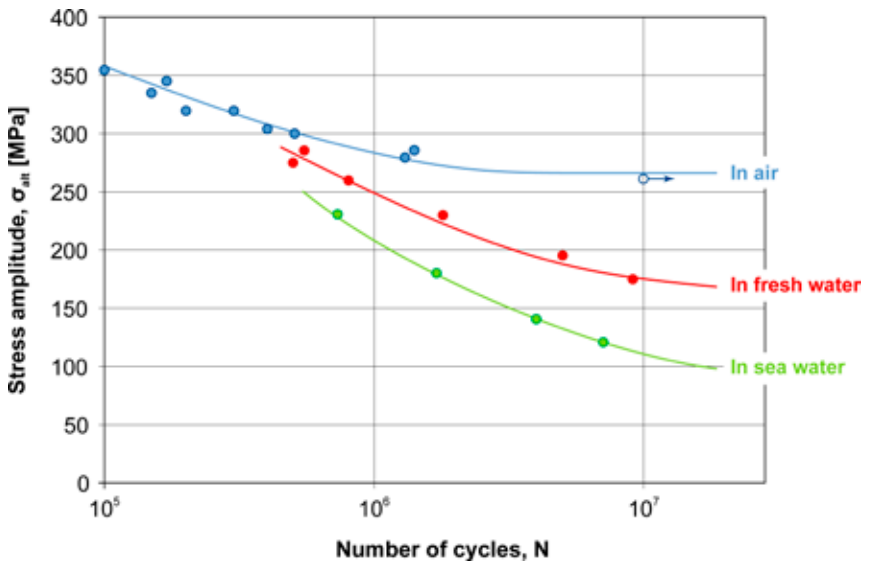

Figure 6.18 – Trend of Wöhler curves in rotating bending fatigue conditions (R = -1) for an EN C45 steel grade (YS = 410 MPa; UTS = 630 MPa) in air, in freshwater and in seawater [from Endo and Miyao 1958].

Last but not least, you have to take into account the issue of residual stress that might exist in steel.
In general, you can say that tensile residual stresses negatively affect fatigue resistance while compressive residual stresses actually improve it. These effects depend on the fact that compressive residual stresses (with a negative sign) oppose the external stresses applied (with a positive sign), thereby inhibiting initiation and propagation of the fatigue crack. Contrarily, tensile residual stresses (with a positive sign) add to the external stresses applied.
Consequently, tensile residual stresses should be eliminated as much as possible before putting the mechanical component into service. This means that the tempering phase of the Q&T heat treatment should be closely monitored[11] or that suitable strain annealing treatments should be carried out if the semi-finished product or finished component so require[12].

[11] *Post-quenching residual stresses are nullified if steel is temperate using suitable temperatures and times (for more detailed information, see Boniardi M., Casaroli A., "Steel Metallurgy - Volume I", Lucefin - Esine, Italy, 2017).*

[12] *Tensile residual stresses develop after a number of manufacturing processes for the manufacture of mechanical parts (casting, drawing, machining, etc.) or following welding processes.*

On the other hand, all thermal, thermo-chemical and mechanical procedures that induce compressive residual stresses at the part surface, exactly where fatigue stress is at its peak, are to be preferred. Surface quenching, case-hardening and nitriding perfectly meet these requirements. If steel is selected in an appropriate manner and the procedure is performed correctly, you will always observe not only a considerable increase of compressive stresses in the cortical area of the part, but also an increase of its surface hardness (Figure 6.19). The mechanical treatments of shot peening and rolling also provide similar beneficial effects. Shot peening is usually performed in the case of springs, crankshafts and gears while rolling is typically used to increase fatigue resistance in shoulder connections.

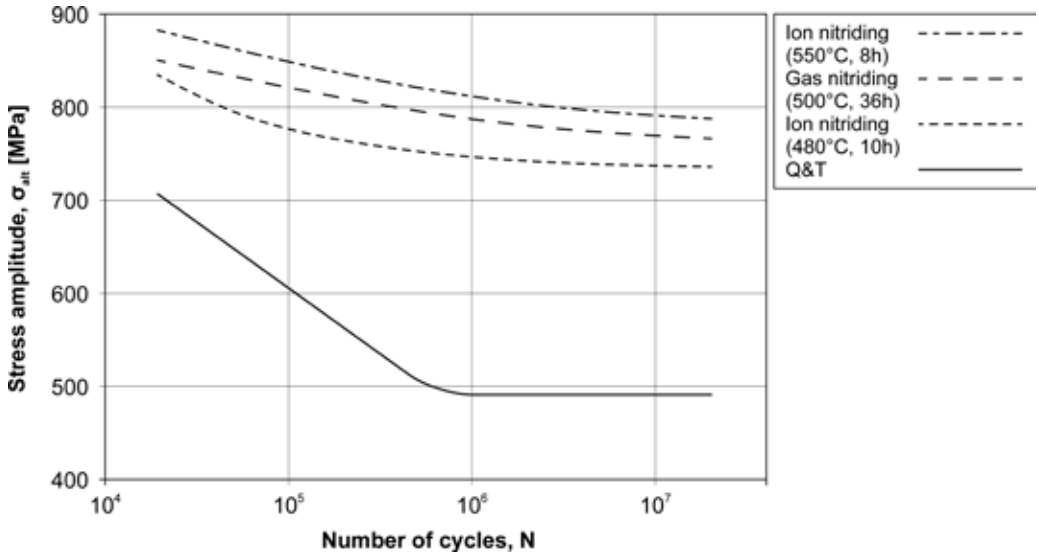

Figure 6.19 – Wöhler curves in rotating bending conditions (R = -1) for an EN 42CrMo4 steel grade (YS = 780 MPa; UTS = 980 MPa), after quenching and tempering and after quenching and tempering followed by nitriding in different modes [from ASM-H.1 1991].

6.6 Fatigue Behaviour of Materials vs Fatigue Behaviour of Components

A major aspect to be always kept in mind as regards steel fatigue is that fatigue behaviour of materials is different from that of components. Under the same stress type applied, the fatigue limit of a mechanical part (σ'_{FA}) is always systematically lower than the fatigue limit of the material with which that part is manufactured (σ_{FA}). In addition to the reduced fatigue limit (from σ_{FA} to σ'_{FA}) when you go from the material to the component, you usually observe a displacement of the number of cycles that marks the transition from finite-life fatigue to infinite-life. Actually, this goes from ~10^6 in steel down to ~10^7 in the component manufactured from that steel (Figure 6.20).

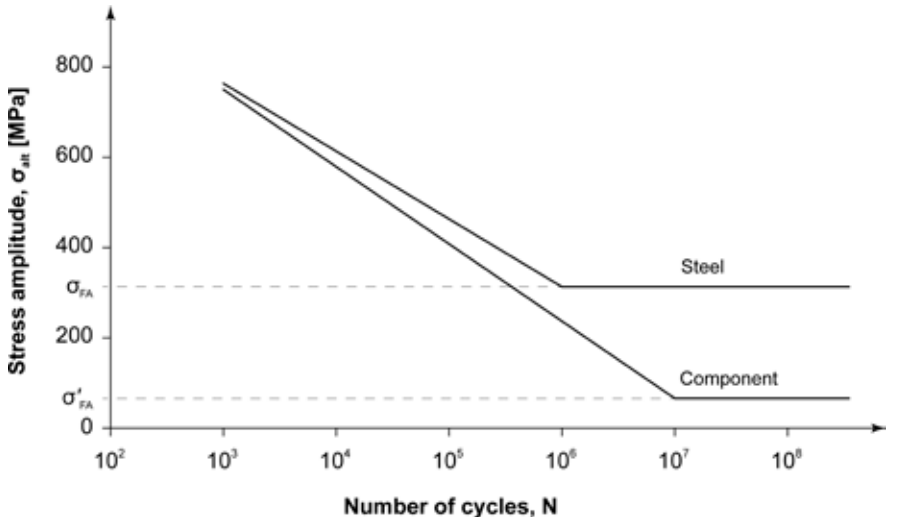

Figure 6.20 – Wöhler curves for a generic carbon steel and for a component manufactured using the same steel. σ_{FA} is the steel fatigue limit and σ'_{FA} is the fatigue limit of the component manufactured using the same steel.

Three main factors diminish the fatigue limit of a mechanical part in comparison with the material from which that part was obtained; they are:

- The size of the mechanical part (dimensional effect),
- The surface finish of the mechanical part (surface finish effect),
- The presence of geometrical discontinuities in the mechanical part (stress concentration effect).

The *Dimensional Effect*. To determine the fatigue limit of a generic steel experimentally, small size specimens are used, with a diameter of 6 to 8 mm in the gauge length. Consequently, due to the bending loads applied, you obtain a high stress gradient. The stress applied (σ_{appl}) is highest at the surface, but suddenly decreases at a distance of few millimetres and goes down to zero along the axis (neutral axis).

In the case of real-life components, stress reduction is less conspicuous than in a specimen with a small diameter (Figure 6.21). In reality, under the same stress applied at the surface (σ_{appl}), the stress gradient gradually decreases as the part size increases.

The difference of the two stress gradients induces a different average stress on a generic volume of material adjacent to the surface where fatigue cracks normally develop. In brief, as the component size increases, the stress gradient decreases, with consequent increase of average stress in the material portion examined. Experimental data enable observing that, as the diameter increases, the component fatigue limit (σ'_{FA}) gradually decreases in comparison with the fatigue limit measured in a small diameter specimen (σ_{FA}).

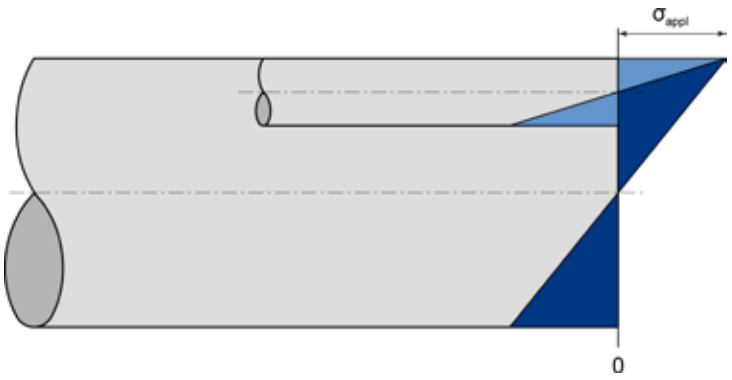

Figure 6.21 – Stress trend along the sections of two components with different diameter, both subjected to bending and under the same stress applied at the surface (σ_{appl}). In the smaller component, the stress gradient is remarkably higher (light blue) than in the larger component (dark blue).

The dimensional effect is normally expressed by means of a coefficient, b_2, ranging between 0 and 1 and defined by the ratio σ'_{FA}/σ_{FA} (Figure 6.22). Alternatively, you can evaluate b_2 using the following formula:

$$b_2 = 1.189 \cdot d^{-0.097} \quad \text{[eq. 6.15]}$$

where d is the component diameter in mm (if $d \leq 8$ mm, we presume $b_2 = 1$). In the case of axial fatigue, the coefficient b_2 is always equal to 1 because in tensile-compression conditions stress is constant all along the section.

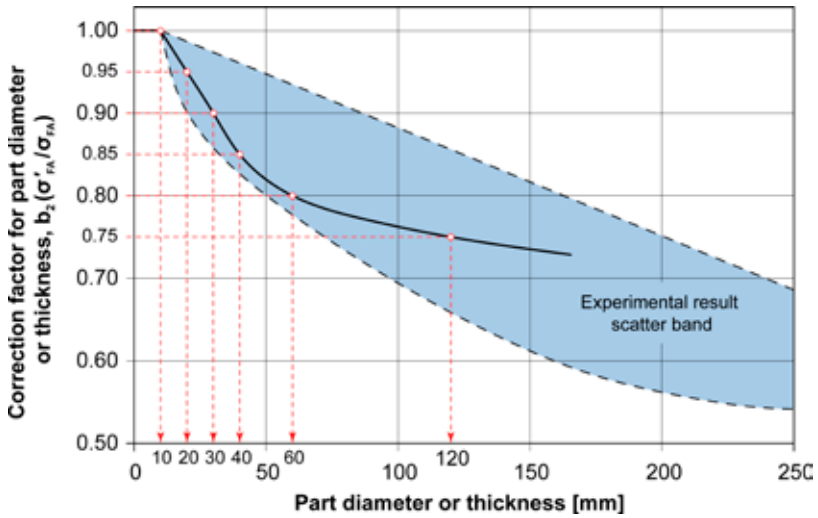

Figure 6.22 – Trend of the dimensional coefficient b_2 that allows defining the component fatigue limit (σ'_{FA}) starting from the material fatigue limit (σ_{FA}) as a function of the component size [from Davoli et al. 2003].

The Surface Finish Effect . When you determine the fatigue limit of a material experimentally, you use specimens with a very low roughness level ($R_a \leq 0{,}05$ µm). Such an extremely low roughness can be obtained only by mirror-polishing. Perfect surface finishing removes all micro-geometrical discontinuities (peaks and valleys in the roughness profile) that can act as preferential points of initiation for fatigue cracks.

Figure 6.23 – Values of average arithmetic roughness, R_a, due to the different machining processes.

Instead, with real-life components, roughness due to traditional machining processes (turning, milling, grinding, etc.) is definitely worse (Figure 6.23) and involves a gradual reduction of fatigue resistance (σ'_{FA}) relative to the value measured in a mirror-polished specimen (σ_{FA}).
The effect of surface roughness is usually represented by a coefficient, b_3, between 0 and 1, and defined by the ratio σ'_{FA}/σ_{FA} (Figure 6.24). It should be noticed that the diagram in Figure 6.24 also shows the effects of corrosion on surface roughness and, consequently, on its coefficient b_3.

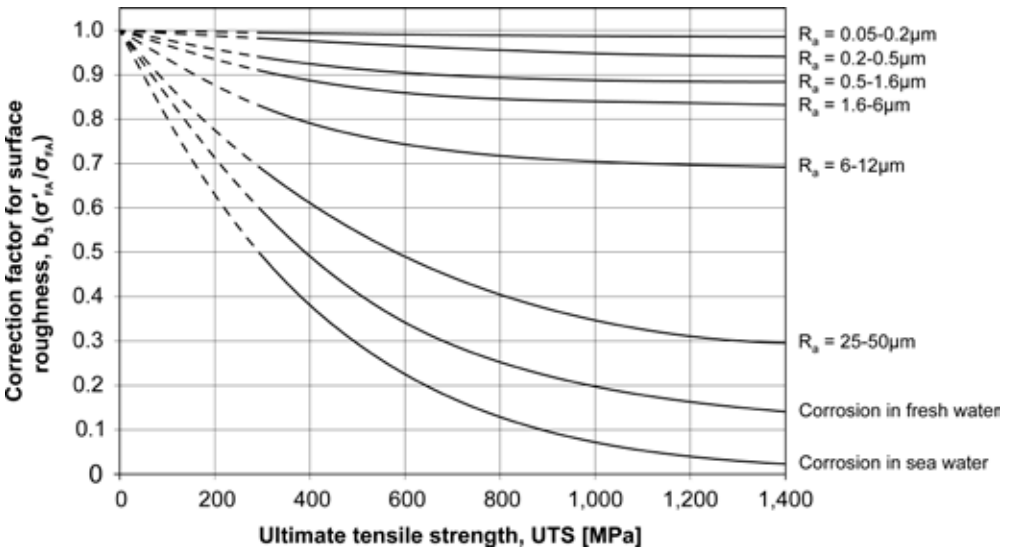

Figure 6.24 – Trend of the surface finish coefficient b_3 that enables defining the component fatigue limit (σ'_{FA}) starting from the material fatigue limit (σ_{FA}) as a function of component roughness. The entry value plotted in the abscissa axis is steel Ultimate Tensile Strength [from Brand et al. 1991].

The Stress Concentration Effect . The specimens used to determine the fatigue limit do not have geometrical discontinuities. We talk about smooth specimens where nominal stress, σ_0 , is applied[13]. But real-life parts normally exhibit stress concentration effects resulting from section changes due to the presence of shoulders, keys, holes, etc. These discontinuities produce local over-stressing, thereby enhancing the stresses applied that raise from the nominal value, σ_0 , to the maximum value, σ_{max}. The stress concentration effect is well represented by the theoretical stress concentration factor, k_t, obtained from opportune nomograms depending on discontinuity geometry and load type. A typical example is given in Figure 6.25[14]

[13] In the case of tensile or compressive stresses, nominal stress is $\sigma_0 = P/A$ where P is the force applied and A is the section. In the case of bending or torsion, it is $\sigma_0 = M/W$ where M is the moment applied (either bending or twisting) and W is the modulus (to bending or torsion) of the section.

[14] In literature you can find many texts that give the values of k_t for a great number of geometries and stress conditions. For example, see Pilkey, W.D., Peterson's Stress Concentration Factors, 2nd ed., John Wiley & Sons, Hoboken, New Jersey, USA, 1999.

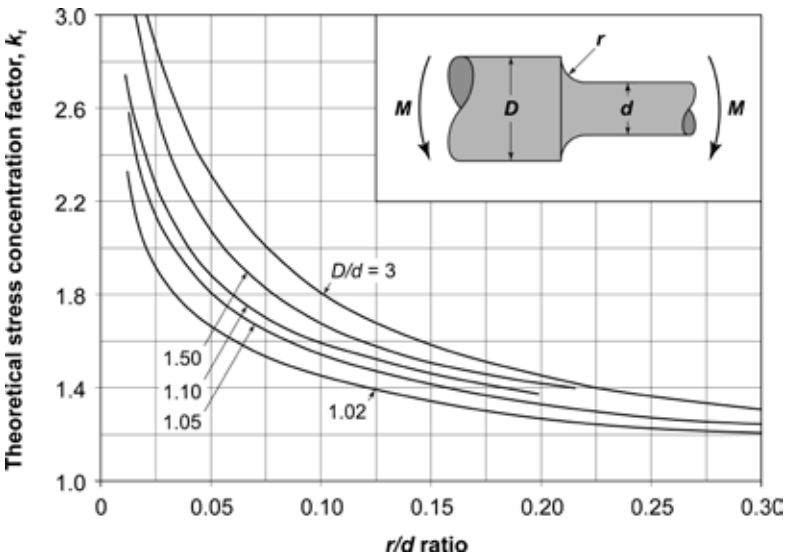

Figure 6.25 – Nomogram for determining theoretical stress concentration factor in a shouldered shaft subjected to bending moment *M*. For example, if $D = 110$ mm, $d = 100$ mm and $r = 5$ mm, then $D/d = 1.10$ and $r/d = 0.05$, thence you will have: $k_t \cong 1.9$ at the shoulder [from Pilkey 1997].

In brief, k_t is a figure higher than 1 that multiplies the nominal stress, σ_0, existing in a certain point and gives back the maximum local stress:

$$\sigma_{max} = k_t \cdot \sigma_0 \qquad \text{[eq. 6.16]}$$

Unlike static load conditions, where k_t depends only on notch geometry, things are different with fatigue. Experimental tests show that a geometrical discontinuity influences fatigue behaviour in a different manner depending on whether steel is more or less mechanically resistant. In particular, harder steel grades are more sensitive to stress concentration than the less hard ones.
In case of components under fatigue, stress concentration is described by means of the fatigue stress concentration factor, k_f, and the *notch sensitivity, q*, in accordance with the following relations:

$$\sigma_{max} = k_f \cdot \sigma_0 \qquad \text{[eq. 6.17]}$$

$$k_f = 1 + q \cdot (k_t - 1) \qquad \text{[eq. 6.18]}$$

where q is calculated by means of the diagram in Figure 6.26. k_f is a figure greater than 1 and defined as the ratio between the fatigue limit of a notched component compared with that of a specimen, as follows:

$$k_f = \frac{\sigma'_{FA}}{\sigma_{FA}} \qquad \text{[eq. 6.19]}$$

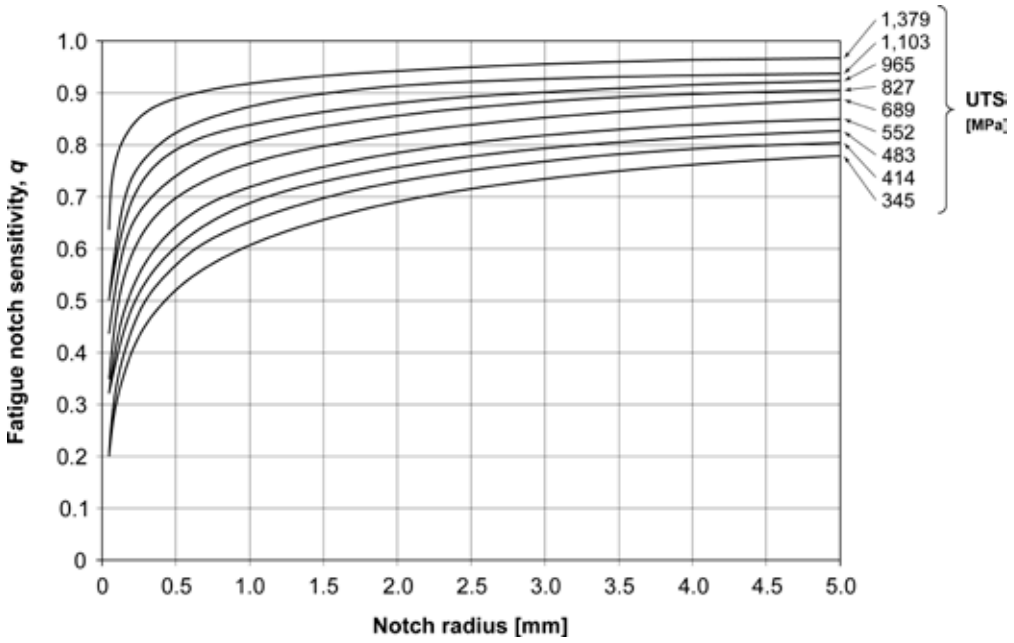

Figure 6.26 – Trend of the notch sensitivity, q, as the notch radius and steel Ultimate Tensile Strength change due to fatigue bending and axial stresses. In the case of torsional stress, you should consider a curve with Ultimate Tensile Strength exceeding by 138 MPa that of the steel actually used [from Norton 1997].

In conclusion, if you consider at the same time the three main factors (dimensional effect, surface finish effect and stress concentration) that reduce steel fatigue limit, σ_{FA}, down to that of the component made from the same steel, σ'_{FA}, you obtain:

$$\sigma'_{FA} = \frac{b_2 \cdot b_3 \cdot \sigma_{FA}}{k_f} \qquad \text{[eq. 6.20]}$$

Let's now develop an example to better understand this difference.
For sake of simplicity, we will consider a shouldered shaft (Figure 6.25) under bending stress (either rotating or reverse) with $R = -1$ (no average stress), in the air, at room temperature.
Reference data are as follows:

- Material: EN 25CrMo4 steel; YS = 540 MPa; UTS = 760 MPa;
- Dimensions: $D = 110$ mm; $d = 100$ mm; $r = 5$ mm;
- Final machining process: turning with $R_a = 2$ to 3 µm.

First of all, we calculate steel fatigue limit. Given that the load applied is bending (rotating or reverse) with R = -1, we can presume the following:

$$\sigma_{FAb} = \frac{UTS}{2} = \frac{760}{2} = 380MPa \;\; (R = -1) \qquad \text{[eq. 6.21]}$$

To evaluate the dimensional effect (coefficient b_2), we take into account the smaller section including stress concentration, i.e. the section where d = 100 mm. From Figure 6.22 we obtain:

$$b_2 = 0.76 \quad \text{[eq. 6.22]}$$

To evaluate the surface finish effect (coefficient b_3), we take into account both machining roughness (R_a = 2 to 3 µm) and steel Ultimate Tensile Strength (UTS = 760 MPa). From Figure 6.24 we obtain:

$$b_3 = 0.85 \quad \text{[eq. 6.23]}$$

Finally, we evaluate fatigue stress concentration factor (k_f). To this aim, theoretical stress concentration factor (k_t) and steel notch sensitivity (q) should be determined in advance.
On the basis of the shoulder geometrical characteristics (D = 110 mm; d = 100 mm; r = 5 mm) and Figure 6.25 we obtain:

$$k_t = 1.9 \quad \text{[eq. 6.24]}$$

If we consider steel Ultimate Tensile Strength (UTS = 760 MPa) and the notch radius (r = 5 mm) on the basis of Figure 6.26, we find that notch sensitivity is:

$$q = 0.90 \quad \text{[eq. 6.25]}$$

thence:

$$k_f = 1 + q \cdot (k_t - 1) = 1 + 0.90 \cdot (1.9 - 1) = 1.81 \quad \text{[eq. 6.26]}$$

Therefore, the part fatigue limit, σ'_{FAf}, at the shoulder, i.e. at the most stressed point, is:

$$\sigma'_{FAb} = \frac{b_2 \cdot b_3 \cdot \sigma_{FA}}{k_f} = \frac{0.76 \cdot 0.85 \cdot 380}{1.81} \cong 135.6MPa \quad \text{[eq. 6.27]}$$

It should be emphasised that this case study regards the simple condition of a shouldered cylindrical shaft subjected only to bending with R = -1. However, this example enables demonstrating that the fatigue limit of a component (σ'_{FAf} = 135.6 MPa) is systematically lower than that of the steel (σ_{FAf} = 380 MPa) the component is made of. Consequently, extreme attention must be paid at design level to the stresses that are actually applied and that must be considerably lower than the component fatigue limit (σ'_{FAf}) calculated in the most critical conditions.

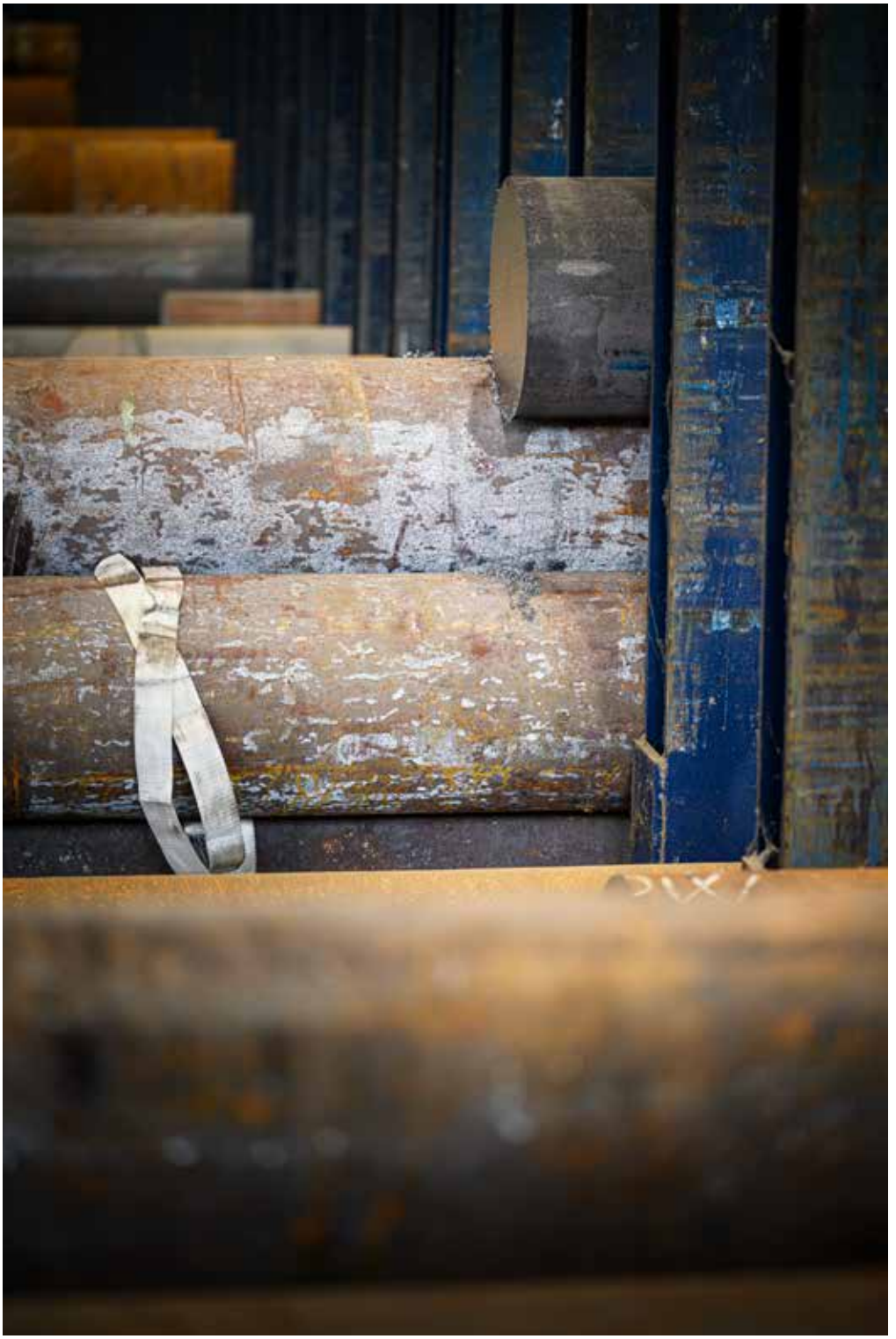

7. STEEL CLASSIFICATIONS AND STANDARDS

7.1 Possible Steel Classifications

Steels are iron and carbon alloys with carbon contents below 2.11%. Alloys with carbon contents above 2.11% are referred as cast iron.

Most steels used at industrial level have a carbon content below 0.77%; therefore, they are classified as hypoeutectoidic steels[1]. Typical examples are general-purpose structural steels, special structural steels and some steel grades used for special applications (steels for high temperatures, steels for low temperatures, stainless steels, etc.).

Hypereutectoid steels are also available on the market; they are Fe-C alloys with carbon contents between 0.77% and 2.11%[2]. Tool steels and some grades of bearing steels belong to this second category that, in any case, includes much fewer steels than the previous one.

Also, it is worth adding that all steels (both hypoeutectoid and hypereutectoid) can exist in the non-alloy carbon steel and low-alloyed/alloyed formulations. The difference consists in the presence of one or more alloying elements in addition to carbon. As better explained in the next pages, the regulations further discriminate between low alloy steels and alloy steels depending on whether they contain a chemical element in a content higher than or same as 5% (Figure 7.1).

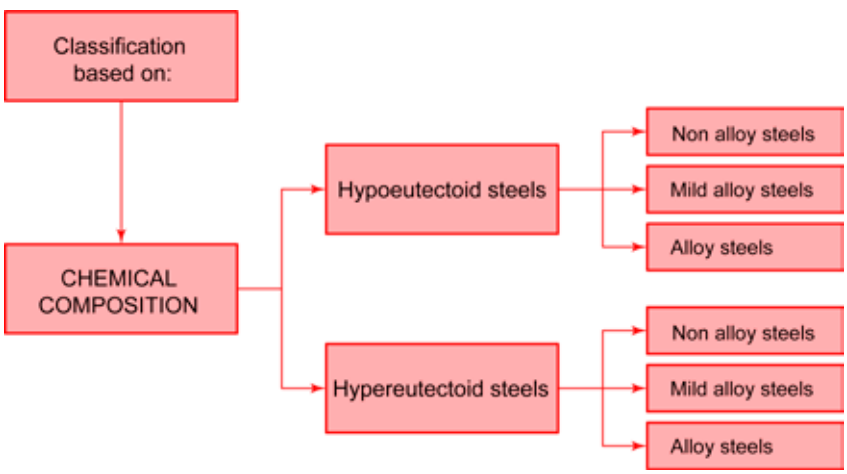

Figure 7.1 – Classification of steels based on their chemical compositions.

[1] *The alloy with C = 0.77% is referred to as eutectoid alloy; therefore, alloys with lower carbon contents are called hypoeutectoid alloys and those with higher carbon contents are called hypereutectoid alloys.*

[2] *Keep in mind that 0.77% is the carbon content of the eutectoid of the iron-carbon alloy without alloying elements. If other alloying elements are present, the eutectoid value tends to decrease as the additional elements increase, and can even be much lower than 0.77%. Indeed, there are hypereutectoid alloy steel grades with carbon contents as low as 0.3 to 0.4%.*

Another possible division is based on steel end use. To this regard, you can identify three main categories[3] (Figure 7.2):

- General-purpose structural steels also known as carbon steels or non-alloy carbon steels[4];
- Special structural steels or steels for special applications, divided into steels for quenching and tempering, surface hardening steels, self-hardening steels, spring steels, case hardening steels and nitriding steels;
- Steels meant for selected applications, such as bearing steels, steel for wire and ropes, rail steels, steels for magnetic applications, stainless steels, tool steels, maraging steels, Hadfield steels, steels for high temperatures, steels for low temperatures, etc.

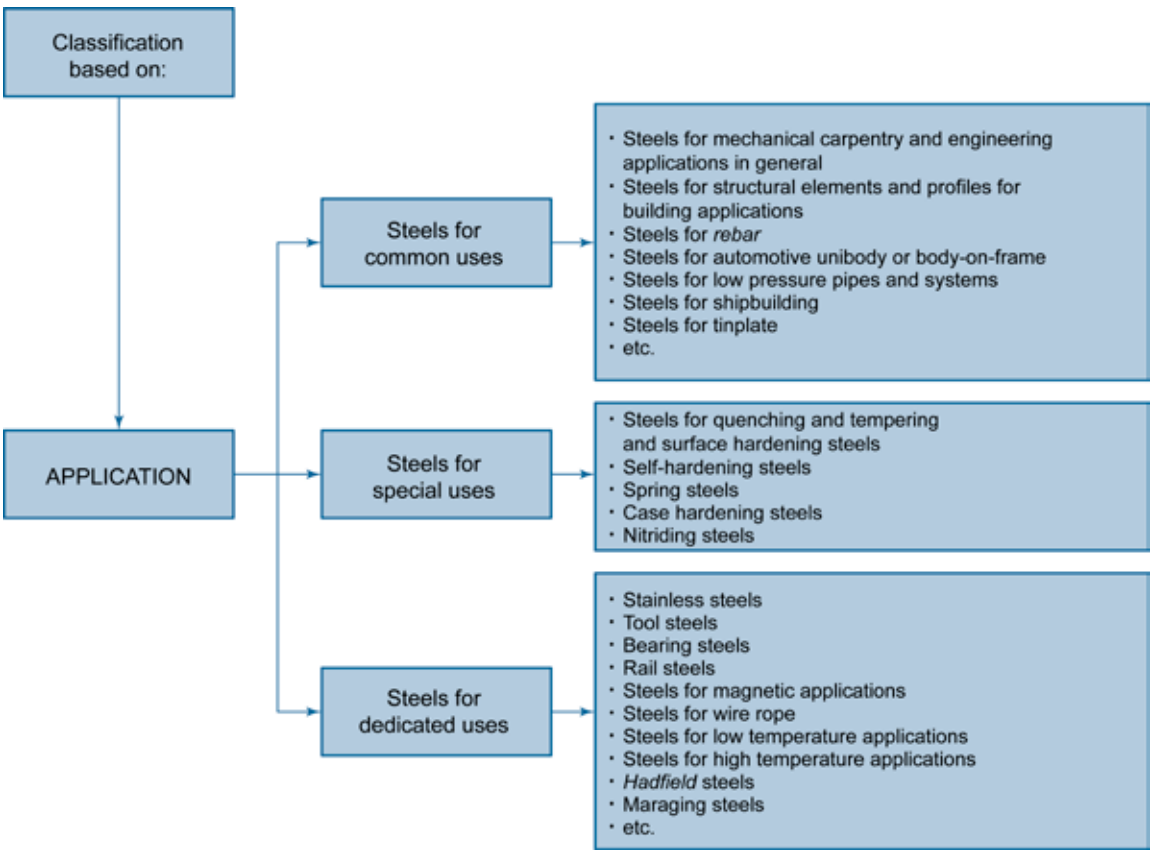

Figure 7.2 – Classification of steels based on their intended use.

[3] *This division is taken from Nicodemi W., Acciai e leghe non ferrose, 2nd ed., Zanichelli - Bologna, Italy, 2008.*

[4] *In addition to "acciai comuni" (common steels), in Italy this steel family is also identified using the English terminology "carbon steels". Even though it may sound quibbling, the term "carbon steel" is not correct. The term "steel" already indicates an iron and carbon alloy; therefore, specifying that these are "carbon steels" is tautological. It would be better to say "non-alloy carbon steels", which highlights that steels also exist that, in addition to carbon, contain different alloying elements contributing to obtain the properties desired (low alloy steels and alloy steels).*

However, probably the most appropriate distinction, also used in European regulations, is dividing steels into two families in accordance with the methods used to obtain their physical and mechanical properties (Figure 7.3). In this case, you talk about:

- Steels that are put into service with no previous heat treatment;
- Steels that are put into service only after a specific heat treatment.

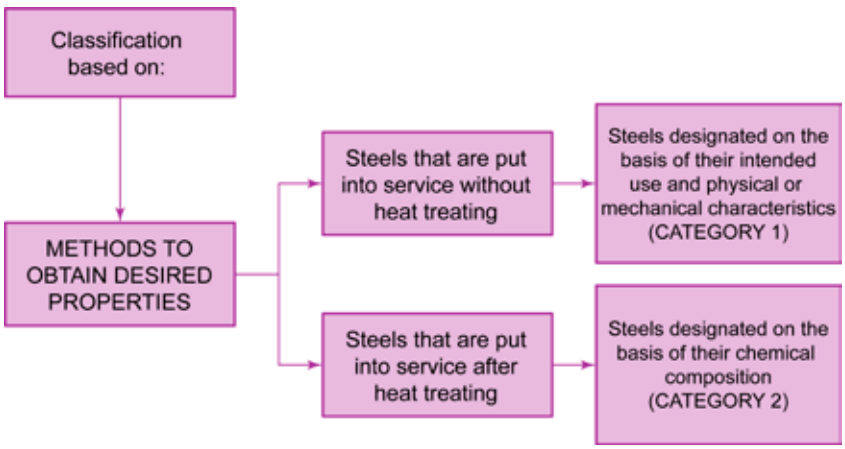

Figure 7.3 – Classification of steels based on the methods used to obtain their physical properties and mechanical characteristics.

The first category includes steels that already possess the physical, micro-structural and mechanical characteristics required in operation at the end of the manufacturing process. These steels do not require additional heat treatments by the user of the semi-finished product. Their properties are not remarkably modified by post-manufacturing processes (cold forming, cutting, welding, machining, etc.).

This is the case of steel grade EN B450C[5] used to manufacture hot-rolled rebars normally used to reinforce concrete. This is a low carbon steel (C ≅ 0.16 to 0.20%) with no alloying elements. At the end of the production process, i.e., after hot rolling and subsequent air cooling, the rod mechanical strength and ductility are more than suitable for its final application and no additional heat treatment performed by the user is required. Also, steel properties remain almost unaltered even if the rod is cut, bent or welded.

[5] *This steel is very similar to the one originally designated as Fe B44K by the UNI 6407 standard and mentioned in Eurocode 2 (EN 1992-1-1) and in the Italian Ministerial Decree of 14 January 2008.*

The same applies to steel EN S275J0[6], used to fabricate girders, beams and steel profiles for structural applications, and to steel EN P295GH used to make pipes and pressure vessels. It also applies to steel EN M140-30S whose characteristics are suitable for the manufacture of magnetic transformer core laminations.

Things are very different with steels belonging to the second category. They owe their properties to the heat treatment performed by the user on the semi-finished product before final machining operations and preliminary to putting into service.
This category includes Q&T steels such as EN C40 (non-alloy carbon steel) or EN 42CrMo4 (low alloy steel), both used to manufacture small and medium size mechanical components. After rough machining, the semi-finished products are quenched and tempered, then they are finished by means of fine turning and/or grinding. The parts so obtained (shafts, pins, crank gears, etc.) exhibit high strength characteristics resulting from the steel chemical composition and Q&T heat treatment. The same happens in the manufacture of gears for which Q&T steels such as EN 17NiCrMo6-4 or nitriding steels such as EN 31CrMo12 are typically used.
Another example is represented by stainless steels. For example, if you have to make a pot or a sink by deep drawing, the austenitic stainless steel strip should undergo cold deformation. This first step is followed by the solution annealing treatment to optimise steel corrosion resistance. Now the item finished by polishing. If it is a pot, handles are welded on before polishing. Also in this case, it is exactly the combination of the steel chemical composition and final heat treatment that guarantees the properties required from the component during operation (in this example, corrosion resistance)

7.2 European Standards on Steels

The EN 10027 standard (Designation systems for steels - Part 1: Steel names. Part 2: Numerical system) is the reference standards for steel designation.

First, we will consider the steel names consisting of letters and digits. This alphanumeric or *symbolic designation system* is used more commonly than the *numerical system* and allows immediate evaluation of steel metallurgical and mechanical characteristics. According to this reference system, a steel belongs only to one of the following two categories:

- Category 1 - Steels designated on the basis of their intended use and physical or mechanical characteristics;
- Category 2 - Steels designated on the basis of their chemical composition.

[6] *Carbon steel S275J0 roughly corresponds to steel Fe430C in the old UNI 7070 standard.*

Category 1

Steels belonging to the first category are designated by means of an initial letter representing the intended use, followed by some digits that define the value of the reference physical or mechanical characteristic for the intended use. Sometimes, the designation includes *additional letters* that provide more information on the steel characteristics or properties.

For Category 1, the standard lists the following *initial letters* representing the intended use:

S - Steel for structural applications;

P - Steel for pressure purposes;

L - Steel for line pipe;

E - Steel for engineering applications;

B - Steel for reinforcing concrete;

Y - Steel for prestressing concrete;

R - Steel for or in the form of rails;

D - Steel for flat products for cold forming;

H - High strength steel flat products for cold forming;

T - Steel for tin mill products;

M - Steel for electrical applications.

As to the digits to be associated to the initial letter representing steel intended use, it is always opportune to consult the EN 10027-1 standard because various indications exist. The same applies to other additional letters that you may find in steel designation.

In the commonest cases (intended use classes S, P, L, E and B), the digit after the initial letter indicates the guaranteed minimum Yield Strength (in MPa) for the format with the minimum available thickness.

Let's come back to the example seen above: EN B450C. This designation represents a steel for rebars (thence the first letter B that stands for *béton*, meaning concrete in French), with characteristic Yield Strength of 450 MPa[7] (the additional letter C refers to the ductility class).

Another example is the designation EN E295. This is a steel for industrial engineering applications (first letter E) with guaranteed minimum Yield Strength of 295 MPa for semi-finished products in the minimum available thickness. In this case, there are no additional letters.

Similarly, the designation EN E355K2 identifies the same applications as for the steel previously examined (first letter E meaning steel for engineering applications), but with a higher guaranteed minimum Yield Strength (355 MPa). The additional letter K2 indicates a transversal impact strength of minimum 40 J at -20°C (see EN 10027-1).

---

[7] *The words "characteristic Yield Strength" define the steel Yield Strength value representing the 5% quantile of the population, as statistically evaluated based on mechanical test results from samples taken from a certain population. Therefore, this means that 95% of the sample population tested mechanically provided a result above the characteristic value.*

Another example is the designation EN P355M. It identifies a steel for pressure purposes (first letter P) with a guaranteed minimum Yield Strength of 355 MPa for semi-finished products in the minimum available thickness. The additional letter M informs that semi-finished product was obtained by means of thermo-mechanical rolling (see EN 10027-1).

Remember that the purpose of designations is to provide an alphanumeric code containing all the information that the user must know to use steel at best. Thus, given that carbon steels or general-purpose structural steels (steels in Category 1) do not require being heat-treated by the user before being put into service, it suffices to indicate the intended use and the design reference mechanical characteristics. In the case of EN E355K2, these are the guaranteed minimum Yield Strength and minimum impact strength at a certain temperature.

To avoid misunderstandings, it should be pointed out that the number after the letter does not always represent steel Yield Strength. For example, take the designation EN R320Cr. This is a rail steel with minimum Brinell hardness of 320 HB, low alloyed with chromium (about 1%). Or the designation EN M140-30S that identifies a conventional oriented grain silicon steel for electrical applications (magnetic core laminations), with a maximum specific loss of 1.40 W/kg and nominal thickness of 0.03 mm.

It is worth repeating that steels in Category 1, that are designated on the basis of their intended use and physical or mechanical characteristics, are put into service without undergoing any heat treatment. However, keep in mind that sometimes also these steels can be heat-treated during the manufacturing process. Normalization is the typical case. This treatment is performed by the manufacturer of the hot-rolled products to reduce the average size of the grain and improve steel mechanical strength and fracture toughness.

In any case, at the end of the manufacturing process at the factory, steel will not be subjected to whatever heat treatment by the final user because it already has the properties suitable for its intended use.

Category 2

Let's examine now steels belonging to the second category that are designated based on their chemical composition.

In Category 2 the designation method differs depending on whether alloying elements are present or not. Four families are found:

- Family no. 1: Non-alloy Carbon steels, namely not alloyed steels with a manganese content below 1%.
- Family no. 2: Low alloy steels with a manganese content above or same as 1% and contents of every other alloying element below 5%.
- Family no. 3: Alloy steels, i.e., steels with a content of at least one alloying element above or same as 5%.
- Family no. 4: High-speed tool steels.

Family no. 1

Non-alloy carbon steels are designated by means of the letter C followed by a number representing the nominal carbon content multiplied by 100. Sometimes, there is a letter after the number that is used to specify steel additional characteristics (see EN 10027-1).

For example, this family includes EN C20 and EN C60. These are two non-alloy carbon steels and contain a nominal carbon content of 0.2% (i.e., 20 divided by100) and 0.6% (60/100), respectively. The code EN C60E identifies a steel that is similar to standard EN C60 steel, except that it has a controlled maximum sulphur content, which is indicated by the letter E. Or the code EN C85S where the letter S indicates a steel specially designed to manufacture springs (S from Spring).

Family no. 2

Low alloy steels are designated using a number that represents the nominal carbon percentage multiplied by 100. After the number you find the chemical symbols of the alloying elements listed in order of decreasing concentration and followed by one or more numbers separated by a hyphen. These numbers represent the nominal concentration of the alloying elements multiplied by a pre-defined coefficient. The multiplying coefficient is 4 for *Cr, Co, Mn, Ni, Si, W,* 10 for *Al, Be, Cu, Mo, Nb, Pb, Ta, Ti, V* and *Zr* , 100 for *N, P, S* and *Cs* , 1000 for *B* .

For example, the code EN 34CrNiMo6 identifies a low alloy steel containing a nominal carbon content of 0.34% (34/100), a nominal chromium content of 1.5% (i.e., 6 divided by 4) and decreasing contents of nickel and molybdenum that are not specified in the code. The code EN 42CrMo4 identifies a low alloy steel containing a nominal carbon content of 0.42% (42/100), a nominal chromium content of 1% (i.e., 4 divided by 4) and a lower content of molybdenum that is not specified in the code.

Steel coded as EN 33CrMoV12-9, that also is a low alloy steel, features a nominal carbon content of 0.33% (33/100), a nominal chromium content of 3% (12/4), a nominal molybdenum content of 0.9% (9/10) and lower vanadium contents. Or the code EN 11SMnPb30 that identifies a steel containing a nominal carbon content of 0.11% (11/100), a nominal sulphur content of 0.3% and lower contents of manganese and lead.

Family no. 3

Alloy steels are designated using letter X, followed by a number representing the nominal carbon percentage multiplied by 100. After the number you find the chemical symbols of the alloying elements listed in order of decreasing concentration, followed by one or more numbers separated by a hyphen. In this case, the numbers represent the nominal concentration of the alloying elements indicated. A typical alloy steel is EN X5CrNi18-10 that contains a nominal carbon content of 0.05% (5/100), a nominal chromium content of 18% and a nominal nickel content of 10%. Another example is the case of EN X40CrMoV5-1 that is an alloy steel containing a nominal carbon content of 0.4% (40/100), a nominal chromium content of 5%, a nominal molybdenum content of 1% and a lower content of vanadium.

Family no. 4

High-speed tool steels are designated in a totally different manner. Their designation includes using the two letters HS (that stand for High Speed) followed by a series of numbers separated by a hyphen that specify the nominal contents of tungsten (W), molybdenum (Mo), vanadium (V) and cobalt (Co). These are the chemical elements characteristic of this class of steels.

For example, this family includes HS 2-9-1-8 that is a high-speed steel containing a nominal tungsten content of 2%, a nominal molybdenum content of 9%, a nominal vanadium content of 1% and a nominal cobalt content of 8%. Or HS 6-5-2 that is a high-speed steel with a nominal tungsten content of 6%, a nominal molybdenum content of 5% and a nominal vanadium content of 2%.

Finally, we consider the numerical designation system that is borrowed from the German DIN standards and is less used than the previous one. It is based on a five-digit numerical code uniquely identifying each steel grade.

In the case of steels, the first digit is always 1 (being 1 the digit associated with steels) followed by a dot and four other digits. The first two digits refer to the sub-category the steel belongs to and the second two digits are the sequence number in the sub-category[8].

Now, let's take a look at how some of the steels previously designated using the steel names system are designated using the numerical system.

According to numerical coding, steel EN P355M is classified as 1.8821: 1 is for steel, 88 is the sub-category of high strength weldable steels and 21 is the sequential number; steel EN E295 is classified as 1.0050, which means a steel (1), specifically a base steel (00) with sequential number 50[9].

Therefore, EN 42CrMo4 becomes 1.7225 (72 being the sub-category of Cr-Mo or Cr-Mo-B steels) and EN C40 is coded as 1.0511 (05 being the sub-category of steels with a medium carbon content, namely $0.25\% \leq C < 0.55\%$). Steel EN X5CrNi18-10 is classified as 1.4301, where 43 is the sub-category of stainless steels containing $Ni \geq 2.5\%$ and without Mo, Nb or Ti.

[8] More detailed information is available in the EN 10027-2 standard.

[9] 1.8821 is read as "one point double eight twenty-one" and 1.0050 as "one point double zero fifty".

7.3 The Technical Standards

The technical standards are public documents[10] that represent the "state of the art[11]" of a certain sector or field. They indicate the highest level of development and/or knowledge attained about a certain product, process or service and define their dimensional, performance, environmental, quality, safety, organisational characteristics and other aspects. You can say that the technical standards present the latest achievements of consolidated research works in single specific fields (a material, a product, a technology, a service, a phenomenon, a scientific domain, etc.) to provide a summary of confirmed data from different research sectors. The standards instruct the reader about the state of the subject matter as it is known on the date when the standard is published. In brief, every standard contains both theoretical and practical requirements based on the experience of many experts and researchers in a certain domain.

All standards are characterised by "voluntary application", which means that they are valid exclusively if the parties concerned give their mutual consent. They are not state laws and/or regulations that have a mandatory nature; they are not binding obligations[12].

You can easily understand that the technical standards are a sort of "common language" that all engineers speak and understand in their sector of activity. The scope of the technical standards is extremely wide and steel are only a small part of it.

Just think that the technical standards cover the whole life cycle of whatever product, process or service (from steel plates to electrical wires, from glass bottle manufacture to the safety systems for a paper mill, from firefighting systems to technical drawing rules).

The following example on the case of a gas cylinder for storing technical gases will better illustrate this concept to readers that are not familiar with these subjects.

There are standards for designing gas cylinders depending of their end use, standards for drawing and dimensioning gas cylinders, standards for selecting the steel grade and the heat treatment to be used to manufacture gas cylinders, standards for running the mechanical tests on gas cylinders steel, standards for sampling the gas cylinders to be tested, standards for testing the gas cylinders, standards for marking and painting gas cylinders, standards on the accessories connected with gas cylinders, standards about how to fill, transport and store gases into gas cylinders, standards for gas cylinder maintenance and routine checks, standards on safe use of gas cylinders, etc. Not enough, the technical standards are often supplemented with laws and regulations issued at national level and also circulars issued by specific competent bodies (such as the Firefighting authorities, the Prevention and protection services, etc.). Therefore, you can assert that all segments of all technical activities at industrial level or of a civil nature are regulated by standards.

---

[10] Technical standards are documents available to the public; they are sold by the standardisation bodies to all who ask.

[11] Formerly "Status of the Art", later State of the Art. In the technical sector, it indicates the latest scientific achievements in a certain discipline; more simply it is a synonym of "last generation", "of excellence" or "forefront".

[12] The technical standards become mandatory only if they are expressly mentioned in regulations, directives or laws.

7.4 Technical Standards Issuing Bodies

All technical standards are written, approved and issued by the standardisation bodies that operate at both national and international level and carry out their activities almost autonomously. The system of the standardisation bodies and technical standards is, by nature, very dynamic and continuously changing. In this paragraph we are going to exhaustively describe the standardisation systems, even if some simplifications are necessary.

The Italian reference body is UNI, the national Italian standardisation body that manages the standardisation activity in Italy together with CEI, the Italian electro-technical committee[13]. Both organisations represent Italy at European and international levels.

All industrialised countries have standardisation bodies that operate in manners similar to those of the two Italian organisations. For example, we can mention the *British Standards Institution* (BSI BS) in the United Kingdom, the *Deutsches Institut für Normung* (DIN) in Germany, the *Association Française de NORmalisation* (AFNOR NF) in France, the *Turkish Standards Institution* (TSI TS) in Turkey, the *Japanese Industrial Standards* (JIS) in Japan and the *GOsudarstvennyy STandart* (GOST) in ex-USSR countries.

The standards issued by these organisations are identified by the acronym of the issuing body affixed as a reference prefix. For example, "UNI 5381 - Trattamenti termici dei materiali metallici, Cementazione" is a standard issued by the Italian standardisation body (UNI), while "BSI BS 8201 - Code of practice for installation of flooring of wood and wood-based panels" is issued by the standardisation body of the United Kingdom (BSI BS).

The situation is more complicated in the United States where several organisations take care of standardisation on an autonomous basis.

The *American National Standards Institute* (ANSI) carries out autonomous standardisation activities at national level and represents the United States at the international one. There are many other important organisations that issue technical standards, such as the *American Society of Mechanical Engineers* (ASME), the *American Society for Testing Materials* (ASTM), the *American Society of Electrical Engineers* (IEEE[14]) and the *American Society of Civil Engineers* (ASCE). Side by side with the main associations listed above, there are other American sources of technical standards intended for specific industrial sectors, among which the *Society of Automotive Engineers* (SAE), the *American Iron and Steel Institute* (AISI) and the *American Welding Society* (AWS). There even exists the Military standard (MIL) that originates from the American Department of Defense. As in the other countries, also in the United States the standards are published bearing the acronym of the issuing body.

---

[13] CEI, established in 1909, takes care of standardisation in the electrotechnical, electronic and telecommunications fields. UNI, established in 1921 under the acronym of UNIM, changed in UNI in 1928, carries out the standardisation activity in all industrial, marketing and services sectors to the exclusion of those cared by CEI.

[14] IEEE is the acronym of the Institute of Electrical and Electronic Engineers.

From this short account, you can easily understand that the approach to standardisation in the United States broadly differ from what happens in the European countries. In this crowded situation, it is normal to have two or more technical standards issued by different bodies that may partially overlap in terms of the subject matters dealt with. To have an idea, compare the following standards: "ASTM A29 - Standard Specification for General Requirements for Steel Bars, Carbon and Alloy, Hot-Wrought", "SAE J403 - Chemical Compositions of SAE Carbon Steels" and "MIL-S-11310E - Steel Bars, Carbon, Hot Rolled, for Cold Shaping Including Cold Extrusion". On the other hand, the opposite is also often true, namely you can have technical standards that are acknowledged by two different bodies. For example, "ASME/ANSI B16 - Standards for Pipes and Fittings" makes clear reference to ASTM standards to select the materials to be used.

In addition to the standardisation activities of the single countries, there are the international issuing bodies. In Europe you find the *Comité Européen de Normalisation* (CEN) the *Comité européen de normalisation en électronique et en électrotechnique* (CENELEC) and the *European Telecommunications Standards Institute* (ETSI) whose activities are aimed at issuing and harmonising European technical standards, eventually implementing homogeneous standards mutually shared by all EU countries.
The acronym EN is the reference prefix for all of the three above mentioned organisations. Most European technical standards bear the acronym of the issuing body of the implementing country (i.e., UNI EN, DIN EN, NF EN, etc.) before the acronym EN. This means that you are reading a harmonised European standard that is acknowledged as a national standard in the country concerned. A typical example is the standard "UNI EN 10088 - Acciai inossidabili" that also exists in the German version as "DIN EN 10088 - Nichtrostende Stähle", French version as "NF EN 10088 - Aciers inoxydables", English version "BS EN 10088 - Stainless Steels", etc.[15]

At still a higher level there is the *International Organization for Standardization* (ISO[16]). This body with offices in Geneva is involved in issuing and harmonising standards at international level. Its function is similar to that of the European bodies, but with a worldwide impact. ISO and the European bodies are directly connected, consequently the standards are often identified as EN ISO or UNI EN ISO (DIN EN ISO, AFNOR EN ISO, etc.) standards. Acronyms are meant to provide a geographical reference of the environment where a certain standard is implemented. For example, you have the standard "ISO 643 Steels - Micrographic determination of the apparent grain size" together with its national sister standards UNI EN ISO 643, DIN EN ISO 643 and BSI BS ISO 643.

---

[15] Not all standards are harmonised at European level. Thus, you can find UNI EN standards and UNI standards: the former are harmonised at European level and acknowledged by the Italian standardisation body, the latter are issued by the Italian organisation only. To this regard, it is useful to reiterate that the standards are always applied voluntarily, they are never binding. A standard issued by a standardisation body shall not be necessarily implemented in its country of origin.

[16] Unlike the other issuing bodies mentioned and unlike what the designation can make you presume, ISO is not an acronym, but takes from the Ancient Greek word ἴσος that means "equal".

On the other hand, no corresponding UNI EN ISO 6336 or DIN EN ISO 6336 standards exist for the standard "ISO 6336 - Calculation of load capacity of spur and helical gears" (and its sister standards NF ISO 6336 and BS 6336).
Notice that no hierarchical order exists among the issuing bodies or the standards; implementing a certain standard or not is always a voluntarily decision. For example, ISO standards are no more acknowledged and accepted than ASTM ones even if they come from an international organisation, while the latter come from a national body (U.S.).
One of the main problems is exactly that there are no common globally-accepted standards. Therefore, a standard is selected exclusively on the basis of the mutual consent of the parties concerned. Implementing a certain standard always depends on an agreement. If both the customer and the supplier (of a product, process or service) decide to be mutually bound by a certain standard, that standard becomes the reference standard for the technical activity to be carried out.

7.5 The Purposes of Technical Standards

Technical standards are very important because, as already said, they represent the state of the art in a certain domain. They are a simple and cost-efficient manner to transfer technological and scientific knowledge from the world of applied research to that of industrial applications.
Implementing the technical standards also promotes standardising and harmonising products, processes and services, which allows both enlarging the pool of customers/suppliers and rationalising company activities. Just think of having a stock of standardised products whose characteristics already meet the requirements of a certain reference technical standard for a certain business sector.
Another consequence of using standards is that the barriers between the countries are more easily overcome. Supplying products, processes and services complying with the standards in use in a certain country allows the companies to better penetrate the local market.
Technical standards are also very useful because they simplify defining contract clauses between customers and suppliers and make it easier to write purchase orders. In particular, applying standards at contract level protects both the customer and the supplier from the legal point of view:

- On one hand, agreeing on a standard, the customer clearly provides the supplier with all the characteristics that a certain product, process or service should guarantee or comply with.
- On the other hand, agreeing on a standard, the supplier clearly defines the limits of the customer's request concerning the characteristics that a certain product, process or service should guarantee or comply with.

In brief, the standards allow the customer to let the supplier know exactly what the customer wants to be guaranteed and the supplier to let the customer know what the supplier can guarantee.

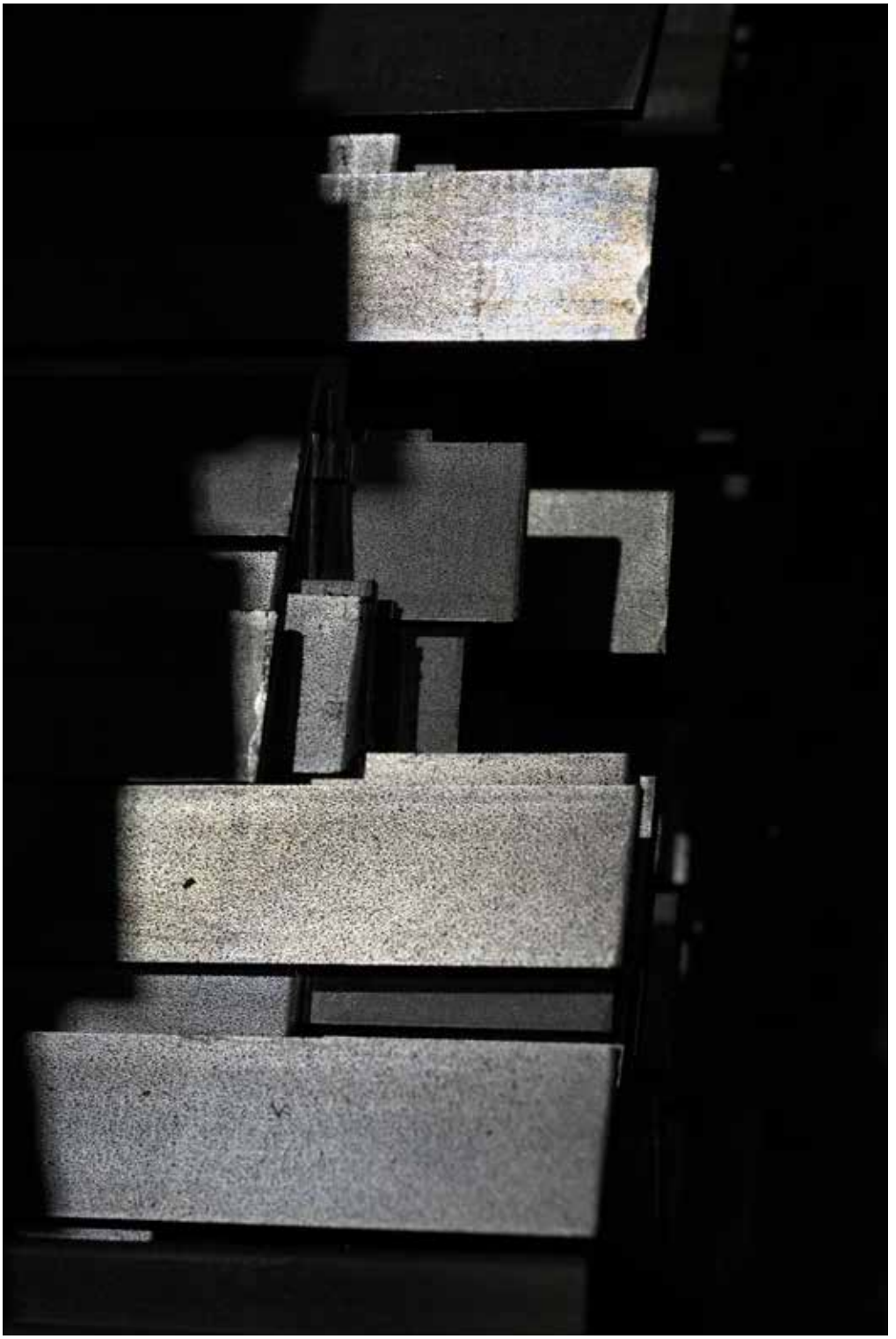

8. GENERAL PURPOSE STRUCTURAL STEELS

General purpose structural steels, also commonly referred to as carbon steels, are hypoeutectoid alloys with a carbon content normally below 0.2%. This is the reason why they are also called mild carbon steels, which means that they contain a low amount of carbon.

Besides carbon, the chemical composition of general purpose structural steels usually does not include other purposely added alloying elements. Remember, however, that due to traditional steelmaking processes, these steels always contain traces of silicon (Si 0.2 to 0.4%) and manganese (Mn 0.3 to 0.7%), which are used as liquid bath deoxidizers, traces of copper (Cu < 0.6%), a scrap iron contaminant, and traces of sulphur and phosphor (S and P < 0.05%) that are noxious elements coming from raw materials[1]. What previously said about manganese traces (0.3 to 0.7%) does not oppose the possibility of adding this element also in higher percentages. In general-purpose structural steels, manganese percentage can be as high as 2.5%.

General purpose structural steels are normally put into service without any prior heat treatment. This means that their mechanical properties and micro structure derive directly from their chemical composition (mainly the carbon content) and from the manufacturing process of the semi-finished products as obtained from hot or cold deformation[2]. However, sometimes it is necessary to perform heat treatments (typically, normalizing or recrystallization annealing) in view of specific applications or to obtain certain properties. General purpose structural steels account for 75 to 80% of the weight of all steel used in all applications.

Mild carbon steels are used to manufacture flat semi-finished products, either hot rolled (sheets, plates, coils, etc.) or cold rolled (sheets, strip, etc.), long semi-finished products, either hot rolled (bars, round bars, profiles, wire rods, etc.) or cold rolled (bars, round bars, wires, etc.), open-die or closed-die forged semi-finished products (flanges, valves, fittings, etc.) as well as hot or cold rolled tubes.

---

[1] It is worth pointing out that the contents of the elements whose traces are present in steels, mainly depend on the steelmaking cycle. Both steels obtained from the "integral cycle" (mineral iron is turned into liquid cast iron in a blast furnace, liquid cast iron is converted into steel in a converter, then the steel liquid bath is worked in the ladle furnace) and steels obtained from the "scrap iron cycle" (scrap iron is molten in an electrical arc furnace and then the steel liquid bath is worked in the ladle furnace) very often contain minuscule quantities (traces) of chemical elements that come from the raw materials used for the steelmaking process (mineral and coke for the "integral cycle", scrap iron for the "scrap iron cycle"). In addition to copper, sulphur and phosphor, steels may exhibit traces of oxygen (O), nitrogen (N), hydrogen (H), antimony (Sb), tin (Sn), arsenic (As), chromium (Cr), nickel (Ni), molybdenum (Mo), aluminium (Al), vanadium (V), niobium (Nb), etc. For more details on steelmaking processes, see the book "Siderurgia - Processi e Impianti" by W. Nicodemi, Associazione Italiana di Metallurgia - Milan, Italy, 1994.

[2] Remember that all semi-finished products commonly used at industrial level (flats and bars as well) are always obtained by hot deformation starting from crude steel (casting ingot or continuous casting billet/slab). After hot deformation, the semi-finished products can be subjected to cold deformation to obtain specific characteristics (limited thickness or diameter, contained geometrical-dimensional tolerances, limited roughness, different mechanical properties, etc.) For example, a 20mm thick plate is obtained by hot deformation starting from an ingot or a billet after several rolling passages whereas a 0.5mm thick strip is the result of a hot rolling process, necessarily followed by cold deformation by means of repeated rolling passages. Obviously, the dimensional tolerances of the two semi-finished products (hot or cold rolled) are widely different.

All these semi-finished products can be used as rolled (i.e., the condition of the material at the end of the production process) or can be surface-coated (plated in zinc, tin, chromium, phosphate, etc.) or pre-painted. Semi-finished products made of general purpose structural steel are put into service to realize several types of structural elements or components. In many cases, these semi-finished products are assembled by welding. For example, think about body-on-frame and unibody car structure, carpentries for the mechanical and civilian sectors or tanks and boilers. Welding allows obtaining lighter and less expensive components in comparison with other joining methods (bolting, nailing or riveting). For all these reasons, steel weldability, which means steel aptitude to provide good-quality flawless welded joints, is an essential feature of this family of materials.

Structural steel semi-finished products are used in numerous applications including, but not limited to, the civilian, building and industrial sectors in general, shipbuilding, tinsmithing, the boiler sector, urban furniture, tubes and piping, fittings, metal shelves, welded pressure cylinders and vessels[3], mechanical carpentry, rebars for reinforced concrete and prestressed concrete, cold formed and/or deep-drawn products, screws and bolts, metal small parts, domestic electric appliances, packaging items and also vehicle structure (either unibody or body-on-frame).

For didactic reasons rather than for application purposes, general-purpose structural steels can be classified on the basis of their mechanical properties. Notwithstanding occurrences of minor overlapping[4], you can identify the three following families:

- *Low strength steels* with UTS $\leq$ 500 MPa, such as non alloy carbon steels for structural or engineering applications (*Carbon steels*), high-speed machining steels (*Free Cutting Steels or Free Machining Steels*), non alloy carbon steels for deep-drawing (*Deep Drawing Steels*), IF steels (*Interstitial Free Steels*) and BH steels (*Bake Hardening Steels*);
- *Medium strength steels* with 500 MPa $<$ UTS $\leq$ 700 MPa, such as carbon-manganese steels for structural or engineering applications (*C-Mn steels*), steels resistant to atmospheric corrosion (*Weathering Steels*) and HSLA steels (*High Strength Low Alloyed Steels*);
- *High strength steels* with UTS $>$ 700 MPa, as DP steels (*Dual-Phase Steels*), TRIP steels (*Transformation Induced Plasticity Steels*), CP steels (*Complex Phase Steels*) and MART steels (*Martensitic Steels*).

---

[3] Components that work under pressure (bottles, vessels, reactors, etc.) can be manufactured by welding together calendered plates of suitable thickness or using semi-finished products with no welded joints. Pressure bottles are an emblematic case. If they are due to work at low pressure (such as for LPG storage or power extinguishers), the bottles are made of general-purpose structural steel plates welded together. It they are used to hold high-pressure gas (such as for storing industrial technical gases or for scuba diving), bottles are made of Q&T steel and obtained from a weldless tube or by deep-drawing.

[4] With reference to the division suggested, it is rather normal that some steel grades fall within two of the families specified. For example, many HSLA carbon steels have mechanical characteristics typical of medium strength steels and actually they are recorded in this family. However, HSLA steels in some chemical compositions and/or following special production processes, can exhibit Rm values typical of high strength steels. The same occurs with Dual-Phase or Complex-Phase steels. Even though they are considered high strength steels, in some cases their mechanical properties make them belong to medium strength steels.

The characteristics of mechanical strength and ductility of general purpose structural steel families are well represented in a graph where Ultimate Tensile Strength, UTS, is plotted in the abscissa axis and its percentage elongation after fracture, A%, is plotted in the ordinate axis (Figure 8.1).

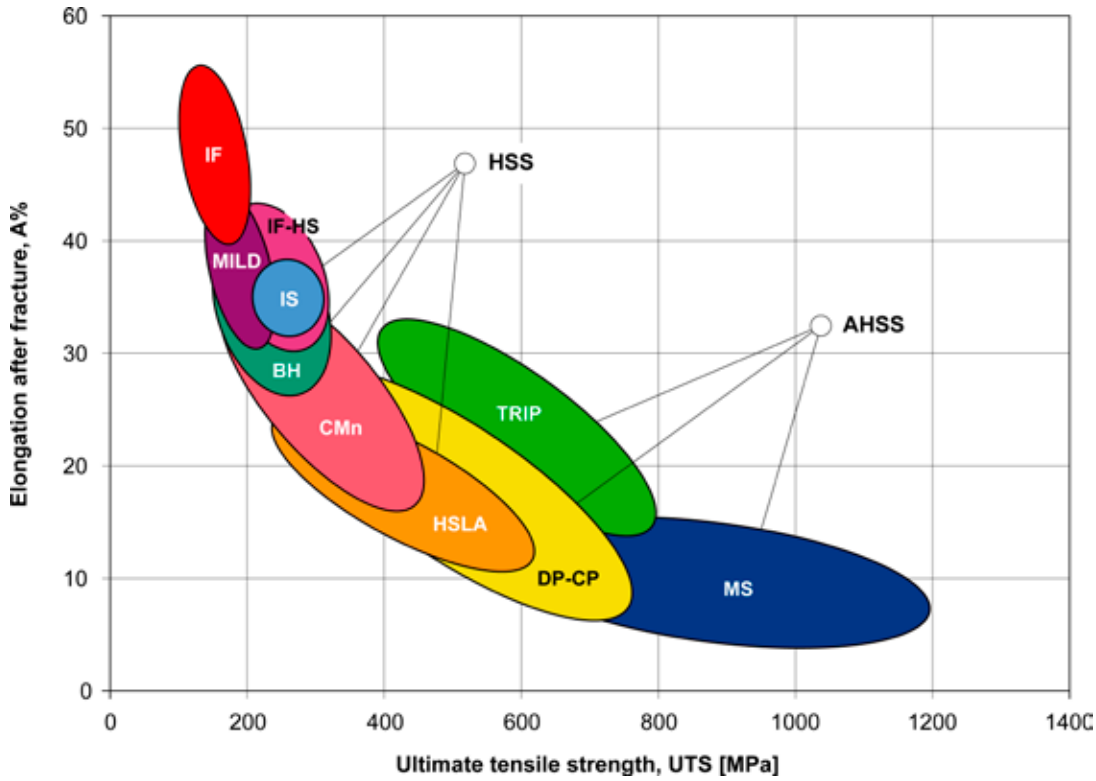

Figure 8.1 – Schematic representation of fields of existence for general purpose structural steels, a.k.a. carbon steels, in an UTS-A% graph [from Sprock et al. 2008].

9. LOW STRENGTH STRUCTURAL STEELS

9.1 Introduction

Low strength steels are Fe-C or Fe-C-Mn hypoeutectoid alloys with a carbon content below 0.20% (typically C ≤ 0.1%) and a manganese percentage not exceeding 1.50%.

From the point of view of ferrous metallurgy, they are killed or controlled-grain killed steels, which means that they are deoxidated in liquid phase by adding silicon and manganese or silicon, manganese and aluminium, respectively. This refining process removes oxygen that is a detrimental element always present in steel baths[1].

Low strength steels have an almost fully ferritic structure, even if sometimes they include small amounts of pearlite elongated along the main hot deformation axis in the semi-finished product. These steels exhibit limited mechanical strength. Their Yield Strength ranges around 150 to 350 MPa and their Ultimate Tensile Strength around 350 to 500 MPa. On the other hand, they exhibit very high cold formability values (percentage elongation after fracture, A%, around 25 to 40%) and excellent weldability (carbon equivalent[2] < 0.4)[3]. Data provided above refer to as-rolled semi-finished products with medium size crystal grains (5 to 7 ASTM = 65 to 32 μm).

---

[1] Through the deoxidation process, oxygen is removed, thereby inhibiting gas development in liquid steel. Gas development results from the carbon oxide gas bubbles that form due to the combination of oxygen and carbon, move in the metal bath and eventually come to the surface and blow causing steel "to boil". If steel was deoxidated (using Si-Mn or Si-Mn-Al), as it happens in modern steel factories, the bath is said to have been killed. If the killing process includes using aluminium, you talk about "fine grain practice" for making killed steels. This is why the very fine aluminium oxide precipitates (Al_2O_3) that form by chemical reaction, remain trapped into solidifying steel and limit crystal grain growth at high temperature during subsequent cooling down.

[2] The carbon equivalent, C_{EV}, is an indicator of steel weldability that can be calculated starting from steel chemical composition according to the formula provided by the International Institute of Welding (IIW) in 1967: $C_{EV} = C + \frac{Mn}{6} + \frac{Cr+Mo+V}{5} + \frac{Cu+Ni}{15}$. The C_{EV} parameter measures steel aptitude to develop cold cracks in a thermally altered area following fast cooling of the joint after welding. In general, if $C_{EV} \leq 0.4$, steel can be welded without special precautions; if $0.4 < C_{EV} \leq 0.6$, steel can be welded after pre-heating the joint; if $C_{EV} > 0.6$, steel might be unweldable. Should welding be required, the joint should be heated before and after welding.

[3] The numerical values provided refer to as-rolled semi-finished products with medium size crystal grains (5 to 7 ASTM = 65 to 32 μm).

Non-Alloy Carbon Steels for Structural Applications

A first field of use of this steel family, mainly in the form of hot rolled semi-finished products or *coils*, includes structural and/or engineering applications that do not require high mechanical strength (section bars for mechanical carpentry and civil buildings, welded tubes, steel plates, zinc-coated structural components, urban furniture, tanks, welded gas cylinders, etc.). Below you find some examples of steels belonging to this sub-category.

- EN S235J0 and EN S275J2: As-rolled steels for structural applications in thickness between 3 and 150 mm, as specified in the EN 10025-2 standard[4] (S refers to the structural application and the number that follows is the guaranteed minimum Yield Strength[5]; J0 and J2 respectively indicate that steel must have a minimum impact strength of 27J at 0°C and 27J at -20°C);
- EN P235S: As-rolled steel for tanks and simple pressure systems, as specified in the EN 10207 standard[6] (P refers to the pressure application and the number that follows is the guaranteed minimum Yield Strength; S indicates that is used for naval construction);
- EN E195+N: Normalized steel suitable for the manufacture of welded tubes for engineering applications, as specified in the EN 10296-1 standard[7] (E refers to the engineering application and the number that follows is the guaranteed minimum Yield Strength; +N indicates that the semi-finished product was normalized by means of heat treatment);
- EN S220GD+ZF: As-rolled or hot zinc-plated steel for structural applications in thickness between 0.2 and 3 mm, as specified in the EN 10346 standard[8] (S refers to the structural application and the number that follows is the guaranteed minimum Yield Strength; GD+ZF indicates that the semi-finished product was zinc-plated in a zinc-iron bath).

Tables 9.1 and 9.2 show the reference standards, chemical composition and mechanical properties of non-alloy carbon steels for the structural or engineering applications listed above. Figures 9.1 and 9.2 highlight the typical ferrite-pearlite micro-structure elongated in the rolling direction for steel grades EN S275J2 and EN P235S.

---

[4] EN 10025-2: Hot rolled products of structural steels - Part 2: Technical delivery conditions for non-alloy structural steels

[5] The guaranteed minimum Yield Strength (YS) always refers to the minimum thickness of the semi-finished products. As the thickness of the semi-finished product increases, the minimum value of YS to be guaranteed tends to gradually decrease. For example, in the case of S235J2, the guaranteed minimum load for metal plates in thickness 16 mm or lower is exactly 235 MPa; with thickness of the semi-finished product between 150 and 200 mm, the minimum YS value would be 185 MPa. To this regard, it is always opportune to read the applicable standards to know the correct values of the mechanical characteristics to be guaranteed.

[6] EN 10207: Steels for simple pressure vessels. Technical delivery requirements for plates, strips and bars.

[7] EN 10296-1: Welded circular steel tubes for mechanical and general engineering purposes - Technical delivery conditions - Non-alloy and alloy steel tubes.

[8] EN 10346: Continuously hot-dip coated steel flat products for cold forming – Technical delivery conditions.

Designation	Standard	%C	%Si	%Mn	%P	%S	%N	%Cu	%Al_{tot}
S235J0	EN 10025	≤ 0.17	---	≤ 1.40	≤ 0.030	≤ 0.030	≤ 0.012	≤ 0.55	(*)
S275J2	EN 10025	≤ 0.18	---	≤ 1.50	≤ 0.025	≤ 0.025	---	≤ 0.55	(**)
P235S	EN 10207	≤ 0.16	≤ 0.35	0.40-1.20	≤ 0.025	≤ 0.025	≤ 0.010	n.s.	≤ 0.020
E195+N	EN 10296	≤ 0.15	≤ 0.35	≤ 0.70	≤ 0.045	≤ 0.045	n.s.	n.s.	n.s.
S220GD+ZF	EN 10346	≤ 0.20	≤ 0.60	≤ 1.70	≤ 0.10	≤ 0.045	n.s.	n.s.	n.s.

(*) Killed using Si-Mn.

(**) Killed using Si-Mn-Al, with fine grain.

n.s.: not specified.

Table 9.1 – Heat analysis for some low strength non-alloy carbon steels for structural or engineering applications.

Designation	Standard	Yield Strength, YS [MPa]	Ultimate Tensile Strength, UTS [MPa]	Elongation after fracture, A%	Sampling position
S235J0 (*)	EN 10025-2	≥ 235	360-510	≥ 26	longitudinal
S275J2 (*)	EN 10025-2	≥ 275	410-560	≥ 23	longitudinal
P235S (*)	EN 10207	≥ 235	360-480	≥ 26	longitudinal
E195+N (**)	EN 10296-1	≥ 195	≥ 300	≥ 28	longitudinal
S220GD+ZF (***)	EN 10346	≥ 220	≥ 300	≥ 20 (°)	longitudinal

(*) values to be guaranteed in flat semi-finished products in thickness 3 mm $\leq$ tck. $\leq$ 16 mm.
(**) values to be guaranteed in tubes in thickness tck. $\leq$ 40 mm.
(***) values to be guaranteed in flat semi-finished products in thickness tck. > 0.7 mm.
(°) percentage elongation after fracture is determined in an 80 mm L_0 gauge length (A_{80mm}), which is a typical value for non proportional specimens, and not in $L_0 = 5.65 \cdot \sqrt{S_0}$, as with the traditional proportional specimen.

Table 9.2 – Mechanical properties of semi-finished products obtained from low strength non-alloy carbon steels for structural or engineering applications.

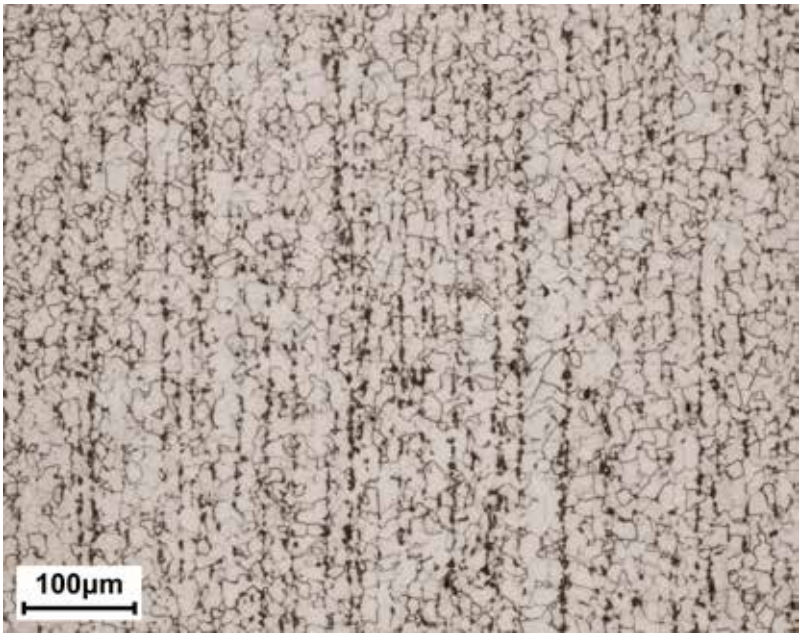

Figure 9.1 – Metallographic appearance of low strength non-alloy carbon steel grade EN S235J0. Notice ferrite and pearlite in banded micro-structure orientated in the rolling direction of the semi-finished product; etching agent: Nital 2% [Omeco S.r.l. Laboratories - Monza, Italy].

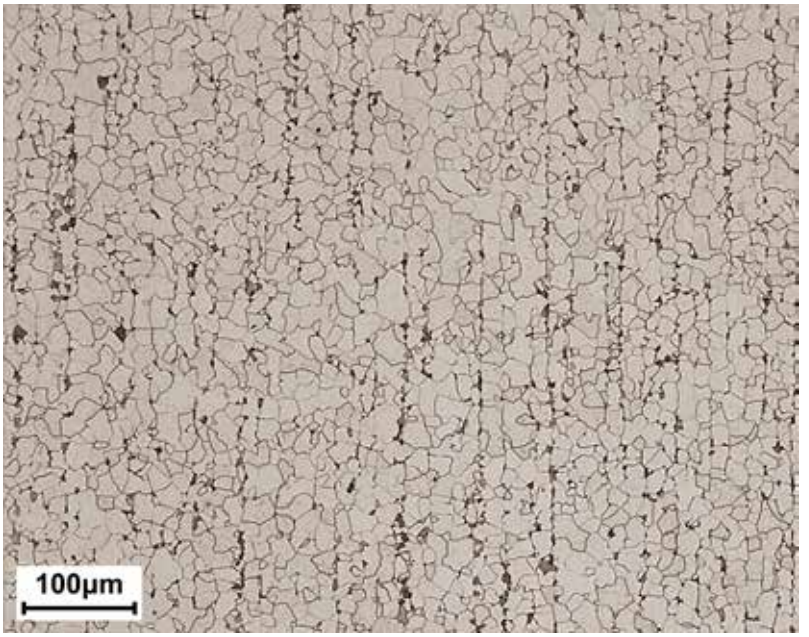

Figure 9.2 – Metallographic appearance of low strength non-alloy carbon steel grade EN E195+N. Notice ferrite and pearlite in banded structure orientated in the rolling direction of the semi-finished product; etching agent: Nital 2% [Exova S.r.l. Laboratories - Crema, Italy].

9.3 Free Cutting (*Free Machining*) Steels

Free cutting steels are iron alloys whose chemical composition was specially developed for easier high-speed machining (> 30 m/min). To achieve this target, several characteristics are required, namely: chips should easily break into fragments during machining (Figure 9.3), built-up edge formation should be limited[9], and tool wear, nicks, heat micro-cracks and cratering should be reduced. In addition to these properties, free cutting steels are also required to develop a sort of self-lubricating action upon contact with the tool.

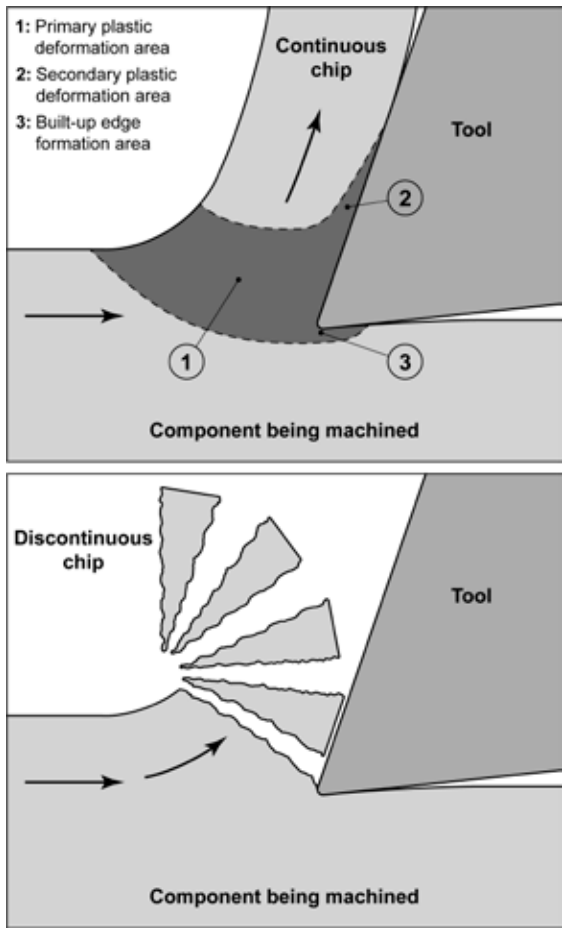

Figure 9.3 – Chip formation upon tool contact with the part: (a) continuous chip; (b) discontinuous fragmented chip.

[9] *The term built-up edge defines the portion of material that, after being heavily strain hardened by cutting, does not detach from the tool flank, but almost "clutches" to it, thereby changing tool geometry. The built-up edge worsens both tool wear and the surface finish of the components being machined.*

Free cutting steels are very similar to steels for structural or engineering applications, but they are characterised by the presence of sulphur and/or lead. These chemical elements are added during manufacture to improve steel machinability.

The presence of sulphur in contents of approximately 0.30 to 0.40% and of manganese around 1 to 1.5% promotes the formation of manganese sulphides (MnS) forming inclusions elongated in the direction of maximum plastic strain, while avoiding that the metallic mass becomes excessively brittle[10]. Another chemical element used to improve machinability is lead, which sometimes is present in contents between 0.20 to 0.35%. This element is not soluble in steel and forms small-sized roundish discontinuities[11].

Both manganese sulphide inclusions and lead inclusions support chip breakage and exert a self-lubricating action at the tool/part interface. Not only cutting forces, tool wear and built-up edge are lower than in traditional steels, but also you observe an improvement of dimensional stability and surface finish of machined parts (Figure 9.4). In general, the best machinability conditions exist when inclusions are small, roundish and evenly distributed in the metallic mass (Figure 9.5).

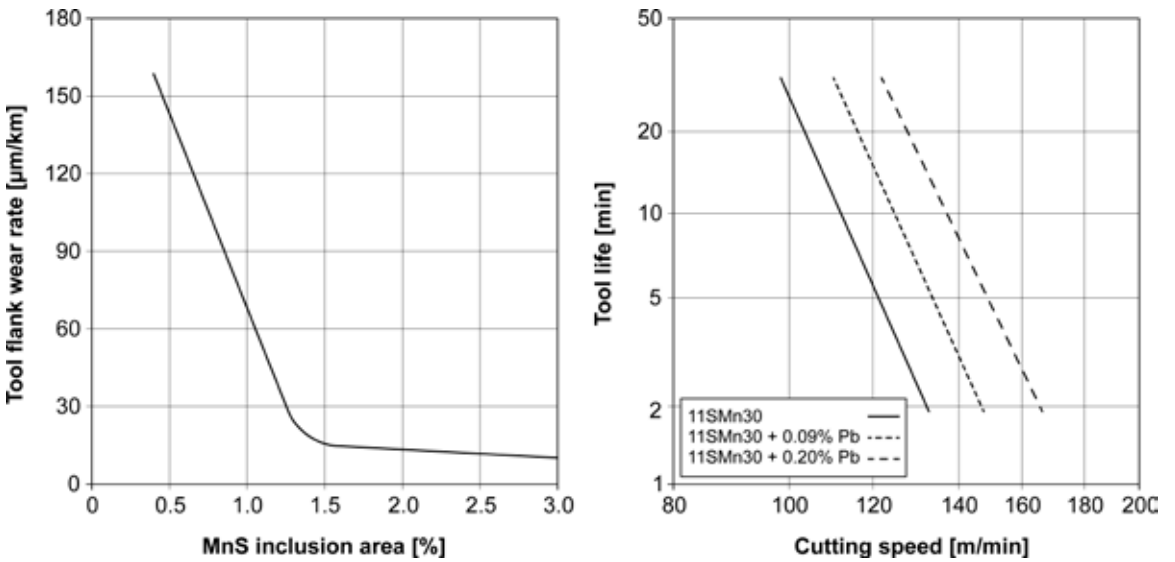

Figure 9.4 – Effect of (a) sulphur and (b) lead on cutting tool wear [from Wannel 1977].

[10] Sulphur is known to be detrimental to steels. The presence of free sulphur causes considerable brittleness problems in the metallic mass, both at room temperature and in hot conditions. Without manganese, high sulphur percentages lead to the formation of iron sulphides with melting temperatures of about 1000°C at grain boundary. The presence of these low-melting compounds should be avoided because it results in steel disintegration during the industrial processes performed at high temperature (hot rolling, forging, welding, etc.). Brittleness caused by iron sulphides provokes considerable problems also in cold conditions, both in terms of impact strength and fracture toughness.

[11] Lead is toxic for man and the environment; therefore, it is being gradually eliminated from many industrial applications. In this study case, it will be replaced with other chemical elements performing a similar "chip-breaking" action such as tellurium, selenium or bismuth.

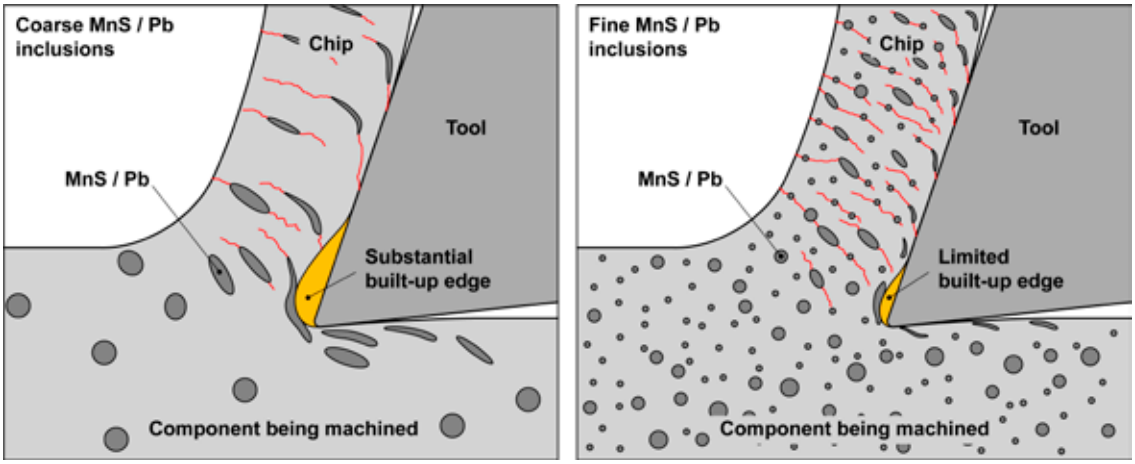

Figure 9.5 – Effect of inclusion size/distribution on formation of chips and built-up edge: (a) large inclusions, (b) small inclusions. The red lines indicate the possible chip fracture planes during machining by chip removal while the orange area highlights the built-up edge on the tool [from Hashimura et al. 2007].

Free-cutting steels are mainly used to manufacture screws and bolts, nuts, metal fittings and small parts, small components for the automotive sector and for the mechanical industry in general. High sulphur and phosphor contents drastically decrease free-cutting steel weldability in comparison with carbon steels.
Below you find some examples of steels belonging to this sub-category.
EN 11SMn30 and EN 11SMnPb30: Free-cutting steels in hot-rolled bars and wire rods, as specified in the EN ISO 683-4 standard[12]. Their designation is based on the chemical composition even if they are general-purpose structural steel to all effects (the first number is the nominal carbon percentage multiplied by 100; the letters represent the chemical elements, sulphur and manganese or sulphur, manganese and lead, listed in order of decreasing amount; the last number is the nominal content of the first element in the previous sequence, in this case sulphur, multiplied by 100[13]).
Tables 9.3 and 9.4 show the reference standards, chemical composition and mechanical properties for the free cutting steels listed above. Figure 9.6 illustrates the ferrite-pearlite micro-structure with MnS and Pb inclusions typical of 11SMnPb30 steel.

[12] *EN ISO 683-4: Heat-treatable steels, alloy steels and free-cutting steels - Part 4: Free-cutting steels.*

[13] *Remember that the multiplying factor for Cr, Co, Mn, Ni, Si and W is 4; for Al, Be, Cu, Mo, Nb, Pb, Ta, Ti, V and Zr is 10; for N, P, S and Cs is 100; and for B is 1,000.*

Designation	Standard	%C	%Si	%Mn	%P	%S	%Pb
11SMn30	EN ISO 683-4	≤ 0.14	≤ 0.05 (*)	0.90-1.30	≤ 0.11	0.27-0.33	---
11SMnPb30							0.20-0.35

(*) For special steelmaking processes, you can foresee 0.10 ≤ %Si ≤ 040.

Table 9.3 – Heat analysis for some free-cutting steels.

Designation	Standard	Yield Strength, YS [MPa]	Ultimate Tensile Strength, UTS [MPa]	Brinell hardness, [HB]	Sampling position
11SMn30 (*)	EN ISO 683-4	non indicato	380-570	≤ 169	longitudinal
11SMnPb30 (*)					

(*) Values to be guaranteed in long semi-finished products in dia. 5 mm < Ø ≤ 40 mm.

Table 9.4 – Mechanical characteristics of semi-finished products obtained from some free-cutting steels.

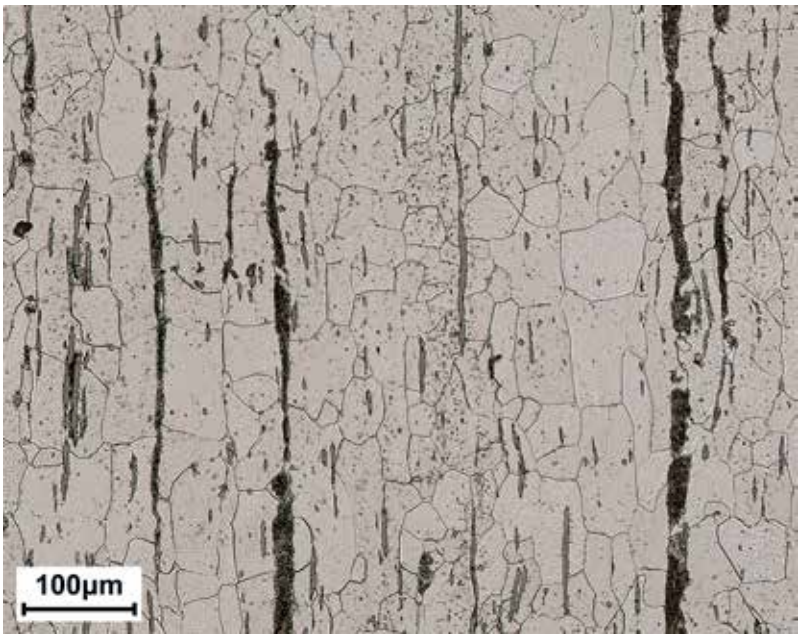

Figure 9.6 – Metallographic appearance of free-cutting steel grade EN 11SMnPb30. Notice the presence of MnS and Pb inclusions and of ferrite and pearlite in the typical banded micro-structure orientated in the rolling direction of the semi-finished product; etching agent: Nital 2% [Laboratories of the Department of Mechanical Engineering of Politecnico di Milano – Milan, Italy].

9.4 Steels for Deep-Drawing and Cold Forming

A third application sector for low strength steels, and definitely a more substantial one in terms of volumes and market shares in comparison with those previously dealt with, includes the automotive sector (chassis, wheels, car body[14]), the food *packaging* sector and the electrical appliances sector.

The semi-finished products used in these sectors include steel sheets and strips for cold-forming, sheet metal drawing, deep-drawing and shearing, either as-rolled, painted or zinc-, tin- or chromium-plated. In most cases, they are fine grain killed steels that were deoxidated using silicon, manganese or aluminium with the minimum possible attainable carbon and free nitrogen contents in the iron lattice.

Normally, the steel strip is cold rolled to give it the geometrical/dimensional tolerances and roughness typically required in deep-drawing applications (as it happens with automotive car body). Subsequently, the semi-finished product is annealed for recrystallisation purposes to restore the original ductility characteristics of the material[15].

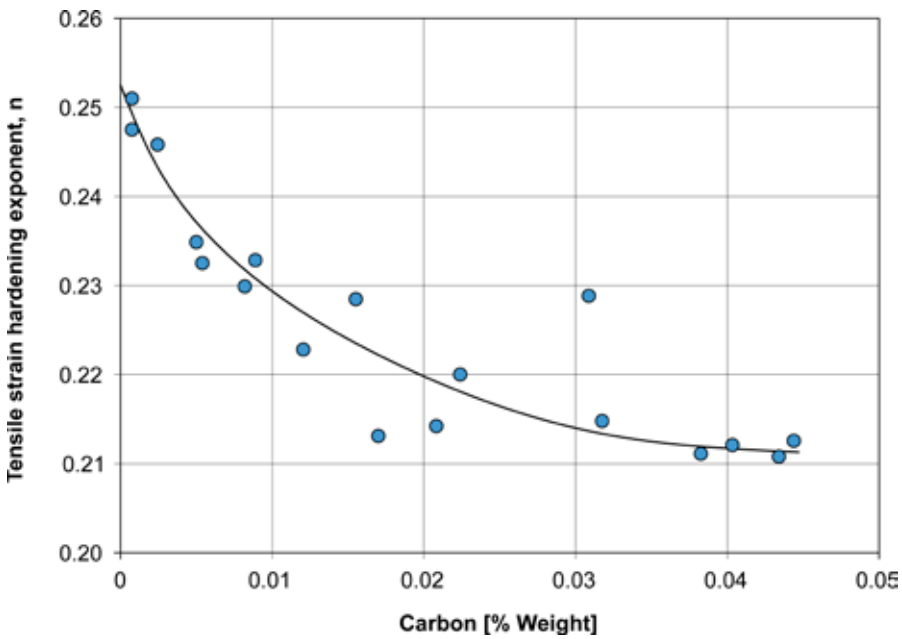

Figure 9.7 – Trend of the strain hardening index *n* from Hollomon equation as a function of steel carbon content (steels with a very low carbon content, steels killed using aluminium and annealed in line at 700°C and 850°C) [from Ono et al. 1982].

[14] Keep in mind that in most cases, car body (hood, roof, doors, etc.) are made of steel strips in thickness between 0.7 and 0.9 mm.

[15] Recrystallisation annealing can be performed in chamber furnaces or in furnaces lined up after the last cold rolling mill stands.

To this regard, a first property to be considered to evaluate steel cold formability is the strain hardening index *n* that can be obtained from Hollomon equation after tensile tests[16]. High values of *n* indicate a considerable aptitude of the steel strip to being formed by *stretching* together with its homogeneous and even behaviour as to ductility in view of preventing crack formation and premature necking in the semi-finished product. Typically, the value of the index *n* tends to increase as the interstitial chemical elements (carbon and nitrogen) and the manganese content decrease (Figure 9.7). Also, *n* increases as the average crystal grain size increases, at least up to an average size of approximately 40 µm beyond which no further noticeable improvement occurs (Figure 9.8). The presence of second phases and/or of precipitates improves ductility as a function of the increase in their average distance.

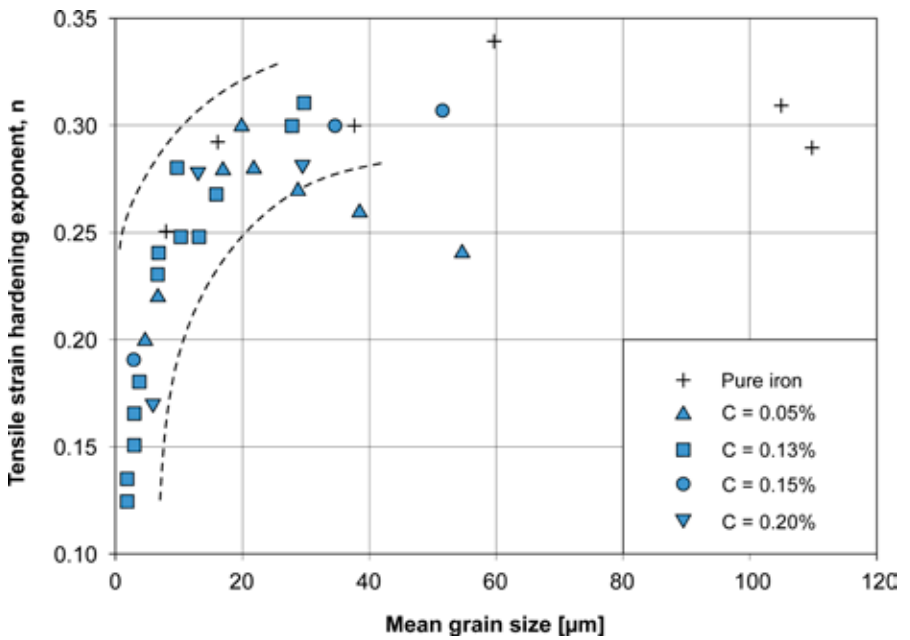

Figure 9.8 – Trend of the strain hardening index *n* from Hollomon equation as a function of mean grain size for pure iron and for low carbon steels [from Morrison 1966].

The other important parameter to be taken into account with cold-forming steels is the plastic strain ratio *r* or Lankford coefficient that can also be obtained from simple tensile tests.

[16] *See Chapter 1, para. 1.4.*

The plastic strain ratio r varies depending on the sampling direction. This is the reason why you usually calculate an average value, r_m, starting from r measured along three different directions relative to the strip rolling axis (r_0, r_{45}, r_{90})[17].
High r_m values guarantee excellent sheet drawability (drawing), together with limited wrinkling. Also in this case, the decrease of the interstitial chemical elements in solution in the crystal lattice (typically carbon and nitrogen) leads to a gradual increase of the average plastic strain ratio r_m (Figure 9.9).

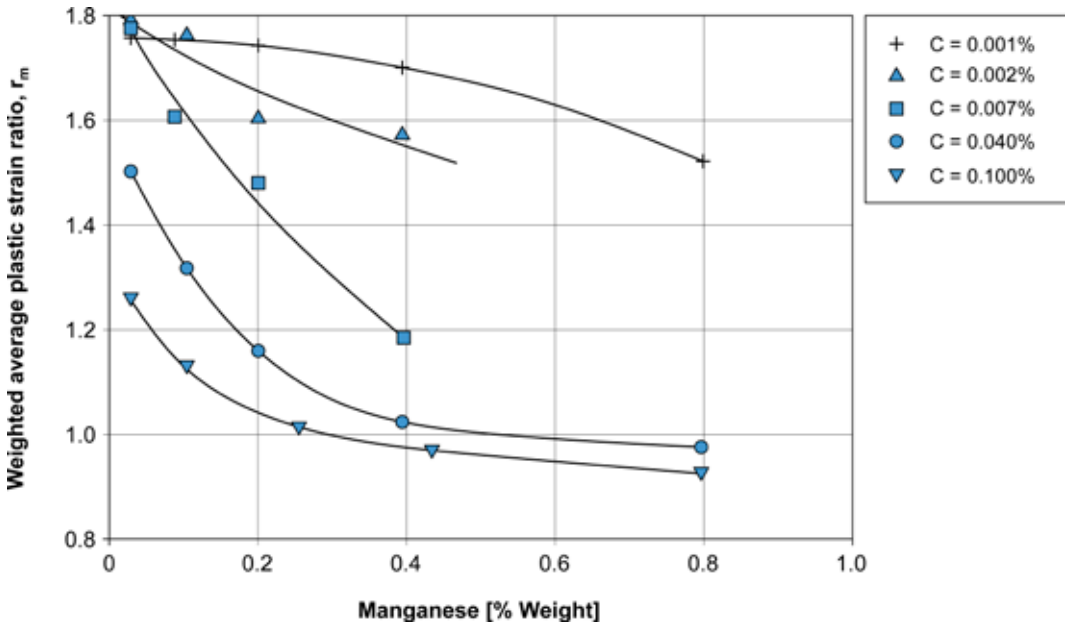

Figure 9.9 – Trend of the average plastic strain ratio r_m with reference to carbon and manganese contents in steel [from Osawa et al. 1984].

Using the plastic strain ratio r, you can also evaluate the strip planar anisotropy according to the following formula:

$$\Delta r = \frac{1}{2} \cdot (r_0 - 2r_{45} + r_{90}) \quad \text{[eq. 9.1]}$$

Values of Δr close to zero allow steel homogeneous formability along all directions (isotropic material); if $\Delta r > 0$ (the commonest case) or if $\Delta r < 0$, earring is bound to occur in deep-drawn semi-finished products (Figure 9.10).

[17] See Chapter 2 in this book on steel tensile testing. Remember that while calculating the average plastic strain ratio, r_m, the value r_{45} should be considered twice.

Finally, notice that non-alloy carbon steels for structural and engineering applications as well as those for cold-forming/deep-drawing come with excellent weldability. This characteristic is absolutely important in all industrial applications for this family of materials.

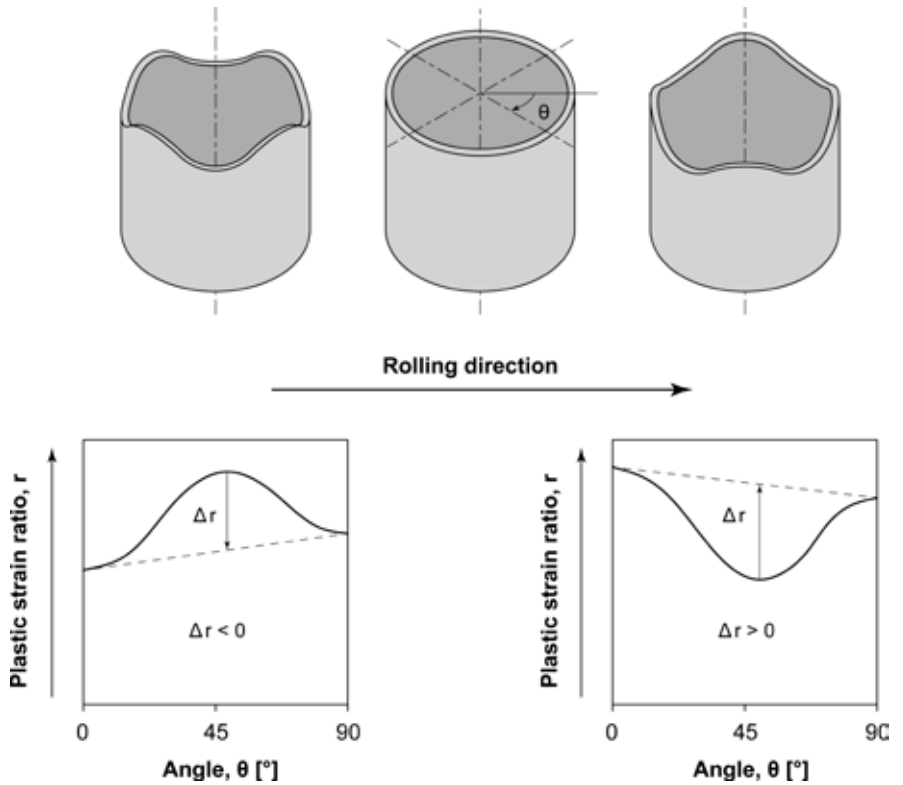

Figure 9.10 – Earring trend in deep-drawn semi-finished products with reference to the planar anisotropy value Δr of the steel strip [from Wilson and Butler 1961-1962].

Below you find some examples of steels belonging to this sub-category. It should be pointed out that such designations focus on steel cold formability and not on its mechanical strength.

- EN DD14: Hot rolled steel plate/strip for cold forming in thickness between 1 and 11 mm, as specified in the EN 10111 standard[18] (the first D refers to a flat semi-finished product meant for cold forming while the second D explains that the semi-finished product was obtained by hot deformation; the number is a progressive formability value according to an arbitrary scale defined in the standard);

[18] *EN 10111: Continuously hot rolled low carbon steel sheet and strip for cold forming – Technical delivery conditions.*

- EN DC05: Cold rolled steel strip for deep-drawing in thickness between 0.35 and 3 mm, as specified in the EN 10130 standard[19] (D refers to a flat semi-finished product meant for cold forming while C explains that the semi-finished product was obtained by cold deformation; the number is a progressive formability value according to an arbitrary scale defined in the standard);
- EN DX51D+Z: Zinc-plated steel strip for deep-drawing in thickness between 0.7 and 3 mm, as specified in the EN 10346 standard[20] (D refers to a flat semi-finished product meant for cold-forming while X explains that the finish rolling method is not specified; the number is a progressive formability value according to an arbitrary scale defined by the standard; D+Z refers to a semi-finished product whose characteristics are conditioned by hot zinc-plating in a zinc bath);
- EN TS260: Steel strip for food packaging in thickness between 0.13 and 0.49 mm, as specified in the EN 10202 standard[21] (the letter T indicates that this is white latten while S explains that the semi-finished product was annealed in a non-continuous furnace; the number that follows is the guaranteed minimum Yield Strength).

Tables 9.5 and 9.6 show the reference standards, chemical composition and mechanical properties for the cold forming steels listed above. Figure 9.11 highlights the typical micro-structure composed of homogeneous ferritic grains in a cold-forming/deep-drawing steel.

Designation	Standard	%C	%Si	%Mn	%P	%S	$\%Al_{tot}$	%Ti
DD14	EN 10111	≤ 0.08	n.s.	≤ 0.35	≤ 0.025	≤ 0.025	(*)	n.s.
DC05	EN 10130	≤ 0.06	n.s.	≤ 0.35	≤ 0.025	≤ 0.025	(*)	n.s.
DX54D+Z	EN 10346	≤ 0.12	≤ 0.50	≤ 0.60	≤ 0.10	≤ 0.045	(*)	≤ 0.30
TS260 (**)	EN 10202	0.04-0.08	≤ 0.030	≤ 0.025	≤ 0.020	≤ 0.020	0.02-0.08	n.s.

(*) killed using Si-Mn-Al, with fine grain.
(**) the chemical composition of white latten steels also includes: Cu ≤ 0.080; Ni ≤ 0.080; Cr ≤ 0.080; N ≤ 0.008; and for any other X element ≤ 0.020.
n.s.: not specified.

Table 9.5 – Heat analysis of some low strength non-alloy carbon steels for deep-drawing and cold forming.

[19] *EN 10130: Cold rolled low carbon steel flat products for cold forming. Technical delivery conditions.*

[20] *EN 10346: Continuously hot-dip coated steel flat products for cold forming – Technical delivery conditions.*

[21] *EN 10202: Cold reduced tinmill products. Electrolytic tinplate and electrolytic chromium/chromium oxide coated steel.*

Designation	Standard	Yield Strength, YS [MPa]	Ultimate Tensile Strength, UTS [MPa]	Elongation after fracture, A%	Index r_{90}	Index n_{90}	Sampling position
DD14 (*)	EN 10111	170-310	$\leq$ 380	$\geq$ 36	---	---	transversal
DC05 (**)	EN 10130	$\leq$ 180	270-330	$\geq$ 40 (°)	$\geq$ 1.9	$\geq$ 0.20	transversal
DX54D+Z (***)	EN 10346	120-220	260-350	$\geq$ 36 (°)	$\geq$ 1.6	$\geq$ 0.18	transversal
TS260	EN 10202	260±50	360±50	---	---	---	n.s.

(*) values to be guaranteed in flat semi-finished products in thickness 3 mm $\leq$ tck. $\leq$ 16 mm.
(**) values to be guaranteed in tubes in thickness tck. $\leq$ 40 mm.
(***) values to be guaranteed in flat semi-finished products in thickness tck. > 0.7 mm.
(°) percentage elongation after fracture is determined in an 80 mm L_0 gauge length (A_{80mm}), which is a typical value for non proportional specimens, and not in $L_0 = 5.65 \cdot \sqrt{S_0}$, as with the traditional proportional specimen.

Table 9.6 – Mechanical characteristics of semi-finished products obtained from some low strength non-alloy carbon steels for deep-drawing and cold forming.

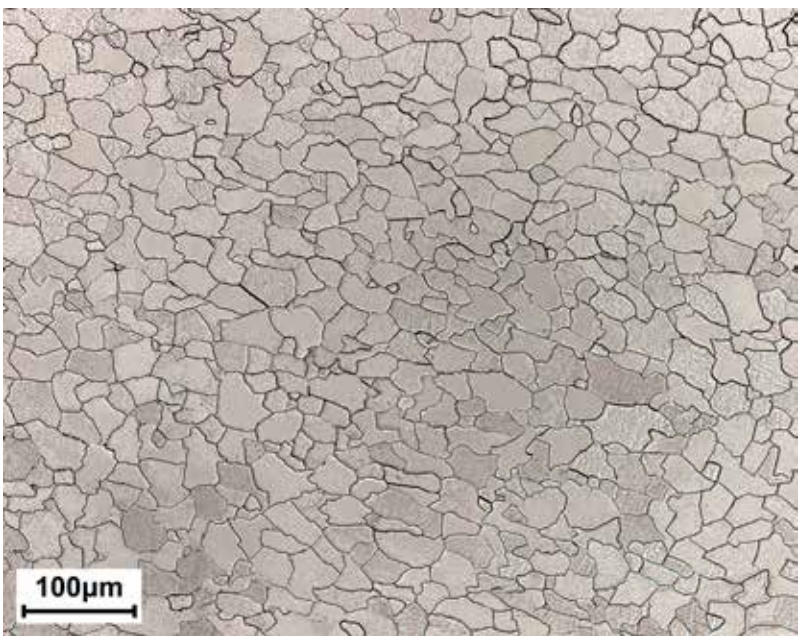

Figure 9.11 – Metallographic appearance of cold forming steel grade EN DD14. Notice the fully recrystallised ferritic structure; etching agent: Nital 2%. [Laboratories of the Department of Mechanical Engineering of Politecnico di Milano – Milan, Italy].

9.5 *Interstitial Free* (IF) Steels

This family, that was developed in the Seventies of the last century in Japan, is composed of very low carbon steels. These steels are used for cold forming complex shapes in the automotive sector, especially to make the car frame structural elements (side members, cross members, wheelhouses, etc.). They are widely diffused due to increasing demand for improved mechanical strength with reduced car weight.

As their name suggests, these steels are manufactured with extremely low amounts of carbon and nitrogen (interstitial elements); typically, carbon is present in contents ranging around 40 to 70 ppm (0.004% to 0.007%). It is worth mentioning that an IF steel sub-family also exists that is called Ultra Low Carbon Interstitial Free (ULC-IF) where carbon and nitrogen contents are below 30 ppm.

Additional stabilising elements, such as titanium and niobium (sometimes also vanadium and boron), are added to IF and ULC-IF steels. In this manner, you neutralise all carbon and nitrogen that are free in solution as carbides/carbonitrides, thereby significantly increasing steel aptitude to cold forming. If you need to increase mechanical strength, you can add phosphor (P ≤ 0.1%) and manganese (Mn ≤ 1%).

Similar to deep-drawing steels, also IF steel strips are subjected to recrystallisation annealing after hot and cold rolling.

From the mechanical point of view, these steels have a very low Yield Strength (200 to 280 MPa) and an YS/UTS ratio around 0.6. They exhibit considerable cold-forming and deep-drawing characteristics with high values of percentage elongation after fracture, A%, strain hardening index, n, and plastic strain ratio, r_m).

Below you find some examples of steels belonging to this sub-category.

EN HC180Y and EN HC260Y: Cold rolled steel strips for cold forming in thickness up to 3 mm, as specified in the EN 10268 standard[22] (H refers to a high-strength flat product for cold forming; C refers to a cold-finished semi-finished product; the number that follows is the guaranteed minimum Yield Strength; Y is the symbol representing *Interstitial Free steels*);

EN HX180YD and EN HX180YD: Cold rolled hot coated steel strips for cold forming in thickness up to 3 mm, as specified in the EN 10346 standard[23] (H refers to a high-strength flat product for cold forming; X refers to a semi-finished product without indication on the finishing process; the number that follows is the guaranteed minimum Yield Strength; Y is the symbol representing *Interstitial Free steels* and D indicates hot coating).

[22] *EN 10268: Cold rolled steel flat products with high Yield Strength for cold forming. Technical delivery conditions.*

[23] *EN 10346: Continuously hot-dip coated steel flat products for cold forming. Technical delivery conditions.*

Tables 9.7 and 9.8 show the reference standards, chemical composition and mechanical properties for the IF steels listed above. Their micro-structure is composed of very fine homogeneous ferritic grains, with nanometric precipitates (carbides, nitrides and carbonitrides) that are not visible using the traditional techniques of optical microscopy (Figure 9.12).

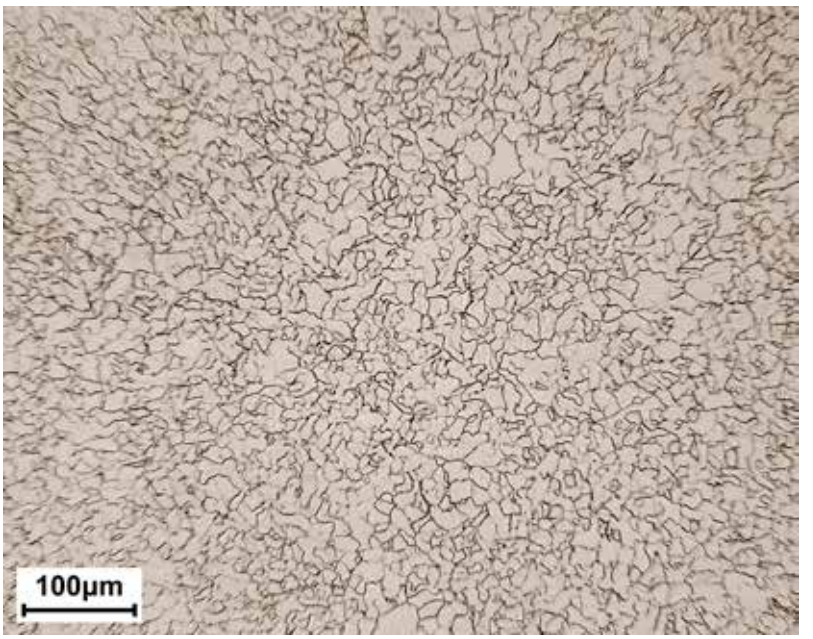

Figure 9.12 – Metallographic appearance of *interstitial Free steel* grade EN HC180Y. Notice the fully recrystallised ferritic structure; etching agent: Nital 2%. [Laboratories of the Department of Mechanical Engineering of Politecnico di Milano – Milan, Italy].

Designation	Standard	%C	%Si	%Mn	%P	%S	$\%Al_{tot}$	%Ti	%Nb
HC180Y	EN 10268	≤ 0.01	≤ 0.30	≤ 0.7	≤ 0.06	≤ 0.025	≥ 0.01	≤ 0.12	≤ 0.09
HC260Y		≤ 0.01	≤ 0.30	≤ 1.6	≤ 0.10	≤ 0.025	≥ 0.01	≤ 0.12	≤ 0.09
HX180YD	EN 10346	≤ 0.01	≤ 0.30	≤ 0.70	≤ 0.06	≤ 0.025	≥ 0.01	≤ 0.12	≤ 0.09
HX260YD		≤ 0.01	≤ 0.30	≤ 1.60	≤ 0.10	≤ 0.025	≥ 0.01	≤ 0.12	≤ 0.09

Niobium and titanium can be used as individual alternatives or in combination to obtain the characteristics desired. In addition, you may also use vanadium and boron, provided that their total amount (Nb + Ti + V + B) does not exceed 0.22%. Al_{tot} means both free aluminium and aluminium combined into oxides.

Table 9.7 – Heat analysis for some *interstitial free steels*.

Designation	Standard	Yield Strength, YS [MPa]	Ultimate Tensile Strength, UTS [MPa]	Elongation after fracture, A%	Index r_{90}	Index n_{90}	Sampling position
HC180Y (*)	EN 10268	180-230	330-400	≥ 35 (°)	≥ 1.7	≥ 0.19	transversal
HC260Y (*)		260-320	380-440	≥ 31 (°)	≥ 1.4	≥ 0.17	transversal
HX180YD (**)	EN 10346	180-240	330-390	≥ 34 (°)	≥ 1.7	≥ 0.18	transversal
HX260YD (**)		260-320	380-440	≥ 30 (°)	≥ 1.4	≥ 0.16	transversal

(*) values to be guaranteed in semi-finished products in thickness 0.7 mm < tck. ≤ 2 mm.
(**) values to be guaranteed in semi-finished products in thickness 0.7 mm < tck. ≤ 1.5 mm.
(°) percentage elongation after fracture is determined in an 80 mm L_0 gauge length (A_{80mm}), which is a typical value for non proportional specimens, and not in $L_0 = 5.65 \cdot \sqrt{S_0}$, as with the traditional proportional specimen.

Table 9.8 – Mechanical characteristics of semi-finished products obtained from interstitial free steels.

9.6 *Bake Hardening* (BH) Steels

The chemical composition, mechanical characteristics and applications of BH steels, which were developed in the late Eighties of the last century, are very similar to those of IF steels. The main difference lies in the presence of limited carbon and nitrogen contents, purposely left in solution in the α-iron lattice to promote *Bake Hardening*. In IF steels, instead, all carbon is combined into carbides or carbonitrides.

The *Bake Hardening* effect derives from the combined action of strain hardening due to cold deformation and subsequent ageing that occurs during hot painting (temperature is kept at 160° to 180°C for 20 to 30 minutes). Ageing improves steel mechanical strength and increases its Yield Strength. This phenomenon is caused by carbon and nitrogen diffusing towards high dislocation areas, specifically where strain hardening was effectively performed. Migration of interstitial elements causes the carbon and nitrogen atoms to closely gather forming the so-called Cottrell atmospheres[24], where dislocations are pinned. This process considerably increases the stress level necessary to set the dislocations in motion, thereby increasing steel Yield Strength[25].

BH steels offer the advantage of having low Yield Strength and high formability before cold deformation. After hot painting, the component's Yield Strength increases by approximately 50 MPa, depending on the strain hardening level attained.

[24] Cottrell atmospheres are thick gatherings of carbon and nitrogen atoms in the iron lattice where they are attracted by the energy fields generated by dislocation piling-up.

[25] If not controlled, aging of mild carbon steels can have very negative effects and, in critical conditions, result in brittle fracturing of the semi-finished product or of the finished component.

Below you find some examples of steels belonging to this sub-category.

- EN HC180B, EN HC220B and EN HC260B: Cold rolled steel strips for cold forming in thickness up to 3 mm, as specified in the EN 10268 standard[26] (H refers to a high strength flat product for cold forming; C refers to a cold rolled semi-finished product; the number that follows is the guaranteed minimum Yield Strength; B is the symbol for *Bake Hardening steels* ;

Tables 9.9 and 9.10 show the reference standards, chemical composition and mechanical properties for the BH steels listed above. Their micro-structure is composed of very fine homogeneous ferritic grains, similar to that of IF steels in Figure 9.12.

Designation	Standard	%C	%Si	%Mn	%P	%S	%Al_{tot}
HC180B	EN 10268	≤ 0.06	≤ 0.5	≤ 0.7	≤ 0.06	≤ 0.030	≥ 0.015
HC220B		≤ 0.08	≤ 0.5	≤ 0.7	≤ 0.085	≤ 0.030	≥ 0.015
HC260B		≤ 0.1	≤ 0.5	≤ 1.0	≤ 0.1	≤ 0.030	≥ 0.015

Table 9.9 – Heat analysis for some *bake hardening steels*.

Designation	Standard	Yield Strength, YS [MPa]	Ultimate Tensile Strength, UTS [MPa]	Elongation after fracture, A%	Index r_{90}	Index n_{90}	Sampling position
HC180B (*)	EN 10268	180-230	290-360	≥ 34 (°)	≥ 1.6	≥ 0.17	transversal
HC220B (*)		220-270	320-400	≥ 32 (°)	≥ 1.5	≥ 0.16	transversal
HC260B (*)		260-320	360-440	≥ 29 (°)	---	---	transversal

(*) values to be guaranteed in semi-finished products in thickness 0.7 mm < tck. < 2 mm. The minimum increase to be guaranteed in YS due to the Bake Hardening effect is equal to 35 MPa.
(°) percentage elongation after fracture is determined in an 80 mm L_0 gauge length (A_{80mm}), which is a typical value for non proportional specimens, and not in $L_0 = 5.65 \cdot \sqrt{S_0}$, as with the traditional proportional specimen.

Table 9.10 – Mechanical characteristics of semi-finished products obtained from *bake hardening steels*.

[26] *EN 10268: Cold rolled steel flat products with high Yield Strength for cold forming. Technical delivery conditions.*


63
63

10. MEDIUM STRENGTH STRUCTURAL STEELS

10.1 Introduction

Medium strength steels are Fe-C-Mn hypoeuctetoid alloys very similar to low strength steels. In this case, however, carbon and manganese are present in slightly more substantial contents, between 0.1 and 0.2% and between 0.8 to 2%, respectively. These additions are made in the aim of improving mechanical strength while preserving a high level of resistance to brittle fracture. Normally, their micro-structure is ferritic-pearlitic type with increasing pearlite percentages relative to carbon and manganese contents. If micro-alloying elements are present, the micro-structure is mainly ferritic.

This steel family has Yield Strength of about 350 to 500 MPa and Ultimate Tensile Strength of 500 to 700 MPa. Both cold formability and weldability are good; percentage elongation after fracture, A%, is between 20% and 25% and the carbon equivalent is about 0.4[1]. The mechanical properties of this second steel category can be improved by means of two metallurgical/technological mechanisms: micro-alligation and thermo-mechanical rolling.

Micro-alligation. A first possibility to raise steel tensile strength consists in modifying its chemical composition through small additions of niobium, titanium and/or vanadium. The effect of these elements (also called micro-alloying elements) occurs during hot deformation of semi-finished products. Niobium, titanium and/or vanadium generate compounds of nanometric dimensions with carbon and nitrogen that are present in solution in steel. The carbides, nitrides and carbonitrides so formed are normally evenly dispersed in the metal. The presence of precipitates of a coherent nature (also called dispersoids) heavily restrains crystal grain growth during hot deformation operations and allows obtaining semi-finished products characterised by a very fine micro-structure (average grain size 5 to 10 μm). The extremely fine ferritic micro-structure and the precipitates considerably hinder dislocation motion, thereby increasing mechanical strength through strengthening phenomena due to grain refining and precipitation. Besides, the ferritic micro-structure guarantees good ductility and fracture toughness. Pearlite formation is inhibited by carbon and nitrogen depletion in the metal due to precipitate formation.

Thermo-Mechanical Rolling . Another option to increase mechanical strength in medium strength steels is using special hot deformation processes with controlled cooling. These processes, that are always performed concurrently with micro-alligation, drastically decrease the average size of the crystal grain while significantly increasing YS and UTS.

[1] *The values provided above refer to hot rolled semi-finished products with a medium-sized crystal grain (5 to 7 ASTM = 65 to 32 μm).*

A generic semi-finished product, such as a *coil*, a round bar or a wire rod, can be manufactured following a traditional procedure or through a thermo-mechanical rolling process[2] (Figure 10.1).

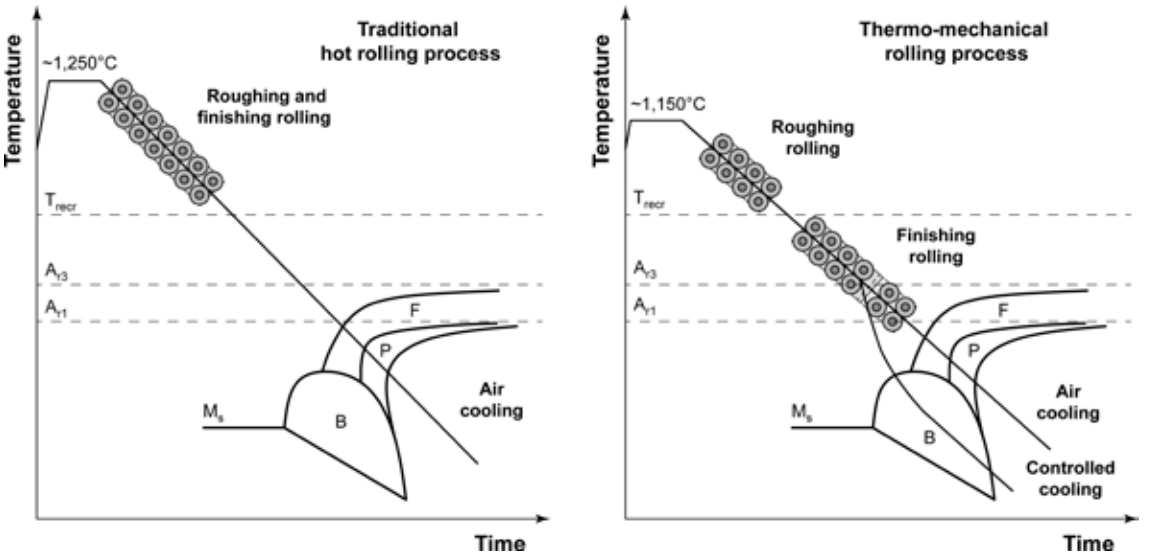

Figure10.1 – Comparison of conventional and thermo-mechanical rolling processes.

The traditional rolling process consists in austenitizing steel up to the ideal hot deformation temperatures (~1,250°C). Thereafter, conventional rolling is performed up to a temperature above dynamic recrystallisation temperature (T_{recr})[3]; by so doing, steel acquires a fully recrystallised austenitic structure. Due to final cooling, a new medium-sized ferritic-pearlitic structure forms. If necessary, you can further refine the grain by means of subsequent normalizing.

---

[2] In English literature this process is called Thermo-Mechanical Process (TMP) or Thermo-Mechanical Rolling (TMR) or even Thermo-Mechanical Control Process (TMCP).

[3] Recrystallisation can be static or dynamic. Static recrystallisation has been already exhaustively described when dealing with recrystallisation annealing heat treatments. If a cold strain-hardened semi-finished product is heat treated at a temperature higher than the critical recrystallisation temperature, new crystal grains form that are considerably finer than the original ones. If steel were not cooled down now, the crystal grain would gradually become larger and larger (for more details, see Chapter 4 of the book "Steel Metallurgy - Volume I", by Boniardi M. and Casaroli A., Lucefin - Esine, 2017).
Dynamic recrystallisation is slightly different. It also occurs at high temperature, but does not require a specific heat treatment given that it takes place during plastic deformation (rolling, forging, etc.) The final result is similar to static recrystallisation with new crystals forming from a deformed-grain micro-structure. In this case, however, recrystallisation is continuous throughout the manufacturing process because hot deformation strain-hardens the crystal grains that rapidly reform in an even and equiaxied manner. This phenomenon takes place without interruption because the metal is above the critical temperature for dynamic recrystallisation. To this regard, it should be pointed out that recrystallisation (static and dynamic as well) depends on both steel nature and the cold work level.

Alternatively, you can implement a controlled thermo-mechanical rolling process. This process foresees an initial heating temperature lower than in the previous case (~1150°C) so that to improve control on the average size of the austenitic grain. Hot rolling continues to temperatures lower than recrystallisation temperature. As a result, plastic deformation partially occurs between the A_{r3} and A_{r1} temperatures, i.e., in the $\alpha + \gamma$ two-phase field of steel (inter-critical field). The resulting austenitic structure (or austenitic-ferritic structure if you are working in the inter-critical field) is heavily strain-hardened, with shear bands[4] characterised by high dislocation density. In English literature, the special micro-structure that forms is referred to as *pancake structure* (Figure 10.2). Now, you can opt for slow cooling in open air and obtain a very fine fully ferritic or ferritic-pearlitic structure or for fast cooling by means of water jets[5] and obtain an extremely fine acicular ferritic or bainitic structure.

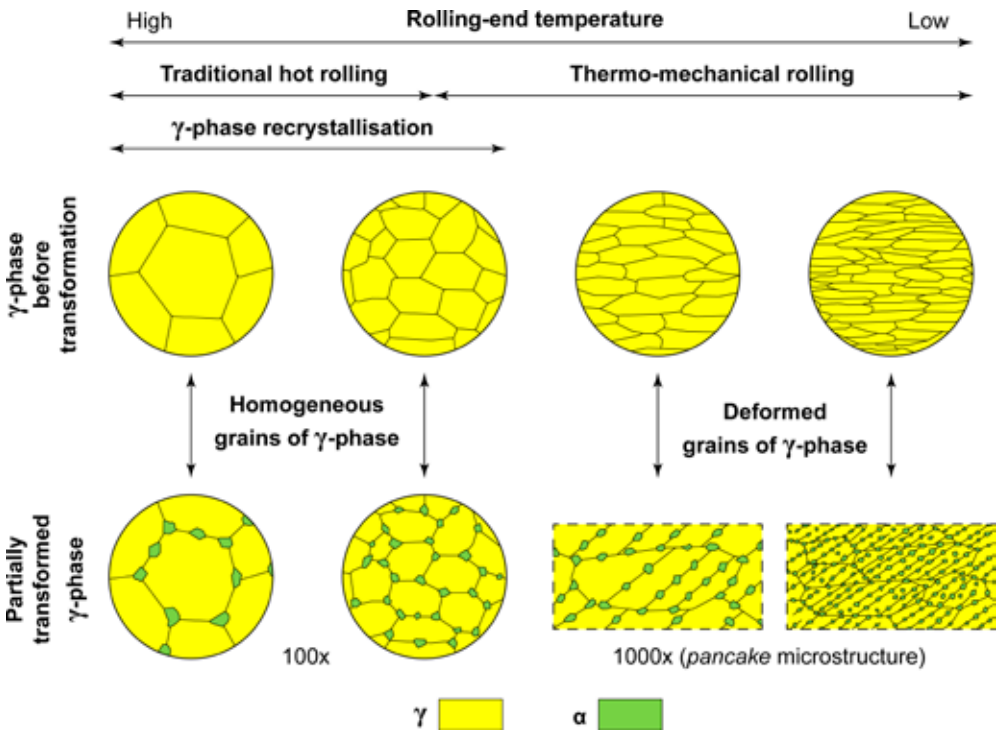

Figure 10.2 – Microstructure development in low carbon steels after thermo-mechanical rolling [from Kozasu 1992].

[4] *Shear bands and grain boundaries are the sites where the new micro-structure is most likely to nucleate.*

[5] *Forced cooling using water jets does not cause martensitic transformation by itself because these steel grades have low hardenability. However, fast cooling allows obtaining a very fine micro-structure.*

Keep in mind an essential and often underrated aspect. Heating above 400°C can be particularly detrimental to the semi-finished products containing micro-alloying elements and subjected to thermo-mechanical rolling with final heat treatment. In these cases, you can experience a worsening of mechanical strength as a consequence of unexpected recrystallisation events with coalescence of micro-precipitates and/or unwanted structural transformations.

These considerations are of the utmost importance to evaluate mechanical strength deterioration in welded joints. Whatever weld bead made on traditional general-purpose structural steels is characterised by local increase of mechanical strength in the molten area and in the thermally altered area compared to base metal. Therefore, the failure normally occurs far from the weld bead and in the area that is mechanically less resistant.

The opposite happens with micro-alloyed steels after thermo-mechanical rolling with final heat treatment. Due to the thermal alteration induced by the welding process, the mechanical characteristics of the molten area or of the thermally altered area worsen and this is where the failure normally occurs.

10.2 Carbon-Manganese Steels for Structural Applications

Carbon-manganese steels (C-Mn Steels) for structural applications are selected when medium to high mechanical strength is required. These steels have a traditional chemical composition, i.e., carbon and manganese where sometimes micro-alloying elements, such as vanadium, titanium and niobium, are added. The semi-finished products are obtained from traditional rolling or thermo-mechanical rolling processes, both of which can be followed by normalizing or quenching and tempering to form fine grain ferrite and pearlite or tempered bainite and/or martensite, as required.

Their application fields are same as structural non-alloy carbon steel. What changes is the level of mechanical strength and, consequently, the possibility to build lighter structures. Below you find some examples of steels belonging to this sub-category.

- EN S355K2: Hot-rolled steel for structural applications in thickness 3 to 150 mm, as specified in the EN 10025-2 standard[6] (S refers to the structural application and the number that follows is the guaranteed minimum Yield Strength; K2 indicates that steel minimum impact strength must be 40 J at -20°C);
- EN P460QH: Quenched and tempered steel for simple pressure vessels, as specified in the EN 10028-6 standard[7] (P refers to the pressure application and the number that follows is the guaranteed minimum Yield Strength; Q indicates that this is a quenched and tempered steel and H that this material is suitable for high temperature applications[8]);

[6] *EN 10025-2: Hot rolled products of structural steels. - Part 2: Technical delivery conditions for non-alloy structural steels*

[7] *EN 10028-6: Flat products made of steels for pressure purposes. - Part 6: Weldable fine grain steels, quenched and tempered.*

[8] *In this case, maximum application temperature is 300°C.*

- EN E420M: Hot-rolled welded steel tube for mechanical applications, as specified in the EN 10296-1 standard[9] (E refers to the engineering application and the number that follows is the guaranteed minimum Yield Strength; M indicates that the semi-finished product was obtained by means of thermo-mechanical rolling);
- EN L415NE: Normalized steel for oil product pipelines, as specified in the EN ISO 3183 standard[10] (L refers to the pipeline application and the number that follows is the minimum guaranteed Yield Strength; NE indicates a semi-finished product whose characteristics result from a normalizing process).

Tables 10.1 and 10.2 show the reference standards, chemical composition and mechanical properties of carbon-manganese steels for the structural or engineering applications listed above. Their micro-structure is normally composed of homogeneous ferritic-pearlitic grains elongated in the rolling direction. If the semi-finished product was heat treated, you can also have bainitic and/or martensitic structures (Figure 10.3).

Designation	Standard	%C	%Si	%Mn	%P	%S	%N	%Cu	%Al_{tot}
S335K2	EN 10025-2	≤ 0.20	≤ 0.55	≤ 1.60	≤ 0.025	≤ 0.025	---	≤ 0.55	(°)
P460QH (*)	EN 10028-6	≤ 0.18	≤ 0.50	≤ 1.70	≤ 0.025	≤ 0.010	≤ 0.015	≤ 0.30	(°)
E420M (**)	EN 10296-1	≤ 0.16	≤ 0.50	≤ 1.70	≤ 0.035	≤ 0.030	≤ 0.020	n.s.	≤ 0.020
L415NE (***)	EN ISO 3183	≤ 0.23	≤ 0.45	≤ 1.40	≤ 0.025	≤ 0.015	≤ 0.012	≤ 0.25	≤ 0.015

(°) killed using Si-Mn-Al, with fine grain.
(*) can contain the following elements up to: 0.005% B; 0.50% Cr; 0.50% Mo; 1% Ni; 0.05% Nb; 0.03% Ti; 0.08% V; and 0.05% Zr.
(**) can contain the following elements up to: 0.20% Mo; 0.30% Ni; 0.050% Nb; 0.050% Ti; and 0.12% V.
(***) can contain the following elements up to: 0.10% V; 0.05% Nb; 0.04% Ti; 0.30% Ni; 0.30% Cr; and 0.10% Mo.
n.s.: not specified.

Table 10.1 – Heat analysis of some carbon-manganese steels for structural or engineering applications.

[9] *EN 10296-1: Welded circular steel tubes for mechanical and general engineering purposes - Technical delivery conditions - Non-alloy and alloy steel tubes.*

[10] *EN ISO 3183: Petroleum and natural gas industries. Steel pipe for pipeline transportation systems. Corresponds to API X60NE.*

Designation	Standard	Yield Strength, YS [MPa]	Ultimate Tensile Strength, UTS [MPa]	Elongation after fracture, A%	Sampling position
S335K2 (*)	EN 10025-2	≥ 355	470-630	≥ 20	longitudinale
P460QH (**)	EN 10028-6	≥ 460	550-720	≥ 19	longitudinale
E420M (***)	EN 10296-1	≥ 420	≥ 500	≥ 19	longitudinale
L415NE (****)	EN ISO 3183	415-565	520-760 (°)	≥ 20	longitudinale

(*) values to be guaranteed in flat semi-finished products in thickness 3 mm < tck.< 16 mm.
(**) values to be guaranteed in semi-finished products in thickness tck. < 50 mm.
(***) values to be guaranteed in flat semi-finished products in thickness tck. < 16 mm.
(****) values to be guaranteed in tubes in thickness tck. < 25 mm.
(°) The YS to UTS ratio should be < 0.85.

Table 10.2 – Mechanical properties of semi-finished products obtained from carbon-manganese steels for structural or engineering applications.

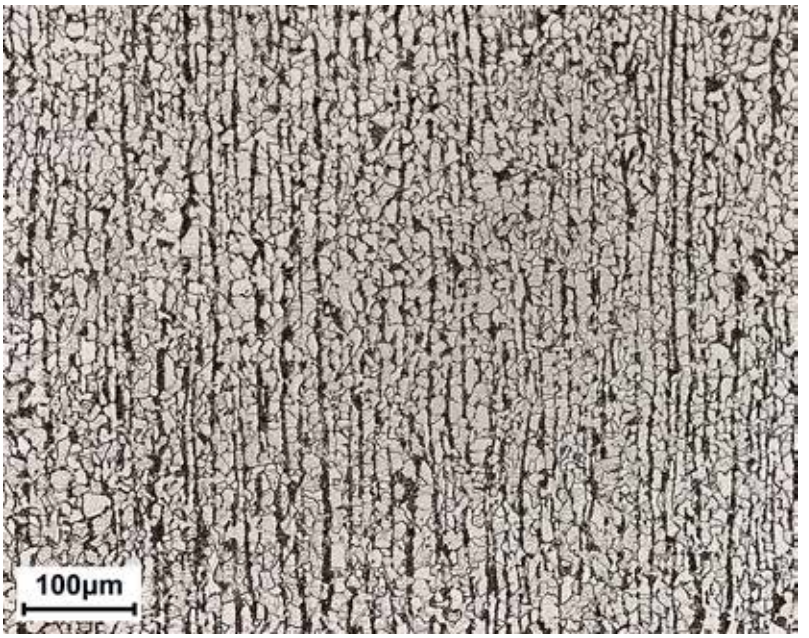

Figure 10.3 – Metallographic appearance of medium strength carbon-manganese steel grade EN S355K2. Notice ferrite and pearlite in banded micro-structure orientated in the semi-finished product rolling direction; etching agent: Nital 2% [Laboratories of the Department of Mechanical Engineering of Politecnico di Milano – Milan, Italy].

10.3 Weathering Steels

Weathering steels should also be mentioned among structural steels with 500 MPa < Rm ≤ 700 MPa. The characteristic of these steels, that also go under the name of Corten[11] steels, is to resist atmospheric corrosion. They are iron-carbon-manganese alloys with balanced additions of copper, chromium and phosphor (in some cases also nickel) in overall contents between 1% and 5%. These steels provide good resistance to atmospheric corrosion in mildly aggressive environments (mildly aggressive rural, urban or industrial environments), to a definitely higher level than traditional non-alloy carbon or carbon-manganese steels (Figure 10.4). Corten steels are mainly designed for structural applications that do not require being protected before putting into service (no painting, zinc-plating or similar treatments).

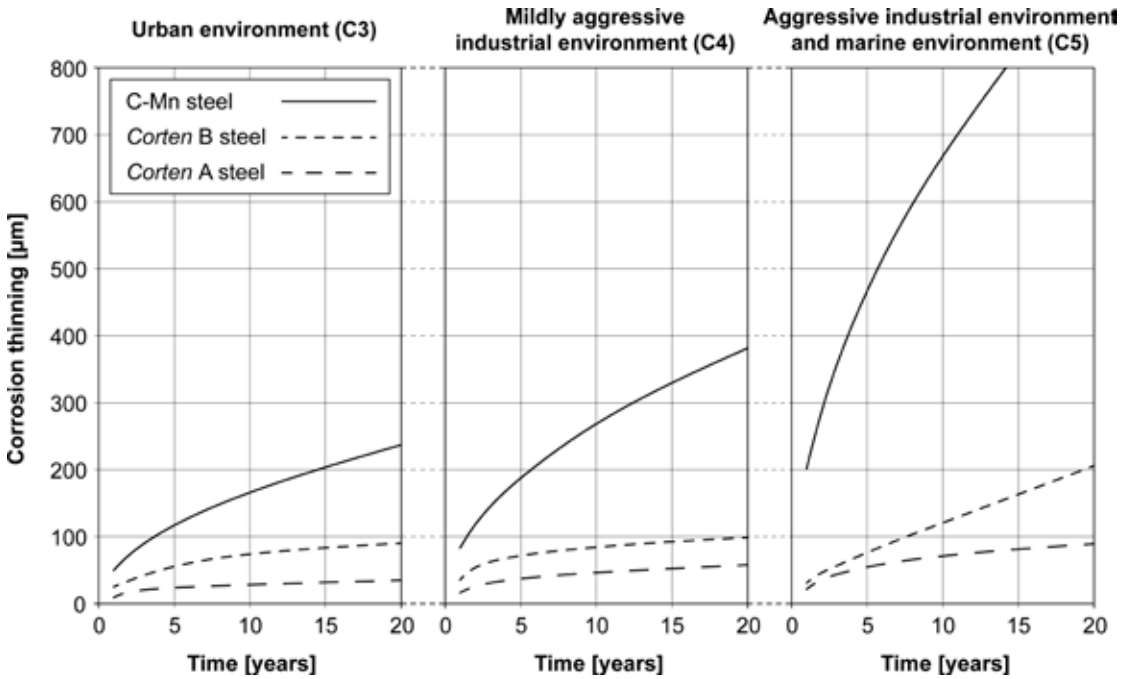

Figure 10.4 – Corrosion thinning of a generic non-alloy carbon steel, *Corten* A steel and *Corten* B steel. [Data relating to non-alloy carbon steel refer to the categories of atmospheric environment corrosivity specified in the EN ISO 9223 and EN ISO 9224 standards[12] (C3 - urban environment; C4 - mildly aggressive industrial environment; C5 - aggressive industrial environment and marine environment). Data for *Corten* steels are taken from Morcjillo et al. 2019].

[11] Corten is the acronym of Corrosion-Tensile; this term defines the main characteristics of these steels, i.e., corrosion resistance and Ultimate Tensile Strength. It was patented by the United States Steel Corporation in 1933.

[12] EN ISO 9223: Corrosion of metals and alloys. Corrosivity of atmospheres. Classification, determination and estimation; EN ISO 9224: Corrosion of metals and alloys. Corrosivity of atmospheres. Guiding values for the corrosivity categories.

Corrosion resistance of *Corten* steels is provided by a thick layer of complex iron oxides/hydroxides that forms on the surface and protects it against the aggression of the surrounding environment. If mechanically damaged, the oxide reforms. Its rust-like brownish colour makes *Corten* steel structures compatible with the natural environments where they are set. The main applications of *Corten* steels are in civil sector for the construction bridges, road barriers, sculptures, urban furniture, building façades and roofings. For example, the guard-rails in the A22 Modena-Brenner motorway are made of *Corten* A steel. A typical industrial application of weathering steels is the manufacture of containers for goods transportation.

The two main types of weathering steels are regulated by the EN 10025-5 standard[13]:

- *Corten* A, or phosphor-containing, steel as EN S355J2WP (S refers to the structural application and the number that follows is the guaranteed minimum Yield Strength; J2 indicates that minimum steel impact strength must be 27 J at -20°C; W indicates that this a weathering steel and P warns that it contains phosphor). It is a medium strength steel mainly used in architectural applications. Its corrosion resistance is approximately 5 to 8 times higher than traditional structural steels. In a mildly aggressive rural, urban or industrial atmosphere, corrosion thinning of *Corten* A steel tends to stop after reaching a penetration thickness of about 50 µm. In a marine environment deterioration slowly continues over the years even, but, in any case, it remains at lower levels than non-alloy carbon steels. Its high phosphor content makes it unsuitable to weld joints. If required, welding should be performed using a filler metal with a chemical composition similar to the base metal to avoid corrosion issues in the welded joint once this is put into service.
- *Corten* B, or vanadium-containing, steel as EN S355J2W (S refers to the structural application and the number that follows is the guaranteed minimum Yield Strength; J2 indicates that steel minimum impact strength must be 27 J at -20°C; W informs that this is a weathering steel). Its corrosion resistance is approximately 2 to 4 times higher than traditional structural steels. It does not possess the same good-looking characteristics of *Corten* A and is normally used for structures subjected to high mechanical stresses. This steel is more weldable than the previous one, but here too you have to use a filler metal with a chemical composition similar to the base metal.

Recently, another weathering steel grade has been developed (called *Corten* C). These steels are characterised by improved mechanical strength compared to the previous ones (*Corten* A and B), with corrosion resistance like *Corten* B.

[13] *EN 10025-5: Hot rolled products of structural steels. - Part 5: Technical delivery conditions for structural steels with improved atmospheric corrosion resistance.*

Tables 10.3 and 10.4 show the reference standards, chemical composition and mechanical properties of the *Corten* steels detailed above. Their micro-structure is composed of ferrite and pearlite grains elongated in the rolling direction, as it is typical of steels grade EN S355 for structural applications (Figure 10.5).

Designation	Standard	%C	%Si	%Mn	%P	%S	%Cr	%Cu	$\%Al_{tot}$
S355J2WP (*)	EN 10025-5	≤ 0.12	≤ 0.75	≤ 1.00	0.06-0.15	≤ 0.030	0.30-1.25	0.25-0.55	(°)
S355J2W (**)		≤ 0.16	≤ 0.50	0.50-1.50	≤ 0.030	≤ 0.030	0.40-0.80	0.25-0.55	(°)

(°) killed using Si-Mn-Al, with fine grain.
(*) *Corten* A.
(**) *Corten* B.

Table 10.3 – Heat analysis of some *Corten* steels for structural applications.

Designation	Standard	Yield Strength, YS [MPa]	Ultimate Tensile Strength, UTS [MPa]	Elongation after fracture, A%	Sampling position
S355J2WP (*)	EN 10025-5	≥ 355	470-630	≥ 22	longitudinale
S355J2W (*)					

(*) values to be guaranteed in flat semi-finished products in thickness 3 mm < tck.< 16 mm.

Table 10.4 – Mechanical properties of semi-finished products obtained from *Corten* steels for structural applications.

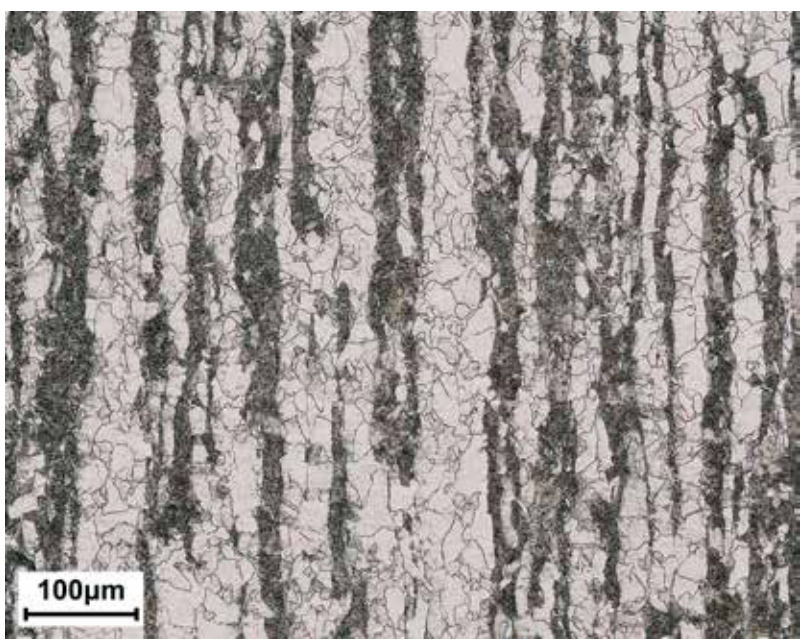

Figure 10.5 – Metallographic appearance of *Corten* A steel grade EN S355J2 WP. Notice the ferrite and pearlite in banded micro-structure orientated in the semi-finished product rolling direction; etching agent: Nital 2% [Laboratories of the Department of Mechanical Engineering of Politecnico di Milano – Milan, Italy].

10.4 *High-Strength Low-Alloy Steels* (HSLA Steels)

HSLA steels originate from the idea of inserting small percentages of niobium, titanium and/or vanadium (sometimes also boron) in a maximum amount not exceeding 0.22% into carbon-manganese steels. Also, nitrogen content is kept under control because it affects the formation of precipitates. Carbon content ranges around 0.05 to 0.15% while manganese content can be as high as 2%. As already stated, the effect of the micro-alloying chemical elements occurs in a combined manner during thermo-mechanical rolling processes. Grain refining and precipitation of nanometric chemical compounds are the two main strengthening mechanisms that play a role in HSLA steels[14]. The first mechanism inhibits dynamic recrystallisation of the micro-structure (in the γ-phase or in the $\gamma + \alpha$ phase) during hot deformation caused by the thermo-mechanical processes. For this to happen, finely dispersed niobium, vanadium and/or titanium nano-precipitates must be present and stable at high temperature. The compounds act as anchor points for the grain boundaries, thereby preventing dynamic recrystallisation and subsequent grain growth (Figure 10.6). For maximum process efficiency, it is important that the micro-alloying elements (Nb, V and Ti) completely dissolve in the crystal lattice when steel is brought into the austenitic phase field (1150° to 1250°C) before hot deformation.

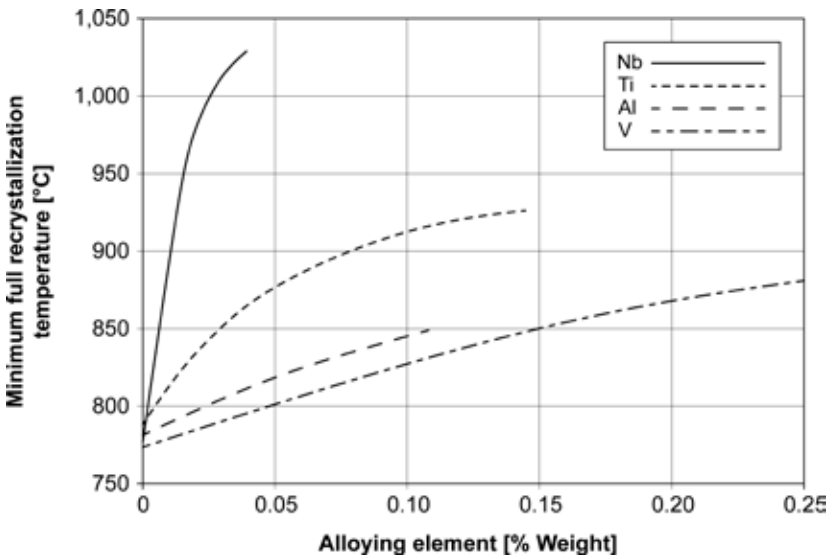

Figure 10.6 – Trend of the minimum full recrystallisation temperature with reference to the amounts of micro-alloying elements added into a steel with C = 0.07%; Mn = 1.4% and Si = 0.25%; plastic deformation equal to 10 to 15% [from Tither 1990].

[14] *In this case, reference is made collectively to carbides [NbC, VC and TiC], nitrides [NbN, VN and TiN] and/or carbonitrides [NbCN, VCN, TiCN, (Nb,V)CN and (Nb,Ti)CN] of the micro-alloying elements.*

Then, it is necessary that the precipitates (small-sized carbides, nitrides and carbonitrides) reform during thermo-mechanical hot rolling and/or during final cooling in order to inhibit grain recrystallisation and growth. The second strengthening mechanism is based on micro-alligation of HSLA steels and the combined addition of niobium and vanadium. Niobium is poorly soluble in the iron lattice, much less than vanadium and titanium. Small amounts of niobium (0.02 to 0.03%) enable the formation of a great number of precipitates that hinder dynamic recrystallisation up to temperatures of 950° to 1,000°C. Also, the presence of niobium promotes the formation of bainitic structures if fast cooling is performed after thermo-mechanical rolling. Vanadium is more soluble than niobium and is added in typical amounts of 0.05 to 0.1%. Vanadium compounds considerably strengthen the metal because, even though they induce a minimum recrystallisation temperature lower than niobium compounds, they are present in a greater amount. Also, titanium can be used as a micro-alloying element given that, as vanadium, it exhibits high solubility in the iron lattice. However, using it is more complicated due to the high temperature at which its compounds solubilise (1,200° to 1,300°C). This characteristic has positive and negative consequences. On one hand, it prevents austenitic grain growth during heating, on the other hand it requires substantial additions of titanium (0.10 to 0.15%) because it is not possible to solubilise all of the compounds initially present[15]. As to strengthening, titanium compounds have an intermediate effect compared to vanadium and niobium, both in terms of crystal grain refinement and precipitation hardening.

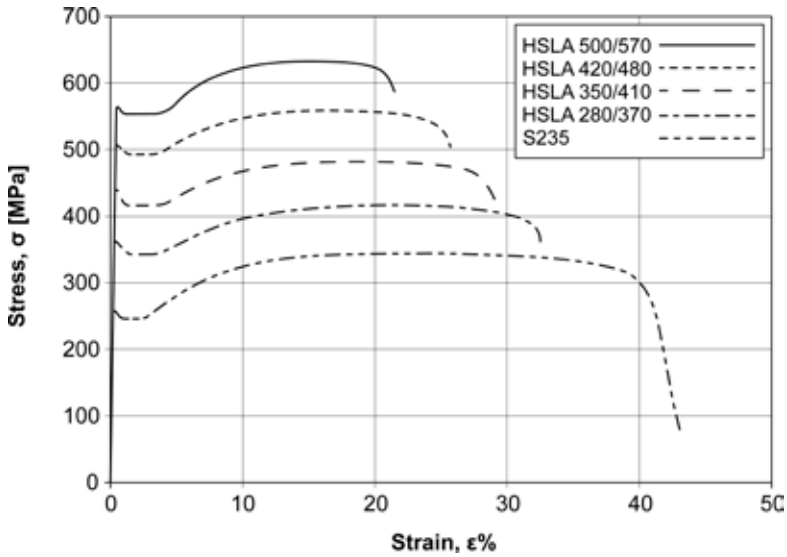

Figure 10.7 – Stress-strain curves for some micro-alloyed steels (identified by the acronym *HSLA* followed by the minimum values of YS and UTS) compared with generic steel grade EN S235 [from Keeler et al. 2017].

[15] *Titanium is extremely reactive with many other chemical elements (O, S, N and C); therefore, you have to be very careful when adding it into the steel metal bath.*

Typical Yield Strength values for micro-alloyed steels oscillate between 300 MPa and 600 MPa and tensile strength values between 450 MPa and 750 MPa. With some chemical compositions you can reach an YS value around 1,000 MPa and an UTS value of 1,200 MPa. But, as mechanical strength increases, elongation after fracture gradually decreases ranging around 30% and 10%. The low carbon content and very fine grain enable these steels to be extremely tough with transition temperatures between -50°C and -75°C approximately. Thus, HSLA steels cover the entire range of mechanical strength featured by general-purpose structural steels (Figure 10.7).

Below you find some examples of steels belonging to this sub-category.

- S355MC and S460MC, hot rolled steels for structural applications in thickness between 1.5 mm and 20 mm, as specified in the EN 10149-2 standard[16] (S refers to the structural application and the number that follows is the guaranteed minimum Yield Strength; M indicates thermo-mechanical rolling and C the possibility of cold-forming the semi-finished product).
- HC380LA and HC460LA, cold rolled uncoated steels for cold forming in thickness equal to or lower than 3 mm, as specified in the EN 10268 standard[17] (HC refer to a cold rolled high Yield Strength steel; the number that follows is the guaranteed minimum Yield Strength; LA indicates a micro-alloyed steel).

Tables 10.5 and 10.6 show the reference standards, chemical composition and mechanical properties of the HSLA steels detailed above. Their micro-structure is normally composed of extremely fine ferritic grains that are homogeneous or elongated in the rolling direction (Figure 10.8). You can also have bainitic and/or martensitic structures is the semi-finished product is heat treated.

HSLA steels are widely used in the automotive sector to make frames, in the mechanical sector in general to manufacture shelving units and metal furniture, and for the production of structural elements obtained by profiling, bending and/or sheet metal drawing. HSLA steels offer good weldability even tough, after welding, the molten area and the thermally altered area provide impaired mechanical strength compared to the base metal.

[16] *EN 10149-2: Hot rolled flat products made of high Yield Strength steels for cold forming. - Part 2: Technical delivery conditions for thermomechanically rolled steels.*

[17] *EN 10268, Cold rolled steel flat products with high Yield Strength for cold forming. Technical delivery conditions.*

Designation	Standard	%C	%Si	%Mn	%P	%S	%Al_{tot}	%Nb	%V	%Ti
S355MC	EN 10149-2	≤ 0.12	≤ 0.5	≤ 1.5	≤ 0.025	≤ 0.020	≥ 0.015	≥ 0.09	≥ 0.20	≥ 0.15
S460MC		≤ 0.12	≤ 0.5	≤ 1.6	≤ 0.025	≤ 0.015	≥ 0.015	≥ 0.09	≥ 0.20	≥ 0.15
HC380LA	EN 10268	≤ 0.12	≤ 0.5	≤ 1.6	≤ 0.030	≤ 0.025	≥ 0.015	≥ 0.09	(*)	≥ 0.15
HC460LA		≤ 0.14	≤ 0.6	≤ 1.8	≤ 0.030	≤ 0.025	≥ 0.015	≥ 0.09	(*)	≥ 0.15

(*) V and B can be added provided that the total amount of chemical micro alloying elements is < 0.22%.

Table 10.5 – Heat analysis of some HSLA steels for structural applications.

Designation	Standard	Yield Strength, YS [MPa]	Ultimate Tensile Strength, UTS [MPa]	Elongation after fracture, A%	Sampling position
S355MC (*)	EN 10149-2	≥ 355	430-550	19 (°)	longitudinale
S460MC (*)		≥ 460	520-670	14 (°)	longitudinale
HC380LA (**)	EN 10268	380-480	440-580	19 (°)	longitudinale
HC460LA (**)		460-580	510-660	13 (°)	longitudinale

(*) values to be guaranteed in flat semi-finished products in thickness 1.5 mm < tck. < 20 mm.
(**) values to be guaranteed in flat semi-finished products in thickness 0.7 mm < tck. < 3 mm.
(°) percentage elongation after fracture is determined in an 80 mm L_0 gauge length (A_{80mm}), which is a typical value for non proportional specimens, and not in $L_0 = 5.65 \cdot \sqrt{S_0}$, as with the traditional proportional specimen.

Table 10.6 – Mechanical properties of semi-finished products obtained from some HSLA steels for structural applications.

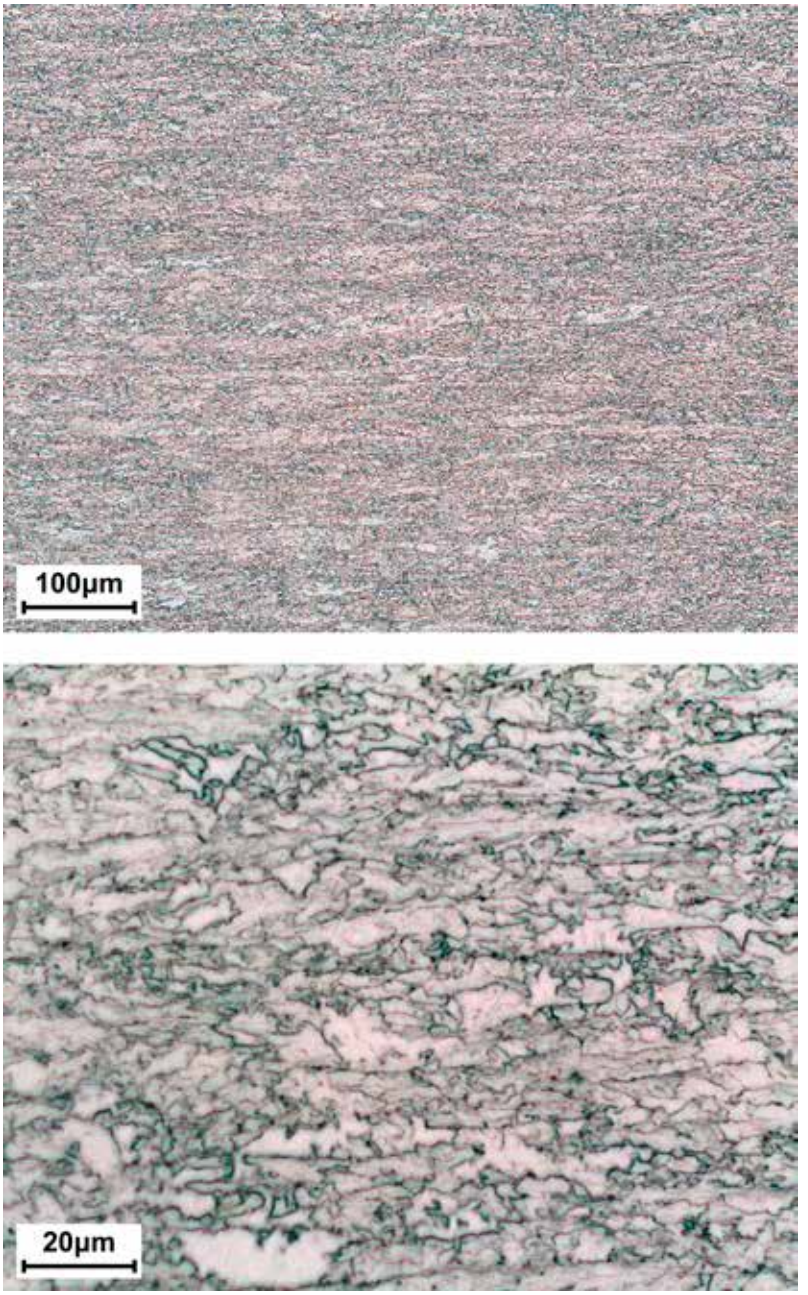

Figure 10.8 – Metallographic appearance at low and high magnification of HSLA steel grade EN HC460LA. Notice the extremely fine ferritic micro-structure orientated in the semi-finished product rolling direction; etching agent: Nital 2%. [Laboratories of the Department of Mechanical Engineering of Politecnico di Milano – Milan, Italy].

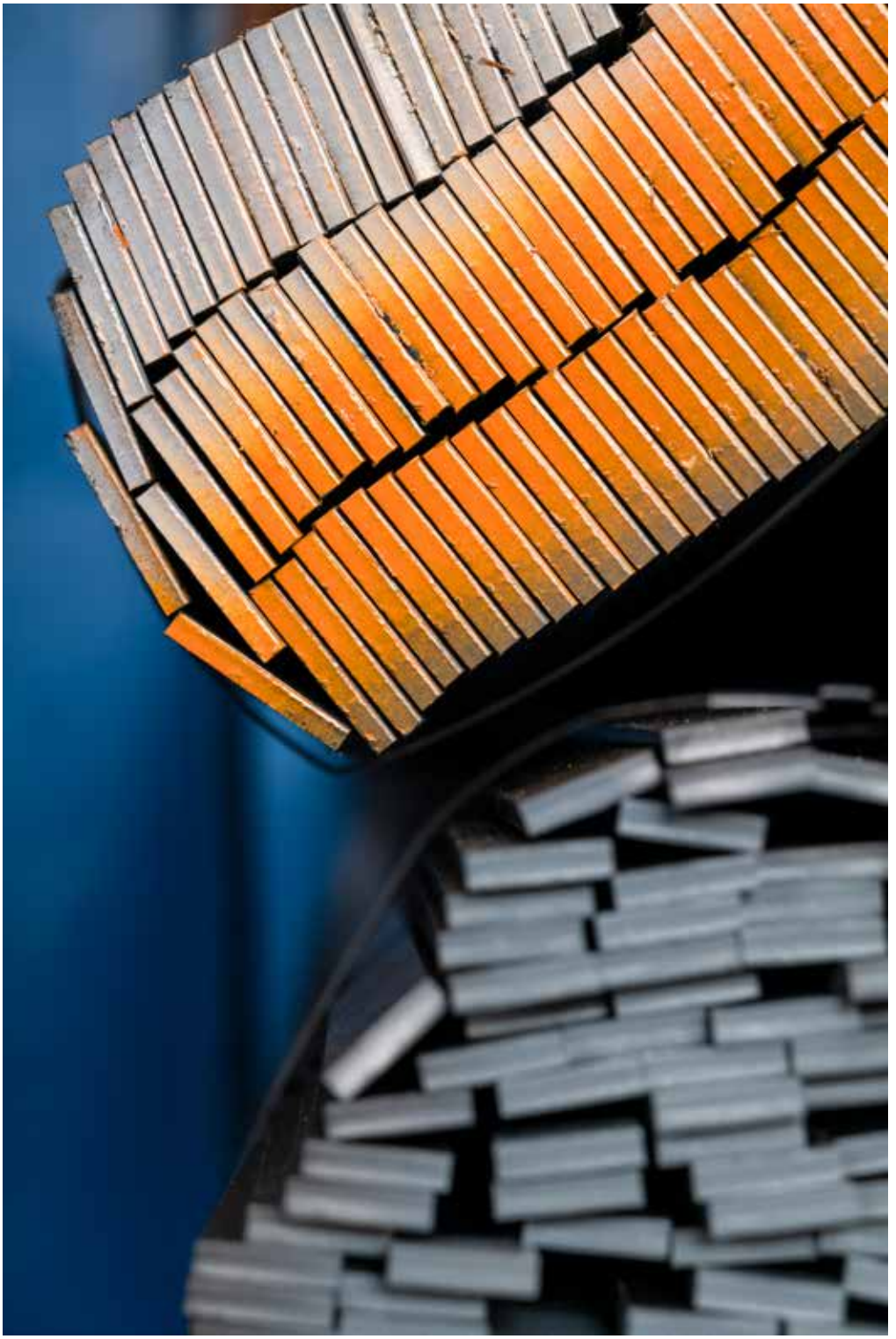

11.HIGH STRENGTH STRUCTURAL STEELS

11.1 Introduction

The last carbon steel family is the family of high strength steels. They are Fe-C-Mn hypoeutectoid alloys characterised by YS values above 500 MPa and UTS values above 700 MPa. To further increase Ultimate Tensile Strength in comparison with medium strength steels, not only it is necessary to perform specific alligations and/or thermo-mechanical processes, but also opportune heat treatments. In this manner, you obtain steels with a mixed micro-structure composed of ferrite, pearlite, bainite and/or martensite, as shown in Figure 11.1.

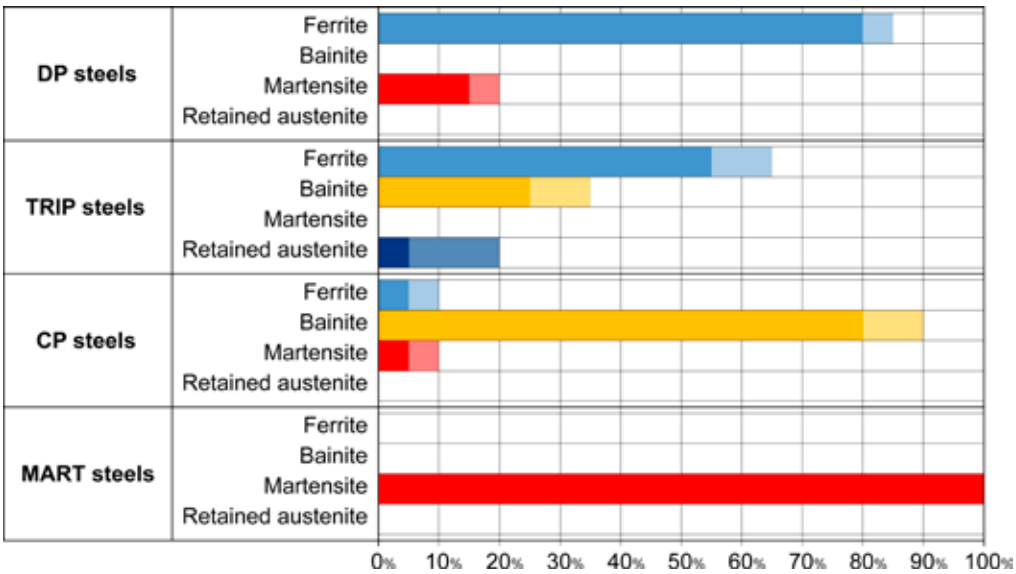

Figure 11.1 – Percentage volumetric fraction of micro-structures in high strength steels of non traditional type [from Heller and Nuss 2003].

Keep in mind that these steel grades should be used with great attention because, as tensile strength increases, you also experience the increase of some metallurgical issues that should not be underestimated. For example, as UTS increases, brittle fracture resistance gradually decreases together with a deterioration of steel welding and galvanising features. Proneness to hydrogen embrittlement also tends to increase as Ultimate Tensile Strength increases. So, be careful: *the stronger the better*[1] not always is the ideal solution.

[1] *Typical English motto.*

11.2 *Dual-Phase* (DP) Steels

These steels have a carbon content below 0.2% with high silicon and manganese contents (Si = 0.5 to 1%; Mn = 2 to 2.5%). Titanium, niobium and vanadium as well as chromium and molybdenum (Cr + Mo = 1 to 1.4%) are added to enhance steel tensile strength.

DP steels are characterised by a fine micro-structure composed of a matrix of ferrite grains surrounding small martensite islands. The martensitic structure is obtained by heat treatment. Its volumetric fraction can range from 15 to 60% of the total, even though martensite content in DP steels for industrial use normally does not exceed 20%. In metallurgical terms, martensite is determinant to steel tensile strength while ferrite affects its cold formability (Figure 11.2).

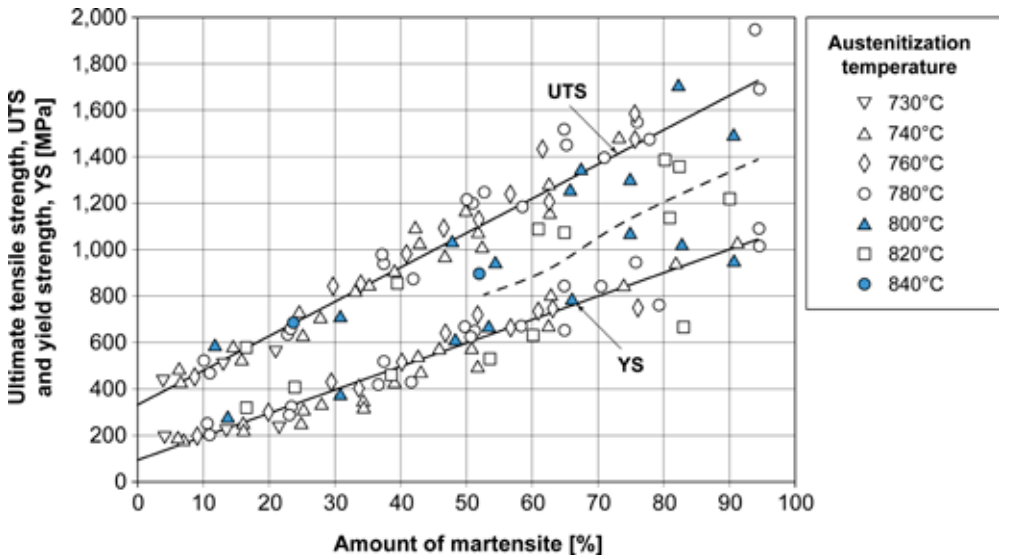

Figure 11.2 – Influence of martensite percentage on Yield Strength, YS, and Ultimate Tensile Strength, UTS, for *Dual Phase* steels [from Davis 1978].

The mixed ferrite/martensite micro-structure allows obtaining very special ductile and tensile features. The Ultimate Tensile Strength values are around 600 to 1,000 MPa with a very low YS/UTS ratio, equal to 0.4 to 0.5. The remarkable cold formability is underlined by Yield Strength without kink on the stress-strain curve, as well as by high values of both the strain hardening index, n, and percentage elongation after fracture A% (Figure 11.3).

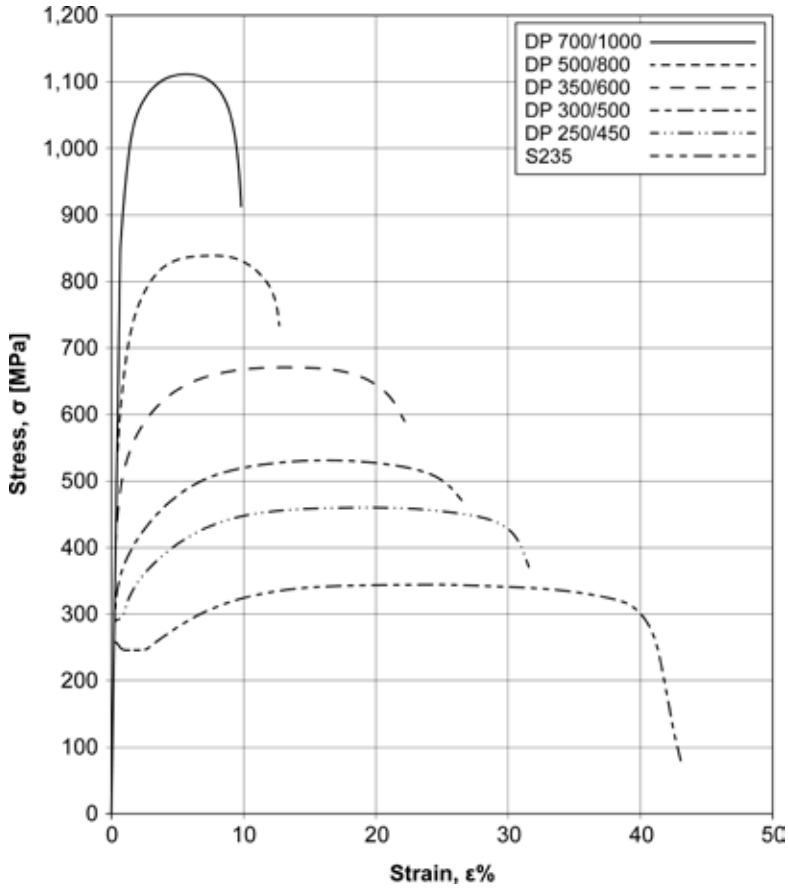

Figure 11.3 – Stress-strain curves for some DP steels (identified by the letters DP followed by their minimum YS and UTS values) compared with a generic EN S235 steel [from Keeler et al. 2017].

The semi-finished products typically include low-thickness strip and are obtained through a traditional hot deformation process, followed by cold rolling. At the end, steel is heat-treated in line, at temperatures where the α and γ phases coexist (intercritical interval). Thereafter, sudden cooling is performed. Recrystallization of the cold strained structure which provides the desired ferrite-austenite ratio, occurs during the austenitizing phase in the intercritical field. During cooling, austenite transforms into martensite while ferrite remains unchanged. Sometimes, depending on martensite *start and finish* temperatures in steel, you can also have lower bainite and/or retained austenite.

Should you wish to obtain a rather thick semi-finished product from DP steel, as in the case of plates, you proceed to traditional hot rolling followed by slow in-line cooling down to the $\alpha + \gamma$ intercritical temperature. Sudden cooling terminates the cycle.

Notice that, normally, DP steels are not obtained by thermo-mechanical rolling because their ferrite structure would be partially hard-strained with consequent limited cold formability.
The chemical composition should be carefully balanced to improve steel hardenability, necessary to make martensite formation easier without negatively affecting weldability. DP steels contain carbon and manganese: the former hardens martensite, the latter reinforces ferrite by solid solution and both stabilise austenite. Besides, they can be added with small percentages of chromium and/or molybdenum (to delay austenite transformation into pearlite), boron (to promote hardenability), silicon (to assist ferrite formation) as well as vanadium and niobium (as grain refiners and micro alloying elements).
DP steels are mainly used in the automotive sector to manufacture car frames and wheels.
EN HCT780X and EN HCT980X are typical examples. In particular, they are hot coated steels for cold forming in thickness 0.2 to 3 mm, as specified in the EN 10346 standard[2] (the initial letters HCT refer to a cold rolled high Yield Strength steel for cold forming; the number that follows is its guaranteed minimum Ultimate Tensile Strength; X indicates that this is a *Dual Phase* steel).

Tables 11.1 and 11.2 show the reference standards, chemical composition and mechanical properties for the steels listed above. Figure 11.4 shows the typical micro-structure of Dual Phase steels.

Designation	Standard	%C	%Si	%Mn	%P	%S	%Al_{tot}	%Cr+%Mo	%Nb+%Ti
HCT780X (*)	EN 10346	≤ 0.18	≤ 0.80	≤ 2.5	≤ 0.08	≤ 0.015	0.015-2.0	≤ 1.4	≤ 0.15
HCT980X (*)		≤ 0.20	≤ 1.00	≤ 2.9	≤ 0.08	≤ 0.015	0.015-2.0	≤ 1.4	≤ 0.15

(*) %V < 0.20; %B < 0.005.

Table 11.1 – Heat analysis of some DP (*Dual Phase*) steels for structural applications.

Designation	Standard	Yield Strength, YS [MPa]	Ultimate Tensile Strength, UTS [MPa]	Elongation after fracture, A%	Sampling position
HCT780X (*)	EN 10346	440-550	≥ 780	≥ 14 (°)	longitudinale
HCT980X(*)		590-740	≥ 980	≥ 10 (°)	longitudinale

(*) values to be guaranteed in flat semi-finished products in thickness 0.6 mm < tck. < 3 mm. The minimum increase to be guaranteed in YS due to the *Bake Hardening* effect is equal to 30 MPa.
(°) percentage elongation after fracture is determined in an 80 mm L_0 gauge length (A_{80mm}), which is a typical value for non proportional specimens, and not in $L_0 = 5.65 \cdot \sqrt{S_0}$, as with the traditional proportional specimen.

Table 11.2 – Mechanical properties of semi-finished products made from some DP (*Dual Phase*) steels for structural applications.

[2] *EN 10346: Continuously hot-dip coated steel flat products for cold forming.*

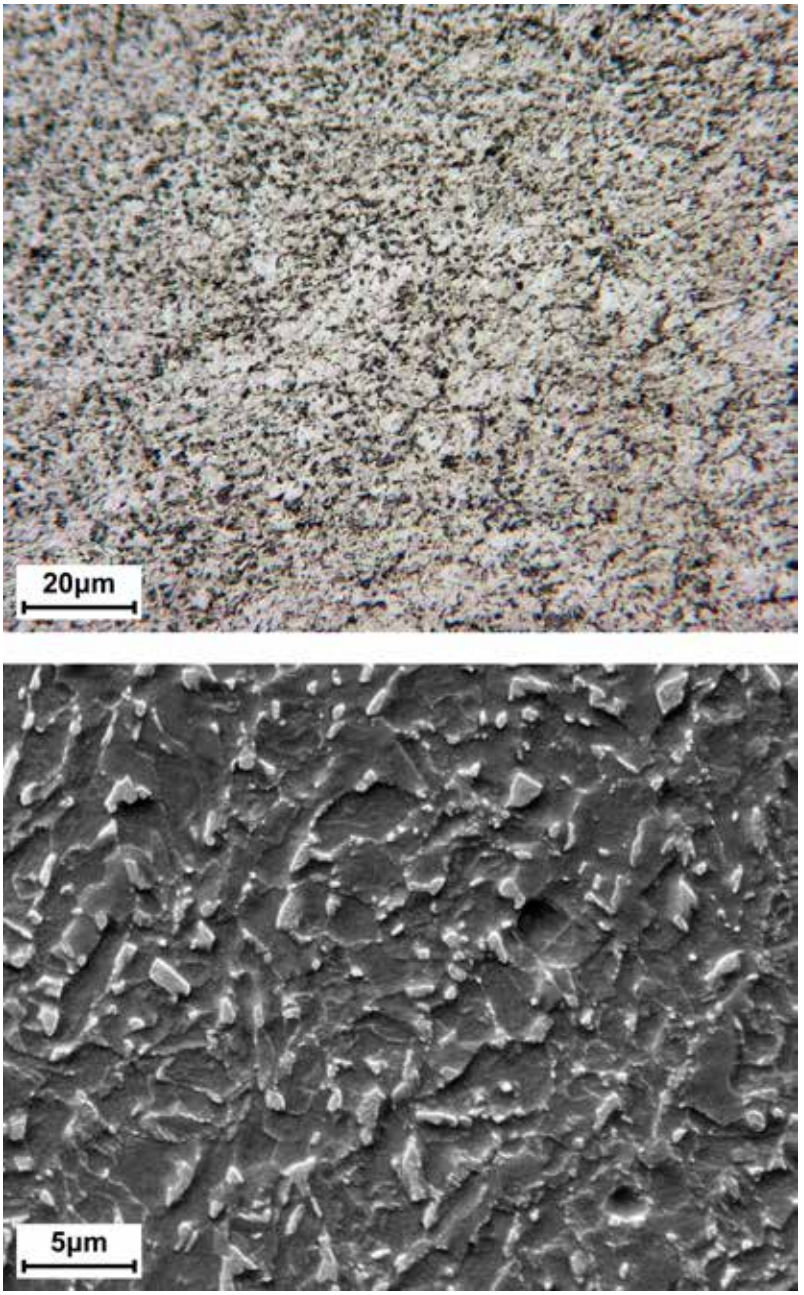

Figure 11.4 – Metallographic appearance of DP steel grade EN HCT980X at low and high magnification. Notice the martensite islands surrounded by the very fine ferritic micro-structure; etching agent: Nital 2%. [Laboratories of the Department of Mechanical Engineering of Politecnico di Milano – Milan, Italy].

11.3 *Transformation Induced Plasticity* (TRIP) Steels

TRIP is the acronym of *Transformation Induced Plasticity*: they are high strength steels characterised by a micro-structure that, at room temperature, undergoes $\gamma \rightarrow \alpha$ partial transformation when the semi-finished product is subjected to plastic strain to obtain the finished component.

TRIP steels have a carbon content between 0.1% and 0.4% and high contents of silicon and manganese (Si = 0.5 to 1%; Mn = 2 to 2.5%); titanium, niobium and vanadium can be added to improve steel tensile strength. As the carbon content increases, also austenite stability increases together with the cold deformation level triggering the $\gamma \rightarrow \alpha$ transformation. But, as carbon increases, weldability decreases. Most TRIP steels come with carbon contents around 0.1 to 0.2%, this being a fair compromise of these two opposite needs.

TRIP steel micro-structure is formed by retained austenite islands ($A_r > 5\%$) surrounded by a mainly ferritic matrix; small bainite and martensite grains are also present. Their structure is the result of a clever manufacturing process, characterised by hot and cold rolling passages and specific isothermal treatments. The semi-finished products typically include strip and are largely used to cold form complex shapes. This is the phase when the TRIP effect occurs. After cold deformation, a more or less substantial amount of austenite (depending on the deformation degree) transforms into martensite with considerable increase of steel tensile strength.

TRIP steels possess remarkable formability given that their strain hardening index is higher than in DP steels ($n > 0.2$) and their YS/UTS ratio is around 0.6 to 0.7. After hot painting, this steel family exhibits the *bake hardening* effect (YS $\cong$ 50 to 70 MPa). Figure 11.5 shows the stress/strain curves for some TRIP steels compared to a generic EN S235 steel.

Main applications of TRIP steels are found in shipbuilding and in the automotive sector for the manufacture of structural elements with high shock absorption capacity. They are also used to make tie-rods, piping and tanks that work at low temperature. EN HCT690T and EN HCT780T are typical examples. In particular, they are hot coated steels for cold forming in thickness 0.2 to 3 mm, as specified in the EN 10346 standard [3] (the initial letters HCT refer to a cold rolled high Yield Strength steel for cold forming; the number that follows is its guaranteed minimum Ultimate Tensile Strength; T indicates that this is a TRIP steel). Tables 11.3 and 11.4 show the reference standards, chemical composition and mechanical properties for the steels listed above.

[3] *EN 10346: Continuously hot-dip coated steel flat products for cold forming.*

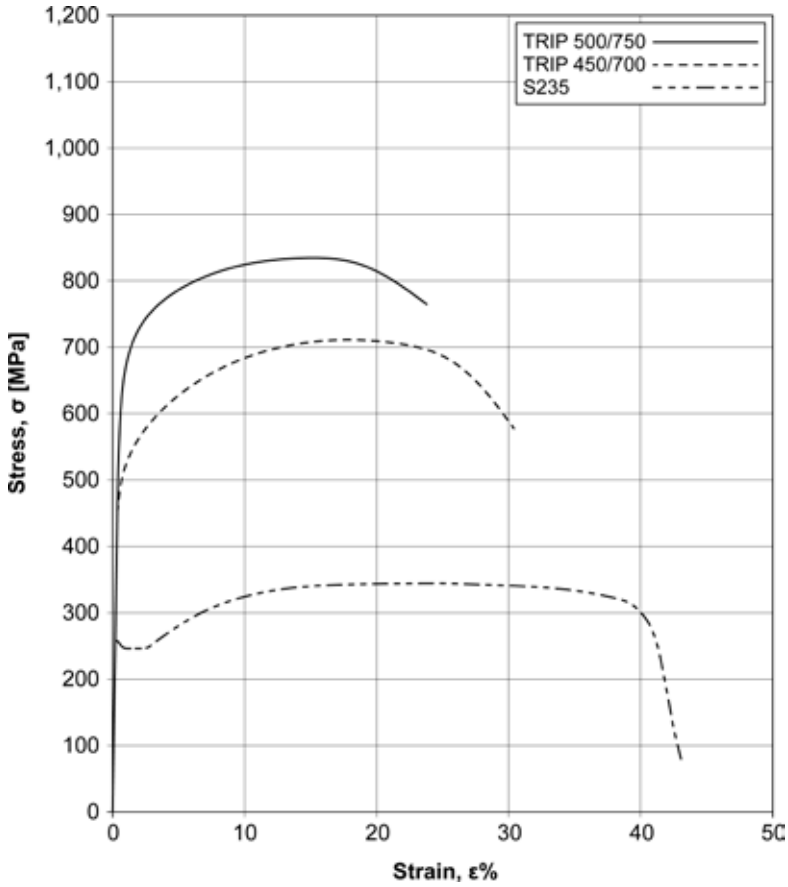

Figure 11.5 – Stress/strain curves for some TRIP steels (identified by the TRIP acronym followed by their minimum YS and UTS values) compared to a generic EN S235 steel [from Keeler et al. 2017].

Designation	Standard	%C	%Si	%Mn	%P	%S	%Al_{tot}	%Cr + %Mo	%Nb + %Ti
HCT690T (*)	EN 10346	≤ 0.24	≤ 2.0	≤ 2.2	≤ 0.080	≤ 0.015	0.015-2.0	≤ 0.6	≤ 0.20
HCT780T (*)		≤ 0.25	≤ 2.2	≤ 2.5	≤ 0.080	≤ 0.015	0.015-2.0	≤ 0.6	≤ 0.20

(*) %V < 0.20; %B < 0.005.

Table 11.3 – Heat analysis of some TRIP (*Transformation Induced Plasticity*) steels for structural applications.

Designation	Standard	Yield Strength, YS [MPa]	Ultimate Tensile Strength, UTS [MPa]	Elongation after fracture, A%	Index n_0 (°°)	Sampling position
HCT690T (*)	EN 10346	400-520	≥ 690	≥ 23 (°)	≥ 0.19	longitudinale
HCT780T (*)		450-570	≥ 780	≥ 21 (°)	≥ 0.16	longitudinale

(*) values to be guaranteed in flat semi-finished products in thickness 0.6 mm < tck. < 3 mm. The minimum increase to be guaranteed in YS due to the *Bake Hardening* effect is equal to 40 MPa.
(°) percentage elongation after fracture is determined in an 80 mm L_0 gauge length (A_{80mm}), which is a typical value for non proportional specimens, and not in $L_0 = 5.65 \cdot \sqrt{S_0}$, as with the traditional proportional specimen.
(°°) Index n_0 is measured in the 10 to 20% strain interval.

Table 11.4 – Mechanical properties of semi-finished products made from some TRIP (*Transformation Induced Plasticity*) steels for structural applications.

11.4 *Complex Phase* (CP) Steels

Complex Phase steels are similar to TRIP steels, compared to which they have retained austenite contents close to zero. They are characterised by a mixed ferrite and bainite structure, with limited martensite percentages. CP steels have a carbon content below 0.18%; they feature high contents of silicon and manganese (Si = 0.5 to 1%; Mn = 1.5 to 2.5%) and always contain micro alloying elements such as titanium, niobium and vanadium. Also the steelmaking process is similar to that of TRIP steels. It consists in thermo-mechanical rolling followed by one or more isothermal heat treatments to obtain the micro-structure desired with an extremely fine grain. With the same Ultimate Tensile Strength, Complex Phase steels have higher Yield Strength than Dual Phase steels, while remaining fairly ductile. Figure 11.6 shows the stress/strain curves for some CP steels compared to a generic EN S235 steel.
The main applications of CP steels are found in the automotive sector, where these steels are used to make frame components, especially those exposed to shocks. EN HCT780C and EN HCT980C are typical examples. In particular, they are hot coated steels for cold forming in thickness 0.2 to 3 mm, as specified in the EN 10346 standards (the initial letters HCT refer to a cold rolled high Yield Strength steel for cold forming; the number that follows is its guaranteed minimum Ultimate Tensile Strength; C indicates that this is a CP steel). Tables 11.5 and 11.6 show the reference standards, chemical composition and mechanical properties for the steels listed above.

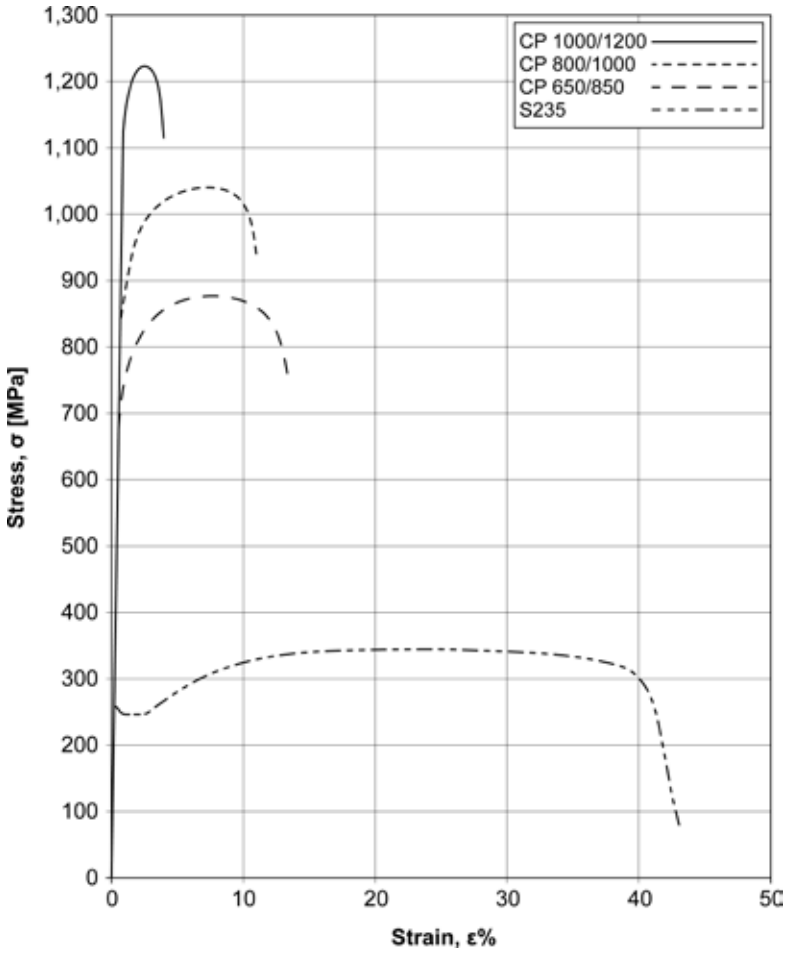

Figure 11.6 – Stress/strain curves for some CP steels (identified by the letters CP followed by their minimum YS and UTS values) compared to a generic EN S235 steel [from Keeler et al. 2017].

Designation	Standard	%C	%Si	%Mn	%P	%S	%Al_{tot}	%Cr + %Mo	%Nb + %Ti
HCT780C (*)	EN 10346	≤ 0.18	≤ 1.0	≤ 2.5	≤ 0.080	≤ 0.015	0.015-2.0	≤ 1.0	≤ 0.15
HCT980C (*)		≤ 0.23	≤ 1.0	≤ 2.7	≤ 0.080	≤ 0.015	0.015-2.0	≤ 1.0	≤ 0.15

(*) %V < 0.20; %B < 0.005.

Table 11.5 – Heat analysis of some CP (*Complex Phase*) steels for structural applications.

Designation	Standard	Yield Strength, YS [MPa]	Ultimate Tensile Strength, UTS [MPa]	Elongation after fracture, A%	Sampling position
HCT780C (*)	EN 10346	570-720	≥ 780	≥ 10 (°)	longitudinale
HCT980C (*)		780-950	≥ 980	≥ 6 (°)	longitudinale

(*) values to be guaranteed in flat semi-finished products in thickness 0.6 mm < tck. < 3 mm. The minimum increase to be guaranteed in YS due to the *Bake Hardening* effect is equal to 30 MPa.
(°) percentage elongation after fracture is determined in an 80 mm L_0 gauge length (A_{80mm}), which is a typical value for non proportional specimens, and not in $L_0 = 5.65 \cdot \sqrt{S_0}$, as with the traditional proportional specimen.

Table 11.6 – Mechanical properties of semi-finished products made from some CP (*Complex Phase*) steels for structural applications.

11.5 *Martensitic Steels* (MS)

Last but not least, we are going to examine the structural steel family of *Martensitic Steels*. These steels have carbon and manganese contents that vary from 0.09 to 0.23% and from 0.5 to 1.2%, respectively. Increased hardenability can be obtained by adding silicon, chromium, molybdenum and vanadium together with extremely low amounts of boron (B < 0.001%). After suitable quenching and tempering, you can reach Ultimate Tensile Strength values, UTS, up to 900 to 1,400 MPa, depending on the carbon content. These steels come with limited ductility and values of elongation after fracture around 5%, which, in any case, is enough to cold form parts styled as required. Figure 11.7 shows the stress/strain curves for some martensitic steels compared to a generic EN S235 steel.

MS steel micro-structure is mainly composed of martensite obtained by sudden cooling in water starting from the temperature where steel is in the γ or $\gamma+\alpha$ phase (intercritical temperature). Ferrite and/or bainite traces are also often present.

Martensitic steels are obtained by implementing two different methods. On one hand, cold pressed parts can be quenched and tempered at the end of the production process; on the other hand, hot or cold rolled semi-finished products can be heat treated during the steelmaking process and before final forming. In the case of plates and strip, the heat treatment is performed in line by means of water jets. In the case of cold formed parts, quenching takes place using water-cooled moulds. Tempering is normally required after quenching to give steel the desired fracture toughness.

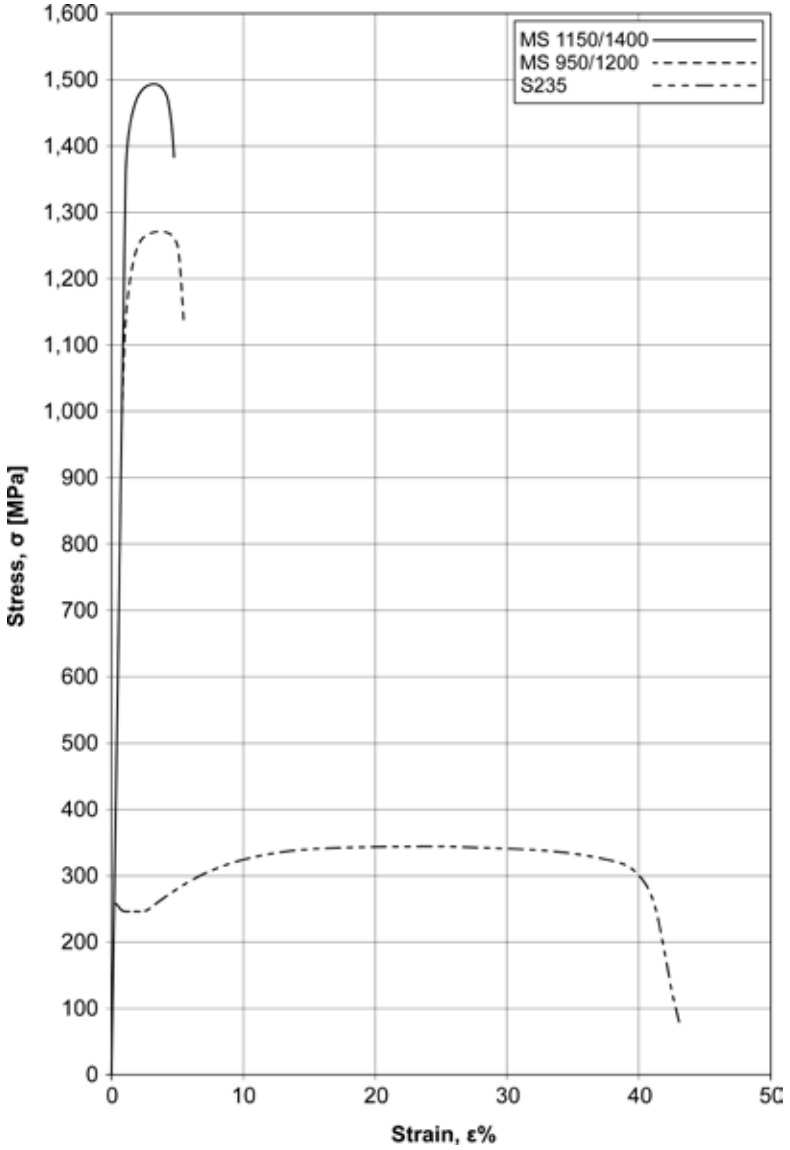

Figure 11.7 – Stress/strain curves for some martensitic steels (identified by the letters MS followed by their minimum YS and UTS values) compared to a generic EN S235 steel [from Keeler et al. 2017]

MS steels are used in the structural sector (profiles and lightweight frames) and in the automotive field to make bumpers, side members and side impact bars. EN S960QL is a typical example. It comes in hot rolled flat products for structural applications in thickness 3 up to 50 mm, as specified in the EN 10025-6

standard[4] (the initial letter S refers to the structural application; the number that follows is steel guaranteed minimum Yield Strength; Q indicates that this steel was quenched and tempered and L that it must have a minimum impact strength of 30J to -40°C).

At present, no special EN standards exist that cover cold rolled strip made of MS steel. Thus, reference should be made to VDA[5] 239-100, that are widely used by the leading steel manufacturers in the automotive sector. An example in this sense is steel CR1220Y1500T-MS for cold rolled steel strip in thickness 0.2 to 3 mm. Tables 11.7 and 11.8 show the reference standards, chemical composition and mechanical properties for the steels listed above. As previously stated, the micro-structure of MS steels is composed almost exclusively of martensite (Figure 11.8).

Designation	Standard	%C	%Si	%Mn	%P	%S	%N	%Cr	%Cu	%Mo	%Ni
S960QL (*)	EN 10025-6	≤ 0.20	≤ 0.8	≤ 1.7	≤ 0.020	≤ 0.010	≤ 0.015	≤ 1.5	≤ 0.5	≤ 0.7	≤ 2.0
CR1220Y1500T-MS (**)	VDA 239-100	≤ 0.28	≤ 1	≤ 2	≤ 0.020	≤ 0.025	---	(°)	≤ 0.2	(°)	---

(*) %Ti < 0.05; Nb < 0.06; %V < 0.12; and %B < 0.005. Steel should be deoxidized and with fine grain; to this aim Al_{tot} content should be equal to 0.018% minimum.
(**) %Ti + %Nb < 0.15; and %B < 0.01. Steel should be deoxidized and with fine grain; to this aim Al_{tot} content should be equal to 0.010% minimum.
(°) %Cr + %Mo < 1;

Table 11.7 – Heat analysis of some MS steels (*Martensitic Steels*) for structural applications.

Designation	Standard	Yield Strength, YS [MPa]	Ultimate Tensile Strength, UTS [MPa]	Elongation after fracture, A%	Sampling position
HCT780C (*)	EN 10346	≥ 960	980-1,150	≥ 10 (°)	longitudinale
CR1220Y1500T-MS (*)	VDA 239-100	1,220-1,520	1,500-1,750	≥ 3 (°)	longitudinale

(*) values to be guaranteed in flat semi-finished products in thickness 0.6 mm < tck. < 3 mm. The minimum increase to be guaranteed in YS due to the *Bake Hardening* effect is equal to 30 MPa.
(°) percentage elongation after fracture is determined in an 80 mm L_0 gauge length (A_{80mm}), which is a typical value for non proportional specimens, and not in $L_0 = 5.65 \cdot \sqrt{S_0}$, as with the a traditional proportional specimen.

Table 11.8 – Mechanical properties of semi-finished products made from some MS steels (*Martensitic Steels*) for structural applications.

[4] *EN 10025: Hot rolled products of structural steels - Part 6: Technical delivery conditions for flat products of high Yield Strength structural steels in the quenched and tempered condition.*

[5] *VDA 239-100, Sheet Steel for Cold Forming. VDA is the acronym for Verband der Automobilindustrie, the German Association of the Automotive Industry.*

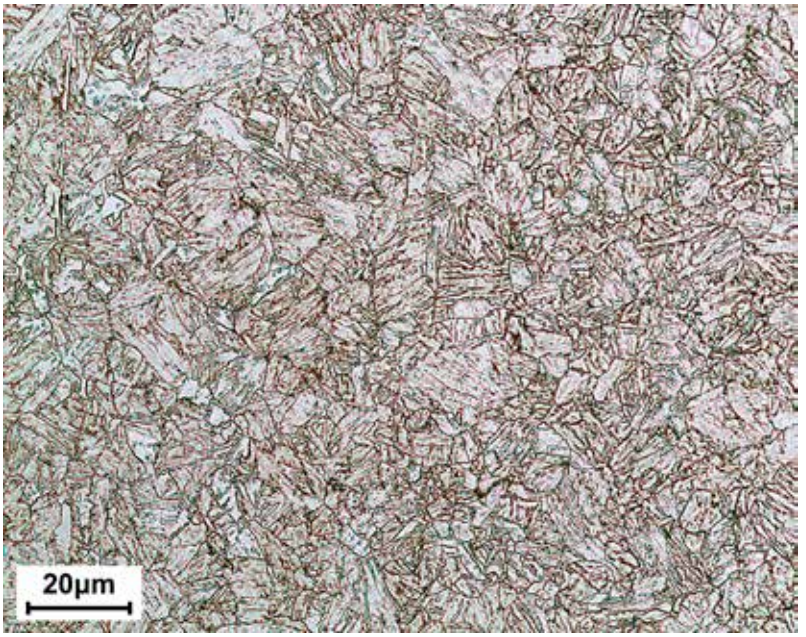

Figure 11.8 – Metallographic appearance of a martensitic steel grade EN S960QL. Notice the fully martensitic micro-structure; etching agent: Nital 2%. [Laboratories of the Department of Mechanical Engineering of Politecnico di Milano – Milan, Italy].

12. SPECIAL STRUCTURAL STEELS

12.1 What are Special Structural Steels

Special structural steels are widely used in many industrial engineering fields, in particular in the mechanical and metallurgical sectors, chemical and process industry, in the *automotive* sector, in production, transformation and distribution of energy and in the military industry. They should possess excellent mechanical properties in terms of static strength, fatigue resistance, impact strength and resistance to brittle fracture.

Together, all the properties mentioned above, that must be guaranteed in small-sized parts as well as in medium-sized to large components, make special structural steel highly suitable to manufacture driveshafts, camshafts, crankshafts, drive axles, railway axles, rotors, stems, pins, cams, tappets, valves, connecting rods, cranks, sliding rails, gears, power hammer and press columns, cylinders for high-pressure technical gases, coil and leaf springs, torsion bars, rolling bearings, firearm barrels and shutters, etc.

There are five main families of special structural steels:

- Steels for quenching and tempering and surface hardening steels,
- Self-hardening steels,
- Spring steels,
- Case hardening steels, and
- Nitriding steels.

Each family is meant for special application fields and, consequently, comes with specific properties.

The distinctive feature shared by these five steel families is that *quenching and tempering* are performed on the components before they are put into service. The Q&T heat treatment allows obtaining the best mechanical properties through the formation of tempered martensite.

12.2. Alloying Elements in Special Structural Steels

Before dealing with the metallurgical and mechanical characteristics of the five families of special structural steels, it is opportune to dwell on the effect that the various chemical elements produce when they are alloyed with iron.

The first element to be considered is *carbon* that is present in special structural steels in contents between 0.1% and 1%. Carbon is an austenitizing alloying element that widens the γ phase field in the *Fe-C* phase diagram, thereby gradually reducing temperature at the critical points A_3 and A_1. As far as steel hardenability is concerned, carbon has intermediate effectiveness.

The real function of carbon is to increase hardness and tensile strength (Yield Strength, Ultimate Tensile Strength and fatigue resistance) of the metallic mass.

The mechanism responsible for such increase is connected with the interstitial solid solution of carbon atoms in the iron lattice. The most effective condition is associated with the presence of temered martensite. On the other hand, an increase in carbon content always results in gradual worsening of impact strength, which is the reason why carbon content in special structural steels generally remains between 0.15% and 0.55%.
Silicon and manganese are two alloying elements that you always find in the chemical composition of special structural steels. They are used to deoxidize the liquid bath during the steelmaking process. For this reason, silicon traces of 0.2% to 0.4% and manganese traces of 0.4% to 0.8% are commonly found in special structural steels.
Silicon is a ferrite-forming element and is purposely added into spring steels only in amounts up to 2%. With these contents, tensile strength and mainly Yield Strength significantly increase, but a slight reduction of impact strength is also recorded. Silicon moderately affects hardenability.
Manganese is the element that most enhances hardenability in special structural steels, especially when its content exceeds 0.8%. It is an austenitizing element that considerably increases the tensile strength of the metallic mass. Its presence promotes carbon diffusion in case hardening processes. Being prone to form sulphides (MnS), manganese inhibits the occurrence of both hot and cold embrittlement induced by sulphur in solution in the iron lattice. In particular applications, manganese sulphides have beneficial effects on machining. In these cases, they are referred to as free-cutting steels or sulphur-controlled steels.
Also chromium, nickel and molybdenum are alloying elements often added into special structural steels in view of improving specific properties.
Chromium is a ferrite-forming element and raises temperature at critical points A_3 and A_1. It is used in contents up to 4% to increase hardenability in special structural steels while improving their tensile strength (static and under fatigue) and fracture toughness. When in high concentrations, it tends to form carbides and nitrides. Remember that in special structural steels, chromium without molybdenum, can originate temper embrittlement in the temperature interval from 370° to 590°C (with critical peaks at 525°C)[1].
Nickel is an austenitizing alloying element that lowers temperature at the critical points A_3 and A_1. Nickel has low chemical affinity with carbon and nitrogen and does not form carbides or nitrides.
Nickel is used in amounts up to 4% because it significantly improves impact strength and fracture toughness. It only marginally affects the other mechanical and metallurgical properties causing a limited increase of tensile strength and with a modest effect on hardenability.

[1] Temper embrittlement occurs in low-alloy chromium, chromium-nickel or chromium-manganese steels with a martensitic structure. Fracture toughness deteriorates if steel is tempered in temperatures from 370°C to 590°C (critical interval) or if, after being tempered at temperatures above 590°C, steel remains in the critical interval for a long time during the cooling phase, for example it is left to cool down slowly in the furnace after tempering. The most critical condition occurs around 525°C. Temper embrittlement is strongly inhibited, but not cancelled, by adding a limited amount of molybdenum (0.15 to 0.3%) to steel. This is the reason why almost all low alloy steels contains small percentages of molybdenum.

Similarly to chromium, molybdenum is a ferrite-forming element that forms carbides and nitrides. It supports hardenability and greatly improves tensile strength (Yield Strength, Ultimate Tensile Strength and fatigue resistance). Its presence, in amounts from 0.15 to 0.3%, is necessary to inhibit temper embrittlement.

Sometimes, two other elements are included in the chemical composition of special structural steels. They are *aluminium* and *vanadium*.

Like silicon and manganese, aluminium is normally used to thoroughly deoxidize the liquid bath. Aluminium concentrations around 0.010 to 0.025% are normally found in the chemical composition of special structural steels[2]. Aluminium is used as an alloying element in special nitriding steels only. Its presence is often required in amounts up to 1% due its high chemical affinity with nitrogen and the possibility to form very stable nitrides.

Vanadium is a highly ferrite-forming element added into special structural steels in amounts not exceeding 0.2%. It forms stable carbides and nitrides and promotes grain refining, which greatly increases tensile strength and partially also fracture toughness. It is used in the chemical composition of some spring steels because it inhibits steel relaxation.

Boron can be occasionally added in extremely low amounts, namely between 0.0005% and 0.005%. It considerably increases steel hardenability, especially in low carbon chemical compositions (0.2 to 0.3%).

12.3. Classification and Identification

You can immediately figure out to which of the five above mentioned families (quenching and tempering, self-hardening, springs, case-hardening or nitriding) a steel belongs starting from its designation.

To this aim, see Table 12.1 that lists the specificities of the five main families of special structural steels in terms of chemical composition, heat treatment and tensile strength.

[2] *Steel deoxidation in liquid phase is performed using silicon and manganese. Aluminium is also often added to boost the deoxidation process and for its strong grain refining property. Special structural steels that were deoxidized using silicon, manganese and aluminium are referred to as killed steels.*

Alloying elements	Q&T steels	Self-hardening steels	Spring steels	Case hardening steels	Nitriding steels
Carbon	> 0.2%	> 0.2%	≅ 0.5%	≤ 0.2%	> 0.2%
Silicon	(1)	(1)	1.5-2%	(1)	(1)
Manganese	(2)	(1)	(1)	(2)	(1)
Chromium	(2)	5% < C+Cr+Ni < 7%	(2)	(2)	YES; > 1.5%
Nickel	(2)		(2)	(2)	NO
Molybdenum	(2)	0.15-0.3%	(2)	(2)	YES; 0.15-0.3%
Aluminium	(1)	(1)	(1)	(1)	YES; 0.3-1%
Vanadium	(2)	(2)	(2)	(2)	(2)
Q&T heat treatment with tempering temperature of:					
Temperature	~600°C	~200°C / ~600°C	~450°C	~150°C	~600°C
Ultimate Tensile Strength, UTS (3)	600-1,500 MPa	1,100-2,500 MPa	1,300-1,800 MPa	600-1,500 MPa	600-1,500 MPa

(1) Normally, it is not purposely added as an alloying element (which does not means that it is not present at all).

(2) It can be used as an alloying element, but it might even not be present as an alloying element.

(3) In tensile specimens obtained from semi-finished product section not above 40 in dia.

Table 12.1 – At-a-glance classification of special structural steels based on chemical composition.

Let's examine a few examples to appreciate the usefulness of Table 12.1.

The first column is devoted to steels for quenching and tempering. Q&T steels typically have carbon content above 0.2% and can be alloyed with manganese, chromium, nickel, molybdenum and vanadium (but they might even not include any of these alloying elements). They are quenched and tempered at temperatures around 600°C. After the Q&T heat treatment, their tensile strength is between 600 MPa and 1,500 MPa, depending on the chemical composition.

Spring steels typically exhibit carbon contents around 0.5% and silicon contents between 1.5% and 2%. These steels can be alloyed with chromium nickel, molybdenum and vanadium. After quenching, they are tempered at temperatures around 450°C and reach an Ultimate Tensile Strength, UTS, around 1,300 MPa to 800 MPa.

Table 1 can also be used the other way round, which means that you can start from steel designation to infer the family it belongs to.

Let's make a first example based on steel EN 18CrMo4. This designation certainly refers to a case hardening steel because its nominal carbon content is 0.18% and the case hardening steel family is the only one where the carbon content is below or equal to 0.2%. The steel in question also has a nominal chromium content of 1% and a nominal molybdenum content of 0.2%. Consequently, we know that steel EN 18CrMo4 is quenched and tempered at about 150°C, thereby obtaining an Ultimate Tensile Strength in the range of 1,150 MPa to 1,250 MPa (values within the 600 to 500 MPa interval that is common to all case hardening steels).

Steel EN 41CrAlMo7-4 is a nitriding steel because it has a nominal aluminium content of 1%; this family is the only that includes aluminium as an alloying element.

Another example is steel EN 36NiCrMo16 that contains the following alloying elements: 0.36% nominal carbon content, 4% nominal nickel content and approximately 1.8% nominal chromium content together with small percentages of molybdenum (0.25%). Given that the sum of the nickel, chromium and carbon contents (4% + 1.8% + 0.36% = 6.16%) falls between 5% and 7%, this steel belongs to the family of self-hardening steels that can be also quenched and tempered at 200°C, not only at 600°C. In the first case, they reach an Ultimate Tensile Strength around 2,100 to 2,200 MPa and in the second case around 1,100 to 1,200 MPa (values within the 1,100 to 2,500 MPa interval that is common to all self-hardening steels).

As a last example, let's consider steel EN 42CrMo4 (0.42% nominal carbon content, 1% nominal chromium content and approximately 0.2% molybdenum content). EN 42CrMo4 cannot be a case hardening steel because its carbon content is too high, not a nitriding steel because it does not contain aluminium, not a self-hardening steel because the total amount of alloying elements is not enough to obtain $5\% < Cr + Ni + C < 7\%$ and it cannot be a spring steel because the carbon value is too low for this family and no silicon is present. By exclusion, only one solution is left: 42CrMo4 is a steel for quenching and tempering.

However, keep in mind that, even though Table 12.1 may prove extremely helpful, certainly it is not exhaustive. Actually, spring steels do exist that do not contain silicon (such as spring steels with a high carbon content and spring steels alloyed with chromium, chromium-vanadium or chromium-molybdenum-vanadium) and even nitriding steels that do not contain aluminium do exist (such as nitriding steels alloyed with chromium-molybdenum or chromium-molybdenum-vanadium). Furthermore, sometimes families slightly overlap to one another, as it happens with EN C60 that can be used as a high-carbon Q&T steel and as a spring steel or with EN C20 that can be used as a case hardening steel and as a low-carbon Q&T steel.

An overview of the main special structural steels, as classified by the standards, is given in Table 12.2.

Special Structural Steels	
Q&T steels ([1])([2]) EN ISO 683-1 EN ISO 683-2	Non alloy carbon steels: C20, C25, C30, C35, C40, C45, C50, C55 ([4]), C60 ([4]). Manganese steels: 23Mn6, 28Mn6, 36Mn6, 42Mn6. Chromium steels: 34Cr4, 34CrS4, 37Cr4, 37CrS4, 41Cr4, 41CrS4. Chromium-vanadium steels: 51CrV4. Chromium-molybdenum steels: 25CrMo4, 25CrMoS4, 34CrMo4, 34CrMoS4, 42CrMo4, 42CrMoS4, 50CrMo4. Chromium-nickel-molybdenum steels: 30CrNiMo8, 34CrNiMo6, 36CrNiMo4, 41CrNiMo2, 41CrNiMoS2. Boron (manganese-boron or manganese-chromium-boron) steels: 20MnB5, 30MnB5, 39MnB5, 27MnCrB5-2, 33MnCrB5-2, 39MnCrB6-2.
Self-hardening steels ([3]) EN10083-3	Nickel-chromium-molybdenum steels: 30NiCrMo16-6; 36NiCrMo16.
Spring steels EN 10089 EN 10132	Non alloy carbon steels: C55 ([4]), C60 ([4]), C67, C75, C85, C90, C100, C125. Silicon steels: 38Si7, 46Si7, 56Si7. Chromium steels: 55Cr3, 60Cr3, 102Cr6, 125Cr2. Silicon-chromium steels: 54SiCr6, 56SiCr7, 61SiCr7. Chromium-vanadium steels: 51CrV4, 80CrV2. Silicon-chromium-vanadium steels: 45SiCrV6-2, 54SiCrV6, 60SiCrV7. Silicon-chromium-molybdenum steels: 46SiCrMo6, 50SiCrMo6. Silicon-chromium-nickel steels: 52SiCrNi5. Chromium-molybdenum-vanadium steels: 52CrMoV4. Chromium-molybdenum steels: 60CrMo3-1, 60CrMo3-2, 60CrMo3-3.
Case hardening steels ([1]) EN ISO 683-3	Non alloy carbon steels: C10, C15, C16. Manganese steels: 22Mn6. Chromium steels: 17Cr3, 17CrS3, 20Cr4, 20CrS4, 28Cr4, 28CrS4. Manganese-chromium steels: 16MnCr5, 16MnCrS5, 16MnCrB5, 20MnCr5, 20MnCrS5. Chromium-molybdenum steels: 18CrMo4, 18CrMoS4, 20MoCr4, 20MoCrS4, 22CrMoS3-5, 24CrMo4, 24CrMoS4. Nickel-chromium steels: 16NiCr4, 16NiCrS4, 18NiCr5-4, 17CrNi6-6, 15NiCr13. Nickel-chromium-molybdenum steels: 20NiCrMo2-2, 20NiCrMoS2-2, 17NiCrMo6-4, 18CrNiMo7-6.
Nitriding steels EN ISO 683-5	Chromium-aluminium steels: 32CrAlMo7-10, 34CrAlMo5-10, 41CrAlMo7-10, 34CrAlNi7-10. Chromium-molybdenum steels: 24CrMo13-6, 31CrMo12. Chromium-molybdenum-vanadium steels: 31CrMoV9, 33CrMoV12-9, 40CrMoV13-9.

([1]) The chemical compositions including sulphur (S) are referred to free-cutting steels (with improved machinability).

([2]) The chemical compositions including boron (B) are referred as improved hardenability steels.

([3]) Self-hardening steels do not exist any longer in the new EN ISO 683-2 standards; those mentioned in this table were covered by the EN 10083-3 standard, withdrawn in 2018.

([4]) EN C55 and EN C60 are included in both standards for Q&T steels and for spring steels.

Table 12.2 – List of the designations for the five families of special structural steels (quenching and tempering, self-hardening, spring, case hardening and nitriding steels).

12.4 Assessing Tensile Strength in Special Structural Steels

Once you know the family a steel designation refers to, you can calculate the approximate Ultimate Tensile Strength, UTS, of that steel after quenching and tempering, which means in the condition where the material will operate once put into service.

Even though it is a simplified approach, the schematisation proposed by Raffaello Zoja in the Fifties of the last century certainly proves useful to[3] estimate the tensile properties of all special structural steels.

According to Zoja, the basic idea is that the Ultimate Tensile Strength, UTS, of a generic special structural steel is given by the sum of pure iron strength added with the contribution provided by carbon and the other alloying elements. Therefore, you have:

$$UTS = UTS_{Iron} + \Delta UTS_{Carbon} + \Sigma \Delta UTS_{Alloying\ elements} \quad \text{[eq. 12.1]}$$

where R_{Iron} is iron contribution, ΔR_{Carbon} is the increase due to carbon and $\Sigma \Delta R_{Alloying\ elements}$ is the summation of steel strength increases due to the various alloying elements.

If you convert the three contributions into numerical terms, you obtain:

$$UTS\,[\text{MPa}] = 300 + 1{,}000 \cdot \text{n} \cdot \%\text{C} + 100 \cdot (\%\text{Si} - 0.3\%) + 150 \cdot (\%\text{Mn} - \%\text{C}) + 40 \cdot \%\text{Ni} + \\ + 150 \cdot \%\text{Cr} + 300 \cdot \%\text{Mo} + 700 \cdot \%\text{V} + 50 \cdot \%\text{Al} \qquad \text{[eq. 12.2]}$$

The formula applies to 40mm dia. specimens made of quenched and tempered special structural steel. The validity interval of the formula with reference to steel chemical composition is as follows:

$$C \leq 0{,}7\% \quad Si \leq 1{,}5\% \quad Mn \leq 2\% \quad Ni \leq 5\% \quad Cr \leq 3\% \quad Mo \leq 1{,}2\% \quad V \leq 0{,}3\% \quad Al \leq 1{,}5\%;$$

The margin of error involved in using [eq. 12.2] is approximately ±10% of the value calculated[4].

However, it is necessary to make some considerations regarding [eq. 12.2].

The chemical symbols represent the element percentage that is present in the designation[5] while n is a multiplying factor for the carbon content only, which increases as the tempering temperature decreases. The value of n is given in Table 12.3.

---

[3] Zoja R., Lezioni di Metallurgia e Metallografia - Siderurgia, Tamburini - Milan, 1957. Laboratory technical manager with Cogne steel works (in the Aosta Valley, Italy), later adjunct professor of Metallurgy and Steelmaking Process Technology at Politecnico di Milano until the Seventies of the last century.

[4] Even though the formula in [eq. 12.2] seemingly contains a significant error (±10%), remember that during the designe phase, you generally adopt a safety factor of about 1.5 to 2 relative to the stresses calculated. This represents the possibility that the calculation hypotheses may carry an error between 50% and 100%, which is normally accepted by designers.

[5] The addends relating to alloying elements not listed in steel designation should not be considered in the summation.

Tempering temperature	Factor *n*
600°C	1
450°C	2.3
200°C	3.8
150°C	4

Table 12.3 – Trend of the *n* factor in the formula in [eq. 12.2] as a function of the tempering temperature.

The numerical coefficients in [eq. 12.2] represent the effect that the single alloying elements have on steel Ultimate Tensile Strength. You can easily notice that carbon is the chemical element that gives the highest contribution to tensile strength, with a coefficient varying from 1,000 to 4,000 with reference to the *n* factor that varies from 1 to 4. The coefficients of the other alloying elements contained in steels (Si, Mn, Ni, Cr and Mo) range from 40 to 300. This result is easily explained on the basis of the different nature of the alloying elements in question, carbon being the only interstitial chemical element while all the others are substitutional chemical elements.
Also notice the special form of the addends connected with silicon and manganese. In both cases, the content of the alloying element has decreased by a certain amount, namely -0.3% for silicon and -%C for manganese. This peculiarity is due to the fact that all steels always contain an amount of silicon of about 0.2 to 0.4% and of manganese in contents approximately same as the carbon percentage. This is because manganese and silicon are added during steelmaking due to their liquid bath deoxidizing capability. Therefore, these amounts of manganese and silicon are present also in non alloy carbon steels. Should you not subtract them, you would mistakenly count their contribution twice.

Let's now see how to apply the formula in [eq. 12.2] in practice with reference to some special structural steels commonly used. For example, consider the following steel grades: EN C40, EN 36CrNiMo4, EN 17NiCrMo6-4 and EN 51CrV4.
C40 is a steel for quenching and tempering with a nominal carbon content of 0.4%; this being a Q&T steel, it is quenched and tempered at 600°C (*n* factor = 1). Its Ultimate Tensile Strength UTS is as follows (notice that only the alloying elements actually listed in the designation should be introduced in the formula [12.2]):

$$UTS[\mathrm{MPa}] = 300 + 1{,}000 \cdot \mathrm{n} \cdot \%\mathrm{C} = 300 + 1{,}000 \cdot 1 \cdot 0.4\% = 700 \pm 70\ \mathrm{MPa} \quad \text{[eq. 12.3]}$$

Also 36CrNiMo4 is a Q&T steel quenched and tempered at 600°C (n factor = 1). In addition to its nominal carbon content of 0.36% and nominal chromium content of 1%, let's presume that it has a nickel content equal to 0.7% and a molybdenum content equal to 0.24%. Thence:

$$UTS\,[\mathrm{MPa}] = 300 + 1{,}000 \cdot \mathrm{n} \cdot \%\mathrm{C} + 40 \cdot \%\mathrm{Ni} + 150 \cdot \%\mathrm{Cr} + 300 \cdot \%\mathrm{Mo} = \\ = 300 + 1{,}000 \cdot 1 \cdot 0.36\% + 40 \cdot 0.7\% + 150 \cdot 1\% + 300 \cdot 0.24\% = 910 \pm 91\ \mathrm{MPa}$$

[eq. 12.4]

17NiCrMo6-4 is a case hardening steel (0.17% nominal carbon content, 1.5% nominal nickel content, 1% nominal chromium content and approximately 0.2% nominal molybdenum content) that is quenched and tempered at 150°C (n factor = 4); its Ultimate Tensile Strength is as follows:

$$UTS\,[\mathrm{MPa}] = 300 + 1{,}000 \cdot \mathrm{n} \cdot \%\mathrm{C} + 40 \cdot \%\mathrm{Ni} + 150 \cdot \%\mathrm{Cr} + 300 \cdot \%\mathrm{Mo} = \\ = 300 + 1{,}000 \cdot 4 \cdot 0.17\% + 40 \cdot 1.5\% + 150 \cdot 1\% + 300 \cdot 0.2\% = 1{,}250 \pm 125\ \mathrm{MPa}$$

[eq. 12.5]

Finally, 51CrV4: this is a spring steel containing vanadium; it is quenched and tempered at 450°C (0.51% nominal carbon content, 1% nominal chromium content and about 0.1% nominal vanadium content; n factor = 2.3). Its tensile strength is as follows:

$$UTS\,[\mathrm{MPa}] = 300 + 1{,}000 \cdot \mathrm{n} \cdot \%\mathrm{C} + 150 \cdot \%\mathrm{Cr} + 700 \cdot \%\mathrm{V} = \\ = 300 + 1{,}000 \cdot 2.3 \cdot 0.51\% + 150 \cdot 1\% + 700 \cdot 0.1\% \cong 1{,}700 \pm 170\ \mathrm{MPa}$$

[eq. 12.6]

According to Zoja, once you know steel Ultimate Tensile Strength, you can estimate the other mechanical properties of engineering interest. In particular, starting from the value UTS estimated by means of [eq. 12.2], you can calculate:

- The Yield Strength, YS,
- The fatigue limit under rotating bending stress, σ_{FAb}, and
- Vickers (HV) or Brinell hardness (HB)

for a generic special structural steel after quenching and tempering.

The Ultimate Tensile Strength is correlated to the other characteristics listed above approximately as follows:

YS = 0.7-0.8 · UTS (for Q&T, self-hardening, case hardening and nitriding steels) [eq. 12.7]

YS = 0.85-0.88 · UTS (for spring steels) [eq. 12.8]

σ_{FAb} = 0.45-0.55 · UTS (σ_{FAb} max = 700 MPa) [eq. 12.9]

HV (or HB) = 0.3-0.33 · UTS [eq. 12.10]

If you apply the formulae suggested above to the four steels under examination (EN C40, EN 36CrNiMo4, EN 17NiCrMo6-4, EN 51CrV4), you will obtain the values shown in Table 12.4.

Designation	Family	Factor *n*	Ultimate Tensile Strength, UTS [MPa]	Yield Strength, YS [MPa]	Fatigue limit, σ_{FAf} [MPa]	Hardness, HV (o HB)
EN C40	Quenching & Tempering	1	~700 ± 70	~490 ± 49	~330 ± 33	~220 ± 22
EN 36CrNiMo4	Quenching & Tempering	1	~910 ± 91	~680 ± 68	~430 ± 43	~290 ± 29
EN 17NiCrMo6-4	Case hardening	4	~1,250 ± 125	~930 ± 93	~600 ± 60	~400 ± 40
EN 51CrV4	Springs	2.3	~1,700 ± 170	~1,400 ± 140	~700 ± 70	~550 ± 55

Table 12.4 – Estimate of mechanical properties for steel grades EN C40, EN 36CrNiMo4, EN 17NiCrMo6-4 and EN 51CrV4.

13. QUENCHING AND TEMPERING (Q&T) STEELS

13.1 What are Quenching and Tempering Steels

Quenching and tempering steels are special structural steels with a medium carbon content ($0.2 < \%C < 0.6$). At regulatory level, there are Q&T steels that are either non-alloy carbon or carbon-manganese steels and Q&T steels that are low-alloyed mainly with chromium, chromium-molybdenum, nickel-chromium-molybdenum, manganese-boron or manganese-chromium-boron steels.

This steel family is the most widespread (accounting for 75 to 80% of all special structural steels) thanks to their perfectly balanced combination of fracture toughness and resistance to static stresses and fatigue.

Q&T steels are mainly used to manufacture machine components that will be subjected to high static and dynamic load conditions. However, if a medium to low stress is applied, you can also make recourse to general-purpose structural steels. In any case, typical applications of Q&T steels include driveshafts (solid or hollow), rotors, camshafts, tappets, crankshafts, axles, railway axles, connecting rods, crank mechanisms, stems, pins, manipulators, press columns, heavy-duty hardware, technical gas cylinders, firearm barrels and shutters, etc.

The chemical compositions of Q&T steels are designed to guarantee the best performances after quenching and tempering, i.e. after quenching followed by tempering at 600°C. This is the reason why hardenability is an essential feature of Q&T steels.

After quenching and tempering, this steel family provides Ultimate Tensile Strength, UTS, in values ranging between 600MPa and 1,500MPa, depending on the different amounts of the chemical elements they contain.

Notwithstanding the above mentioned advantages, many Q&T steels are still put into service after full annealing or normalizing, without enhancing their properties through a correct heat treatment.

13.2 Q&T Steels Metallurgy

Q&T steels are normally available on the market under the form of forgings or hot-worked semi-finished products (plates, bars, wire rods, etc.) in their as-rolled state, i.e. in the condition where the material is at the end of the production process. Delivery in the normalized or fully annealed state is requested for some special applications only.

EN ISO 683 is the basic standard covering Q&T steels. Part 1 (683-1) deals with non-alloy carbon and carbon-manganese Q&T steels. Part 2 (683-2) deals with low-alloy Q&T steels[1]. The metallurgical and mechanical properties of Q&T steels can be described starting from their chemical composition.

[1] *EN ISO 683-1: Heat-treatable steels, alloy steels and free cutting steels - Part 1: Non-alloy steels for quenching and tempering; EN ISO 683-2: Heat-treatable steels, alloy steels and free-cutting steels - Part 2: Alloy steels for quenching and tempering.*

Carbon is the element that confers hardness, especially when the micro-structure is martensitic type. As the carbon content increases, also steel hardness gradually increases in accordance with the martensite percentage[2] (Figure 13.1). However, carbon increase tends to gradually impair fracture toughness and resistance to brittle fracture. For this reason, Q&T carbon steels for industrial applications usually contain a carbon amount between 0.25% and 0.45%.

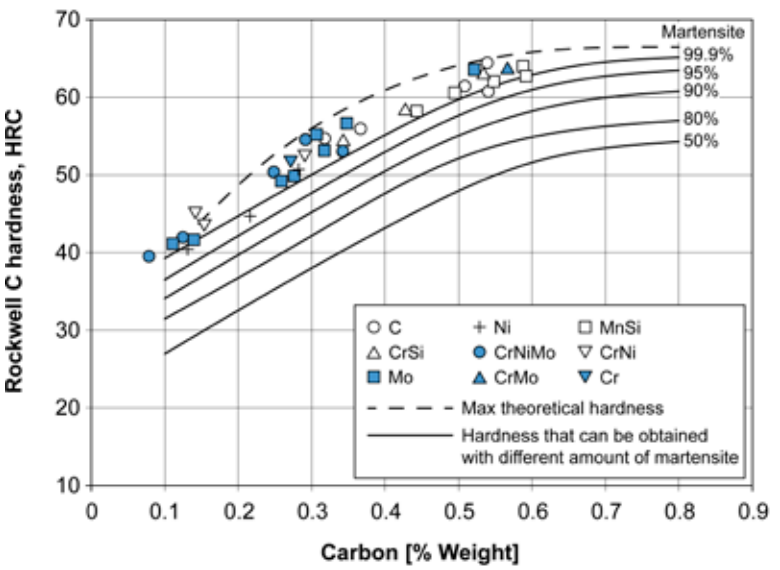

%C	$HRC_{50\%M}$	%C	$HRC_{50\%M}$
0.10	26.2	0.36	40.5
0.12	27.3	0.38	41.5
0.14	28.4	0.40	42.4
0.16	29.5	0.42	43.4
0.18	30.7	0.44	44.3
0.20	31.8	0.46	45.1
0.22	33.0	0.48	46.0
0.24	34.2	0.50	46.8
0.26	35.3	0.52	47.7
0.28	36.4	0.54	48.5
0.30	37.5	0.56	49.3
0.32	38.5	0.58	50.0
0.34	39.5	0.60	50.7

Figure 13.1 – HRC hardness trend as a function of carbon content and martensite percentage for quenched and tempered steels with different chemical compositions [from Liščič et al. 1992].

Chromium and manganese are alloying elements that are often added to Q&T steels to improve their mechanical strength (static and fatigue) and hardenability. Manganese also fairly improves brittle fracture resistance. Boron guarantees a significant hardenability increase and is normally present in an extremely low amount (0.0005 to 0.005%), often combined with manganese and chromium.

Nickel is mainly used to confer high fracture toughness and brittle fracture resistance while its contribution to improve mechanical strength is modest. The presence of this alloying element also brings about a small increase in hardenability.

Last comes molybdenum: this element induces excellent mechanical strength and good hardenability. It is used in contents ranging from 0.15 to 0.3% to inhibit temper embrittlement that occurs in chromium, nickel-chromium or chromium-manganese steels.

[2] *Hardness of martensite after hardening depends exclusively on the steel carbon content.*

Non-alloy carbon and manganese Q&T steels. This is the least expensive sub-category of Q&T steels. They exhibit both a low level of mechanical strength (UTS ≈ 600 MPa to 900 MPa for diameters 40 mm to 60 mm) and poor fracture toughness. Non-alloy carbon steel hardenability is very limited and is only a bit better in steels containing manganese. They are quenched in water or water added with polymers and are used to manufacture small parts in diameters up to about 60 mm. In addition to the traditional formulation, there also exist improved-workability non-alloy carbon steels where sulphur contents around 0.05% promote the formation of manganese sulphides to improve machinability.
Manganese Q&T steels suffer from temper embrittlement while non-alloy carbon ones are virtually immune. EN C40E3 and EN 36Mn6 are typical examples of this sub-category.

Manganese-boron and manganese-chromium-boron Q&T steels. Steels included in this sub-category are slightly more costly than the previous ones.
In comparison with non-alloy carbon steels, manganese (~1.5%), chromium (~0.5%) and above all boron (0.0005 to 0.005%) increase hardenability and mechanical strength (UTS ≈ 800MPa to 1,200MPa for diameters 40 mm to 60 mm). Manganese-boron steels are normally quenched in water or water added with polymers; manganese-chromium-boron steels are quenched in water added with polymers or in oil. They are used to manufacture small to medium size components in diameters up to 60 mm, which is similar to the value of non-alloy carbon steels but with much higher levels of mechanical strength. Manganese-boron and manganese-chromium-boron Q&T steels suffer from temper embrittlement. EN 30MnB5 and EN 33MnCrB5-2 are typical examples of this sub-category.

Chromium and chromium-molybdenum Q&T steels. Chromium in contents 1 to 1.5% and molybdenum, if present, considerably improve hardenability and mechanical strength in comparison with non-alloy carbon steels (UTS ≈ 800 to 1,200 MPa for diameters 40 mm to 60 mm). Impact strength and fracture toughness are higher than in the previous sub-categorys. The presence of molybdenum solves the issue of temper embrittlement. They are quenched in water added with polymers or in oil. They are used to manufacture medium-sized components in diameters up to 120 mm. In addition to the traditional formulation, there also exist improved-machinability chromium or chromium-molybdenum Q&T steels with sulphur contents around 0.05%. EN 25CrMo4 and EN 42CrMo4 are typical examples of this sub-category.

---

[3] The EN ISO 683-1 standard gives three different specifications for EN C40 steels in accordance with their distinctive sulphur and phosphor contents. The first is C40, with maximum permissible phosphor and sulphur contents equal to 0.045%; the second and the third are C40E and C40R that exhibit reduced values of such elements (steels with controlled maximum sulphur content).
In both cases, phosphor should remain within 0.025%; sulphur should not exceed 0.035% in C40E and remain between 0.020% and 0.040% in C40R. The permissible intervals for all the other alloying elements show no differences among C40, C40E and C40R steels.

Nickel-chromium-molybdenum Q&T steels. Adding nickel contributes improving steel impact strength and fracture toughness. Both hardenability and Ultimate Tensile Strength are slightly higher than in the previous sub-category (UTS ≈ 1,000 MPa to 1,250 MPa for diameters 40 mm to 60 mm). The presence of molybdenum makes these steels immune to temper embrittlement. Also chromium-nickel-molybdenum steels are quenched in water added with polymers or in oil. They are used to manufacture medium to large size components in diameters up to 180 mm.
EN 36CrNiMo4 and EN 30CrNiMo8 are typical examples of this sub-category.

The chemical composition of some Q&T carbon steels according to the EN ISO 683-1 and 683-2 standards is shown in Table 13.1 while their mechanical properties are listed in Table 13.2. The metallographic appearance of a Q&T steel after quenching and tempering is illustrated in Figure 13.2. Figure 13.3 shows the Jominy hardenability bands for three typical Q&T steels.

Designation	%C	%Si	%Mn	%P	%S	%Cr	%Ni	%Mo	Others
EN C40E	0.37-0.44	0.10-0.40	0.50-0.80	≤ 0.025	≤ 0.035	---	---	---	1
EN 36Mn6	0.33-0.40	0.10-0.40	1.30-1.65	≤ 0.025	≤ 0.035	---	---	---	1
EN 30MnB5	0.27-0.33	≤ 0.40	1.15-1.45	≤ 0.025	≤ 0.035	---	---	---	2, 3
EN 33MnCrB5-2	0.30-0.36	≤ 0.40	1.20-1.50	≤ 0.025	≤ 0.035	0.30-0.60	---	---	2, 3
EN 25CrMo4	0.22-0.29	0.10-0.40	0.60-0.90	≤ 0.025	≤ 0.035	0.90-1.20	---	0.15-0.30	3
EN 42CrMo4	0.38-0.45	0.10-0.40	0.60-0.90	≤ 0.025	≤ 0.035	0.90-1.20	---	0.15-0.30	3
EN 36CrNiMo4	0.32-0.40	0.10-0.40	0.50-0.80	≤ 0.025	≤ 0.035	0.90-1.20	0.90-1.20	0.15-0.30	3
EN 30CrNiMo8	0.26-0.34	0.10-0.40	0.50-0.80	≤ 0.025	≤ 0.035	1.80-2.20	1.80-2.20	0.30-0.50	3

1. The following is permissible: Cr < 0.4%; Mo < 0.1%; Ni < 0.4% and Cu < 0.3% (with Cr + Mo + Ni < 0.63%) in non alloy carbon steels for quenching and tempering.
2. Boron content in manganese-boron and manganese-chromium-boron Q&T steels is between 0.0005% and 0.005% (5 to 50 ppm).
3. Cu < 0.4%

Table 13.1 – Heat analysis of some Q&T steels [from EN ISO 683-1 and EN ISO 683-2].

Designation	Ø ≤ 16mm tck. ≤ 8mm				16mm < Ø ≤ 40mm 8mm < tck. ≤ 20mm				40mm < Ø ≤ 100mm 20mm < tck. ≤ 60mm				100mm < Ø ≤ 160mm 60mm < tck. ≤ 100mm			
	YS [MPa]	UTS [MPa]	A%	KV	YS [MPa]	UTS [MPa]	A%	KV	YS [MPa]	UTS [MPa]	A%	KV	YS [MPa]	UTS [MPa]	A%	KV
EN C40E	≥ 460	650-800	≥ 16	³20	≥ 400	630-780	≥ 18	≥ 20	≥ 350	600-750	≥ 19	≥ 20	---	---	---	---
EN 36Mn6	≥ 640	850-1,000	≥ 12	³20	≥ 540	750-900	≥ 14	≥ 25	≥ 460	700-850	≥ 15	≥ 25	≥ 410	650-800	≥ 16	≥ 20
EN 30MnB5	≥ 800	950-1,150	≥ 13	(*)	≥ 650	800-950	≥ 13	≥ 60	---	---	---	---	---	---	---	---
EN 33MnCrB5-2	≥ 850	1,050-1,300	≥ 13	(*)	≥ 800	950-1,200	≥ 13	≥ 50	≥ 750	900-1,100	≥ 13	≥ 50	---	---	---	---
EN 25CrMo4	≥ 700	900-1,100	≥ 12	(*)	≥ 600	800-950	≥ 14	≥ 50	≥ 450	700-850	≥ 15	≥ 50	≥ 400	650-800	≥ 16	≥ 45
EN 42CrMo4	≥ 900	1,100-1,300	≥ 10	(*)	≥ 750	1,000-1,200	≥ 11	≥ 35	≥ 650	900-1,100	≥ 12	≥ 35	≥ 550	800-950	≥ 13	≥ 35
EN 36CrNiMo4	≥ 900	1,100-1,300	≥ 10	(*)	≥ 800	1,000-1,200	≥ 11	(*)	≥ 700	900-1,100	≥ 12	(*)	≥ 600	800-950	≥ 13	(*)
EN 30CrNiMo8	≥ 850	1,030-1,230	≥ 12	(*)	≥ 850	1,030-1,230	≥ 12	≥ 30	≥ 800	980-1,180	≥ 12	≥ 35	≥ 800	980-1,180	≥ 12	≥ 45

Designation	160mm < Ø ≤ 250mm 100mm < tck. ≤ 160mm			
	YS [MPa]	UTS [MPa]	A%	KV
EN C40E	---	---	---	---
EN 36Mn6	---	---	---	---
EN 30MnB5	---	---	---	---
EN 33MnCrB5-2	---	---	---	---
EN 25CrMo4	---	---	---	---
EN 42CrMo4	≥ 500	750-900	≥ 14	≥ 35
EN 36CrNiMo4	≥ 550	750-900	≥ 14	(*)
EN 30CrNiMo8	≥ 750	930-1,130	≥ 12	≥ 45

(*) If the Charpy test with U-notched specimens is required, minimum impact strength value should be agreed upon by the parties.

Table 13.2 – Mechanical properties of Q&T steel semi-finished products after quenching and tempering; Ø: diameter, tck.: thickness [from EN ISO 683-1 and EN ISO 683-2].

Figure 13.2 – Metallographic appearance of the tempered martensitic structure of steel grades EN 42CrMo4 (top) and EN 36CrNiMo4 (bottom) [Exova S.r.l. Laboratories - Crema, Italy].

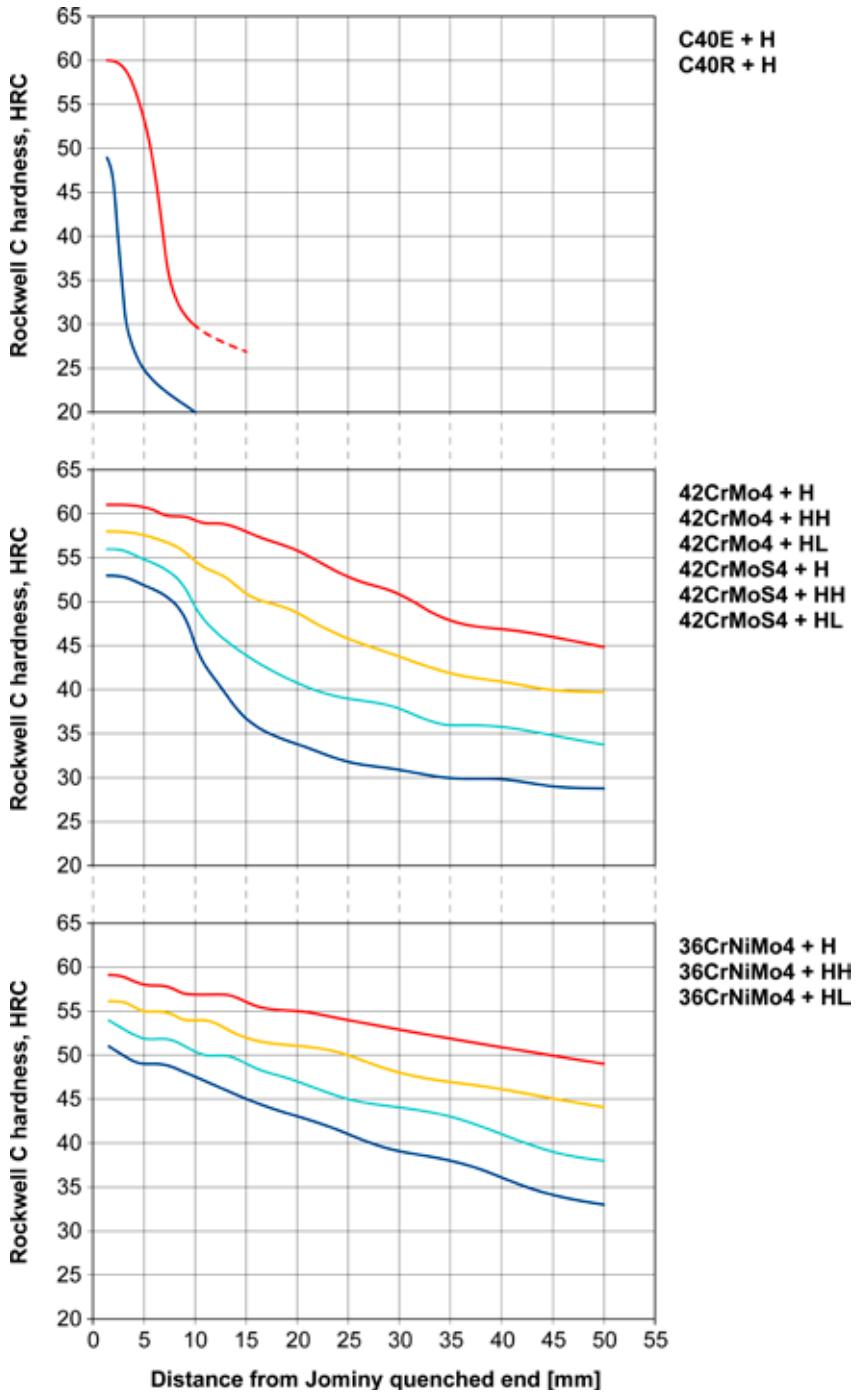

Figure 13.3 – Jominy hardenability bands for steel grades EN C40, EN 42CrMo4 and EN 36CrNiMo4. Upper limit curve (red line); upper limit curve for low hardenability steels (orange line); lower limit curve for high hardenability steels (pale blue line); lower limit curve (dark blue line) [from EN ISO 683-1 and EN ISO 683-2].

13.3 Q&T Steels Selection Criteria

A steel should not be selected at random or exclusively on the basis of money aspects.

Indeed, this choice should be made after careful evaluation of the mechanical strength required by the end use. This means that you have to select steel on the basis of steel hardenability[4] and part size in view of optimizing the amount of martensite throughout the component section.

A component made of Q&T steel should not necessarily have a martensitic structure throughout its hardened section. Typically, a core martensite amount of about 50% is considered acceptable because this value provides suitable mechanical strength throughout the component section. Otherwise, you should make recourse to a steel grade with higher hardenability, independent of costs.

It is also important to keep in mind that the technical standards allow using steels to manufacture components in diameters exceeding the ideal diameter defined by metallurgical criteria on hardenability. For example, the EN ISO 683-2 standard specifies steel grade EN 42CrMo4 for the production of semi-finished products up to a diameter of 250 mm, even though metallurgical considerations indicate 120 mm as the practical limit threshold to have 50% of core martensite[5]; therefore, you can use a semi-finished product made of EN 42CrMo4 with Ø250 mm. However, it is obvious that, if you compare a 250 mm dia. round bar with a 100 mm dia. round bar - after the same quenching process and with the same steel chemical composition - the final mechanical strength values across the two sections will be widely different. This is an important principle that must not be underrated.

To better understand what is described above, we provide some examples justifying the selection of a certain steel grade on the basis of both the Jominy hardenability curves given in the EN ISO 683-1 and EN ISO 683-2 standards and the so-called Grossmann chart. This diagram allows correlating core hardness of a round bar in a certain diameter, D, with quenching intensity factor, H, and distance, d, from the Jominy quenched end where you obtain the desired hardness[6] (Figure 13.4).

[4] Remember that steel hardenability is directly proportional to the amounts of alloying elements steel contains.

[5] Notice that 120 mm is the maximum diameter for an EN 42CrMo4 steel round bar where you can attain 50% of core martensite after quenching. The value indicated might drastically decrease if the amounts of alloying elements actually contained in steel are lower than the maximum permissible, even if they still fall within the limits accepted by the standard.

[6] Rushman W.F., "How to Determine Quench Severity of Oil and Salt Baths", Metal Progress, vol.84, no.6, p.91-92, 1963.

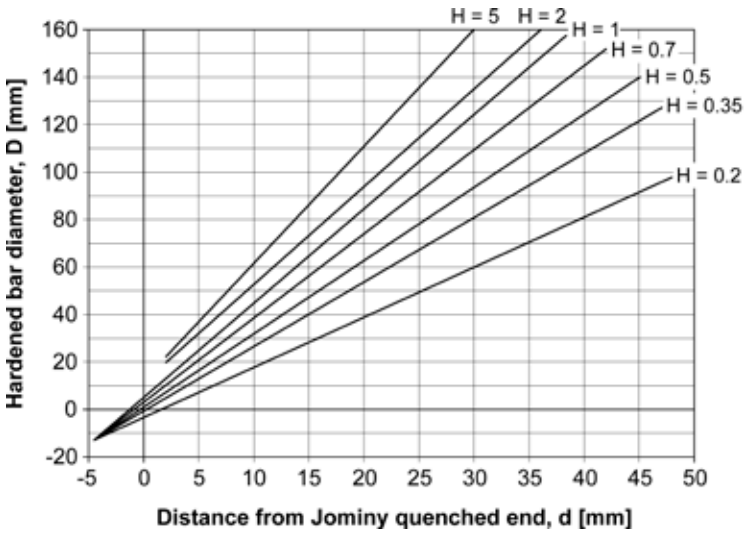

Severity	Correlation $D = f(d)$
H = 0.2	D = 2.11·d - 3.41
H = 0.35	D = 2.72·d - 0.83
H = 0.5	D = 3.10·d + 0.73
H = 0.7	D = 3.55·d + 2.92
H = 1	D = 3.98·d + 4.83
H = 2	D = 4.15·d + 10.40
H = 5	D = 4.93·d + 12.33

Figure 13.4 – Grossmann chart determining core hardness of a generic steel bar as a function of hardened bar diameter (D), distance from Jominy quenched end (d) and quenching intensity factor (H) [from ASM-H.4 1991].

Study case no. 1

Consider steel grade EN C40 and determine the round bar in maximum diameter that can be hardened taking care to attain 50% of core martensite. Assume that steel is quenched in very agitated water ($H = 2$). From Figure 13.1 you know that a steel with C=0.4% and 50% martensite has core hardness of 42.4 HRC. The next step is considering the Jominy hardenability curve for steel EN C40; we presume that it is the curve illustrated in Figure 13.5. Hardness along the Jominy hardenability curve is 42.4 HRC at a distance of approximately 4.5 mm from the quenched end.

Now, you can calculate the part core hardness using the information previously found and the Grossmann chart (Figure 13.5). Based on the distance , d, in the Jominy hardenability curve where you have hardness of 42.4 HRC, i.e. 4.5 mm from the quenched end and on quenching intensity factor, $H = 2$, you will find an equivalent diameter, D, of approximately 30 mm. This is the maximum diameter of the EN C40 steel round bar that has 50% core martensite after hardening using the quenching medium specified. Therefore, bars in diameters below 30 mm have a core martensite percentage above 50% while bars in diameters exceeding 30 mm have a core martensite percentage below 50%.

In brief, this means that you can manufacture a part having a diameter of 30 mm using EN C40 steel while respecting the metallurgical selection criteria based on hardenability. As the standard points out,

you can even go as far as manufacturing round bars in dia. 60 mm, but this would come with a significant reduction of mechanical strength. What is certain is that a part in dia. 100 mm must not be fabricated using EN C40 steel. In these dimensions, steel could not possibly harden at the core[7] and would encounter heavy difficulties in transforming into martensite even at the surface.

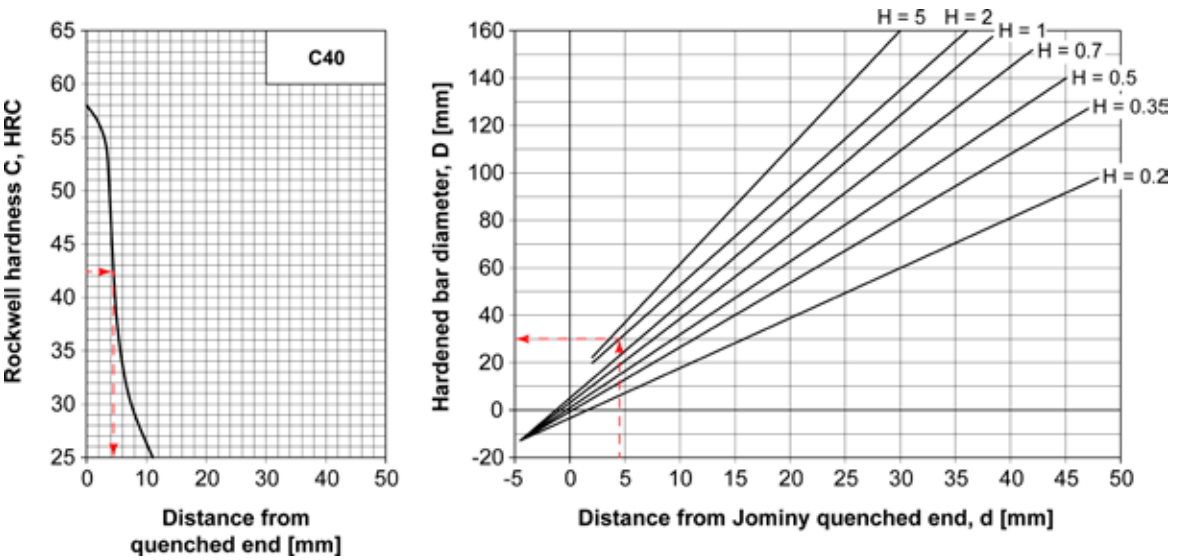

Figure 13.5 – Jominy hardenability curve for steel grade EN C40 and Grossmann chart. Example for calculating the diameter of round bars with 50% core martensite, hardened using a quenching medium with H=2.

Study case no. 2

Consider steel EN 36CrNiMo4 that is much more hardenable than EN C40 above. Also in this case, you will define the maximum diameter of the round bar that can be hardened so that to obtain 50% of core martensite. In this situation, it is opportune to use oil for rapid hardening given that this is a low alloy steel. Let's see what you obtain if the quenching medium is heavily agitated (H= 0.7) or if it is still (H= 0.2).
With steel EN 36CrNiMo6, you obtain 50% of core martensite when hardness is 40.5 HRC (Figure 13.1).
In the Jominy hardenability curve for steel EN 36CrNiMo4 (Figure 13.6) the distance from the quenched end where you find hardness equal to 40.5 HRC is about 33 mm.
Thence, steel EN 36CrNiMo4 round bars with 50% core martensite will have the diameters D (in mm) listed below depending on the different quenching intensity factor (H = 0.7 or H = 0.5), as follows:

if H = 0.7 $D \cong 3.55 \cdot d + 2.92 \approx 120mm \quad if \quad H = 0.7$

if H = 0.2 $D \cong 2.11 \cdot d - 3.41 \approx \ 64mm \quad if \quad H = 0.2$

[7] *By "hardening" we mean steel aptitude to form martensite during the heat treatment.*

This study case highlights another possible use of the Grossman chart. Assume that you have to harden a round bar with a known diameter (Ø120 mm) in heavily agitated oil for hardening ($H = 0.7$). The Grossmann chart shows (Figure 13.6) that hardness obtained at the round bar core will be equal to the value indicated at a distance of approximately 33 mm from the quenched end in the Jominy hardenability curve for that steel.

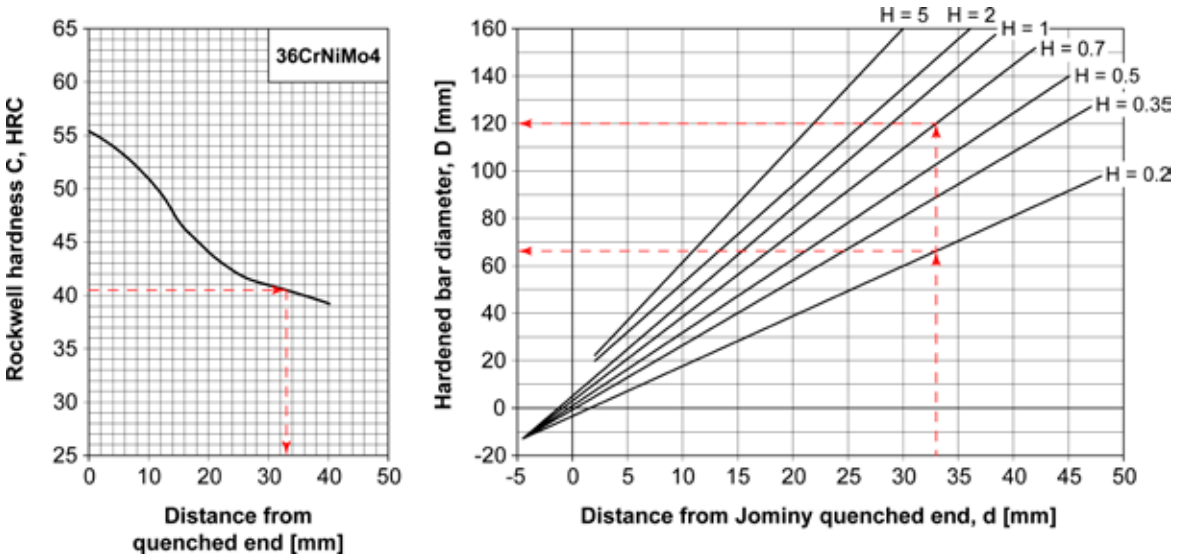

Figure 13.6 – Jominy hardenability curve for steel grade EN 36CrNiMo4 and Grossmann chart. Example for calculating the diameter of bars with 50% core martensite, hardened using quenching media with $H = 0.2$ and $H = 0.7$.

Study case no. 3

The Grossmann chart can also be used to estimate other values regarding steel round bar hardenability. In brief, it is a graph with three variables (namely, the round bar diameter, D, the distance from the quenched end, d, and quenching intensity factor, H). After defining two variables, the third is obtained automatically. Let's see an example based on steel EN 25CrMo4. You want to know which quenching medium should be used to harden a 100 mm dia. round bar and obtain core hardness of minimum 28 HRC.

From the Jominy hardenability curve for steel EN 25CrMo4 (Figure 13.7), you see that hardness of 28 HRC is obtained at a distance of approximately 29.5 mm (Figure 13.7). Now, take the Grossmann chart (Figure 13.7) and plot 29.5 mm (the distance from Jominy quenched end) on the abscissa axis and 100 mm (the round bar diameter) on the ordinate axis: you will find an intermediate point between the straight line with $H = 0.5$ and that with $H = 0.7$. This means that using a heavily agitated oil for rapid hardening ($H = 0.7$), you obtain hardness slightly above 28 HRC at the core of a 100 mm dia. round bar; if oil is moderately agitated, hardness is slightly below 28 HRC.

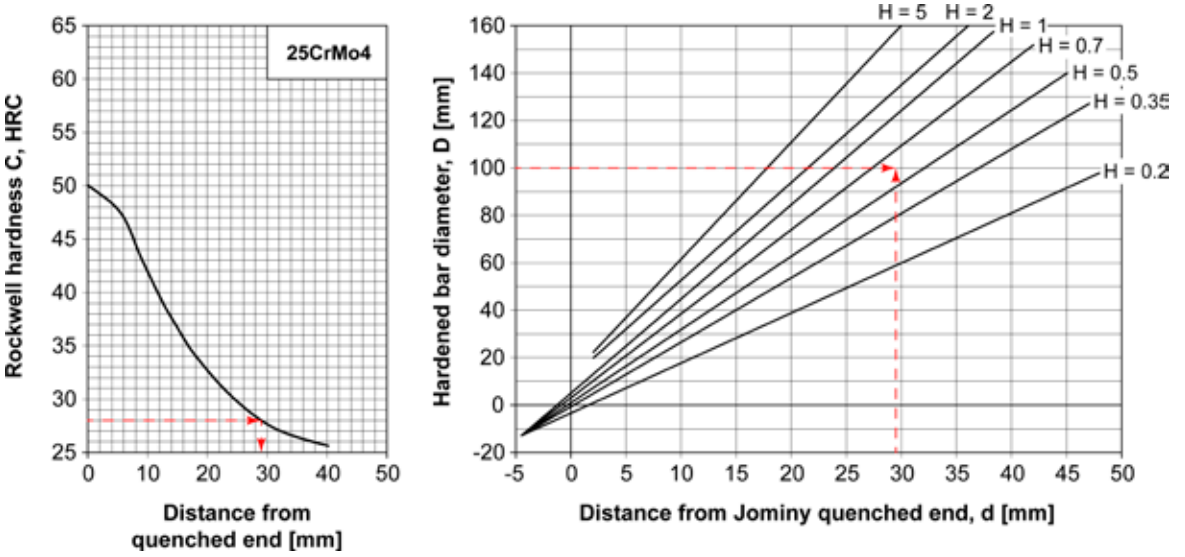

Figure 13.7 – Jominy hardenability curve for steel grade EN 25CrMo4 and Grossmann chart. Example for selecting the quenching medium for a 100 mm dia. round bar with 28 HRC hardness, equal to hardness taken 29.5 mm from the quenched end.

Study case no. 4

Consider a flat semi-finished product in thickness 50 mm and width 300 mm made of EN 25CrMo4 steel. Determine the equivalent diameter to define the quenching medium suitable to obtain 50% of core martensite. Rely on the graph in Figure 13.8 to switch from the flat product to the equivalent round bar. Plot width (300 mm) on the abscissa axis and thickness (50 mm) on the ordinate axis to find the diameter of the equivalent round bar that is approximately 80 mm.

With steel EN 25CrMo4, 50% of core martensite has hardness equal to 34.8 HRC (Figure 13.1). In the associated Jominy hardenability curve, this value is positioned approximately 17 mm from the quenched end (Figure 13.9). In the Grossmann chart (Figure 13.9), where $d = 17$ mm and $D = 80$ mm, you find a point of intersection at the line with quenching intensity factor $H = 2$; this means quenching in heavily agitated water. However, given that EN 25CrMo4 is a low alloy steel, it advisable to quench it in oil ($H = 0.7$ max) to prevent the formation of cracks due to the high residual stresses induced by sudden cooling. Therefore, in a 300x50 mm flat semi-finished product, you are bound to accept a martensite content below 50% and core hardness below 34.8 HRC.

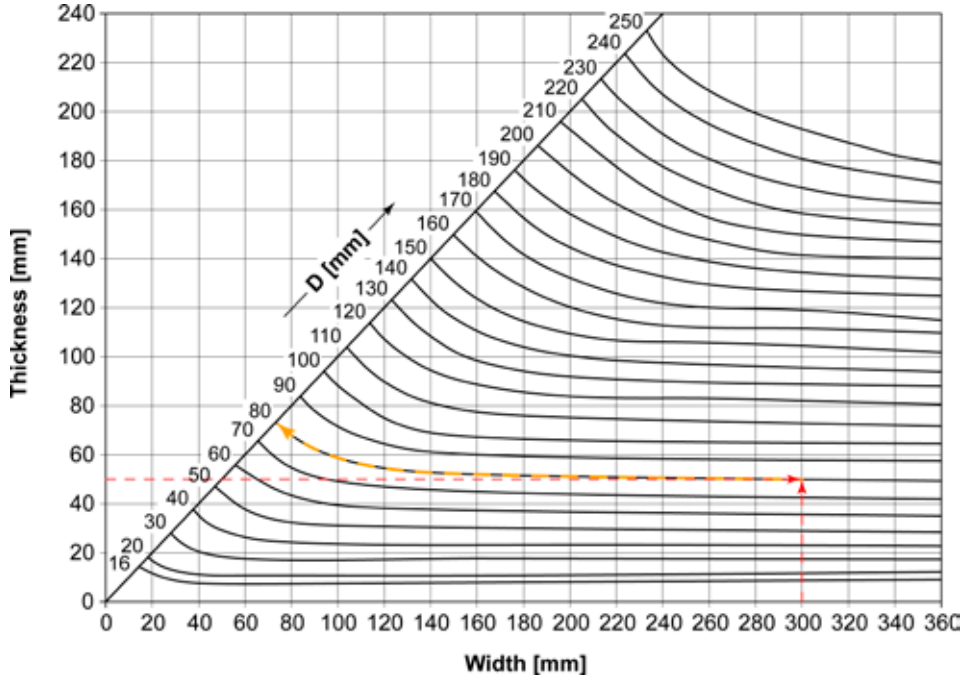

Figure 13.8 – Chart for calculating the equivalent diameter of a round bar starting from a flat product with known thickness and width [from EN ISO 683-2].

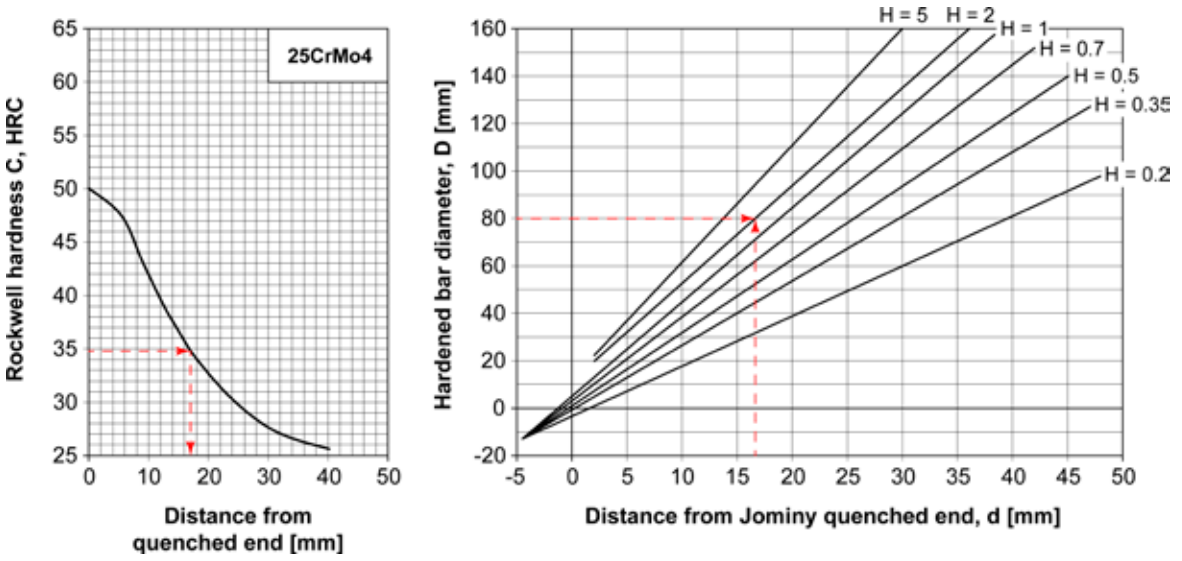

Figure 13.9 – Jominy hardenability curve for steel grade EN 25CrMo4 and Grossmann chart. Example for selecting the quenching medium for a 50mm dia. round bar with hardness equal to that found 17 mm from the quenched end.

13.4 Q&T Steels Manufacturing Cycle

If you are to manufacture a mechanical component from a generic Q&T steel, you should opportunely follow a manufacturing cycle that will bring you from the semi-finished product to the finished part on the basis of steel metallurgical properties and machining operations necessary to shape the component (Figure 13.10).

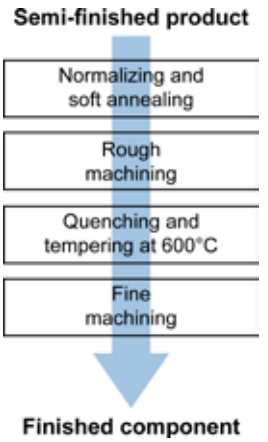

Figure 13.10 – Schematic of the manufacturing cycle necessary to manufacture a component from a generic Q&T steel.

For sake of simplicity, let's imagine manufacturing the driveshaft sketched in Figure 13.11 using Q&T steel grade EN 42CrMo4. The finished part shall be 1275 mm long and have a maximum diameter of 110 mm.

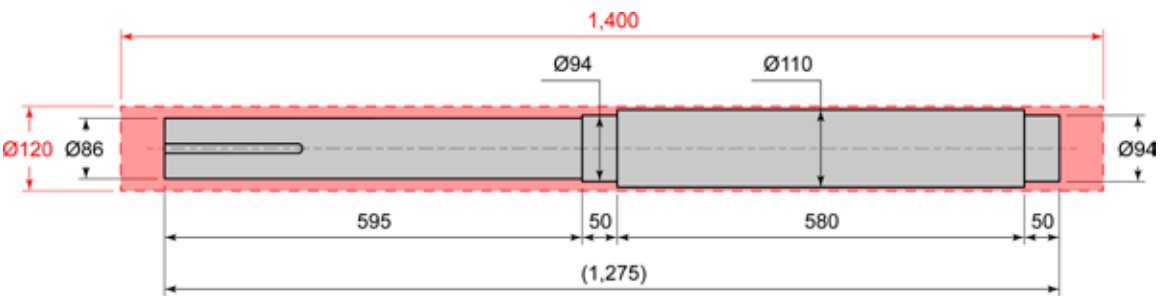

Figure 13.11 – Example of a mechanical component to be manufactured from Q&T steel.

Considering the axial-symmetrical geometry of the part to be manufactured, you have better start from a round bar with a diameter greater than the driveshaft maximum diameter, let's say 120 mm. Then you can proceed by turning.

The same applies to the total length of the semi-finished product. You can set it at 1,400 mm with the intention of securing one round bar end in lathe chuck and positioning the other on a support tailstock.
Given that the part in question is slim (length/diameter > 10), it might prove useful to place a steady rest half-way in the semi-finished product length to prevent weird bending of the part during machining.
Prior to starting machining, steel micro-structure may be opportunely optimized to improve its aptitude to be machined. To this aim, steel should be normalized and then undergo soft annealing.
Normalizing and soft annealing are the first step in the manufacturing cycle[8]. In some cases, these heat treatments can be omitted. For example, if the semi-finished product was sold already normalized and soft annealed, you can avoid incurring other costs associated with additional heat treatments.
But, if you are not certain of the delivery conditions of the semi-finished product, normalizing and soft annealing are a good starting point to obtain an high machinable equiaxiated ferrite-pearlite structure.
The next operation consists in rough machining; in this case it will be rough turning.
Carefully avoid reaching the part's design dimensions in this phase, but leave a machining allowance of a few millimetres to compensate for surface oxidation and deformation that occur in the part after hardening.
Let's say you leave a 2 mm machining allowance at the component radius. Therefore, the semi-finished product after rough machining features a maximum diameter of 114 mm and a minimum diameter of 90 mm. After rough machining, the hardening heat treatment is performed.
The ideal austenitization temperature differs on the basis of steel chemical composition. This information is normally specified in the standards. In the case of EN 42CrMo4, the EN ISO 683-2 standard specifies a temperature between 820°C and 860°C. Usually, the higher temperature is appropriate for steel to be quenched in oil, the lower temperature for steel to be quenched in water.
Holding time is approximately one minute per millimetre of the component radius[9] but should not be shorter than 30 minutes. In this case, minimum holding time is 60 minutes (Ø 114 mm). If you add heating time to holding time, you can presume that the whole treatment will take from one hour fifteen minutes to one hour and a half.
The semi-finished product is now taken from the furnace and quenched in the quenching medium. Also in this case, you can usefully make reference to the standard that suggests using oil or, alternatively, water added with polymers.
Never use only water with a low alloy steel. High quenching intensity factor of this medium might initiate quench cracks in a material featuring good hardenability like EN 42CrMo4[10].

[8] See Chapters 9, 10 and 11 of the book "Steel Metallurgy - Volume I" by Boniardi M. and Casaroli A., Lucefin - Esine, Italy, 2017.

[9] See Chapter 10 of the book "Steel Metallurgy - Volume I" by Boniardi M. and Casaroli A., Lucefin - Esine, Italy, 2017.

[10] Water is suitable for low hardenability steel like EN C40.

In the case under examination, it is opportune to use to an agitated oil for rapid hardening ($H = 0.7$ or $H = 0.5$) in order to obtain a suitable percentage of core martensite.
At cooling end, tempering is performed almost immediately after quenching. Being hard and brittle, as quenched martensite might cause fractures in the metallic mass as a consequence of the high residual stresses induced by quenching.

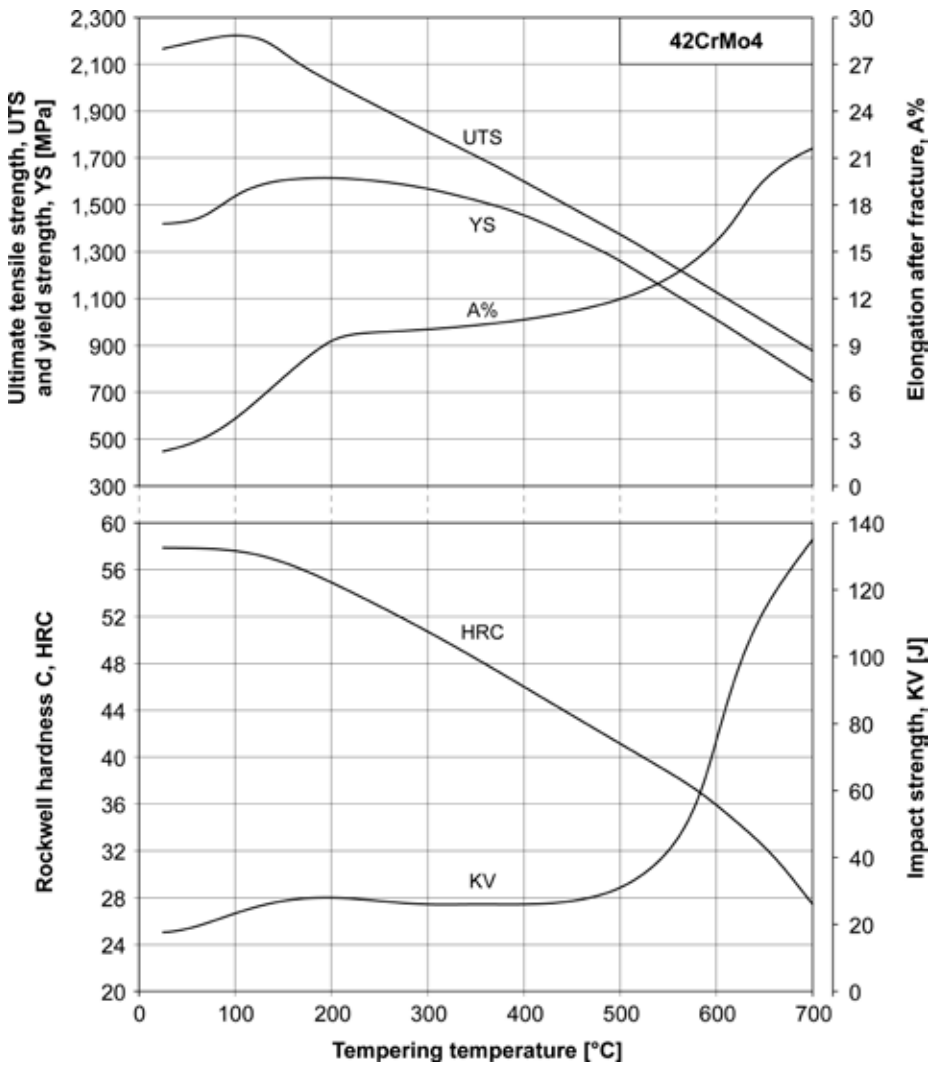

Figure 13.12 – Tempering curve for steel grade EN 42CrMo4 (10 mm dia. rods austenitized at 850°C for 1 hour, and then oil quenched and tempered for 2 hours): correlation between tensile strength (UTS and YS), ductility (A%), hardness (HRC) and impact strength (KV) at different tempering temperatures.

As regards tempering, the EN ISO 683-2 standard specifies a temperature of 540° to 680°C for a period of time normally between one and four hours. In this phase, it is very important to know which characteristics of the finished part are to be prioritized. If you want high hardness and mechanical strength, you should adopt lower temperatures (540° to 580°C); but, if impact strength and fracture toughness should prevail, go for higher temperatures (640° to 680°C). A tempering temperature of 600°C is a good compromise.
During this phase, it may prove useful to evaluate how the mechanical properties change when the tempering temperature changes (Figure 13.11).
However, it is also important to underline that maximizing both properties (YS and UTS vs. KV) is not feasible. This is the typical "short blanket dilemma": either you cover your feet or your head, both is impossible.
Fine machining come as the last manufacturing step. Stock allowances are removed to obtain the final size, geometrical/dimensional tolerances and roughness of the part, as desired. In this phase it is necessary to remove the oxidized surface and compensate for any plastic deformation induced by the heat treatments. Fine turning is the main machining technology used to manufacture this component. It can be supplemented with grinding and lapping, should strict tolerances and low roughness values be required.

14. SURFACE HARDENING STEELS AND THE SURFACE HARDENING PROCESS

14.1 The Surface Hardening Process and Suitable Steel Grades

Surface hardening is a heat treatment developed to locally increase hardness in a mechanical component and guarantee high resistance to wear and fatigue.

The parts to be surface hardened are manufactured using quenching and tempering steels; those with a carbon content around 0.4 to 0.5% are the most suitable for this process. Typical examples of Q&T steels used for surface hardening are the EN C40 and EN C45 grades covered by the EN ISO 683-1 standard[1] and the EN 42CrMo4, EN 50CrMo4, EN 41CrNiMo2 and EN 51CrV4 grades covered by the EN ISO 683-2 standard[2]. You can easily understand that a steel should not be selected at random or exclusively on the basis of money aspects. Indeed, this choice requires careful evaluation of metal hardenability, part size and expected performances.

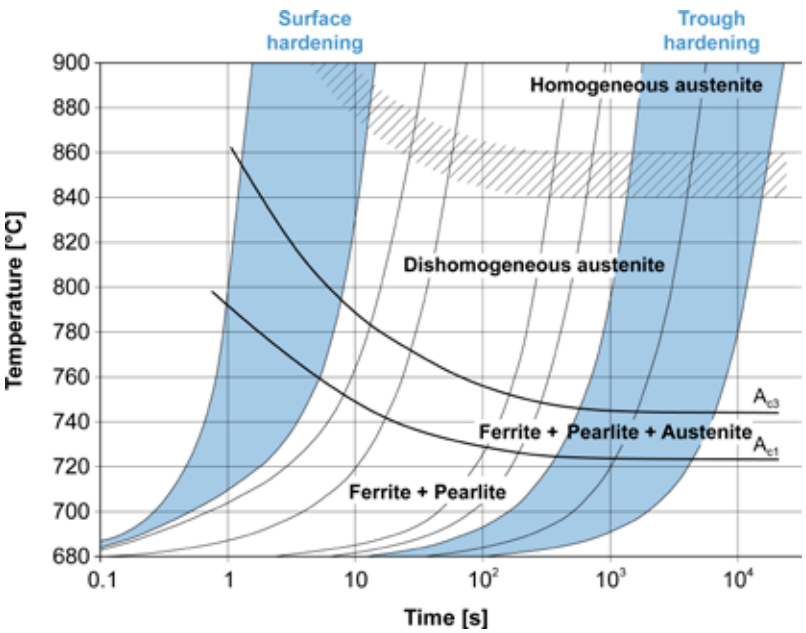

Figure 14.1 – Temperature trend at the critical points A_{c3} and A_{c1} for steel with C = 0.7% at different heating speeds. The concept of homogeneous/dishomogeneous austenite refers to carbon distribution in the γ-phase lattice [from Thelning 1975].

[1] *EN ISO 683-1: Heat-treatable steels, alloy steels and free-cutting steels - Part 1: Non-alloy steels for quenching and tempering.*

[2] *EN ISO 683-2: Heat-treatable steels, alloy steels and free-cutting steels - Part 1: Alloy steels for quenching and tempering Additionally, it should be noticed that in Italy the reference technical standard for surface hardening steels still is the obsolete UNI 7847 – Prodotti finiti laminati a caldo in barre e rotoli di acciaio non legato o legato speciale per tempra superficiale – Qualità, prescrizioni e prove.*

There is no such a thing as a common surface hardening routine for all Q&T steels, but process execution depends on the need to have elevated mechanical strength in the cortical areas. This happens, for example, for gears, sliding rails, racks, driveshafts, crankshafts, camshafts, rollers, bearing races, chain meshes and pins. Surface hardening involves fast steel heating above steel critical points (austenitization) up to 900° to 1,050°C, for a time not exceeding ten seconds. Temperatures are higher than in strandard hardening (about 50° to 150°C higher) given that the critical points A_{c3} and A_{c1} move upwards when heating occurs at very high speed (Figure 14.1).

Immediately after fast heating, the austenitized area is suddenly cooled down by means of water jets or jets of water added with polymers that induce martensitic transformation to minimum 95% of transformed structure. This results in high steel hardness, around 55 to 62 HRC (595 to 745 HV), depending on carbon amount[3]. After quenching, stress relieving is recommended at a temperature of approximately 150° to 200°C for 1 or 2 hours. Hardened layer thickness is usually between 1 and 10 mm, depending on processing methods.

To determine effective depth, reference should be made to the UNI 10932 standard[4]. After sectioning a sample part, you repeatedly measure HV hardness from the surface to the core and draw the curve that interpolates experimental data.

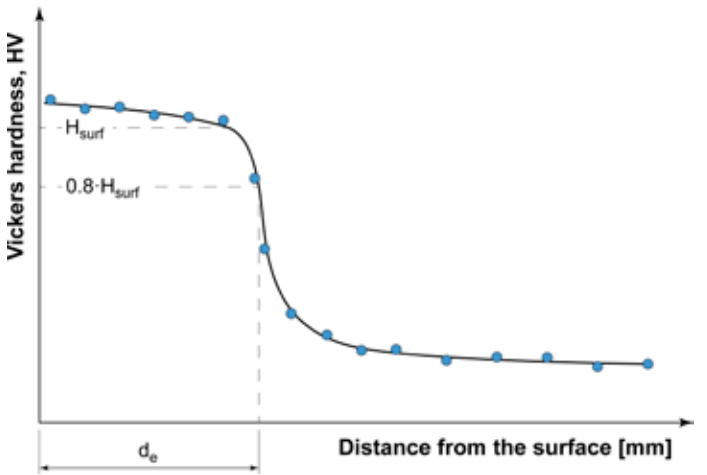

Figure 14.2 – Schematic for determining effective depth, d_e, in a surface hardened layer (H_{surf} minimum hardness required).

[3] *Martensitic structure hardness is a function of the carbon content and not of the cooling speed after the heat treatment.*

[4] *UNI 10932 – Trattamenti termici dei materiali metallici – Tempra superficiale dei materiali ferrosi.*

Effective depth, d_e, defines the distance from the surface to where hardness is 80% of the minimum hardness required for the surface hardening process in question, H_{surf}[5] (Figure 14.2).
If surface hardening is performed correctly, core steel in the part does not sustain substantial thermal alterations because it remains below its critical points (A_{c3} and A_{c1}). Thus, the metal remains in the metallurgical state induced by the heat treatment preliminary to surface hardening, which usually is quenching and tempering. In these cases, the core micro-structure consists mainly in tempered martensite (Figure 14.3).

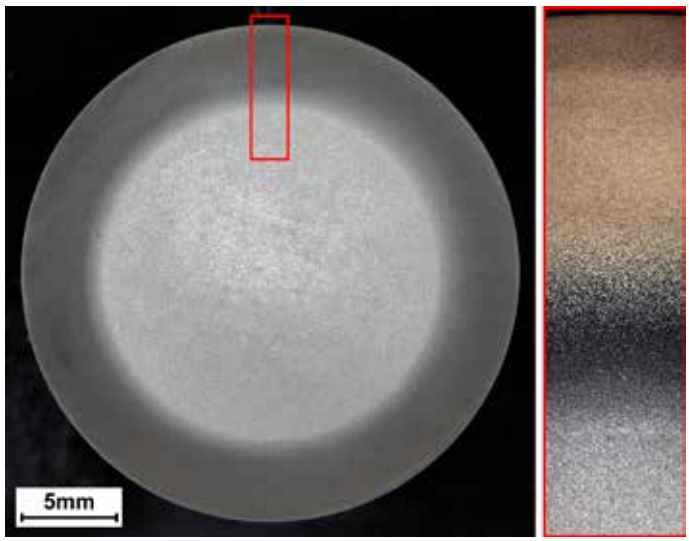

Figure 14.3 – Macroscopic and microscopic appearance of an EN 42CrMo4 steel round bar after induction surface hardening [Omeco S.r.l. Laboratories - Monza, Italy].

In some low cost applications, you can leave steel in the normalized or fully annealed state, with its distinctive fine or coarse pearlitic-ferritic micro-structure. In these cases, however, you usually observe a decrease in hardening depth due carbon dishomogeneity in the austenite lattice[6] (Figure 14.4).

[5] The definition of effective depth provided in the UNI 10932 standard is very different from the one given for case hardening or nitriding (see Chapters 17 and 18 in this book). In the case of surface hardening, reference is made to end customer requests and not to a numerical value, either absolute (as in case hardening) or connected with the steel being processed (as in nitriding). This may lead to different effective depth evaluations even if the same steel grade and process are involved.

[6] Theoretically, carbon is evenly distributed in the martensitic structure lattice; therefore, when quenched and tempered steel is re-austenitized to perform surface hardening, you obtain a homogeneous structure. But if the structure is ferritic-pearlitic, carbon distribution is not homogeneous with a 6.69% carbon content in the Fe_3C phase (pearlite lamellae) and virtually no carbon in the α-phase (ferrite and pearlite lamellae). When this structure is austenitized, exactly because heating is extremely fast, carbon cannot diffuse in the lattice and, consequently, the resulting austenitic structure is not homogeneous. Also, if the ferritic-pearlitic grain is fine (normalizing), the issue is less evident because dishomogeneity is short-range; on the other hand, if the grain is coarse (full annealing), the effect is more evident due to long-range dishomogeneity.

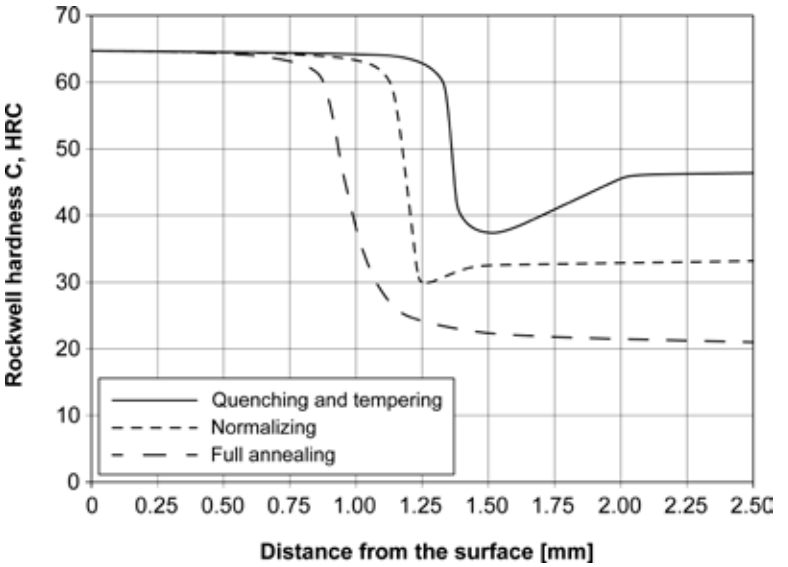

Figure 14.4 – Hardness trend depending on distance from the surface for steel with C = 0.7% subjected to different heat treatments before surface hardening (induction hardening with frequency 450 kHz and power density 25 W/mm^2) [from Rudnev et al. 2003].

Another important result of surface hardening and subsequent stress relieving is that a field of compressive residual stresses creates near the part cortical area. This phenomenon is due to the steel specific volume increase occurring only in the hardened surface layer as a consequence of austenite transformation into martensite.

Refer to Figure 14.5 to better understand what happens in the part. If the surface being hardened could expand freely, you would observe a volume increase (Figure 14.5a). In reality, the surface is bound to the part core; consequently, volume increase is inhibited. It is as if an external force F were acting on the surface, preventing expansion and generating compressive residual stresses in the layer (Figure 14.5b). Remember that compressive residual stresses are particularly beneficial because they decrease the tensile stresses applied to the part surface, thereby significantly improving fatigue resistance.

To obtain high hardness, suitable hardening thickness and compressive residual stresses, it is opportune to start from peeled or ground semi-finished products whose surfaces are free from decarburizing issues.

Figure 14.6 shows the manufacturing cycle to be implemented to obtain a correctly surface hardened mechanical component. It is the same cycle specified for Q&T steels, except for surface hardening that is performed after quenching and tempering and before finish machining.

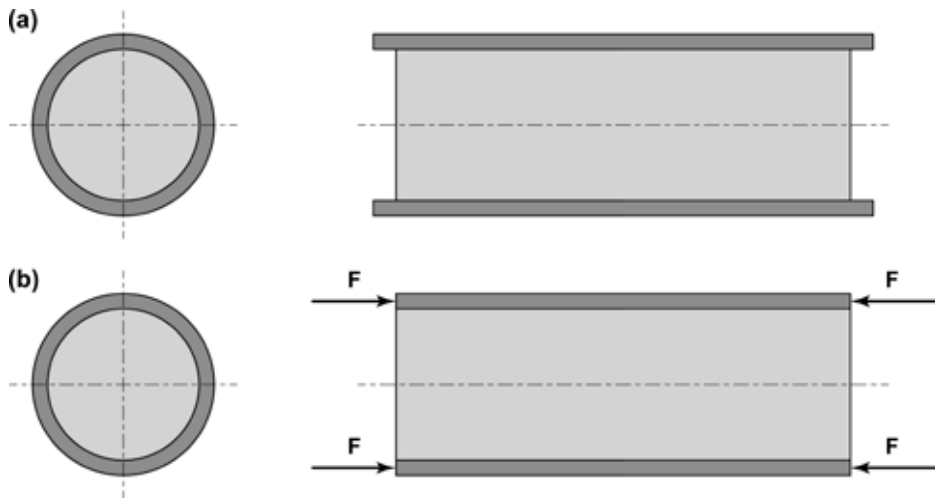

Figure 14.5 – Specific volume increase of the surface hardened layer: (a) the surface is free to move relative to the core, (b) the surface is bound to the core (real-life case).

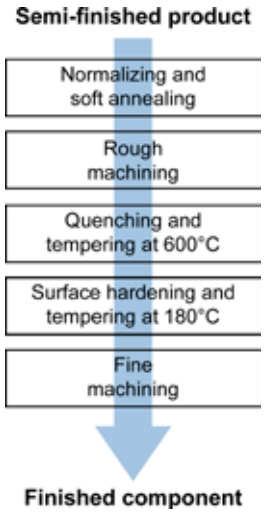

Figure 14.6 – Schematic of the manufacturing cycle for a component obtained from surface hardened Q&T steel.

14.2 Induction Surface Hardening

Surface hardening makes recourse to various technologies to obtain local heating of the metal. Based on these technologies, the processes are classified as induction hardening, flame hardening and laser hardening. Magnetic induction is certainly the commonest technology used at industrial level to perform surface hardening. To heat a component, a special electric circuit, called inductor, is placed in the vicinity of the surface to be hardened. The inductor is made of copper, with an internally water-cooled round or square section.

The electric circuit is supplied with high-frequency alternate current in the range of thousands of Hertz (3 to 450 kHz). Specific powers are between 5 and 30 W/mm^2.
In its simplest layout, the inductor is a solenoid composed of a certain number of coils within which you place the bar to be heat treated (Figure 14.7). As the inductor is close to the surface being hardened, an alternate magnetic flux is induced in the part whose variations in time generate a field of induced currents a.k.a. Foucault's currents or *eddy currents*.
The metal heats up due to the Joule effect[7], but heating occurs only in the areas where the eddy currents flow. Experimentally, you observe that the electric field lines get thicker near the part surface as the electric current frequency increases. This phenomenon is called "skin effect".
The shape, the number of coils and the distance of the inductor from the part (clearance) are some of the parameters that, together with electric current frequency, determine the distribution of the magnetic flux and eddy currents, i.e., of heating efficiency (Figure 14.8). Various technological solutions exist that allow induction hardening also in the case of parts with irregular profiles (Figures 14.9 and 14.10).

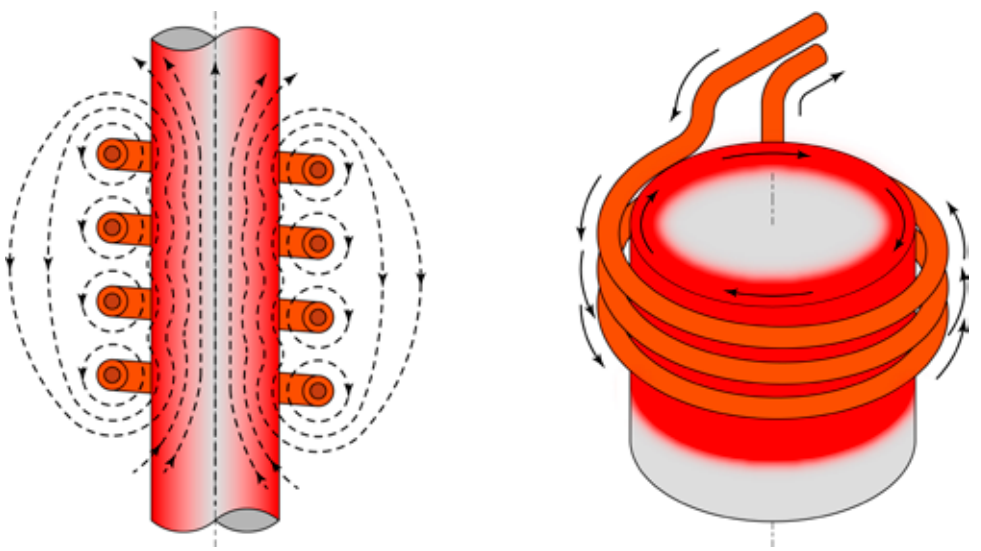

Figure 14.7 – (on the left) Trend of the magnetic field induced in a steel round bar placed into a solenoid inductor through which alternate current is flowing; (on the right) Electric current trend in the inductor and in the round bar [from Thelning 1975].

[7] *Whatever electric circuit with impedance Z, crossed by a current with intensity I, generated by a potential differential V, dissipates electric power in the amount of* $P = V \cdot I = Z^2 \cdot I$ *as heat. Many different applications (incandescent bulbs, fuses, electric ovens, etc.) take advantage of this characteristic that goes under the name of Joule effect that, however, is also responsible for the loss of efficiency experienced by many systems (electric motors, high-voltage cables, etc.).*

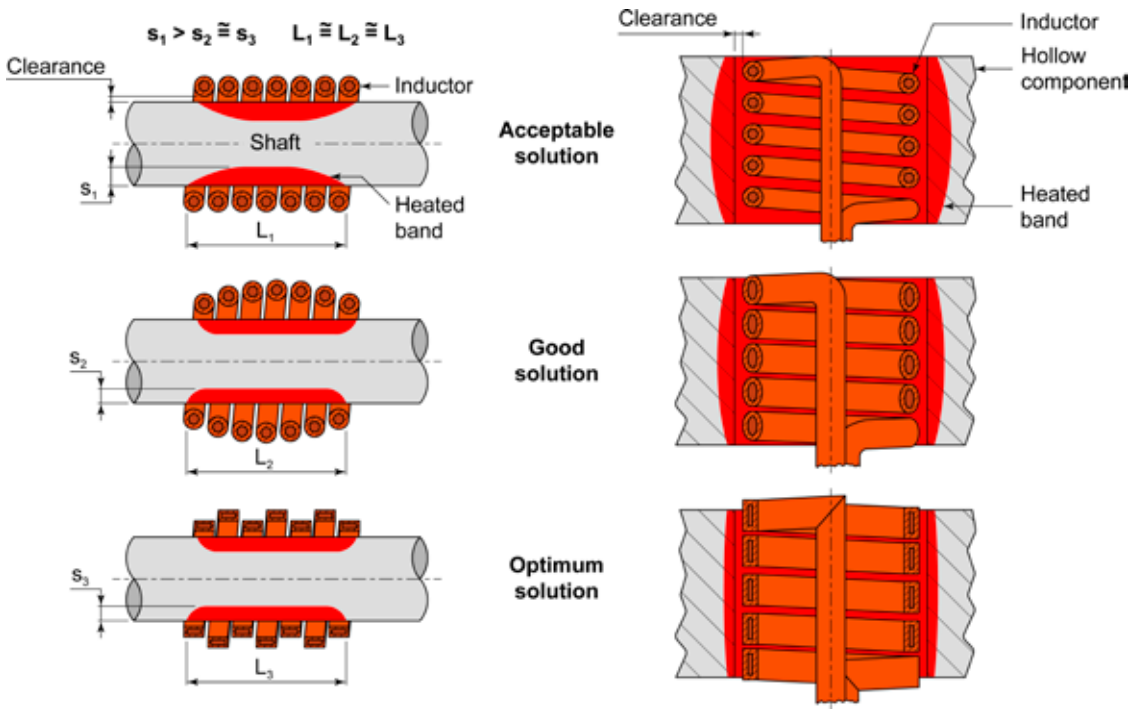

Figure 14.8 – Technological solutions with solenoid inductors to surface-harden cylindrical shafts and internal cavities. Notice how the coils are positioned and their profile with reference to the part being heat treated [from ASM-H.4, 1991 and Rudnev et al. 2003].

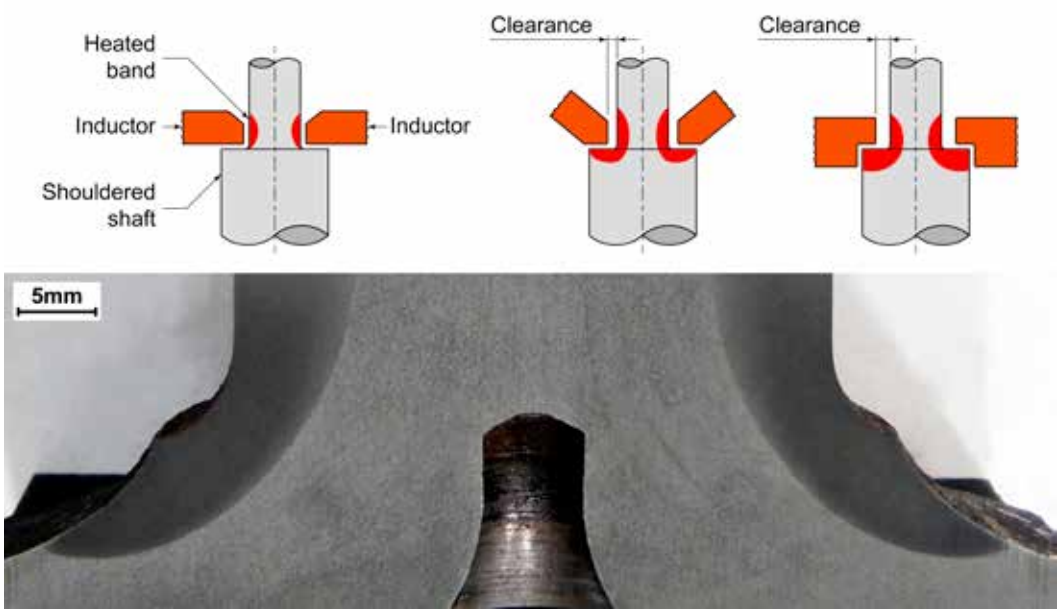

Figure 14.9 – Technological solutions based on specially designed inductors to surface-harden irregular shapes [from Rudnev et al. 2003]; example of a surface hardened driveshaft shoulder [Omeco S.r.l. Laboratories - Monza, Italy].

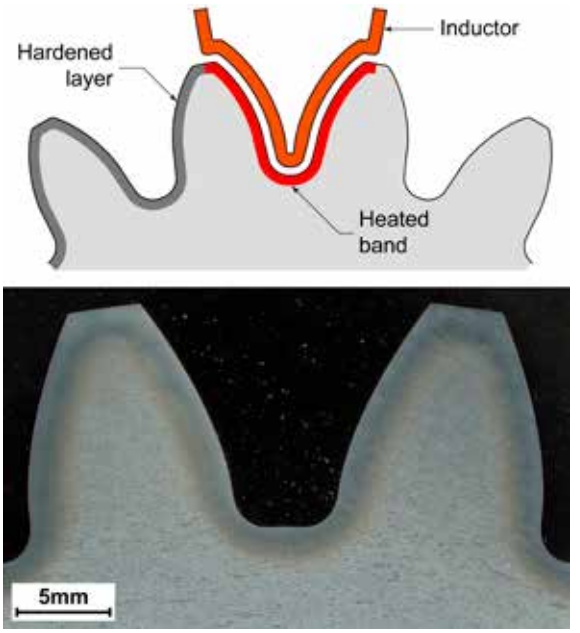

Figure 14.10 – Technological solution based on specially designed inductor to surface-harden irregular shapes [from Rudnev et al. 2003]; example of a surface hardened gear [Bonfiglioli S.p.A. Laboratories, Trasmital Division - Forlì, Italy].

Immediately after heating, coolant is sprayed onto the part surface at high speed. In some cases, a tank is placed near the hardening furnace and the part is quenched by immersion.

Basically, there are two methods to perform induction surface hardening: either *single-shot hardening* (a stationary or localised process) or *progressive hardening* . In both cases, the process is fully automated, which allows excellent repeatability of results.

In *single-shot hardening* , the inductor heats the entire surface to be treated at the same time, and then the cooling system, that can be separate or coupled to the inductor, suddenly cools down the entire austenitized area (Figure 14.11).

In *progressive hardening* , the inductor and the cooling circuit treat only a portion at a time of the part being heat treated. First the inductor heats a section of the part and immediately after the cooling system quenches it. The process goes on until the entire component is surface hardened. A typical example is shown in Figure 14.12: the bar moves downwards and turns on its axis while the inductor and the cooling system heat and quench the bar step by step.

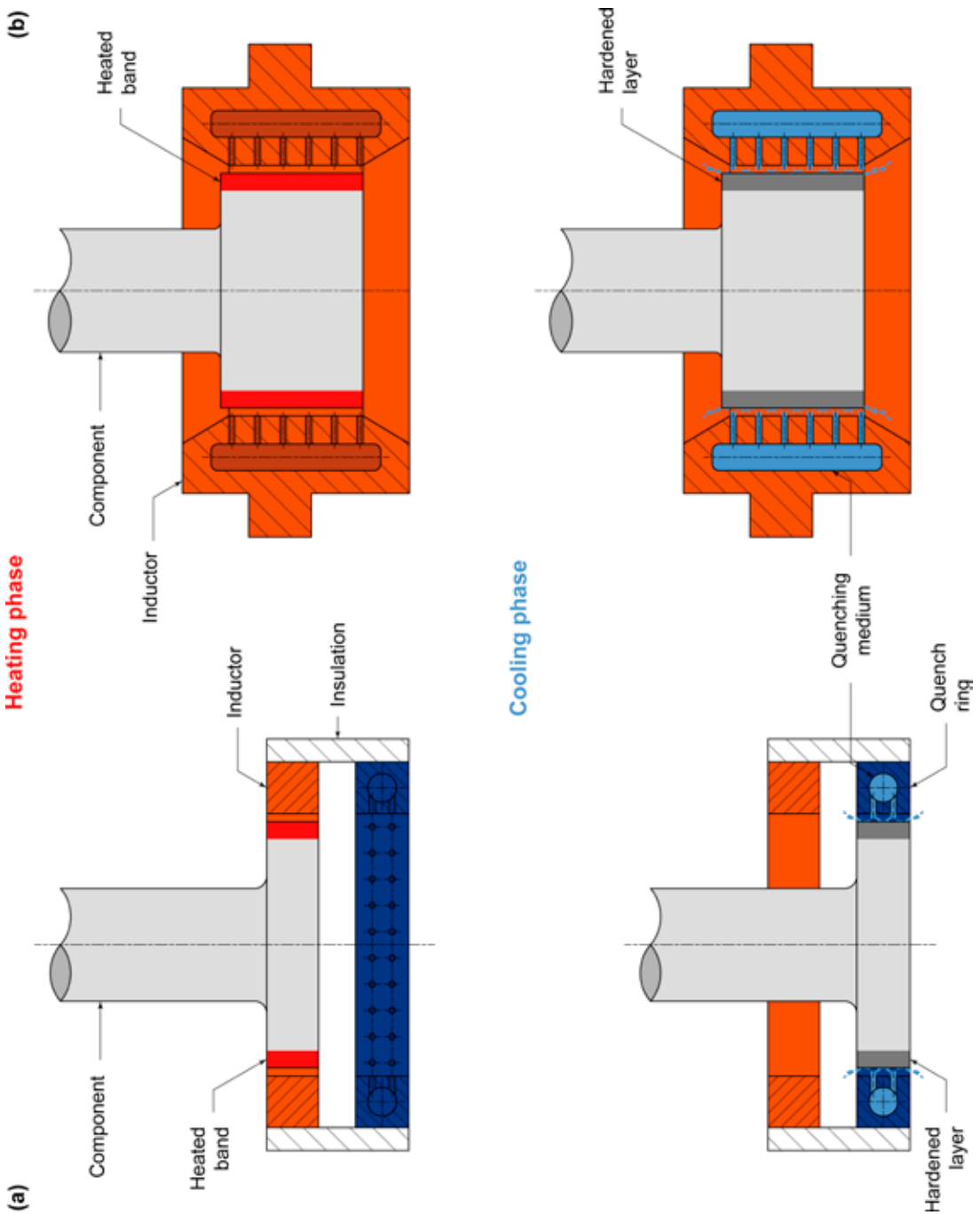

Figure 14.11 – Schematic of the single-shot hardening process - (on the left) Separate inductor and cooling system. After heating, the part moves downwards to be cooled - (on the right) Coupled inductor and cooling system. The part is stationary. First the inductor heats the part surface, then the cooling system quenches it [from Thelning 1975].

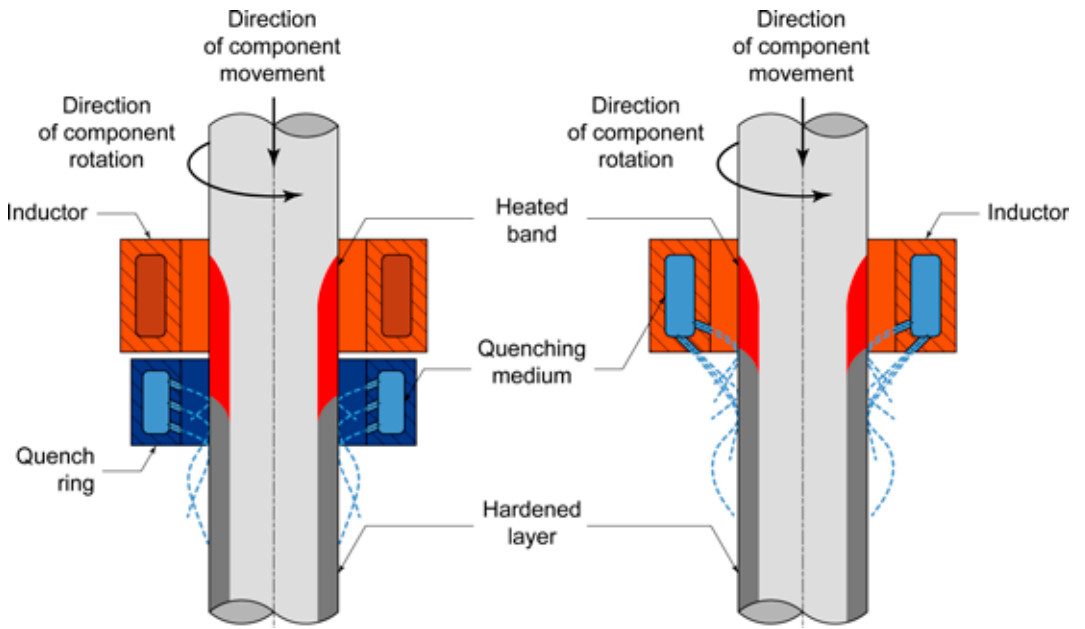

Figure 14.12 – Schematic of the progressive hardening process. Separate inductor and cooling system (on the left). Combined inductor and cooling system (on the right). The arrow indicates the direction of rotary motion of the bar [from Rudnev et al. 2003].

Nominal hardening depth, d_n (in mm), for a generic steel component, can be evaluated by means of the following relation:

$$d_n = 503 \cdot 10^3 \cdot \sqrt{\frac{\rho}{\mu_r \cdot f}} \quad \text{[eq. 14.1]}$$

where ρ is electrical resistivity (in Ω·m), μ_r is the relative magnetic permeability of the metal[8] and f is the frequency of alternate current (in Hz). You can demonstrate mathematically that approximately 63% of the current induced flows through the thickness defined by [eq. 14.1] and that 86% of electric power is dissipated inside such thickness due to the Joule effect (Figure 14.13). This is the so-called "skin effect".

[8] *Remember that for ferromagnetic steels below the Curie temperature (770°C for pure iron), the relative magnetic permeability value, μ_r, is a function of magnetic field intensity; above the Curie temperature and for non-ferromagnetic steels $\mu_r = 1$.*

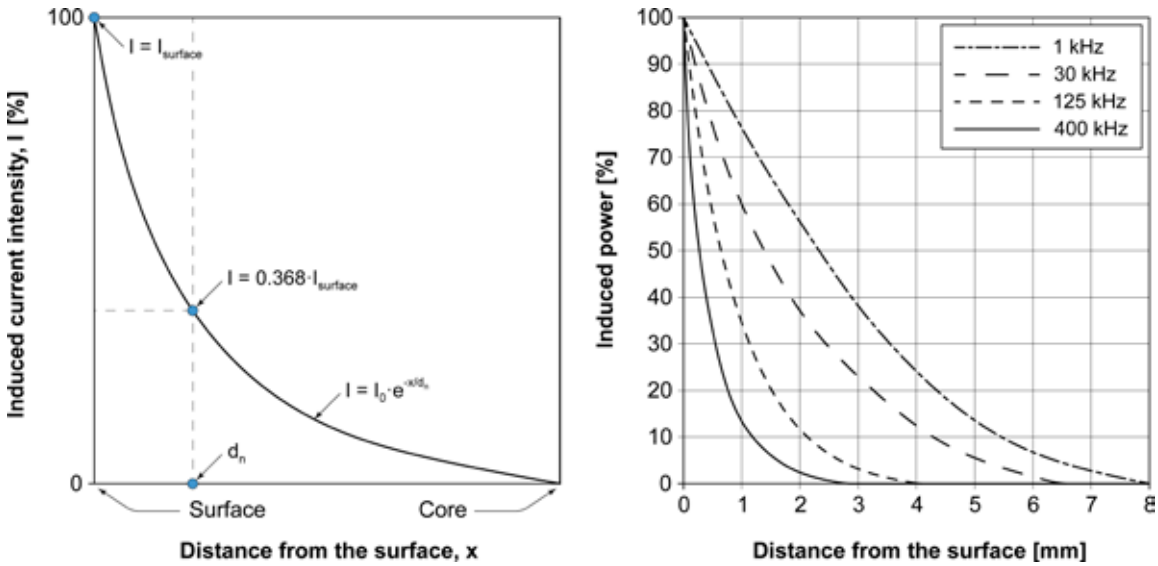

Figure 14.13 – (on the left) Induced current distribution on the part surface due to the skin effect [from Davies and Simpson 1979] - (on the right) Induced power distribution in the part as a function of the current frequency [from ASM-H.4 1991].

If you consider temperatures around 800°C and the average values of the electrical/magnetic properties of steels to be surface hardened ($\rho \cong 10^{-6}$ Ωm e $\mu_r \cong 1$), eq. [14.1] becomes:

$$d_n \cong \frac{500}{\sqrt{f}} \quad \text{[eq. 14.2]}$$

being d_n the nominal hardening depth in mm.

[eq. 14.2] highlights the inverse proportionality between the nominal hardening depth, d_n, and frequency, f, independent of the part dimensions. This relation is normally used to decide the inductor frequency setting during heating. Remember that d_n, as defined by [eq. 14.1] or [eq. 14.2], is slightly lower than total hardness depth, d_t, as follows:

$$d_t = d_n + d_a \quad \text{[eq. 14.3]}$$

where d_a is an additional contribution due heat transmission in the induction-heated part. To make it simpler, the value of d_a (in mm) can be estimated as follows:

$$d_a = 0.1\text{-}0.2 \cdot \sqrt{t} \quad \text{[eq. 14.4]}$$

where t is heating time in seconds.

At industrial level, high frequencies (30 to 450 kHz) and heating times of a few seconds are commonly used whenever hardening thicknesses below 2 mm are required. In these cases, the electric current that heats

the part flows almost completely near the surface. Instead, medium frequency equipment (3 to 10 kHz) and heating times of about ten seconds are preferred to obtain higher thickness values (2 to 6 mm).
For explanatory purposes, table 14.1 shows the nominal hardening depth values, d_n, for a generic surface-hardening steel when the frequency setting and electric power density are changed.

Frequency [kHz]	Power density [W/mm²]	Hardening depth [mm]
500	10.8-18.6	0.38-1.14
500	4.6-12.4	1.14-2.28
10	12.4-24.8	1.52-2.28
10	7.8-23.3	2.86-3.05
10	7.8-21.7	3.05-4.06
3	15.5-26.4	1.52-2.28
3	7.8-24.8	2.86-3.05
3	7.8-2.17	3.05-4.06
1	7.8-18.6	5.08-7.11
1	7.8-18.6	7.11-8.90

Table 14.1 – Trend of nominal hardening depth, d_n, after surface hardening as a function of frequency and electric power density [from Davis 2002].

14.3 Flame Surface Hardening

In flame surface hardening, heating is based on the combustion of a hydrocarbon and oxygen.
Fuels used are acetylene, propane, natural gas (methane) or methilacetylene-propadiene[9] in slightly oxidizing mixtures (10 to 20% higher than stoichiometric conditions). The fuel/comburent *mix* is sent into a heating head (burner) whose flame is opportunely directed towards the surface to be austenitized, normally from top to bottom.
The flame-to-part contact time depends on the fuel calorific power and expected hardening depth and generally lasts a few seconds (Figure 14.14).

[9] The methilacetylene-propadiene (acronym MAPP) is a mix of the two combustible gases widely used in welding and oxygen lance cutting torches. It has a very high calorific power, similar to that of propane.

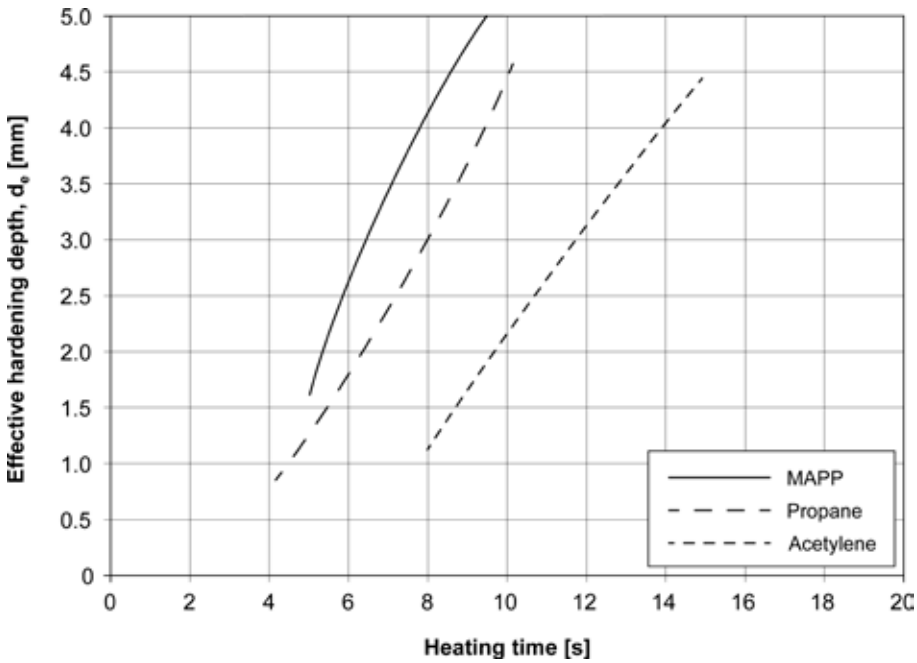

Figure 14.14 – Comparison of heating time and effective depth, d_e, for different fuel types. Flame speed: 170 m/s; part-to-burner distance: 9.5 mm; EN C35 steel; O_2/MAPP = 5; O_2/propane = 4.5; O_2/acetylene = 5 [from ASM-H.4A 2013].

After being heated, the part is sharply cooled down by means of jets of water or water added with polymer. The cooling circuit can be coupled to the burner (by means of nozzles opportunely fabricated in the burner) or work in stand-alone manner.

After surface hardening, low temperature tempering should be performed (stress relieving) at 150 to 200°C to give the hardened layer a certain fracture toughness.

The part being surface hardened and the burner that heats the part surface can be fixed (*stationary hardening*) or move freely relative to one another (*progressive hardening*)[10]. Axial-symmetric parts can be set to rotate on their axis (*spin hardening*) and, if necessary, in translational motion to allow heating the whole circle. In these cases, the burner is stationary (Figure 14.15).

[10] *Normally, one of the two, either the burner or the part, is fixed, while the other can move in translational motion.*

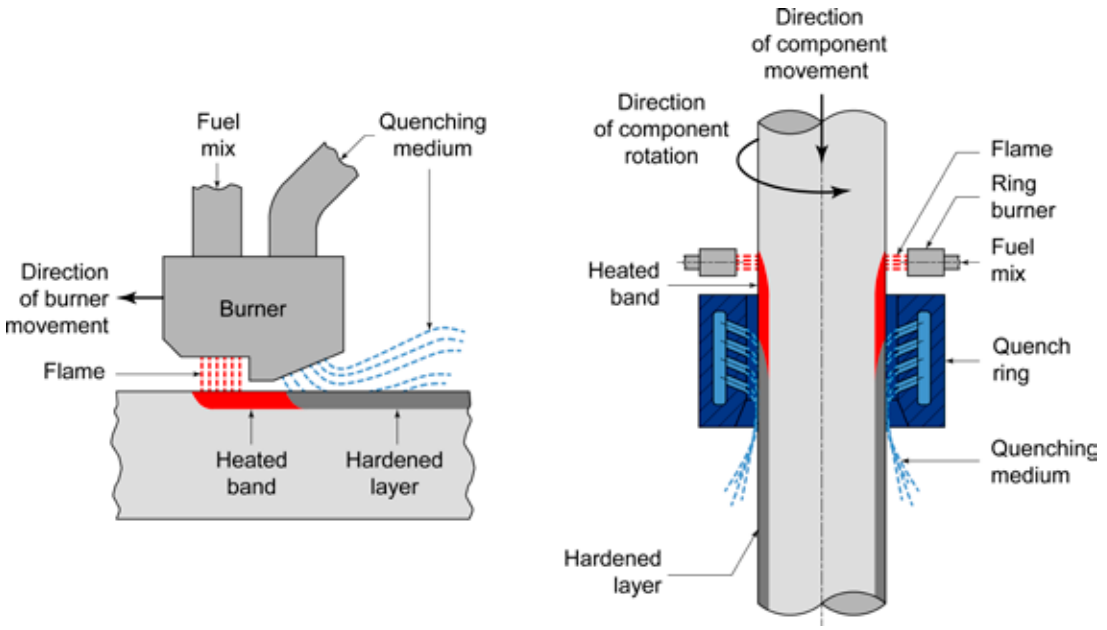

Figure 14.15 – Schematics of flame surface hardening processes: (on the left) *progressive hardening*, (on the right) *spin hardening* with part translational motion.

Surface hardness and effective depth of a flame hardened part fully compare to those obtained by induction hardening. The main difference is the difficulty to automate the process whose repeatability heavily depends on operator skills.

Flame hardening has lower costs than induction hardening, but also lower accuracy, and requires more attention to avoid overheating and surface oxidation. For these reasons, flame hardening is mainly used to obtain considerable effective depths in huge components belonging to small production batches.

14.4 Laser Surface Hardening

Surface hardening is one of the commonest industrial applications of laser technologies[11]. This process offers the advantage of a considerably higher power density (irradiance) compared to induction and flame hardening. This characteristic allows to rapidly transfer huge amounts of thermal energy to a very small area in the metal. The typical irradiance values used in this sector go from 10 to 100 W/mm^2 for times of 1 to 2 seconds.

[11] *Laser is the acronym of light amplification by stimulated emission of radiation. It is an opto-electronic device capable of emitting a directional and monochromatic beam of light that is coherent in time and space; it is also characterised by extreme power density (irradiance). High laser beam irradiance allows cutting, engraving, welding and heat-treating metals. For a deeper knowledge of these subject-matters, see the exhaustive book by Capello E.: Le lavorazioni industriali mediante laser di potenza. La tecnologia, le applicazioni e i sistemi, Maggioli - Santarcangelo di Romagna, Italy, 2008.*

Notwithstanding the high installation costs, using the laser is now ranking among the most versatile and repeatable automated processes. Its usefulness is particularly appreciated in the case of large batches to be manufactured in series.

There are three main laser types that are suitable for steel hardening, each of which comes with its pros and cons:

- CO_2 laser,
- Nd-YAG laser, and
- Diode laser.

If high power levels are required, you should select a CO_2[12] laser source. Once the continuous or pulsed beam is generated, it is directed onto the part by means of series of lenses and mirrors. A special system focusses the laser beam to the work point.

Surface hardening is based on the relative motion between the laser and the part. For this reason, the head drive system (Figure 14.16) should be able to move freely over a certain range of degrees (up to 6 degrees max). High CO_2 laser irradiance allows treating rather large areas also statically.

Unfortunately, overall process efficiency remains at very low values, around 1%, due to the well-known poor efficiency of the laser systems[13]. With CO_2 lasers, you reach 10% of efficiency at best and this value further decreases due to steel low absorbance compared to the energy emitted by CO_2[14] sources. Indeed, steel absorbance gets worse as the wavelength increases and this is particularly high in the case of CO_2 lasers ($\lambda = 10.6$ μm).

To improve material absorption, it is necessary to pretreat the surface with blackish paints, colloidal graphite or layers coated with zinc, iron or manganese phosphates. Even absorbance at all points can be guaranteed only in this manner. Otherwise, there would be a thermal field variation inside steel and the hardened layer profile would consequently exhibit considerable hardness differences. Normally, laser surface hardening is carried out using an inert gas (Ar, Ne or He) in view of avoiding whatever contamination risks from atmospheric oxygen. This consideration always applies no matter the laser source in use.

---

[12] A CO_2 laser source consists in a sealed glass tube containing a gas mix of carbon dioxide, nitrogen and helium. Power outputs typically vary from a few mW to hundreds of kW.

[13] With efficiency we mean the power that actually enters the part compared to the electric power absorbed by the network.

[14] Only a part of the laser energy is absorbed by the surface of the material being treated; the remaining part is reflected. The aptitude to absorb laser beam energy is called absorbance and is inversely proportional to the laser wavelength.

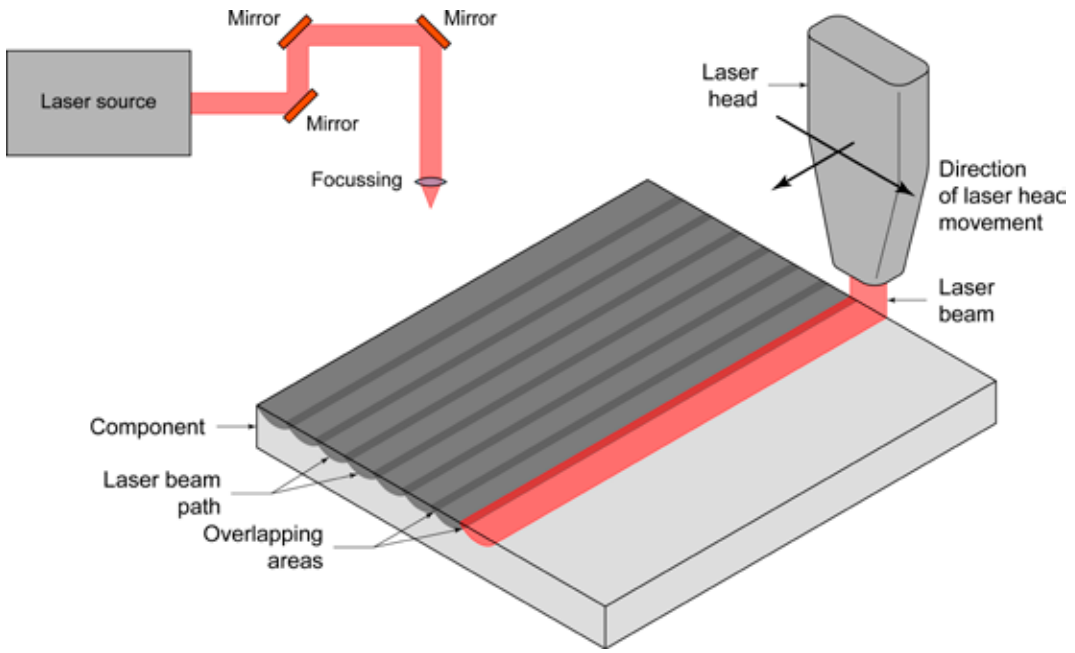

Figure 14.16 – Schematic of a CO_2 laser system including laser source, mirrors and focussing system [from Capello 2008] and associated surface hardening operations [from Dinesh Babu et al. 2011].

Nd-YAG[15] lasers are more versatile than CO_2 lasers given that you can guide the beam using optical fibres. Their main advantage is their short wavelength, equal to 1.064 mm, that enables considerable energy absorption without pretreating the surface to be hardened.

A limit of the Nd-YAG laser systems is their reduced beam size (*spot*). Normally, this problem is solved by rapidly moving the spot over an area of pre-set dimensions, with side of approximately 10 to 20 mm, so that to obtain even part heating. Consequently, the part is gradually hardened until covering the whole surface to be treated (Figure 14.17).

Diode lasers[16] are another alternative. They are small size sources that can be easily moved by means of robotic heads and optical fibres. Also in this case, the part surface does not require being pretreated because this laser type has a very low wavelength (λ = 0.80 to 0.95 μm). Their main disadvantage is the short focal length of the lens which obliges the head to work very close to the part (about 100 mm) with possible clearance problems.

[15] A Nd-YAG source is a solid-state source composed of neodimium ions (Nd^{+3}) enclosed in a synthetic yttrium-aluminium garnet crystal ($Y_3Al_5O_{12}$). Power outputs typically vary from a few Watts up to approximately 6 kW.

[16] A diode source is composed of a semi-conducting crystal that is doped to produce a n type region on one side and a p type region on the other; together, they give origin to the p-n junction diode. Power outputs can be as high as 6 kW.

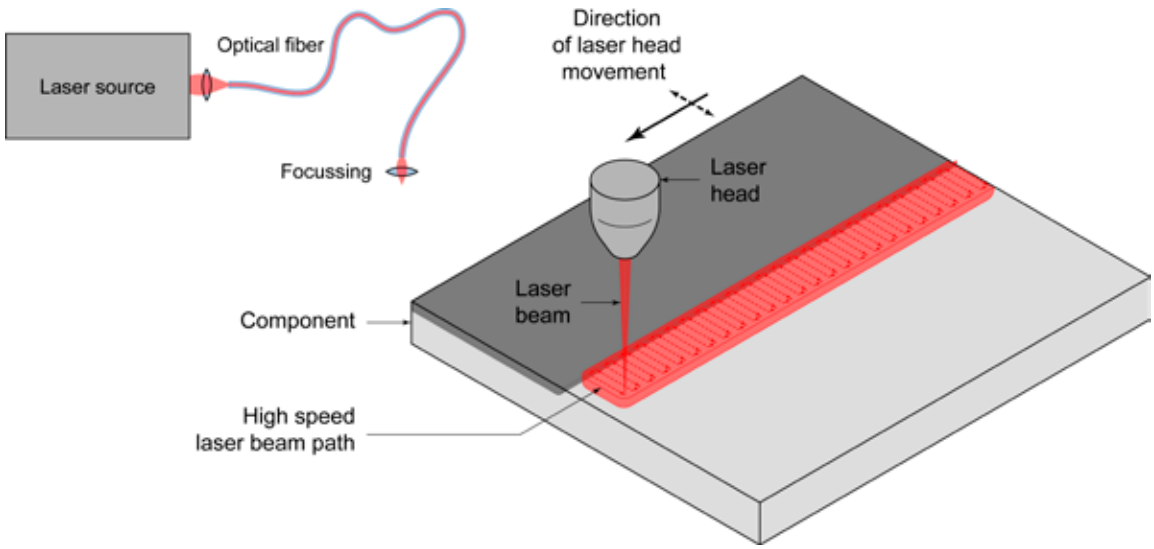

Figure 14.17 – Schematic of a Nd-YAG laser systems including laser source, optical fibre and focussing system [from Capello 2008] and associated surface hardening operations.

Last but not least, a remarkable advantage provided by all laser hardening processes should be mentioned. Laser sources involve heating times around one second, much shorter than induction or flame hardening. This peculiarity allows inducing very fast cooling speeds without using refrigerant fluids because it is the metal adjacent to the austenitized area that causes sudden cooling with consequent steel hardening when the laser source is turned off. This phenomenon is often called "self-hardening".
On the other hand, the possibility to reach temperature around 1,000°C in an extremely short time, causes the critical points A_{c1} and A_{c3} to raise much higher, thereby pushing the austenitization temperature to higher levels than in traditional surface hardening processes. If not correctly managed, this problem poses the risk of partially melting the metal.

15. SELF-HARDENING STEELS

Self-hardening steels are low-alloy steels with medium carbon content. They are similar to steels for quenching and tempering (Q&T steels) and both grades were covered by the EN 10083-3 standard[1]. In 2018 this standard was replaced by EN ISO 683-2[2] that no longer includes self-hardening steels[3]. However, given the importance of self-hardening steels, we have decided to devote a chapter to them and their special utilisation at industrial level.

The difference between self-hardening steels and Q&T steels lies in their chemical composition that for self-hardening steels envisages a cumulative carbon, chromium and nickel content (%C + %Cr + %Ni) between 5% and 7%.

Such a high content of alloying elements causes the isothermal transformation (T.T.T.) curves and anisothermal transformation (C.C.T.) curves of austenite to move downwards and to the right. The resulting hardenability level is too high to allow martensite formation even after a normalizing treatment (Figure 15.1). Technically speaking, you usually say that these steels "harden by cooling in the air".

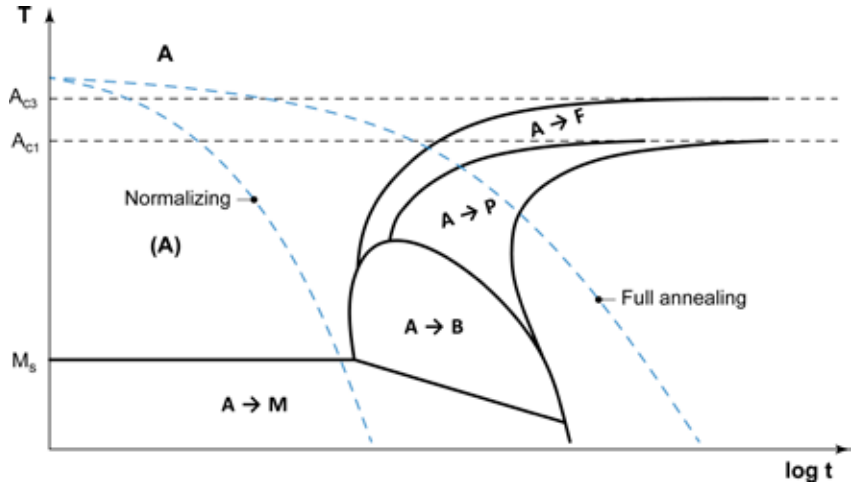

Figure 15.1 – C.C.T. curves for a generic self-hardening steel. After full annealing, the structure consists of ferrite and pearlite; after normalizing, it consists of martensite.

EN 36NiCrMo16 is the only self-hardening steel of a certain importance at industrial level. Its excellent hardenability is confirmed by the Jominy hardenability curve shown in Figure 15.2.

[1] *EN 10083-3: Steels for quenching and tempering - Part 3: Technical delivery conditions for alloy steels.*

[2] *EN ISO 683-2: Heat-treatable steels, alloy steels and free-cutting steels - Part 2: Alloy steels for quenching and tempering.*

[3] *Unluckily, the EN ISO 683-2 standard does not even cover the well-known steel grade EN 39NiCrMo3 that is widely used in Italian industry.*

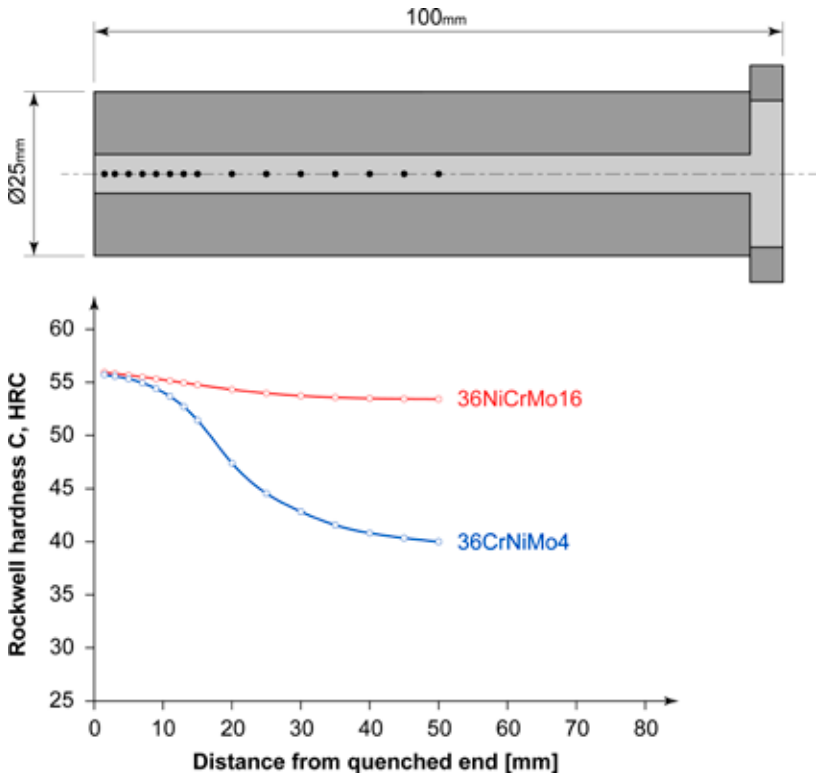

Figure 15.2 – Schematised trend of Jominy hardenability curves for self-hardening steel EN 36NiCrMo16 and for Q&T steel EN 36CrNiMo4.

After the hardening heat treatment, self-hardening steels can be tempered at 200° to 250°C, i.e., at lower temperatures than normally foreseen for Q&T steels[4] (550° to 600°C). There are two reasons for this, namely:

1. The high content of alloyed nickel (4% nominal) confers high fracture toughness to steel, and
2. Cooling in the air is extremely slow due to "air hardening", which allows drastically diminishing the residual stresses generated by martensite transformation.

Low temperature tempering (200° to 250°C) allows obtaining high values of hardness, Ultimate Tensile Strength, UTS, and Yield Strength, YS, without significantly decreasing impact strength and fracture toughness (Figure 15.3). Nonetheless, it should be opportunely pointed out that this alternative needs to be carefully evaluated and that large components requiring high fracture toughness values must always be tempered at temperatures between 550°C and 600°C.

[4] The EN 10083-3 standard provided for tempering at temperatures between 550°C and 650°C. Tempering at low temperature (200° to 250°C) can be performed only if previously agreed upon by the supplier and the customer.

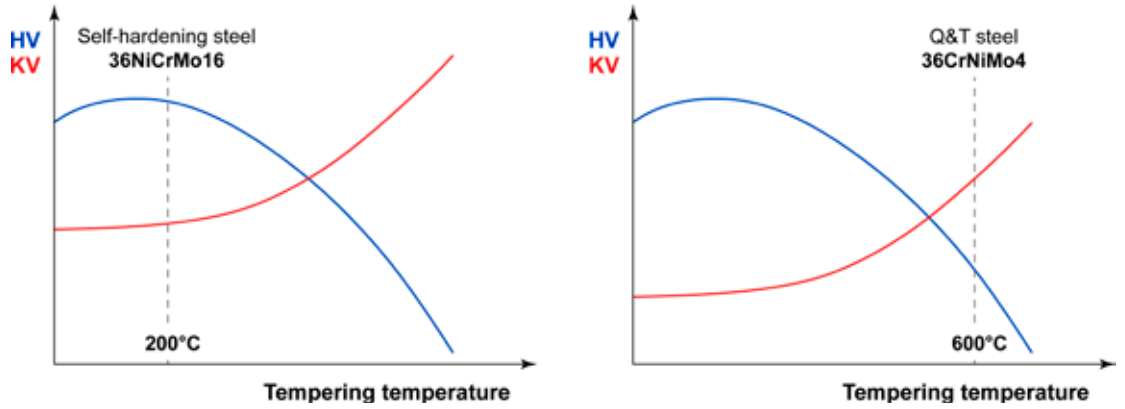

Figure 15.3 – Schematised trends of hardness (HV), Ultimate Tensile Strength (UTS) and impact strength (KV) depending on tempering temperature for self-hardening steel EN 36NiCrMo16 and for Q&T steel EN 36CrNiMo4.

To evaluate the Ultimate Tensile Strength of a self-hardening steel (after hardening and tempering at 200°C), you can apply the known formula[5] that relates Ultimate Tensile Strength, UTS, to steel chemical composition. In steel EN 36NiCrMo16 you have a nominal nickel content of 4%, nominal chromium content of 1.8% and nominal molybdenum content of 0.2% (to inhibit temper embrittlement). The formula used to calculate the Ultimate Tensile Strength of steels gives:

$$UTS = 300 + 1{,}000 \cdot n \cdot C + 150 \cdot Cr + 40 \cdot Ni + 300 \cdot Mo$$

Being n equal to 3.8 (tempering at 200°C), you have:

$$UTS = 300 + 1{,}000 \cdot 3.8 \cdot 0.36 + 150 \cdot 1.8 + 40 \cdot 4 + 300 \cdot 0.2 \approx 2{,}100MPa - 2{,}200MPa$$

As self-hardening steels have a YS/UTS ratio equal to approximately 0.7 (like almost all low alloy special structural steels, except spring steels), you obtain that Yield Strength is around 1,500 MPa.

Consequently, the theoretical fatigue limit of the material is equal to[6]:

$$\sigma_{FAb} \approx 0.45 - 0.55 \cdot UTS\ (\max 700MPa) = 700MPa$$

[5] *See paragraph 4 of Chapter 12.*

[6] *See paragraph 5 of Chapter 6.*

But if you put high temperature tempering (550° to 650°C, $n = 1$) in the picture, you would obtain:

$$UTS = 300 + 1{,}000 \cdot 1 \cdot 0.36 + 150 \cdot 1.8 + 40 \cdot 4 + 300 \cdot 0.2 \approx 1{,}100MPa\text{-}1{,}200MPa$$

From which you can estimate:

$$YS \approx 750MPa\text{-}850MPa$$
$$\sigma_{FAb} \approx 500MPa\text{-}650MPa$$

Its excellent mechanical properties and optimum hardenability allow using this steel for large components (in diameters exceeding 400 mm), such as turbine rotors, marine propeller shafts, chairlift drive systems and large-sized gears. For sake of completeness, we provide a description of the manufacturing cycle necessary to manufacture a component from self-hardening steel. As you can notice from Figure 15.4, it differs from the cycle used with Q&T steels.

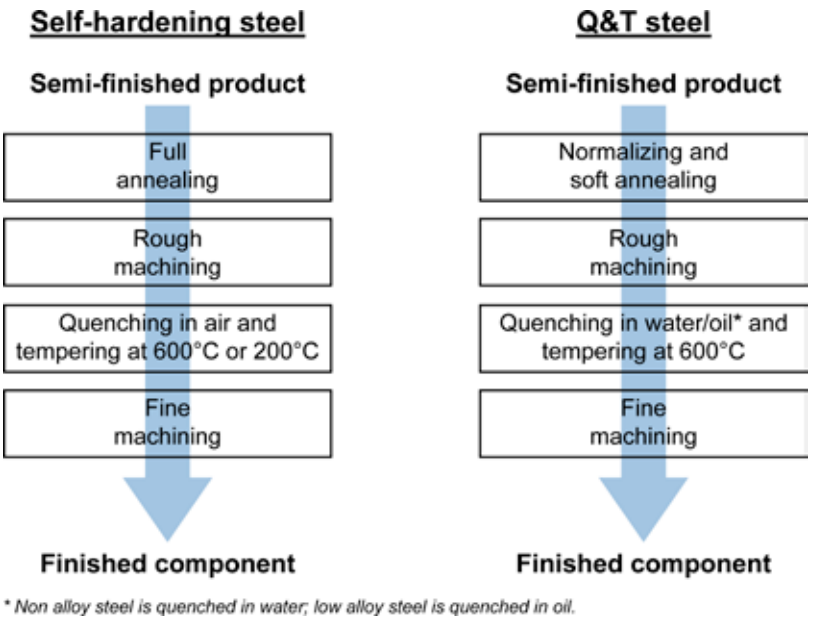

Figure 15.4 – Comparison of the manufacturing cycles to obtain a component from a self-hardening steel (on the left) or from a Q&T steel (on the right).

The main difference is in the first phase that includes full annealing (Figure 15.1) for self-hardening steels versus normalizing and soft annealing for Q&T steels.

Only full annealing allows obtaining the ferritic-pearlitic structure necessary to improve machinability of a self-hardening steel. Implementing the traditional cycle would be a big mistake because the martensitic structure obtained after normalizing would be too hard for rough machining.

The next phases in the manufacturing cycle are basically similar, the only relevant difference being the tempering temperature that, for self-hardening steels, can be performed also at 200° to 250°C.

16. SPRING STEELS

16.1 What Are Spring Steels

Since the beginning, the aim of the spring steel family was to manufacture flexible components such as coil springs, Belleville washers, leaf springs, torsion bars, spring washers, etc.

Springs are machine elements that can absorb high amounts of energy. They are designed to bend and stand elastic deformation without reaching the Yield Strength limit of the material they are made of. An example of coil spring is shown in Figure 16.1.

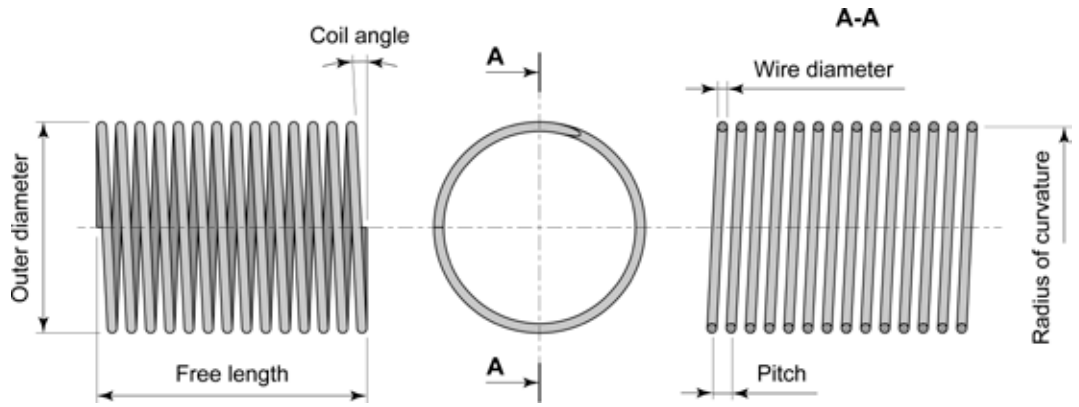

Figure 16.1 – Schematisation of a compression coil spring.

There are many reasons for which springs are installed in mechanical systems: they are used to dampen vibration, mitigate shocks, move controls, apply forces and store energy. Just think about car shock absorbers, railway wagon and locomotive bumpers, roll bars, detachable grip chairlift and so on.

Springs should be manufactured using a metal featuring suitable strength properties: steels, titanium alloys or copper alloys are normally used in this application.

A high value of the elastic modulus E[1] is required to minimise elastic deformation with the same external load applied to the component. Also, material Yield Strength is extremely important and should be very high so that deformations are confined in the elastic field at all times. For all these reasons, springs are typically made of steel,

[1] *Also called Young modulus.*

a material that guarantees an elastic modulus of 190 to 210 GPa[2], much more than titanium and copper, together with high Yield Strength and Ultimate Tensile Strength values (Figure 16.2).

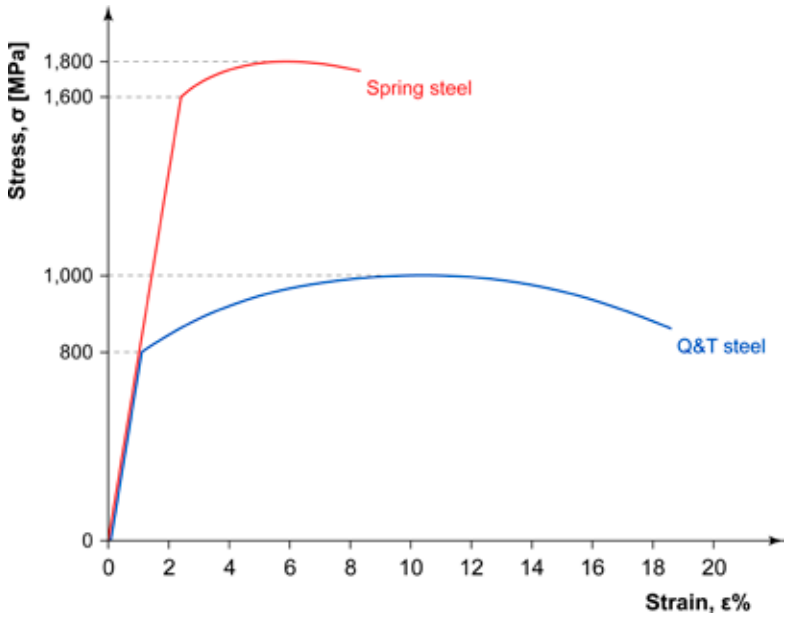

Figure 16.2 – Schematic representation of the stress/strain curves for a generic Q&T steel and a spring steel.

16.2 Spring Steel Metallurgy

Spring steels are delivered under the form of hot rolled semi-finished products such as round bars, plates and wire rods to be quenched and tempered after forming. Alternatively, already quenched and tempered and/or cold rolled wires or strip can be used for small springs (up to 6 mm in diameter).
EN 10089[3], EN 10132[4] and EN 10270 - Parts 1 and 2[5] are the reference standards for spring steels.

---

[2] The elastic modulus E, a.k.a. Young modulus, is a physical characteristic of the material that depends on atomic links in the crystal lattice. Furthermore, the elastic modulus is virtually not affected by heat treatment conditions and strain hardening level of the material. Steels have an elastic modulus E of 190 to 200 GPa (stainless steels) and 200 to 210 GPa (special and carbon steels). Titanium and titanium alloys have an elastic modulus E equal to 103 to 107 GPa, copper and copper alloys 110 to 130 GPa, and aluminium and aluminium alloys 70 to 75 GPa.

[3] EN 10089: Hot rolled steels for quenched and tempered springs - Technical delivery conditions.

[4] EN 10132: Cold rolled narrow steel strip for heat treatment - Technical delivery conditions.

[5] EN 10270-1: Steel wire for mechanical springs - Part 1: Patented cold drawn unalloyed spring steel wire; EN 10270-2: Steel wire for mechanical springs - Part 2: Oil hardened and tempered spring steel wire.

Spring steels have own metallurgical peculiarities compared to the other special structural steels. Generally, spring steels consist in iron-carbon alloys with good hardenability and:

- Carbon content around 0.45 to 0.75%; in some cases, carbon content can even reach 1%,
- Silicon content around 1.5 to -2% and/or other alloying elements such as chromium, molybdenum and vanadium, and
- Tempering at low temperature (400° to 450°C).

These characteristics considerably increase steel Yield Strength until reaching values of the YS/UTS ratio around 0.8 to 0.9 [6]. However, it is necessary that, together with such tensile strength, steel exhibits good resistance to brittle fracture (fracture toughness). Spring steels should also guarantee high resistance to relaxation and cyclic stresses (fatigue resistance) at all times.

As springs are normally subjected to stresses equal to 80 to 90% of the Yield Strength, steel relaxation is commonly observed. In practice, the tensile stresses applied to the component gradually decrease over the time, with consequent loss of the spring load applied by virtue of the spring elastic reaction (Figure 16.3).

The mechanical events originating steel relaxation are similar to creeping. The former occurs at temperatures close to room temperature (±50°C) with an imposed strain rate that remains constant over the time (more correctly referred to as "constant elongation"). The latter takes place at a temperature that exceeds room temperature by far and the forces applied remain constant over the time ("constant load").

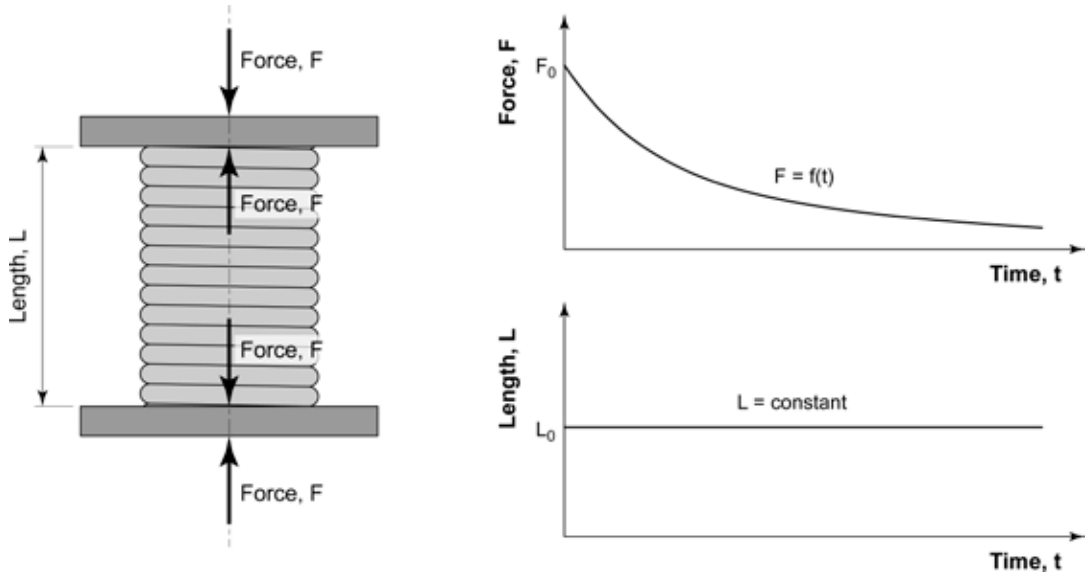

Figure 16.3 – Configuration of a spring in condition of full compression length and possible relaxation trend of the steel the spring is made of (force F is the spring reaction as a result of the pressure applied by the plates positioned at a pre-set distance L_0; the initial value F_0 tends to decrease over time).

[6] *The Yield Strength (YS) to Ultimate Tensile Strength (UTS) ratio is also referred to as yield-to-tensile strength ratio.*

Another important characteristic of spring steels is fatigue resistance. This is strictly related to the operational fitness of all spring types because, as you can easily infer, springs are always subject to cyclic stress over the time. The fatigue phenomenon is the major cause of spring failure, with an incidence exceeding 95% of the cases of breakage in service.

Spring fatigue resistance can be increased by improving the surface finish of the semi-finished product and of the finished product. Both should exhibit extremely limited surface decarburization and a minimum content of non-metallic inclusions. These discontinuities are preferential points for fatigue crack initiation. Springs should also be deprived of high stress concentration areas such as surface micro-flaws and section changes with high stress concentration[7].

To improve fatigue resistance in a part, you usually proceed to mechanical shot-peening at the end of the spring production cycle. Shot-peening is a cold working process that consists in evenly "bombing" the surface with a non-stop flow of tiny steel, cast iron or glass balls hurled at high speed (80 to 120 m/s). Repeated impacts of such shots on the surface generate a field of compressive residual stresses in the spring cortical layers that are compensated by residual tensile stresses at the core. Besides, shot-peening evens out roughness and strain-hardens the material locally (Figure 16.4).

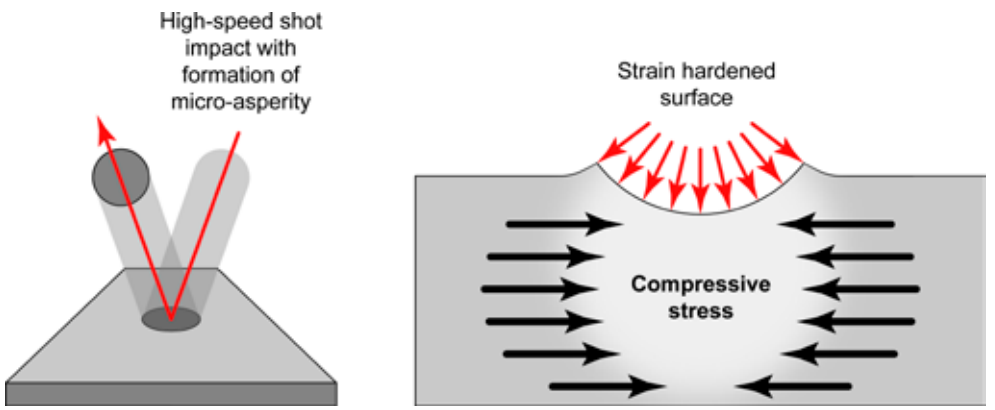

Figure 16.4 – Schematisation of the mechanical effect that repeated shot impacts induce on the surface of a shot-peened spring.

[7] *As seen in Chapter 6, fatigue resistance of a certain steel always exceeds that of a component made from the same steel. In addition to steel fatigue resistance, fatigue resistance of a component depends on its dimensions (the greater the section, the lower the part's fatigue resistance), the presence of notches (the more severe the notch, the lower the part's fatigue resistance), and on surface finish (the rougher the surface, the lower its fatigue resistance). Whereas fatigue resistance in steel is affected exclusively by the steel's own metallurgical characteristics (chemical composition and micro-structure) and by its mechanical strength (Ultimate Tensile Strength).*

If performed correctly, shot-peening significantly increases fatigue resistance in the spring. Its beneficial effect results from the compressive residual stresses that generate across a thickness of a few tenths of a millimetre starting from the component surface (Figure 16.5). Shot-peening considerably improves the fatigue limit that increases by 10 to 20% in springs with ground/polished surfaces and by 50 to 70% in hot rolled steel springs[8].

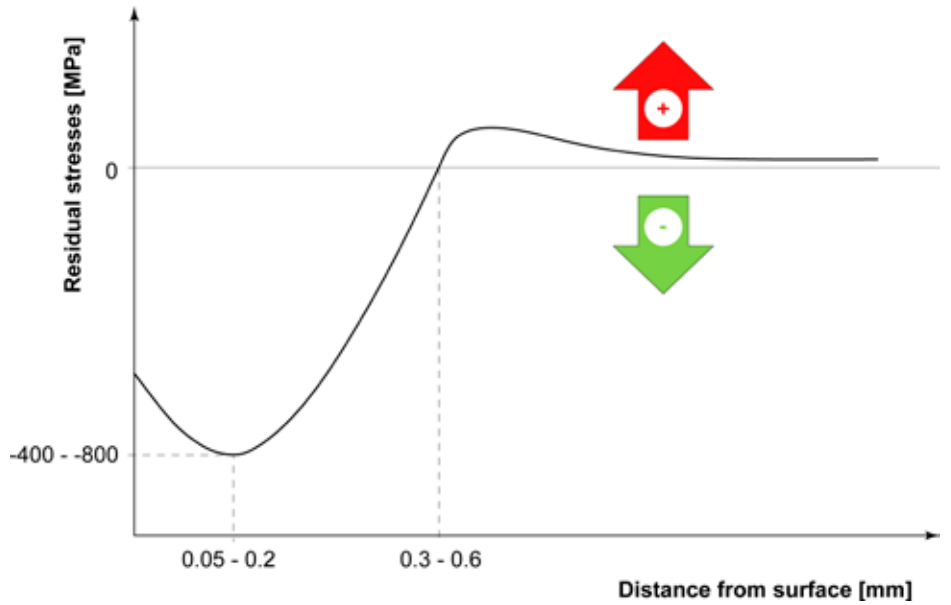

Figure 16.5 – Schematisation of residual stresses that develop under the surface of a shot-peened spring.

16.3 Spring Steel Grades

The first spring steels developed at industrial level were non alloy carbon steels. They have carbon contents between 0.55% and 1% and no other alloying elements. At present, they are rarely used and only for specific applications[9]. EN C60S, EN C75S and EN C90S belong to this category.

Non alloy carbon spring steels are used cold worked or already quenched and tempered under the form of wires or strip with a small section area. Their Ultimate Tensile Strength ranges between 1,200 MPa and 2,000 MPa.

[8] *It is worth observing that shot-peening beneficial effects are so interesting that this process is performed not only to springs, but also to many other types of mechanical parts that work under fatigue, such as gears, crankshafts, connecting rods and cranks in general.*

[9] *Non alloy spring steel applications include the manufacture of music instrument strings (piano strings, guitar strings, etc.), tweezers and retaining springs.*

In this family of materials, maximum strength is found in the thinnest wires, therefore very high reduction ratio are achieved by means of intermediate heat treatments (isothermal annealing). In other cases, steels can be used that are already quenched and tempered, provided that their metallurgical properties are kept under close control: excellent deoxidization, limited silicon and manganese contents, low impurity content (S and P in particular) and low inclusion content.
This steel family is scarcely used at industrial level because of its poor brittle fracture resistance due to its high carbon content necessary to guarantee high Ultimate Tensile Strength and Yield Strength.

Low alloy steels are generally selected for the production of industrial springs, such as leaf springs, coil springs and torsion bars. In this case, steels are put into service after forming followed by quenching and tempering.
This second category includes silicon steels (EN 46Si7 and EN 56Si7) and silicon-chromium steels (EN 54SiCr6 and EN 61SiCr7) together with chromium-vanadium steels (EN 51CrV4), chromium-molybdenum steels (EN 60CrMo3-1), silicon-chromium-vanadium steels (EN 45SiCrV6-2 and EN 54SiCrV6) and silicon-chromium-nickel steels (EN 52SiCrNi5) on the basis of their better performance. Table 16.1 lists the chemical composition of the main low alloy spring steels.
There are multiple reasons for adding these alloying elements.
Silicon is a chemical element that strengthens steel by substitutional solid solution, which causes mechanical effects similar to carbon. It is added to raise the Yield Strength, the YS/UTS ratio and fatigue resistance without drastically deteriorating impact strength. The presence of silicon also confers good resistance to tempering and relaxation. Usually, you obtain the best combination of the above mentioned properties with silicon contents of 1,5% to 2% (Figure 16.6).
A specific silicon-related issue is its strong affinity with oxygen that promotes steel decarburizing during heat treatments. Therefore, chromium is added (0.5 to 1%) to improve oxidation resistance and to increase hardenability and mechanical strength, fatigue resistance in particular.
Sometimes, spring steels contain nickel and vanadium. Nickel is an expensive alloying element that increases steel fracture toughness. Vanadium promotes crystal grain refinement and resistance to relaxation through the precipitation hardening mechanism.
As it happens with non alloy carbon steels, low alloy spring steels exhibit Ultimate Tensile Strength values ranging from 1,400 MPa to 1,900 MPa.

Designation	%C	%Si	%Mn	%P	%S	%Cr	%Ni	%Mo	%Cu	%V	Others
EN C75S	0.70-0.80	0.15-0.35	0.60-0.90	≤ 0.025	≤ 0.025	≤ 0.40	≤ 0.40	≤ 0.10	≤ 0,30	---	(*)
EN 56Si7	0.52-0.60	1.60-2.00	0.60-0.90	≤ 0.025	≤ 0.025	---	≤ 0.40	≤ 0.10	(**)	---	
EN 54SiCr6	0.51-0.59	1.20-1.60	0.50-0.80	≤ 0.025	≤ 0.025	0.50-0.80	≤ 0.40	≤ 0.10	(**)	---	
EN 51CrV4	0.47-0.55	≤ 0.40	0.70-1.10	≤ 0.025	≤ 0.025	0.90-1.20	≤ 0.40	≤ 0.10	(**)	0.10-0.25	
EN 54SiCrV6	0.51-0.59	1.20-1.60	0.50-0.80	≤ 0.025	≤ 0.025	0.50-0.80	≤ 0.40	≤ 0.10	(**)	0.10-0.20	
EN 52SiCrNi5	0.49-0.56	1.20-1.50	0.70-1.00	≤ 0.025	≤ 0.025	0.70-1.00	0.50-0.70	≤ 0.10	(**)	---	

The letter S after the symbol of non alloy carbon steels (such as ENC75S) refers to a steel grade containing sulphur in the maximum content limit.
(*) Cr + Mo+Ni ≤ 0.63.
(**) Cu + 10·Sn ≤ 0.60.

Table 16.1– Heat analysis of some spring steels [from EN 10089 and EN 10132].

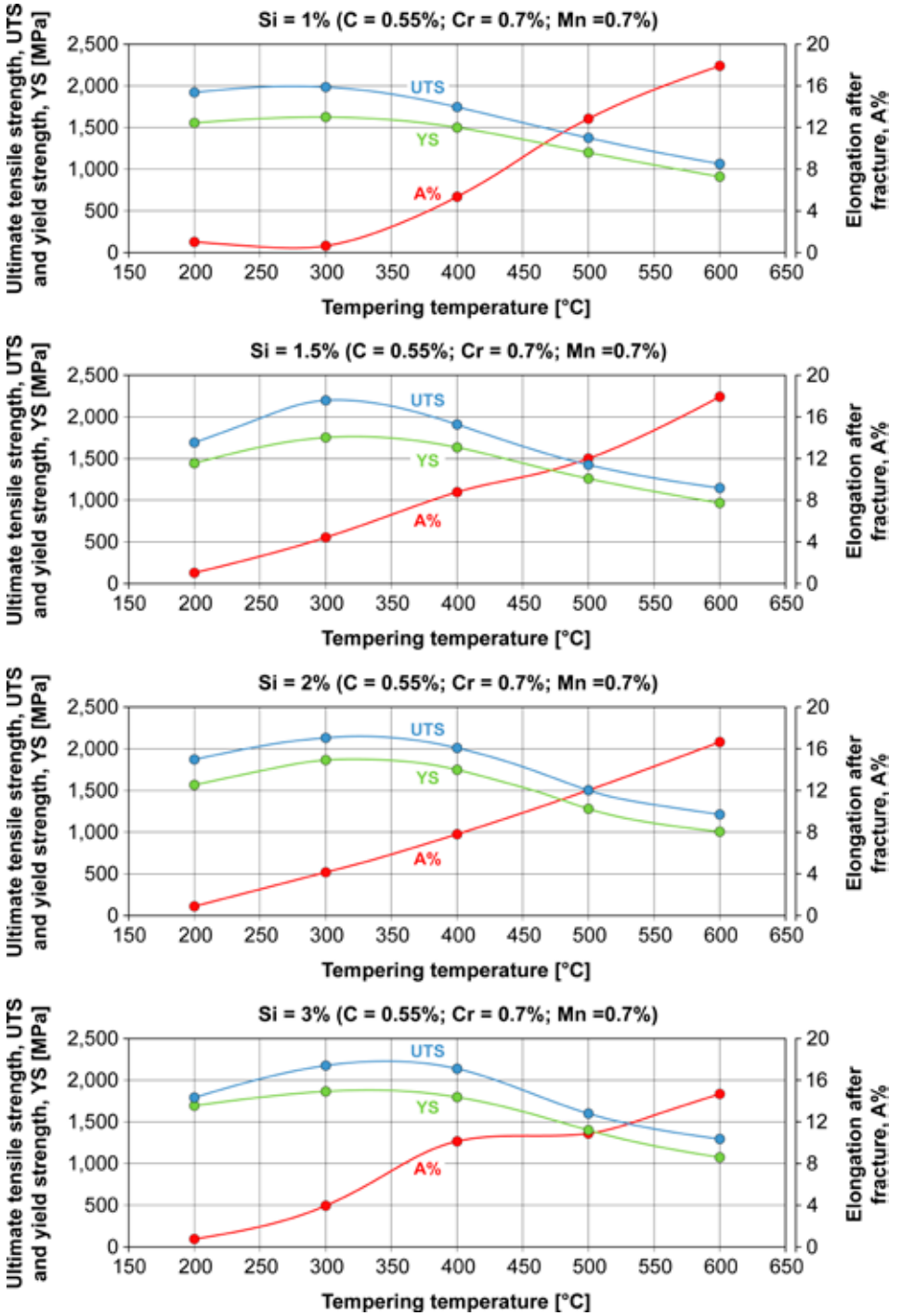

Figure 16.6 – Mechanical properties of spring steel grade SAE 9254 with C = 0.55%, Mn = 0.7% and Cr = 0.7% depending on silicon content changes [from Lee and Choi 1999].

For example, let's compare a non alloy carbon steel grade EN C75S (C = 0.75%) with a low alloy one grade EN 52SiCrNi5 (C = 0.52%; Si = 1.25%; Cr = 0.8%; Ni = 0.6%). From the known formula[10]:

$$UTS = 300 + 1{,}000 \cdot n \cdot C + 100 \cdot (Si - 0.3) + 150 \cdot (Mn - C) + 150 \cdot Cr + \\ + 40 \cdot Ni + 300 \cdot Mo + 700 \cdot V + 40 \cdot Al$$

knowing that both steel grades are tempered at 450°C (n = 2.3), for steel C75 you will have:

$$UTS = 300 + 1{,}000 \cdot 2.3 \cdot 0.75 \cong 2{,}000 MPa$$

$$YS = 0.85 \cdot UTS = 0.85 \cdot 2{,}000 MPa \cong 1{,}700 MPa$$

whereas for steel EN 52SiCrNi5 you will have:

$$UTS = 300 + 1{,}000 \cdot 2.3 \cdot 0.52 + 100 \cdot (1.25 - 0.3) + 150 \cdot 0.8 + 40 \cdot 0.6 \cong 1{,}750\ MPa$$

$$YS = 0.85 \cdot UTS = 0.85 \cdot 1{,}750 MPa \cong 1{,}500 MPa$$

Keep in mind that research efforts on spring steels, in the *automotive* sector in particular, aim at continuous improvement of material performance up to UTS values around 2,300 MPa. In this perspective, Si-Cr-V low alloy spring steels added with minuscule niobium and boron amounts and guaranteeing very high mechanical characteristics (2,200 to 2,400 MPa) have been recently put on the market .

16.4 The Spring Steel Manufacturing Cycle

The manufacturing cycle necessary to manufacture a mechanical spring basically differs from that for a component made of a traditional Q&T steel. To this regard, observe Figure 16.7.

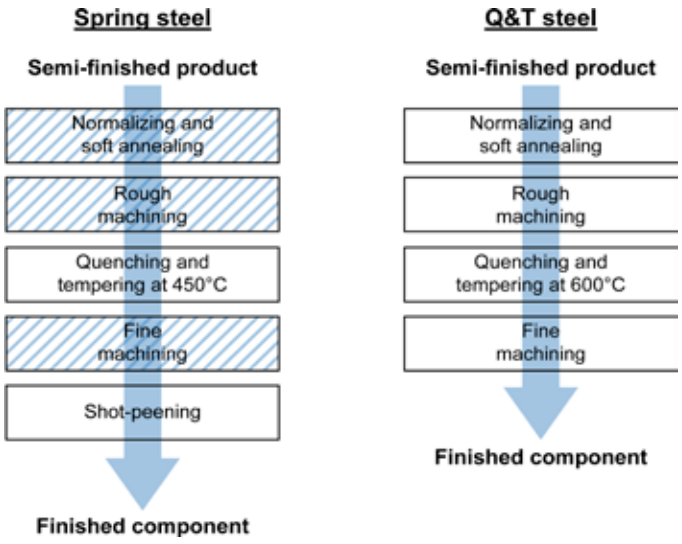

Figure 16.7 – Comparison of manufacturing cycles for a Q&T steel (on the right) and for a spring steel (on the left).

[10] *See paragraph 4 of Chapter 12.*

Let's say that you want to make a simple coil spring or a leaf spring.
In the case of the coil spring, rough machining is not necessary. To make the component, you have to shape a steel wire or a wire rod, in suitable diameter, in accordance with a certain radius of curvature and coil pitch by means of a spring coiling machine. In this case, it initial regeneration is useless given that machining are almost not carried out. Therefore, you can start from a steel wire already quenched and tempered or, in the case of a large diameter, from a wire rod or a normalized bar to be subsequently quenched and tempered.
Also as regards the leaf spring, machining operations are rather marginal. Usually, a steel plate is opportunely cut to obtain the various elements (the leaves) that will be overlapped and secured to one another to form the leaf spring. This is the reason why in Figure 16.7 the squares concerning machining operations are hatched with 45° lines. After forming, the spring is quenched and tempered.
Austenitization temperatures depend on the nominal chemical composition of steel. The spring is usually quenched in oil, even if using water may prove more suitable to low hardenability steels (non alloy carbon steels and some carbon-silicon steels). After quenching, the spring is always tempered at a temperature of 400° to 450°C. To this regard, see Table 16.2.
It is of the utmost importance to avoid surface decarburization while the heat treatments are in progress, as this would drastically lower steel fatigue limit. Also spring surface finish is very important. This is why polishing is often scheduled to remove all traces of the previous machining operations, grinding included. At the end of the manufacturing cycle, the springs are normally shot-peened to increase their fatigue resistance.

Designation	Austenitization temperature [°C]	Quenching medium	Tempering temperature
EN C75S	810-840	Oil	440-460 (*)
EN 56Si7	850-870	Oil	440-460
EN 54SiCr6	850-870	Oil	440-460
EN 51CrV4	840-860	Oil	440-460
EN 54SiCrV6	850-870	Oil	390-410
EN 52SiCrNi5	850-870	Oil	440-460

(*) The EN 10132 standard does not specify the tempering temperature for non alloy carbon spring steels. The value provided is valid on the basis of the metallurgical considerations illustrated in this chapter.

Table 16.2 – Quenching and tempering heat treatment parameters for some spring steels [from EN 10089 and EN 10132].

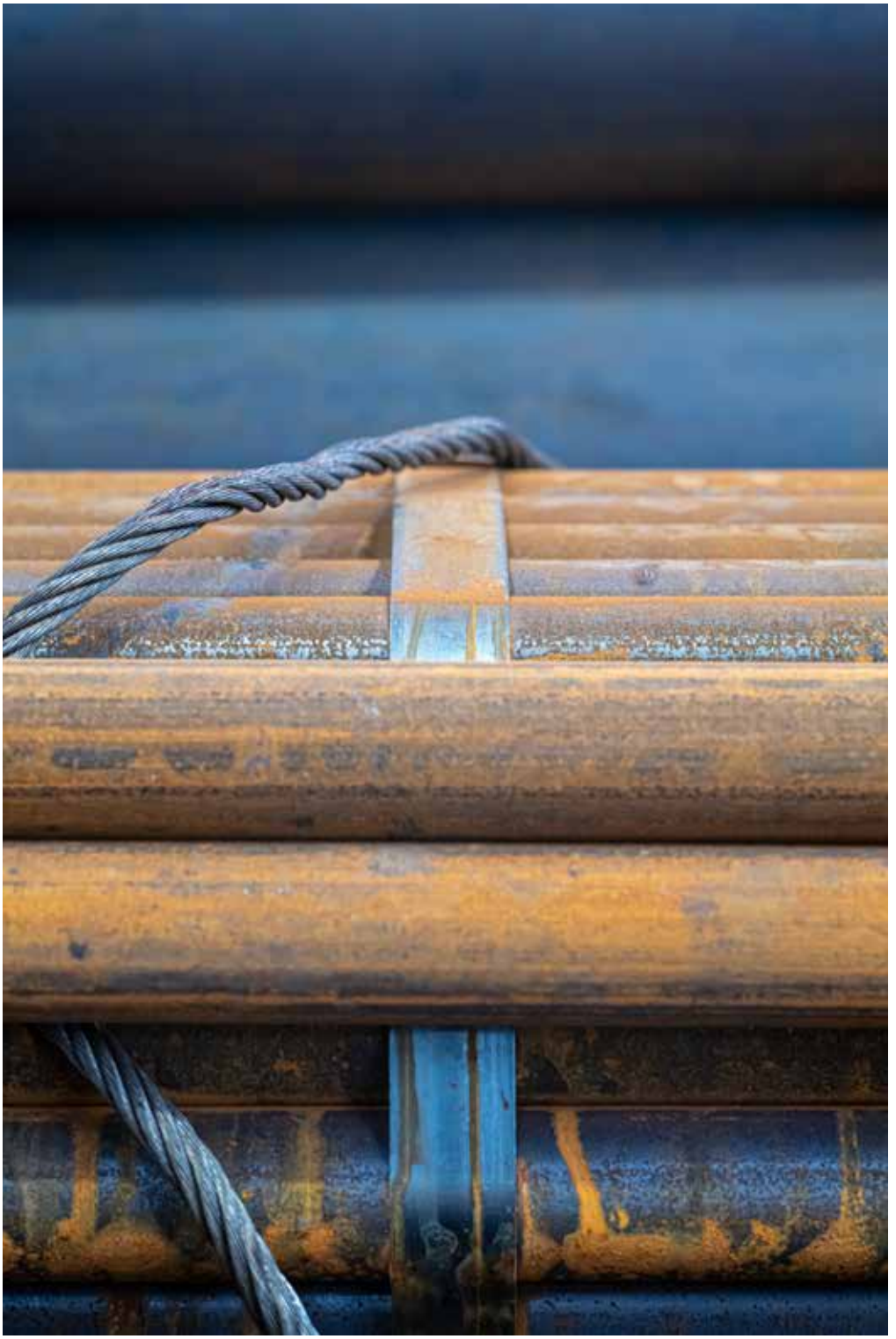

17. CASE HARDENING STEELS AND THE CASE HARDENING PROCESS

17.1 The Case Hardening Process and Its Purposes

Case hardening or carburizing[1] is a thermochemical heat treatment performed on steels with the purpose of carbon enrichment at the surface of the heat treated parts. In practice, only low carbon steels ($C \leq 0.2\%$) are suitable for this type of process.

The purpose of case hardening is to obtain a surface layer rich in carbon and with hardness 650 to 800 HV (equal to approximately 58 to 64 HRC) that penetrates to a depth of 0.5 to 1.5 mm.

After case hardening, components possess good resistance to wear, seizure and surface damages. They also exhibit a considerable improvement of fatigue resistance while the core remains fairly tough thanks to the steel low carbon content.

The case hardening process lasts some hours (2 to 12 hours) and is performed in the range of 900° to 930°C, i.e. at temperatures exceeding the critical point A_{c3} where steel has a γ-phase.

At the end of carbon enrichment, the part is quenched to induce martensitic transformation. Subsequently, low temperature tempering (150° to 200°C) takes place. This step lasts several hours and takes the name of stress relieving.

Typical mechanical components that are case hardened before being put into service include gears, sliding rails spiral bevel gears for the automotive sector, racks, pinions, camshafts, connecting rods, mechanisms in general, dowel pins, pins, rollers, and rolling bearing rings.

17.2 Steel Case Hardening

Experimentally, case hardening is known from the dawn of civilisation. Several research works of archaeo-metallurgical nature on Greek and Etruscan finds report the existence of carbon enrichment processes (case hardening) dating back to the 8th century B.C. and used to harden the cutting edge of weapons and tools. The theoretical studies on this process are much more recent. You have to wait the end of the 19th century for the first industrial applications.

---

[1] In Italian, the term traditionally used to describe the process of carbon enrichment performed on steels is called "cementazione". Another term also used in Italian is "carburazione" and is borrowed from the English words Carburising (UK) or Carburizing (USA). Case Hardening is another term that is often used in specialised literature written in English.

Case hardening is based on diffusing carbon atoms inside the γ-phase of steel. At 900° to 930°C, carbon exhibits high solubility in the crystal lattice of iron and a fairly good diffusion speed[2]. At process temperatures, carbon adsorption is also supported by soaking time increase and high carbon concentration levels between the part being treated and the carburizing atmosphere. Schematically, you can imagine carbon atoms like tiny balls that "penetrate" into the steel crystal lattice that is composed of bigger atoms (Figure 17.1).

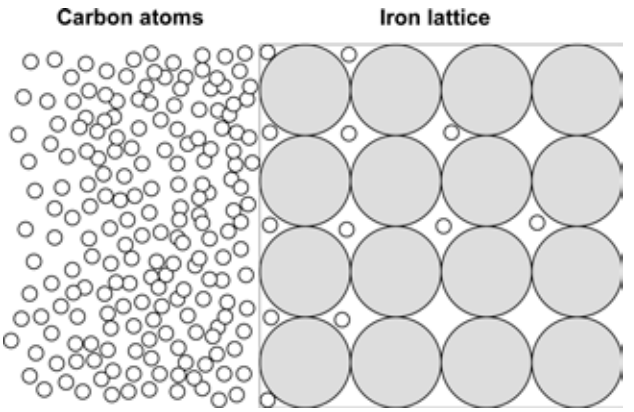

Figure 17.1 – Schematisation of the carburizing environment-to-steel reaction interface: mechanism of carbon atom adsorption into iron crystal lattice.

Whatever the case hardening process used, the main chemical species that acts as carburizing agent is carbon monoxide. When interfaced with a steel part at process temperatures, carbon monoxide, CO, starts the following reaction [eq. 17.1]:

$$Fe + 2CO \rightarrow Fe_{\gamma}(C) + CO_2 \qquad \text{[eq. 17.1]}$$

where the term $Fe_{\gamma}(C)$ represents the carbon solid solution in the γ-iron crystal lattice.
The case hardening results from the decomposition of CO into carbon dioxide, CO_2, with release of carbon atoms that diffuse and enrich the surface layers of the steel component. The greater the amount of carbon monoxide in the reaction environment, the higher the environment ability to case harden the steel being heat treated.
But the reaction [eq. 17.1] involves the formation of CO_2 that acts as a decarburizing agent. Therefore, for the enrichment process to continue, you have to supply the system with new molecules of carbon monoxide (CO).
The carburizing characteristics of the atmosphere can be described in a simple manner by means of the so-called carbon potential parameter indicated as C_p. This parameter quantifies the aptitude of the atmosphere to carburize mechanical parts, i.e. the ability of steel lattice to absorb carbon atoms.

[2] *A practical limit to temperature raise is connected with the issue of grain growth. Theoretically, steel could be case hardened also at 1000° to 1050°C, which would shorten process time, but the layer obtained would result more brittle than with traditional case hardening.*

Once fixed the temperature, the carbon potential of an atmosphere is defined as the amount of carbon obtained at the surface of a pure iron sample when equilibrium conditions are reached in that carburizing atmosphere. For example, if a carburizing atmosphere at 920°C has a carbon potential of 1%, this means that a pure iron sample, placed in contact with that atmosphere at that temperature, will have a surface carbon content of 1% after a period of time long enough to reach equilibrium conditions. As you can easily understand, the index C_p does not depend on the carburizing agent used to obtain it, which means that you can have the same carbon potential value using different substances (wood coal, molten salts, methane, propane, etc.).

For the process to be efficient, the atmosphere carbon potential, C_p, should exceed the carbon content of the steel being treated, generally in the range of 0.15 to 0.20%; the difference between C_p and the material carbon percentage is the driving force of the case hardening process.

In industrial processes, the trend is to operate with carbon potentials that are below carbon saturation in austenite in equilibrium conditions at process temperature. These C_p values are around one.

You should avoid exceeding the carbon solubility limit in the γ-phase as much as possible, otherwise, carbides would form at grain boundary resulting in brittleness and premature flaking of the case hardened layer.

Finally, keep in mind that the limit value of carbon solubility in austenite (and, consequently, the value of C_p to be used for steel case hardening) also depends on the other alloying elements. Usually, steels alloyed with nickel exhibit saturation carbon values that are slightly higher than in *Fe-C* alloy while steels alloyed with chromium, chromium-molybdenum and manganese-chromium are characterised by lower values[3] (Figure 17.2).

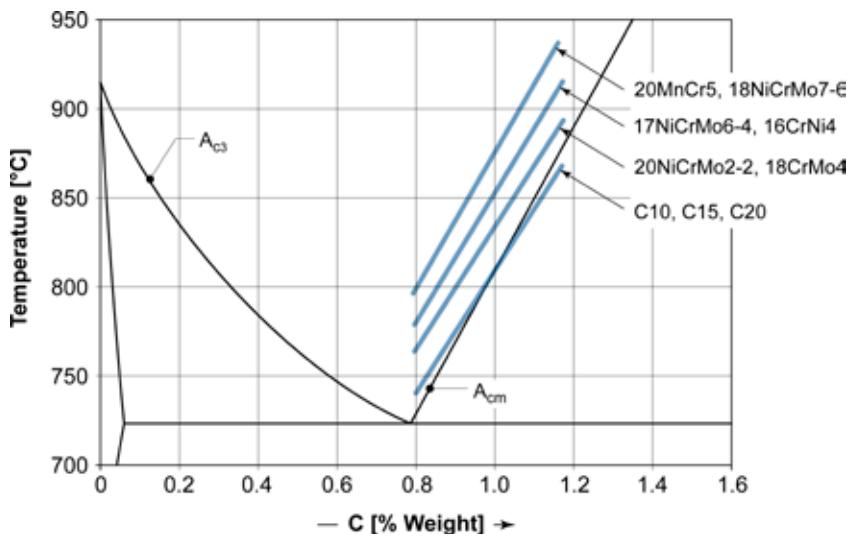

Figure 17.2 – Trend showing the displacement of the value A_{cm} for several case hardening steels relative to the *Fe-C* phase diagram.

[3] *This involves that, during case hardening of steels alloyed with chromium, chromium-molybdenum and chromium-manganese, carbon potentials slightly lower than Fe-C alloy or slightly higher in the case of steels alloyed with nickel should be implemented.*

On the basis of the considerations set forth so far, it derives that case hardening of a component essentially depends on three parameters:

- The carburizing properties of the atmosphere, i.e. its carbon potential, C_p.
- Process temperature, and
- Soaking time during which the part is in contact with the carburizing environment.

Figures 17.3 and 17.4 show the effect of the three above mentioned parameters on the carbon concentration profile.

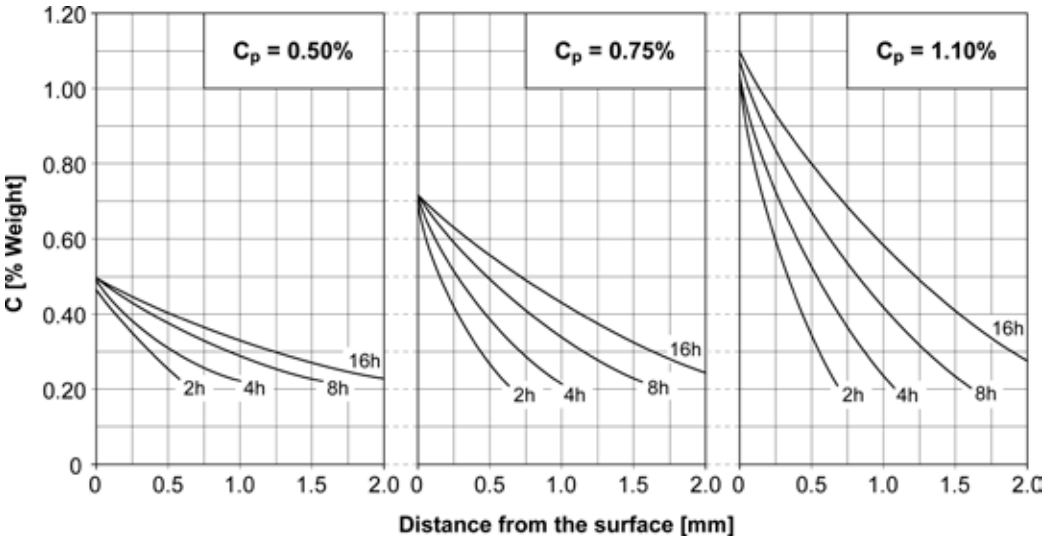

Figure 17.3 – Effect of process time and carbon potential in case hardening processes at 920°C for steel grade EN C20 [from Thelning 1975].

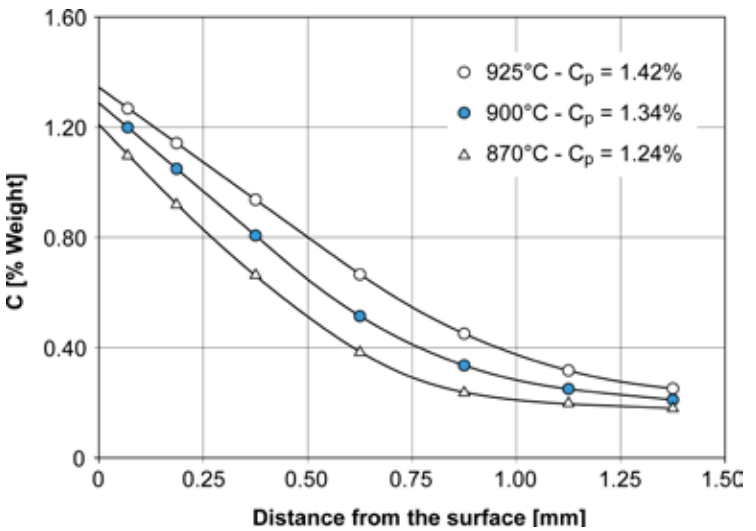

Figure 17.4 – Effect of process temperature and carbon potential (equal to austenite saturation at the different temperatures) in case hardening processes lasting 4 hours for steel grade EN C20 [from Davis 2002].

Figures 17.3 and 17.4 highlight some important aspects that are worth being underlined.

First of all, it is clear that as process time or temperature increase, the depth attained by carbon enrichment inside the part also gradually increases. Generally, increasing temperature is much more effective to improve carburizing depth than increasing process time.

Secondarily, you observe that carbon concentration at the steel surface never exceeds the carbon potential fixed for that atmosphere (constant C_p) and that it can be matched only for prolonged periods of time (for example: 16 hours).

A simplified quantitative description of the case hardening process was provided by Harris[4] starting from diffusion equations. This formula enables estimating carbon diffusion depth starting from process temperature and time in accordance with the following relation:

$$D = 660 \cdot e^{(-8{,}287/T)}\sqrt{t} \quad \text{[eq. 17.2]}$$

where D is case hardening depth in millimetres, T is temperature in Kelvin degrees and t is time in hours.

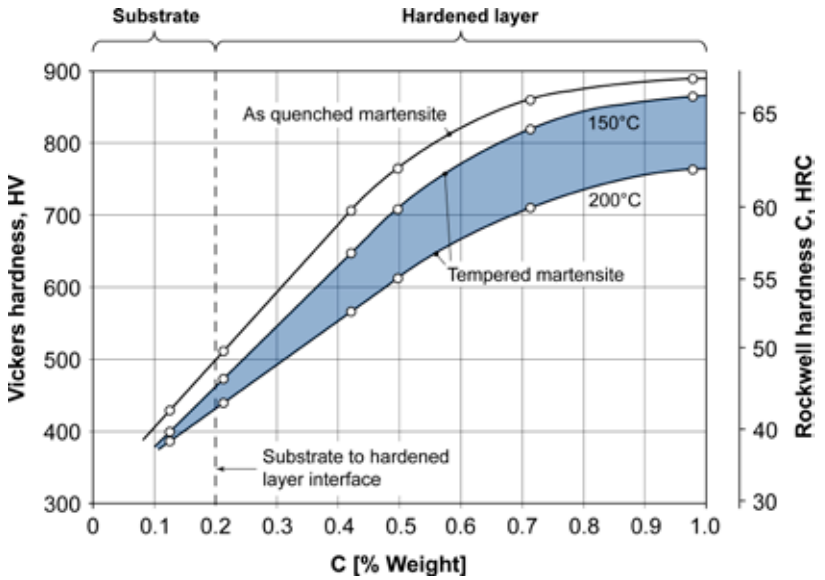

Figure 17.5 – Correlation of carbon content and HV or HRC hardness for a martensitic structure fully quenched, quenched and tempered at 150°C or quenched and tempered at 200°C [from Grange et al. 1977].

[4] *Harris F.E., Case Depth - An Attempt at a Practical Definition, Metal Progress, Vol. 44, no. 2, 1943, p. 265-272. The relation was obtained by assuming that, at process temperatures, austenite at the surface of the case hardened part is saturated with carbon. It is worth noticing that Harris formula generally overestimates case hardening depth in industrial processes. This difference results from the fact that, in practice, the process lasts less than the time required for the part surface to reach equilibrium conditions with the atmosphere carbon potential.*

For example, according to [eq. 17.2] in a 4-hour process at 920°C (1193 K), carbon enrichment depth is approximately 1.27 mm; this value is close to the result that can be obtained experimentally.
At the end of case hardening, steel is quenched in water added with polymers or oil to be transformed into martensite. Then, steel is tempered at 150°-200°C, which is also called stress relieving. As a consequence of the different carbon contents across the part thickness, carburized layer hardness is not constant, but gradually diminishes until reaching the core level[5] (Figure 17.5).
Figure 17.6 shows a typical trend of the carbon concentration profile and Vickers hardness (HV) profile as a function of the distance from the treated surface for steel EN 17NiCrMo6-4.
Measuring hardness across the case hardened layer also allows determining effective case depth, d_e, that is the distance from the surface where you measure 550 HV. Specifically, d_e is determined starting from the micro-hardness values represented in accordance with the graphic construction provided in the standard[6]. To this regard, see Figure 17.7.

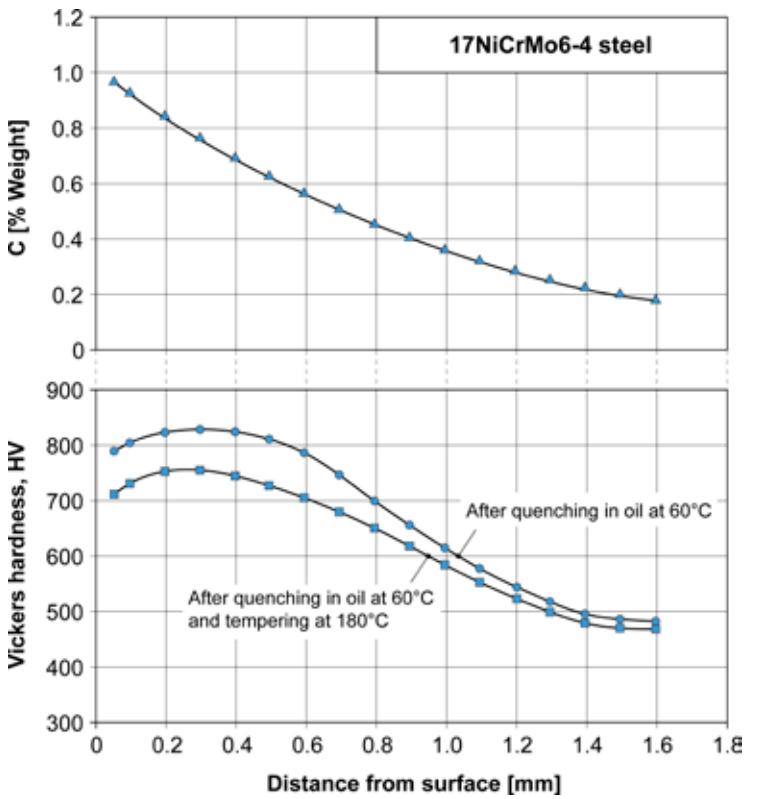

Figure17.6 – Trend of the carbon concentration profile and hardness profile (after quenching and after quenching and tempering) for steel EN 17NiCrMo6-4 case hardened at 920°C for 4 hours [Laboratories of the Department of Mechanical Engineering of Politecnico di Milano – Milan, Italy].

[5] The level depends on the martensite hardness being directly proportional to the carbon content in solution.

[6] UNI 11153-1: Misurazione dello spessore di strati superficiali induriti su elementi di lega ferrosa - Carbocementazione e carbonitrurazione (Measurement of thickness of hardened surface layers of ferrous parts - Carburizing and carbonitriding).

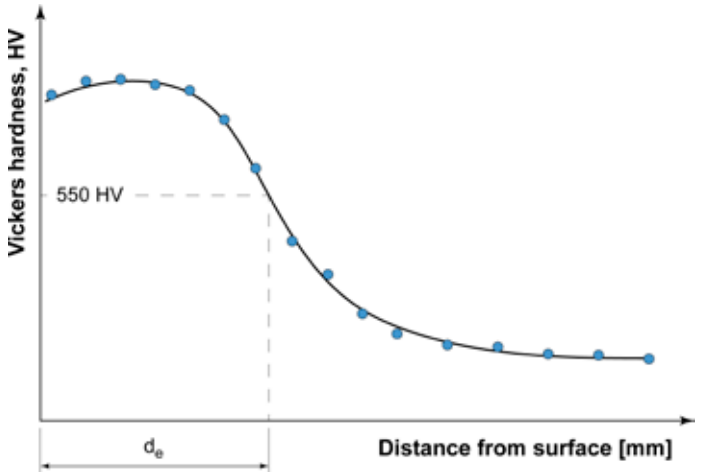

Figure 17.7 – Schematic for determining effective case depth in a case hardened layer [from UNI 11153-1].

17.3 The Commonest Case Hardening Processes

Various industrial processes are used for steel case hardening. They are classified based on the nature of the carburizing source that can be solid, liquid or gaseous.

Pack Carburizing

The first method developed at industrial level to case harden mechanical components was the so-called "pack carburizing" with solid carburizing sources. This is a rather simple process both in terms of execution and necessary equipment. It is still used in artisanal workshops even if it has some technological limits (for example, it is not suitable to process large size components)

In pack carburizing, the part is placed into a metal box together with wood coal and small additions of barium carbonate as accelerating agent. The box is then placed into a furnace at approximately 900°C, at which temperature you experience both carbon incomplete combustion according to the reaction in [eq. 17.3] (a.k.a. Boudouard reaction) and barium carbonate decomposition according to the reaction in [eq. 17.4], as follows:

$$C + CO_2 \rightarrow 2CO \qquad \text{[eq. 17.3]}$$

$$BaCO_3 + C \rightarrow BaO + 2CO \qquad \text{[eq. 17.4]}$$

Both reactions make available carbon monoxide, CO, a chemical species that allows the continuation of the steel carburizing reaction [eq. 17.1].

At the end of carbon enrichment, you can proceed with direct quenching of the metal box containing the part or let the box cool down and then remove the part and quench it. After quenching, stress relieving must always be performed at 150° to 200°C.

Even though the layers obtained from pack carburizing can be of a very high quality, actually you cannot control the enrichment process. The carbon potential is widely variable and irregular between batches. This is not suitable for industrial production where constant reproducibility and quality characteristics are requested.

Salt Bath Carburizing

Another process used to obtain carbon enrichment is salt bath carburizing, with liquid carburizing sources. Starting from the Nineties of the last century, the number of salt bath carburizing plants has drastically decreased due to ecological reasons connected to waste salt disposal.

Steel case hardening requires using molten salt baths based on sodium cyanides (*NaCN*) or potassium cyanides that, reacting with oxygen in the atmosphere, result in the formation of cyanates (*NaCNO*). In addition to cyanides, also variable percentages of barium, sodium and potassium chlorides and carbonates are always present with the function of process catalysts.

From cyanate decomposition, you obtain carbon monoxide (*CO*) and nitrogen (*N*); these chemical species are adsorbed at the surface of the parts being treated. Other reaction products are carbonates (Na_2CO_3) that tend to gradually deplete the bath (reactions in [eq. 17.5] and [eq. 17.6]).

$$2NaCN + O_2 \rightarrow 2NaCNO \qquad \text{[eq. 17.5]}$$

$$4NaCNO \rightarrow 2N + CO + Na_2CO_3 + 2NaCN \qquad \text{[eq. 17.6]}$$

The typical chemical compositions of salt baths are listed in Table 17.1. Usually, you discriminate between baths used at low temperature (850° to 900°C), that result in the formation of carburized layers of limited extent (0.1 to 0.3 mm), and baths used at high temperature (900° to 950°C), that allow obtaining greater hardening depths (1 to 3 mm).

If cyanide concentration is particularly high (30 to 97%), this treatment is referred to carbonitriding in salt baths. As already pointed out, cyanide decomposition leads to the formation of both *CO* and atomic state nitrogen, *N*. Thus, you have simultaneous adsorption of carbon and nitrogen in the component surface layers. The typical composition of these salt baths is shown in Table 17.2.

Salt bath components	Salt baths for low temperature case hardening (850°-900°C) [%]	Salt baths for high temperature case hardening (900°-950°C) [%]
Sodium cyanide	10-23	6-16
Barium chloride	~0	30-55
Chlorides of other alkali metals (Ca, Sr)	0-10	0-10
Potassium chloride	0-25	0-20
Sodium chloride	20-40	0-20
Sodium carbonate	0-30	0-30
Other accelerating chemical species (*)	0-5	0-2
Sodium cyanate	0-1	0-0.5
Salt bath density	~1.76 g/cm^3 a 900°C	~2.00 g/cm^3 a 900°C

(*) Manganese dioxide, boron oxide, sodium fluoride and sodium pyrophosphate.

Table17.1 – Chemical composition of salt baths used for salt bath carburizing [from Davis 2002].

Salt bath components	Salt baths for carbonitriding			
	30% cyanides	45% cyanides	75% cyanides	97% cyanides
Sodium cyanide	30	45.3	75	97
Sodium carbonate	40	37	3.5	2.3
Sodium chloride	30	17.7	21.5	traces
Salt bath density at 860°C	~1.54 g/cm^3	~1.40 g/cm^3	~1.25 g/cm^3	~1.10 g/cm^3

Table 17.2 – Chemical composition of salt baths for carbonitriding [from Davis 2002].

In general, the cycle necessary to carburize or carbonitride a part in a salt bath is shorter than in pack carburizing or gas carburizing. Also, with salt bath carburizing you reach greater effective case depths than in other processes in the same time.
At the end of carbon (or carbon/nitrogen) enrichment, the part is removed from the salt bath to be quenched and stress relieved. Special attention should be paid at the operation of removing the salts stuck to the components that should be washed away in hot water (~80°C), possibly using pressure water jets.

Gas Carburizing

At present, gas carburizing is certainly the most widespread industrial process for steel case hardening. In this process the carburizing source is a hydrocarbon-based gaseous atmosphere.
Case hardening takes place at 900° to 930°C in an environment containing carbon monoxide in excess relative to the chemical equilibrium conditions indicated in the reaction in [eq. 17.1]. The process atmosphere is obtained using a carrier gas of a reducing nature mixed with a hydrocarbon to increase its CO content.
The carrier gas, which cannot harden the part by itself, is composed of endothermic gas[7] (20% carbon monoxide, CO, 40% hydrogen, H_2, and 40% nitrogen, N_2) or a mix of endothermic gas and exothermic gas[8]. The chemical composition of the endothermic/exothermic gas mix can vary; typically, it consists of 17% carbon monoxide, CO, 23% hydrogen, H_2, and 60% nitrogen, N_2.
Methane (CH_4) or propane (C_3H_8) are usually added as a process enrichment gas, even though case hardening processes based on other hydrocarbons (such as ethanol, methanol, ethylene, butane, etc.) are known.
For example, if you consider a typical case hardening process using a methane-enriched endothermic carrier gas, the main chemical reactions involved are the following[9]:

$$Fe + 2CO \rightarrow Fe_\gamma(C) + CO_2 \quad \text{[eq. 17.1]}$$

$$Fe + CH_4 \rightarrow Fe_\gamma(C) + 2H_2 \quad \text{[eq. 17.7]}$$

$$Fe + CO + H_2 \rightarrow Fe_\gamma(C) + H_2O \quad \text{[eq. 17.8]}$$

[7] Endothermic gas is a typical reducing atmosphere that can be obtained through methane stoichiometric combustion in a generator according to the following reaction: $2CH_4 + O_2 + 4N_2 \rightarrow 2CO + 4H_2 + 4N_2$.

[8] Exothermic gas is also a mix produced in a generator through partial combustion of methane, propane or other hydrocarbons. Normally, exothermic gas contains nitrogen (N_2) in amounts exceeding 70%, together with hydrogen (H_2) and carbon dioxide (CO_2). If the mix is not enriched, exothermic gas is a decarburizing atmosphere.

[9] It has been estimated that at least 180 different reactions take place at the same time in a carburizing atmosphere. In the text we mention the three reactions that are considered to be the most relevant to establish carbon transfer speed from the atmosphere to the part.

Enriching the carrier gas with methane (or other hydrocarbons) provides the system with new carbon monoxide and hydrogen molecules that assist steel carburizing and reduce oxidizing chemical species (CO_2 and H_2O) in accordance with the following reactions:

$$CH_4 + H_2O \rightarrow CO_2 + H_2 \quad \text{[eq. 17.9]}$$

$$CH_4 + CO_2 \rightarrow 2CO + 2H_2 \quad \text{[eq. 17.10]}$$

The effectiveness of the carburizing process, i.e. its carbon potential (C_p), can be measured by evaluating the extent of the equilibrium constants of both reactions in [eq. 17.9] and [eq. 17.10] as well as the amounts of the chemical species involved (especially, the ratios CO/CO_2 and H_2/H_2O).
Typically, you use traditional oxygen probes or Lambda probes to monitor O_2, infrared analysers to evaluate the CO/CO_2 ratio, and equipment to measure H_2O content based on dew point determination. All these methods enable correlating the chemical composition of the furnace atmosphere, process temperature and carbon potential, C_p, to a good approximation. A typical example is shown in the diagrams in Figure 17.8 suitable for monitoring the case hardening process when methane is used as the endothermic carrier gas.

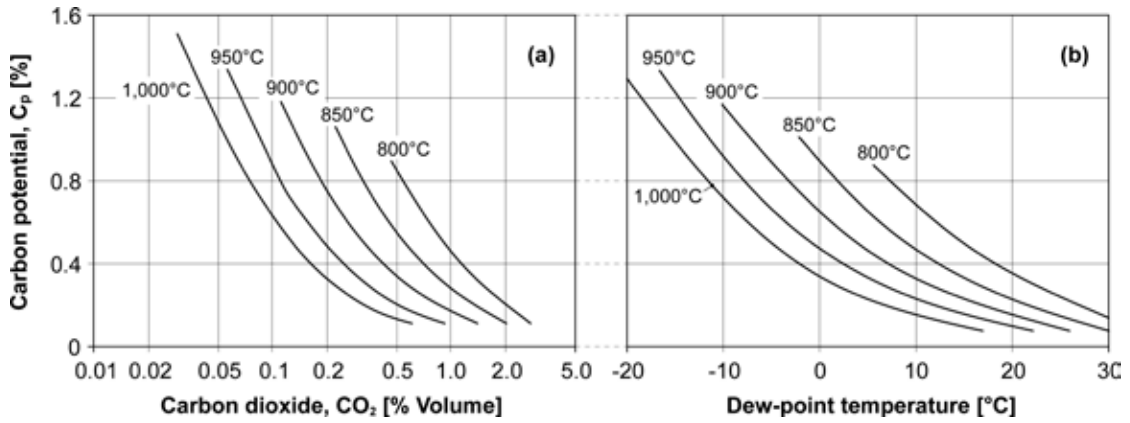

Figure 17.8 – Examples of diagrams suitable for determining the carbon potential C_p in atmospheres enriched with methane as endothermic carrier gas, depending on process temperature and on (a) CO_2 content or (b) dew point [from Davis 2002].

Traditional case hardening processes normally involve constant carbon potentials and slightly higher than the carbon content of the eutectoid of the steel being case hardened (C_p = 0.9 to 1.1%)[10]: in these cases, you talk about single-stage case hardening.

[10] *The maximum carbon content obtained at the surface of case hardened parts can never exceed the carbon potential of the carburizing atmosphere involved. Therefore, it is always opportune to "work" with a carbon potential, C_p, slightly higher than that of the eutectoid of the steel that you are going to process. Also remember that the eutectoid carbon percentage of 0.77% applies exclusively to the Fe-C phase diagram. Carbon steels, either alloyed or not, exhibit widely different eutectoid carbon contents, consequently the carbon value to be aimed at during case hardening will also be different.*

In some cases, you can decide to perform double-stage case hardening, which is also referred to as a *boost and diffusion* process. In the first stage (*boost*), you work with a high carbon potential (such as C_p = 1.2 to 1.4%) to rapidly enrich the surface layers in carbon; in the second stage (*diffusion*), the carbon potential is decreased (C_p = 0.6 to 0.8%) to support carbon diffusion in the steel sub-surface layers. The double-stage process allows homogenising carbon concentration in the hardened layer while reducing consumption of the hydrocarbon used to enrich the process atmosphere. To this regard, see Figure 17.9.

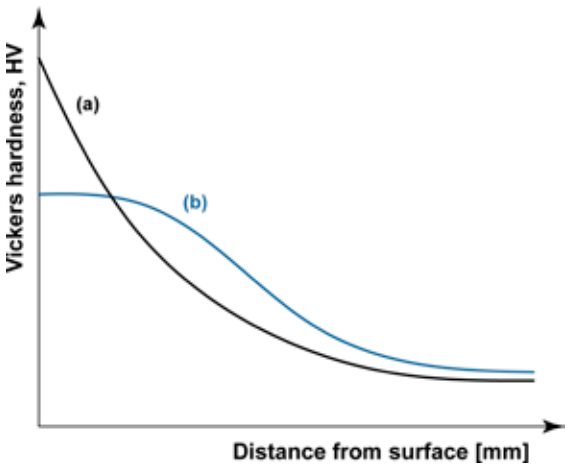

Figure 17.9 – Carbon concentration trend in a case hardened layer obtained by means of (a) a single-stage process or (b) a double-stage process.

17.4 Other Case Hardening Processes

In recent years other innovative case hardening processes have been developed, some of which very interesting, such as low pressure carburizing and ion carburizing.

Low pressure carburizing is a gas carburizing process performed in a chamber furnace where pressure is brought down to value below atmospheric pressure (typically 5 to 20 mbar). Gases used are acetylene (C_2H_2) and propane (C_3H_8)[11]. Due to the special pressure and temperature conditions of the gas, carbon transfer to the steel surface occurs directly, with no intermediate reactions. Case hardening reactions are as follows:

$$C_2H_2 \rightarrow 2C + H_2 \qquad \text{[eq. 17.11]}$$

$$C_3H_8 \rightarrow C + 2CH_4 \qquad \text{[eq. 17.12]}$$

[11] *Normally methane (CH_4) is not used in low pressure carburizing because it has a very low dissociation degree at usual process pressure values.*

For the effect of low pressure, hydrocarbon dissociation in [eq. 17.11] and [eq. 17.12] is considerably shifted to the right (non-equilibrium chemical reaction). Therefore, carbon diffusion flow rates are very high (much higher than in traditional gas carburizing) and the steel surface rapidly attains carbon saturation conditions (carbon saturation in austenite). As a consequence, enrichment occurs very rapidly and the only possibility to control the process is through repeated *boost and diffusion* cycles with opportune adjustment of the gas flow rate[12].
Given that process times are shorter than in traditional case hardening, you can use process temperatures up to 1050°C. Final quenching of the case hardened part is then performed by means of a high-pressure nitrogen flow.
Thanks to its high diffusion speed, low pressure case hardening allows processing also steels with carbon contents slightly higher than in traditional processes (up to 0.25 to 0.28% of carbon), thereby obtaining components with a higher core resistance. Other advantages come from the possibility to obtain a part with an extremely clean surface totally deprived of intergranular oxidation (oxygen being virtually absent in the process atmosphere).
Another innovative process is plasma (ion) carburizing, which is a low pressure gas carburizing process too. In plasma carburizing, the process gas (methane, CH_4, for example) is brought to the state of ionised plasma by applying a potential differential between the parts being heat treated and a counter-electrode, such as, for example, the furnace walls.
Plasma is composed of carbon ions that, due the potential differential, are hurled against the components. Thus, the steel surface becomes the target of a real carbon ion "bombing"[13]. This allows fast enrichment of austenite, followed by diffusion as it happens in the boost and diffusion process. The parts are finally quenched in an oil bath.
The advantages of plasma carburizing are similar to those of low pressure carburizing, namely no intergranural oxidation, limited process times and higher process temperatures than in traditional case hardening. A peculiarity of the plasma process that does not exist in traditional gas or low pressure carburizing, is that you can obtain case hardened layers with an extremely even thickness also in the presence of holes, cavities and/or complex geometries.

[12] The speed at which dissociation reactions take place does not allow in situ measurement of the carbon potential. Also, the almost total absence of oxygen in the furnace chamber excludes using oxygen probes as in traditional case hardening.

[13] The terms normally used with reference to plasma processes are "ion implantation".

Figure 17.10 shows the carbon gradients obtained in an EN 20NiCrMo2-2 steel after case hardening at 980° C for 30 minutes and quenching in oil using traditional gas, low pressure and plasma carburizing processes.

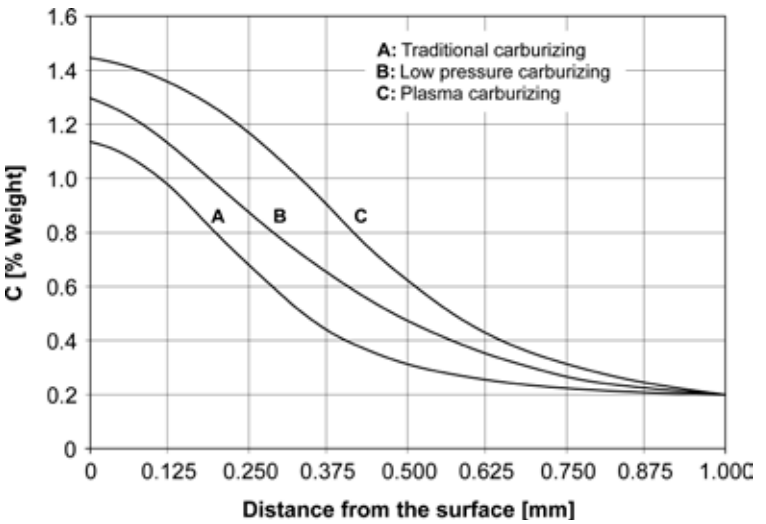

Figure 17.10 – Carbon concentration trend in a case hardened layer for a 20NiCrMo2-2 steel grade after processing at 980°C for 30 minutes through (A) plasma carburizing, (B) low pressure carburizing and (C) traditional gas carburizing.

17.5 The Quenching Heat Treatment and the Tempering of Case Hardened Steels

After carbon enrichment, the parts should be quenched, and then tempered at low temperature (a.k.a. stress relieving). There are several methods to carry out this heat treatment depending on steel grade and part size. To this regards, you should carefully consider that the component surface is very rich in carbon (C = 0.8 to 0.9%, indicatively) and its metallurgical characteristics are very different from the core (C = 0.15 to 0.2%). In particular, the position of the critical point A_{c3} ($\gamma \rightarrow \alpha$ transformation) in the surface layer is very different from the position of the same critical point A_{c3} at the steel core.

To this regard, observe Figure 17.11 showing the *Fe-C* phase diagram with the temperature interval where case hardening is performed (light blue band) and the steel chemical composition at the surface and at the core. In the figure you can clearly see that the transformation temperature A_{c3} is much lower in the case hardened layer than at core level. Ideally, this would involve two different austenitization temperatures. Another element to be taken into account is that usual carburizing temperatures (900° to 930°C) exceed correct austenitization temperatures at the surface and, mainly, at the core.

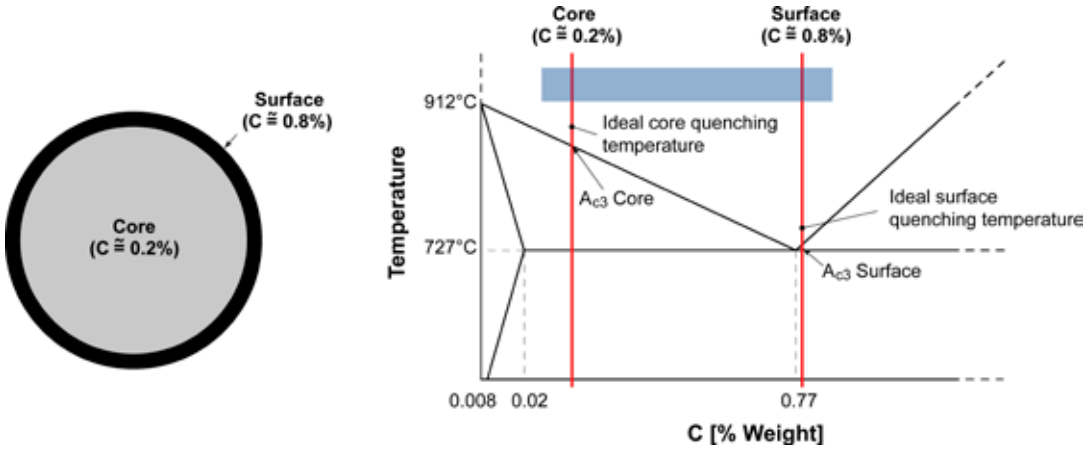

Figure 17.11 – Detail of the *Fe-C* phase diagram highlighting the surface and core positions in a case hardened steel component.

Quenching of case hardening steels derives from a compromise between the surface condition and the core condition as given by the thermal cycle in Figure 17.12 that is called "single quench".

The cycle consists in case hardening the part at the temperature desired, cooling it down to approximately 50°C above the core critical point A_{c3} and then keeping it at that level for a period of time sufficient to support carbon diffusion. Thereafter, the component is actually quenched by immersion in oil or in an adequately drastic fluid (water added with polymers).

An alternative is the cycle in Figure 17.13 where the part is quenched directly from the case hardening temperature (this is called "direct quench").

In both cases, quenching is followed by stress relieving at 150° to 200°C.

These two cycles are largely used for many components fabricated from steels where the temperature difference between $A_{c3\ core}$ and $A_{c3\ surface}$ is below 100°C. In these conditions, austenitization temperature is suitable for the steel core, but it is too high for the steel surface. In most cases, this is an acceptable compromise, mainly for small and/or medium size parts obtained from low alloy steels.

Instead, in the case of large components and/or if the product should be of superior quality, the "double quench" thermal cycle can usefully implemented (Figure 17.14). In this case, first you quench the part from case hardening temperature (or from a slightly lower temperature), then you heat the part again at a level between $A_{c3\ surface}$ and $A_{c3\ core}$ and finally you quench the part again followed by stress relieving.

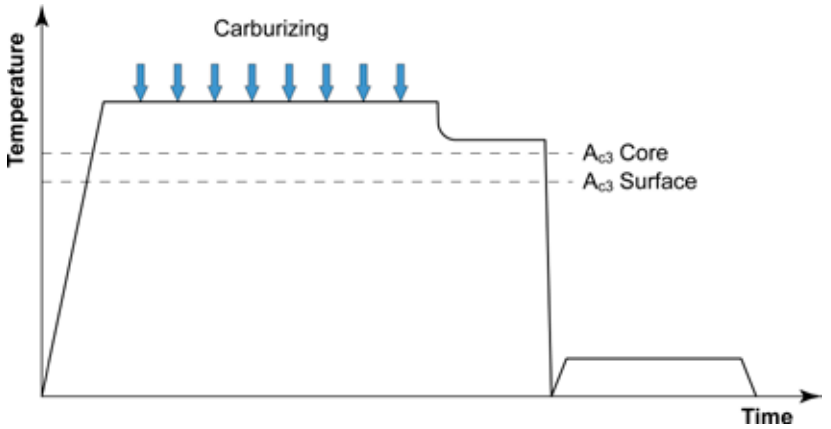

Figure 17.12 – Traditional "single quench" thermal cycle for a generic case hardening steel where temperature is lowered after carburizing to improve carbon diffusion.

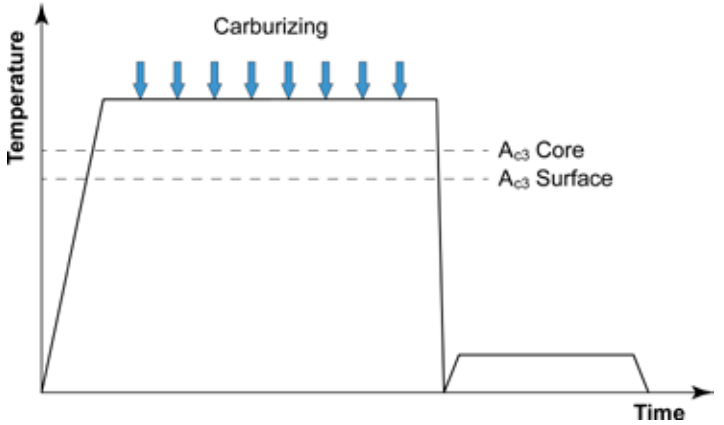

Figure 17.13 – "Direct quench" thermal cycle for a generic case hardening steel

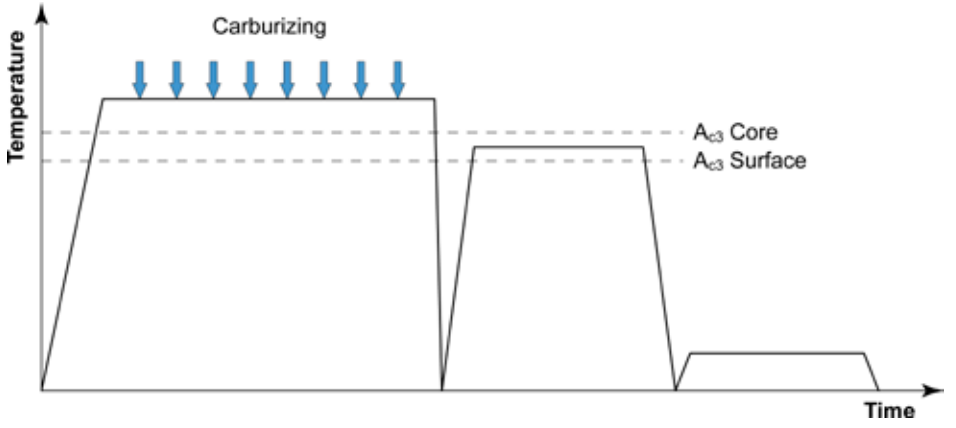

Figure 17.14 – "Double quench" thermal cycle for a generic case hardening steel.

In this manner, both the core and the surface will be quenched starting from a correct austenitization temperature. Second quenching also allows tempering the core. The fact is that "double quench" not only is more expensive than "single quench", but also increases the risk of component bending because the critical points are exceeded two times.

If carburizing, quenching and stress relieving are carried out correctly, you will observe the formation of a field of compressive residual stresses near the surface.

This phenomenon is connected with increased hardenability resulting from carbon enrichment in the hardened layer compared to the core. (Figure 17.15). The different carbon contents at core and surface levels causes the surface C.C.T curves (red lines) to move farther to the right and down relative to the core C.C.T. curves (blue lines). This peculiarity causes austenite transformation to start first at core level (starting from time t_c) and subsequently progress along the surface (starting from t_s). This occurs even if the surface (black dashed line) cools down more rapidly than the core (black solid line).

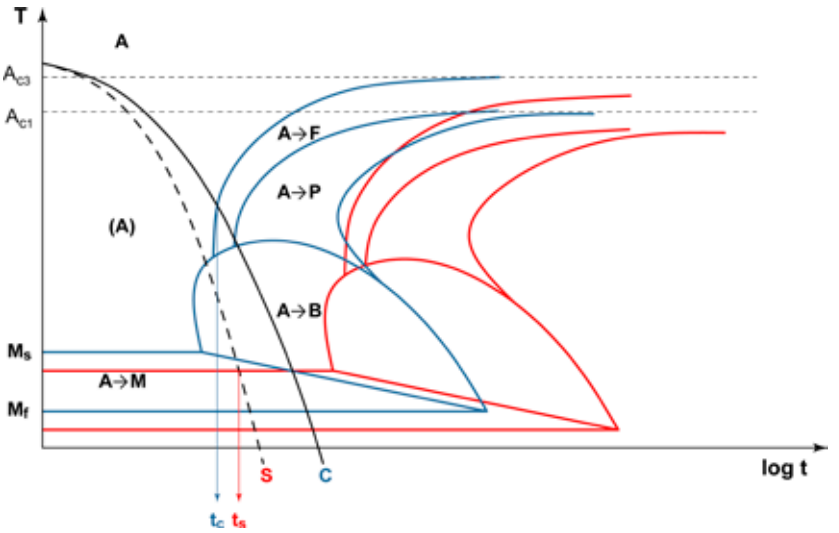

Figure 17.15 – Schematic trend of austenite anisothermal transformation curves for a generic case hardening steel after carburizing. Steel core C.C.T. curves are shown as blue solid lines while the steel surface C.C.T. curves as red solid lines. The black solid curve represents the steel cooling trajectory at the core (C); the black dashed black curve represents the steel cooling trajectory in the hardened surface layer (S).

Austenite transformation, first at the core and then at the surface, creates compressive residual stresses at the surface (Figure 17.16) due to the volume increase constraint in this area during martensite formation.

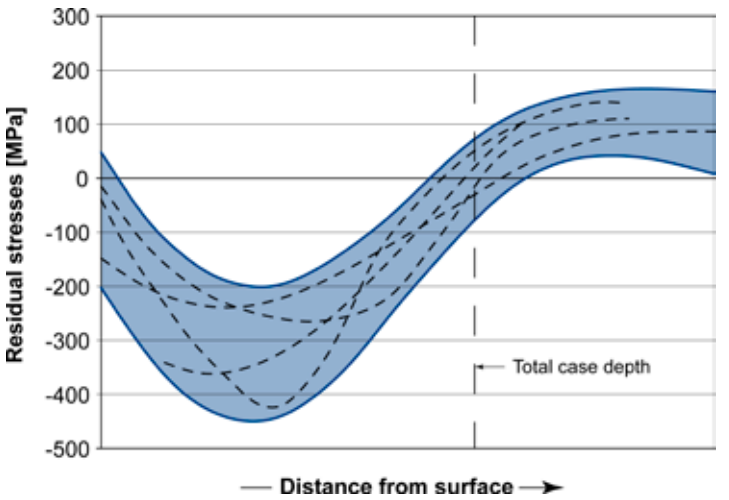

Figure 17.16 – Schematic trend of residual stresses measured in 70 case hardening steels ($0.15\% \leq C \leq 0.20\%$), after carburizing to the depth of 1 mm, oil quenched and stress relieved at 150° to 180°C [from Canale et al. 2008].

17.6 The Characteristics of Case Hardened Layers

The surface layers obtained after case hardening consist of tempered martensite. A typical example is shown in Figure 17.17 and refers to a module 10 tooth taken from a pinion made of EN 17NiCrMo6-4 steel. Figure 17.18 shows the tooth micro-hardness profile together with the indication of effective case depth (d_{eff} = 1.9 mm).

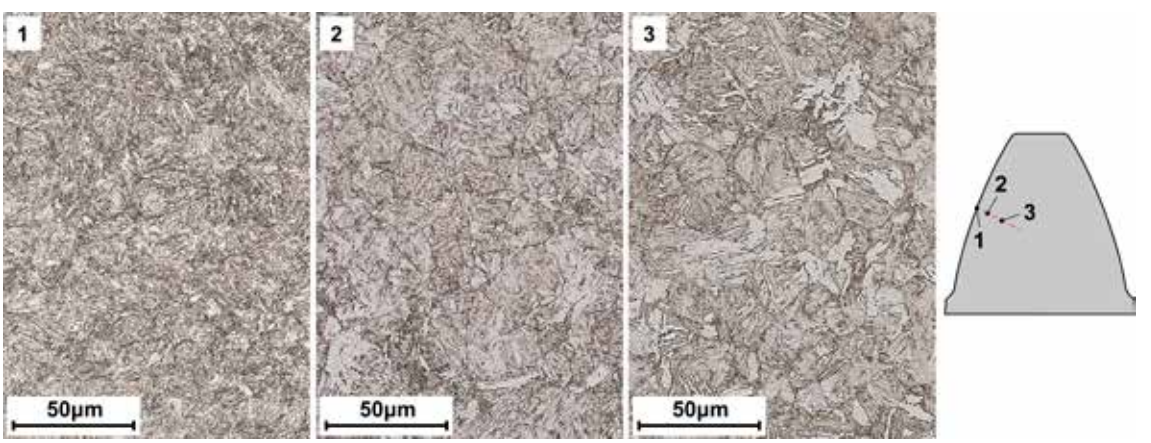

Figure 17.17 – Micro-structure of a case hardened layer found in a gear tooth; etching agent: Nital 2% [Laboratories of the Department of Mechanical Engineering of Politecnico di Milano - Milan, Italy].

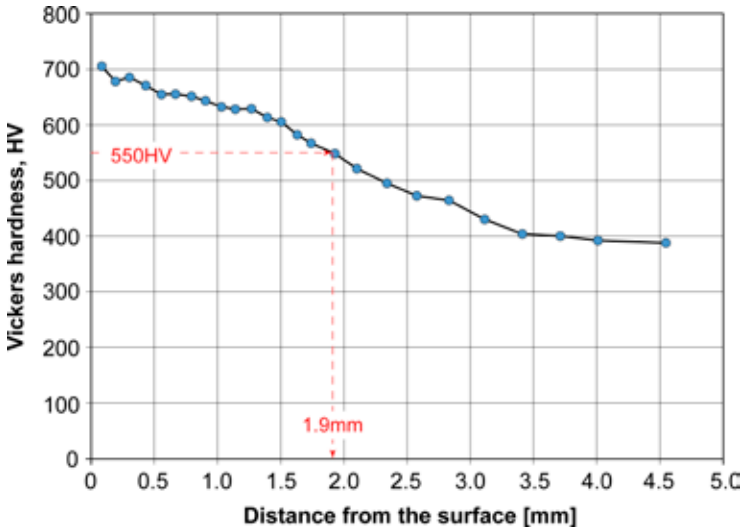

Figure 17.18 – Micro-hardness profile measured along the pitch circle of the tooth shown in Figure 17.17. Red dashed lines indicate the mode of effective case depth determination [Laboratories of the Department of Mechanical Engineering of Politecnico di Milano – Milan, Italy].

To prevent problems arising from case hardened components during operation, you should always consider a number of aspects connected with the micro-structure of the hardened layer.

First of all, you should avoid the formation of oxidized areas near of the surface (Figure 17.19), resulting in high concentrations of oxidizing species in the carburizing atmosphere.

Visually, the problem takes the form of oxidation along the boundaries of the original austenitic grain. If the fault is not very deep, it can be corrected by grinding. Otherwise, intergranular oxidation rapidly damages the case hardened layer as destructive *pitting* [14] occurs after a short service time, even in the presence of limited mechanical stresses.

Another issue connected with the formation of case hardened layers is the presence of retained austenite. This structure can be hardly determined using an optical microscope and can be quantified only by means of X-ray diffraction techniques. Figure 17.20 provides an example that is clearly visible using optical microscopy Retained austenite derives from the considerable carbon content increase in the hardened thickness. This causes the martensite finish temperature (M_f) in the case hardened layer to drop below room temperature, thereby preventing complete austenite transformation after quenching.

[14] *Mechanical damage due to pitting, also known as fatigue wear, should not be confused with corrosive damage that is also called pitting and is a form of localised corrosion typical of stainless steels, aluminium alloys and titanium alloys.*

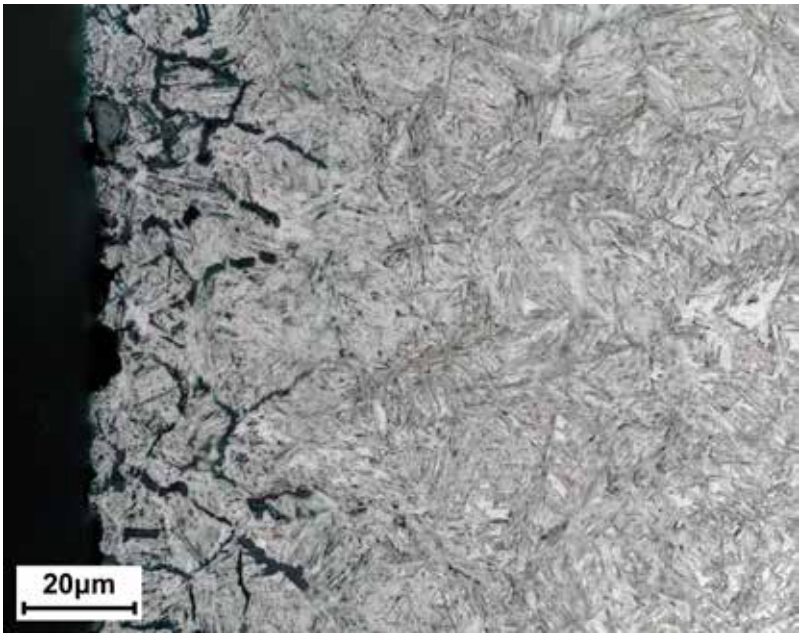

Figure 17.19 – Detail of a case hardened layer affected by intergranular oxidation; fault thickness ~20µm; etching agent: Nital 2% [Laboratories of the Department of Mechanical Engineering of Politecnico di Milano – Milan, Italy].

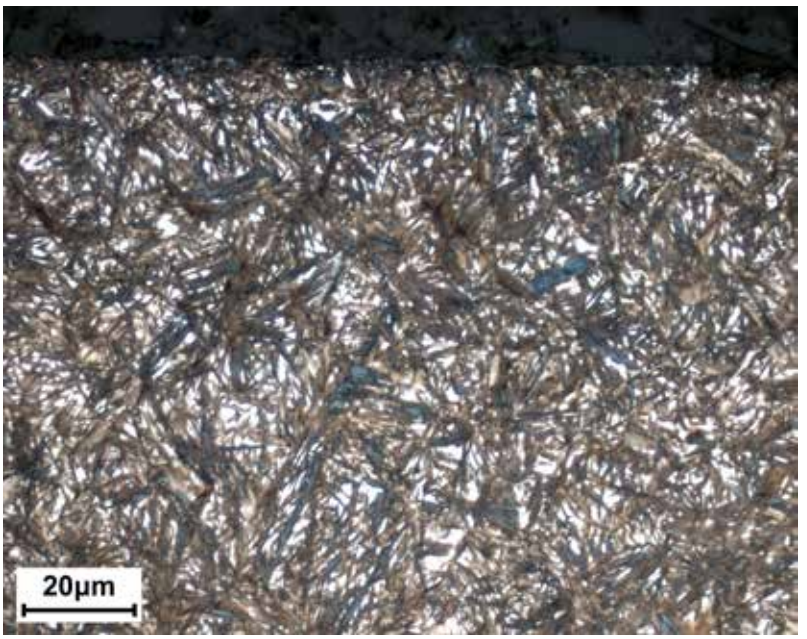

Figure 17.20 – Anomalous amounts of retained austenite (whitish areas) in a case hardened layer; etching agent: Nital 2% [Omeco S.r.l. Laboratories - Monza, Italy].

Opinions differ as to the effect of retained austenite in a case hardened layer. In general, you can say that high deformability of the γ–phase (austenite) produces different effects depending on the characteristics of the case hardened layer and the base material. Under the action of high contact loads, retained austenite islands in the martensitic matrix tend to deform, thereby increasing the contact area and decreasing local pressure. On the other hand, widespread austenite plastic deformation tends to reduce the field of compressive residual stresses, which worsens the component resistance to wear and contact fatigue (*pitting*).

A last important element is the presence of carbides at grain boundary resulting from excessive carbon enrichment in the hardened layer. This defect is connected with using too high carbon potentials during carburizing or too short diffusion times.

In these cases, you observe an iron carbide lattice built up at grain boundary of the original austenitic structure, sometimes in a huge amount. A particularly anomalous situation is shown in Figure 17.21. Being brittle, carbides induce gradual worsening of fatigue wear resistance and promote crack formation during grinding.

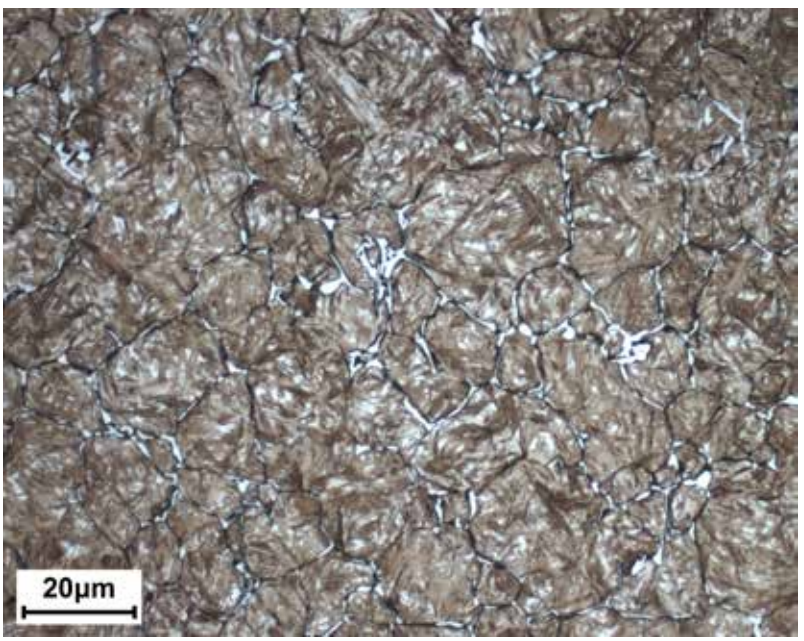

Figure 17.21 – Over-carburized layer; huge amounts of carbides at grain boundary (whitish areas); etching agent: Nital 2% [Omeco S.r.l. Laboratories - Monza, Italy].

17.7 Main Case Hardening Steel grades

Steel grades used to manufacture mechanical components to be case hardened have low carbon content. Even though you can use EN C10 or EN C15 steel grades, recourse is normally made to low-alloy chromium-molybdenum, chromium-manganese, nickel-chromium or nickel-chromium-molybdenum steels[15]. Carbon content should be kept at low levels ($C \leq 0.2\%$) to facilitate case hardening kinetics and guarantee fracture toughness at the component core. Alloying elements are added to increase steel hardenability in view of allowing martensitic transformation also at core level (Figure 17.22).

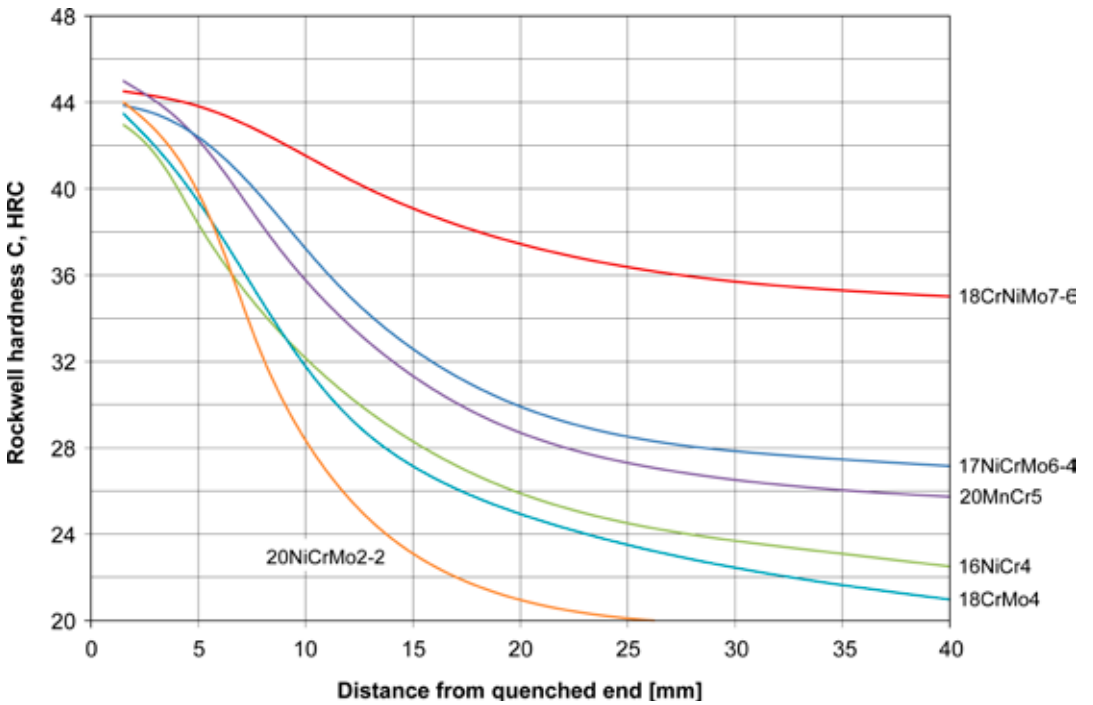

Figure 17.22 – Jominy hardenability curves for some low alloy case hardening steels.

The typical composition that combines these multiple requirements is that of EN 17NiCrMo6-4 steel grade. Actually, this steel grade is the most used in the mechanical sector whenever maximum reliability is a must: pinions, camshafts, gears, dowel pins, pins and rollers are its typical applications.

For heavy-duty applications, high nickel and chromium content case hardening steel grades are available, such as EN 18CrNiMo7-6. Even if expensive, it exhibits high hardenability and excellent fracture toughness values.

---

[15] In comparison with non alloy steels, low alloy steels are more strength, tough and hardenable and offer the advantage of having a difference between $A_{c3\ core}$ and $A_{c3\ surface}$ below 100°C.

When the money aspect is more important, as in the automotive sector, you resort to case hardening steels of the following grades: chromium-nickel or chromium-nickel-molybdenum (EN 16CrNi4 or EN 20NiCrMo2-2), chromium-molybdenum (EN 18CrMo4) or manganese-chromium (EN 16MnCr5 or EN 20MnCr5). With manganese-chromium steels, you can also use alligation with boron to improve hardenability. The properties of manganese-chromium steels are more than acceptable for many applications, even if their fracture toughness is lower than in nickel-alloyed steels.

Table 17.3 lists the chemical composition of some case hardening steels according to the EN ISO 683-3 standard[16]. It should be pointed out that this standard correctly does not provide indications about the mechanical properties of case hardening steels as such properties depend on case hardening conditions.

For maximum machinability, you can select the sulphur-manganese free-cutting steels (11SMn30, 15SMn13, 17SMn20) mentioned in the EN ISO 683-4 standard[17]. Even though they are not specifically designed for this process, their chemical composition is suitable to case hardening.

Designation	%C	%Si	%Mn	%P	%S	%Cr	%Mo	%Ni	%Cu
EN C10	0.07-0.13	0.15- 0.40	0.30-0.60	≤ 0.025	≤ 0.035 (*)	≤ 0.40	≤ 0.10	≤ 0.40	≤ 0.30
EN C15	0.12-0.18	0.15-0.40	0.30-0.60	≤ 0.025	≤ 0.035 (*)	≤ 0.40	≤ 0.10	≤ 0.40	≤ 0.30
EN 20MnCr5	0.17-0.22	0.15-0.40	1.10-1.40	≤ 0.025	≤ 0.035 (*)	1.00-1.30	---	---	≤ 0.40
EN 18CrMo4	0.15-0.21	0.15-0.40	0.60-0.90	≤ 0.025	≤ 0.035 (*)	0.90-1.20	0.15-0.25	---	≤ 0.40
EN 16NiCr4	0.13-0.19	0.15-0.40	0.70-1.00	≤ 0.025	≤ 0.035 (*)	0.60-1.00	---	0.80-1.10	≤ 0.40
EN 20NiCrMo2-2	0.17-0.23	0.15-0.40	0.65-0.95	≤ 0.025	≤ 0.035 (*)	0.35-0.70	0.15-0.25	0.40-0.70	≤ 0.40
EN 17NiCrMo6-4	0.14-0.20	0.15-0.40	0.60-0.90	≤ 0.025	≤ 0.035 (*)	0.80-1.10	0.15-0.25	1.20-1.60	≤ 0.40
EN 18CrNiMo7-6	0.15-0.21	0.15-0.40	0.50-0.90	≤ 0.025	≤ 0.035	1.50-1.80	0.25-0.35	1.40-1.70	≤ 0.40

(*) A controlled-sulphur grade containing 0.020% ≤ S ≤ 0.040% also exists for these steels.

Table 17.3 – Heat analysis of some case hardening steels [from EN ISO 683-3].

Case hardened mechanical components are usually manufactured following the manufacturing cycle shown in Figure 17.23.

The semi-finished product (wire rod, round bar, forging, etc.) is subjected to normalizing and soft annealing heat treatments followed by rough machining. Thanks to their low carbon content, case hardening steels are the most machinable among special structural steels.

[16] *EN ISO 683-3, Heat-treatable steels, alloy steels and free-cutting steels – Part 3: Case hardening steels.*

[17] *EN ISO 683-4, Heat-treatable steels, alloy steels and free-cutting steels – Part 4: Free-cutting steels.*

Then the semi-finished product is case hardened, quenched and tempered at low temperature. During initial austenitization the surface layers are enriched in carbon by effect of the carburizing atmosphere. Then, the part is quenched and stress-relieved.

If requested, some areas of the component can be previously protected from case hardening by means of specific anti-carburizing pastes or through the deposition of copper, nickel or tin over the surfaces that should not be hardened.

At the end of the manufacturing cycle, the component is ground and/or lapped using machine tools, which gives it the dimensions, geometrical/dimensional tolerances and roughness requested by design.

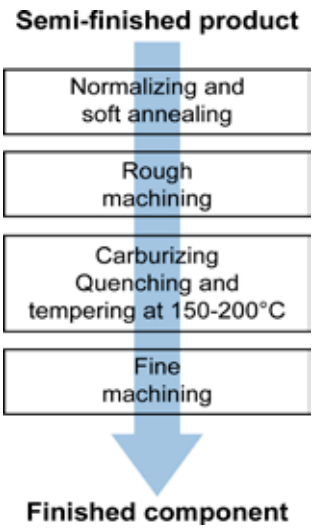

Figure 17.23 – Schematic of the manufacturing cycle used to manufacture a component from a case hardening steel.

18. NITRIDING STEELS AND THE NITRIDING PROCESS

18.1 The Nitriding Process and Its Purposes

Nitriding is a thermochemical treatment performed on steels to enrich the component surface area with nitrogen. Its purpose is to realise an extremely hard layer with thickness of a few tenths of a millimetre (usually between 0.2 and 0.4 mm) to attain optimum resistance to wear, abrasion and seizure. Another result of nitriding is to improve the component fatigue resistance.

Parts are normally nitrided at the end of the manufacturing process, i.e., on steels with a martensitic structure. Nitriding is performed using bell, chamber, pit or fluidised bed furnaces or in salt baths. Temperatures generally range from 480°C and 570°C and process time varies depending on hardening depth (10 to 120 hours).

The nitriding medium can be of a different nature. In most cases, an ammonia-based gaseous atmosphere is used (gas nitriding) while sometimes a nitrogen-hydrogen mix at plasma state (ion nitriding) is used. More rarely, a molten salt bath consisting of sodium/potassium cyanides and cyanates (salt bath nitriding) is preferred.

Nitrided steel takes on the typical dull grey colouring with slight blue hues. Normally, nitrided parts are not subjected to further machining operations.

Nitriding is performed on chromium, aluminium, molybdenum or vanadium low-alloy steels with a medium carbon content that are specially designed for this process. However, other grades of special structural steels are suitable to be nitrided, among which some Q&T steels, case hardening steels or spring steels. Tool steels, *maraging* steels and some grades of stainless steels can also receive the nitriding treatment.

The nitriding process is carried out on components that must resist surface wear and damages (*pitting, scuffing*, etc.) such as bevel spiral gears, Gleason gears, cams, tappets, sliding rails, shafts, valves, extrusion dies, pins, mandrels, pinions, moulds for plastic materials and non-ferrous alloys, pumps and hydraulic components, and cannon barrels.

18.2 Steel Nitriding

Nitriding is based on atomic nitrogen diffusion into the iron crystal lattice, which is similar to what happens with carbon during case hardening. The final result is that the surface layers of the component having been treated will be enriched with nitrogen.

To understand what happens during nitrogen diffusion in the α-iron lattice, you can opportunely make reference to the iron-nitrogen phase diagram in Figure 18.1. Keep in mind that typical process temperatures (480° to 570°C) are below the transformation temperature $\gamma \rightarrow \alpha$ that is equal to 592°C.

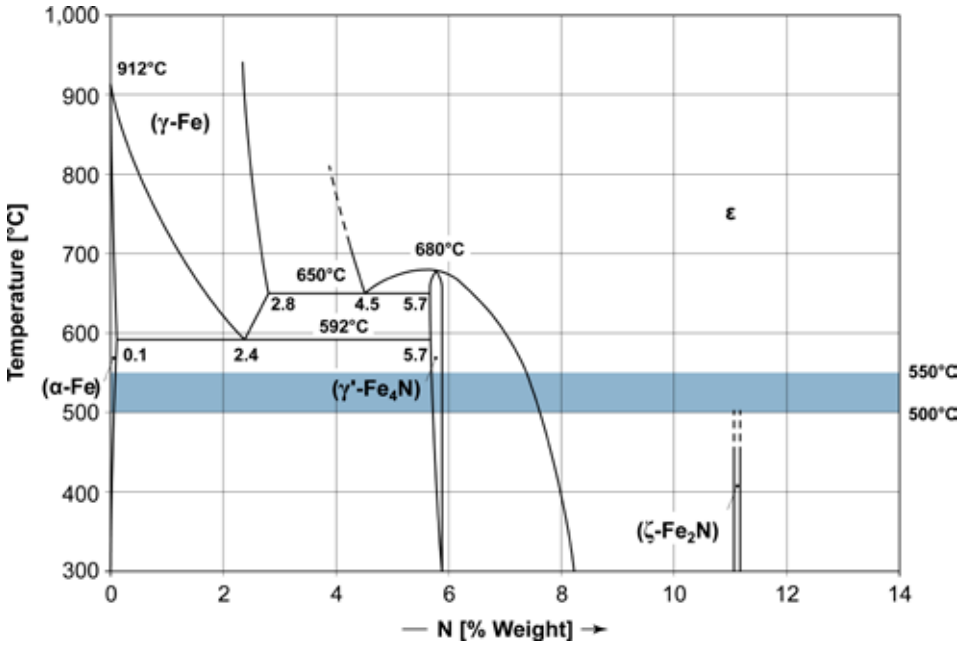

Figure 18.1 – Iron-nitrogen phase diagram with indication of the temperature interval where nitriding takes place (blue band) [from Massalski 1996].

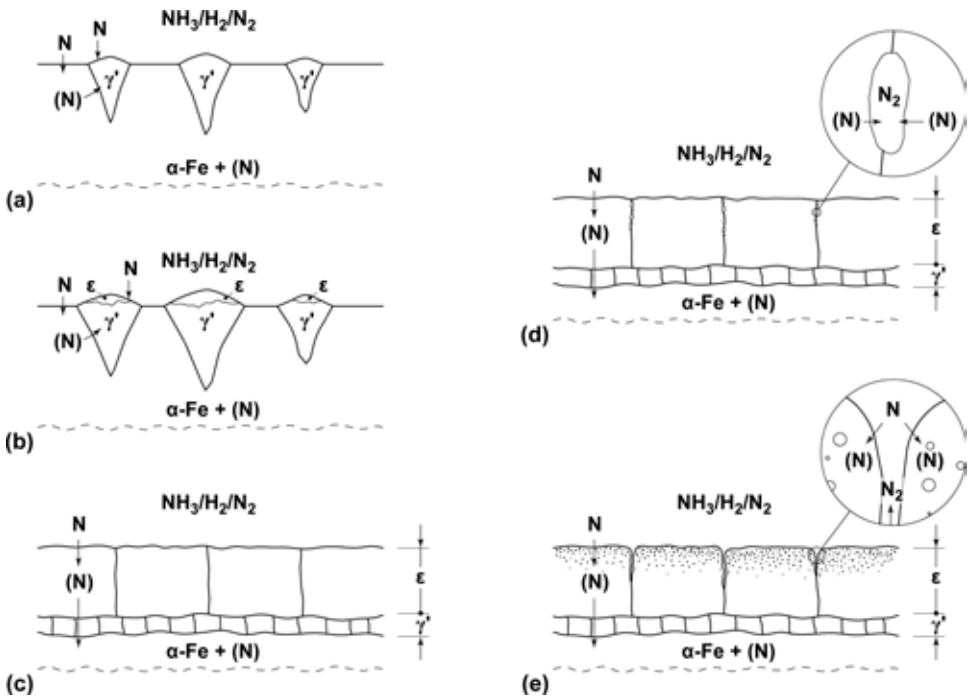

Figure 18.2 – Schematic of the formation of a nitrided layer at iron surface [from Mittemeijer 2013].

In the case of pure iron, once the nitrogen solubility limit in α-phase[1] is exceeded, surplus nitrogen tends to form iron nitrides. Initially, these are Fe_4N type compounds, also called phase γ', with about 6% of nitrogen, later on $Fe_{2-3}N$ type compounds, phase ε, with nitrogen contents above 8%[2]. With nitriding steels containing alloying elements, you also observe the formation of complex chromium, aluminium, molybdenum or vanadium nitrides and/or carbonitrides.

The compounds that nitrogen forms with iron or other alloying elements trigger the typical mechanism of precipitation hardening (Figure 18.3). This type of compounds of nanometric dimensions precipitate and spread very finely in the metallic mass, thereby hindering dislocation motion and causing local distortion of the crystal lattice.

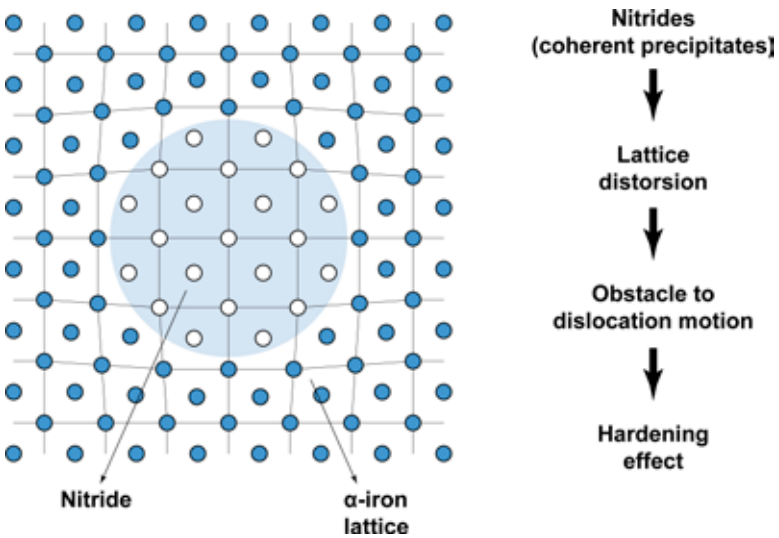

Figure 18.3 – Schematic representation of the iron lattice hardening mechanism following precipitation of coherent nitrides [from Díaz 2007].

When the surface of mild carbon steel is enriched in nitrogen, iron nitrides/carbonitrides (type ε and γ') will mainly form and hardness increase will be rather limited, around 350 to 450 HV. If steel contains alloying elements such as *Cr, Al, Mo* and *V*, the nitrided component will acquire high surface hardness, typically 800 to 1000 HV, even reaching 1200 HV if aluminium is present.

In general, the higher is the percentage of alloying elements, the harder will be the nitrided layer. This is due to the increased number of nitrides that can precipitate in the iron lattice. On the other hand, as alloying elements increase, hardening depth decreases because the presence of precipitates in the lattice

[1] *Nitrogen solubility in iron is equal to 0.1% at 592°C and virtually goes down to zero at room temperature.*

[2] *It should be noticed that Fe_4N and $Fe_{2-3}N$ are sometimes confusingly referred to as "compounds" and other times as "phases".*

is an obstacle to nitrogen diffusion. To the regard, you can usefully observe Figures 18.4 and 18.5 showing the impact of alloying elements on hardness and effective depth of nitrided layers.

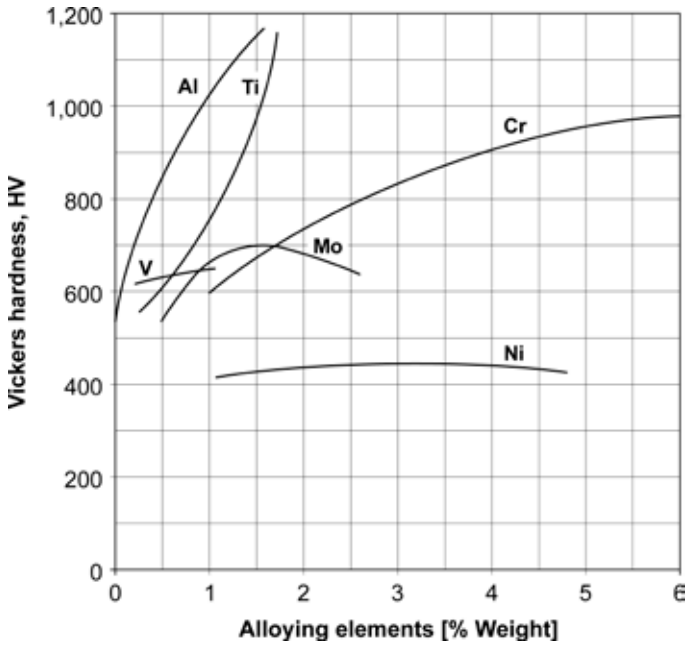

Figure 18.4 – Impact of alloying elements on surface hardness after nitriding (steel with 0.35% C - 0.30% Si - 0.70% Mn) [from Thelning 1975].

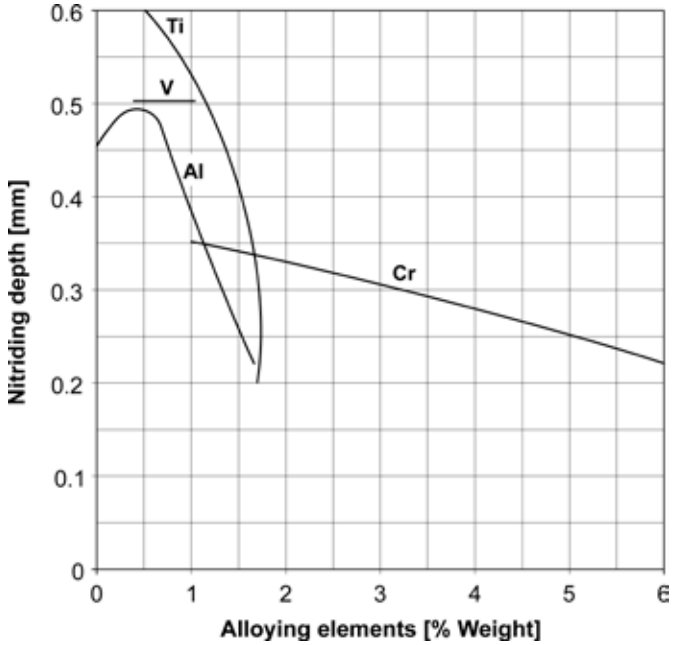

Figure 18.5 – Impact of alloying elements on effective depth of nitrided layers (measured at 400 HV after 8-hour nitriding at 520°C) [from Thelning 1975].

During common nitriding processes, temperature should never exceed the eutectoid temperature of the iron-nitrogen phase diagram at 592°C. Getting past the transformation line $\gamma \rightarrow \alpha$ would result in the formation of an undesired structure, known as braunite[3], that embrittles the nitrided layer.

18.3 Morphology and Characteristics of Nitrided Layers

Figure 18.6 shows the typical aspect of a nitrided layer where two well distinctive areas are clearly visible. Near the surface there is a compact layer, known as *white layer* , consisting of phase γ', phase ε and nitrides/carbonitrides from the alloying elements. The name *white layer* is due to its typical light-colour metallographic appearance. Normally, the white layer is characterised by porosity, as it can be clearly seen in Figure 18.7. The *white layer* properties are very similar to the properties of a ceramic material: low friction coefficient, high hardness values and good corrosion resistance. Normally, its thickness does not exceed a few microns (2 to 20 μm). Some nitriding processes allow obtaining parts virtually deprived of the white layer (< 1 μm).

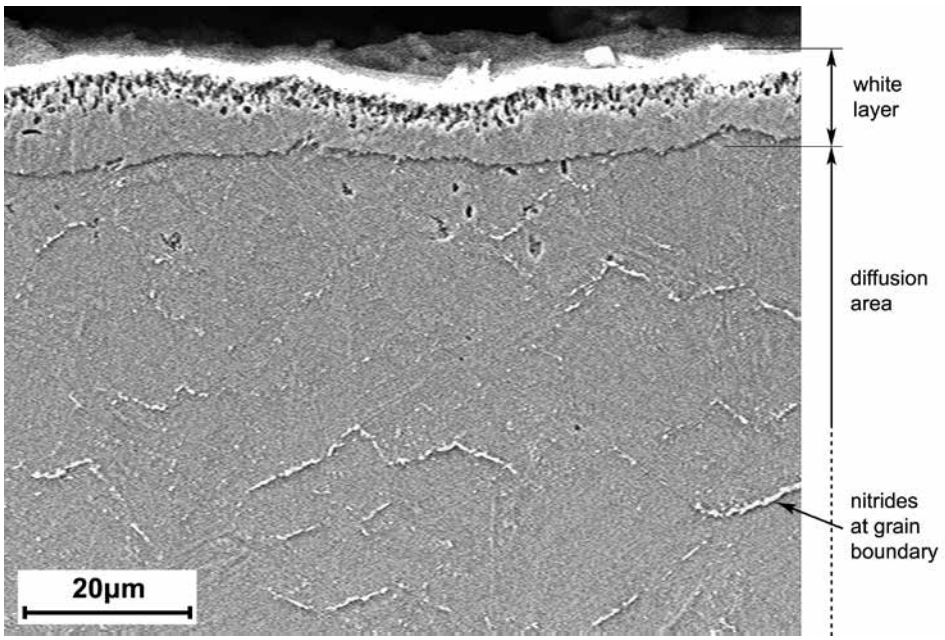

Figure 18.6 – Typical appearance of a nitrided layer for EN 42CrMo4 steel after gas nitriding (30-hour process at 530°C). Electronic scanning microscope; etching agent: Nital 2%. [Laboratories of the Department of Mechanical Engineering of Politecnico di Milano – Milan, Italy].

[3] Braunite is the eutectoid structure of the Fe-N phase diagram that forms from the γ-phase for the effect of slow cooling down. Its structure is similar to that of pearlite, but it is composed of alternating lamellae of phase α and Fe_4N instead of phase α and Fe_3C. Another difference of the two structures lies in the amount of interstitial compound: in equilibrium conditions, the amount of Fe_3C in pearlite is around 12% of the total while in braunite the amount of Fe_4N approximates 44%.

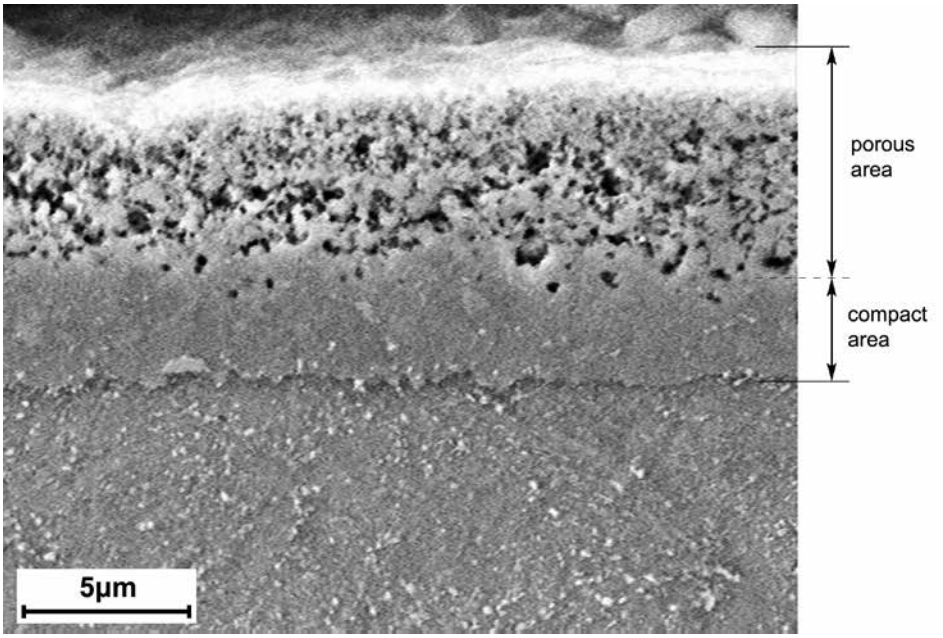

Figure 18.7 – Typical appearance of the white layer in a nitrided layer for EN 42CrMo4 steel. Electronic scanning microscope; etching agent: Nital 2%. [Laboratories of the Department of Mechanical Engineering of Politecnico di Milano – Milan, Italy].

The area immediately underneath the white layer is called diffusion layer. In this area, nitrogen is present both in solid solution in the α-iron lattice and as nitrides/carbonitrides that preferably build up at grain boundary. Nitrogen concentration gradually decreases starting from the surface down to the innermost layers.
Diffusion layer thickness depends on the type and time of the nitriding process; in general, it ranges between 100 µm and 400 µm. You can reach a penetration depth down to 500 to 600 µm only by means of very long nitriding processes
Nitrided layer hardness is not constant all along layer thickness, but it decreases as the nitrogen content decreases until reaching the steel core hardness level.
Typical trends of the Vickers hardness profile (HV) as a function of distance from the surface are reported in Figure 18.8 (as process temperature changes) and in Figure 18.9 (as process time changes). As you can see, hardening depth increases as process temperature increases and, mainly, as process time increases whereas maximum layer hardness tends to decrease as process time decreases.

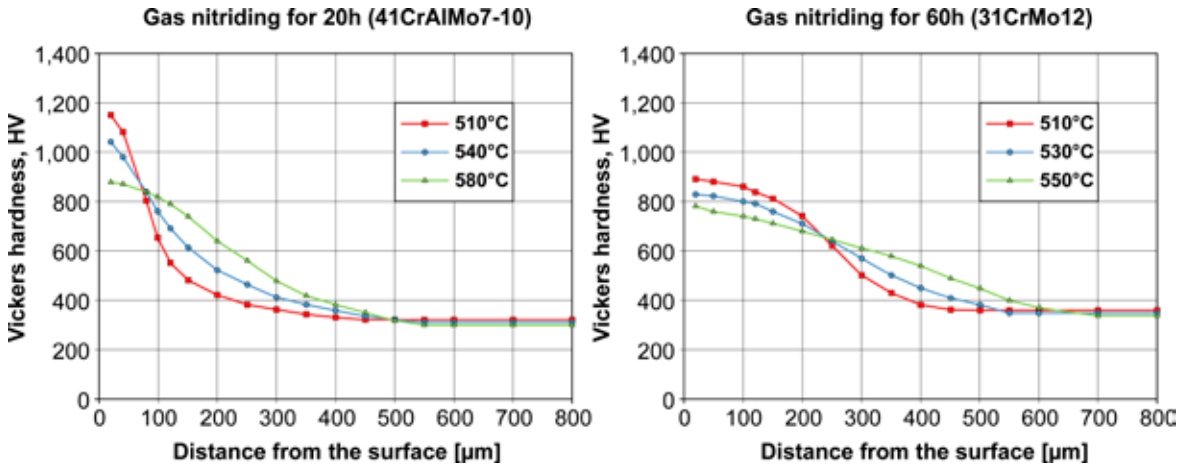

Figure 18.8 – Hardness profile trend after gas nitriding for EN 41CrAlMo7-10 steel, 20 hours process time (on the left) and for EN 31CrMo12 steel, 60 hours process time (on the right) [Laboratories of the Department of Mechanical Engineering of Politecnico di Milano – Milan, Italy].

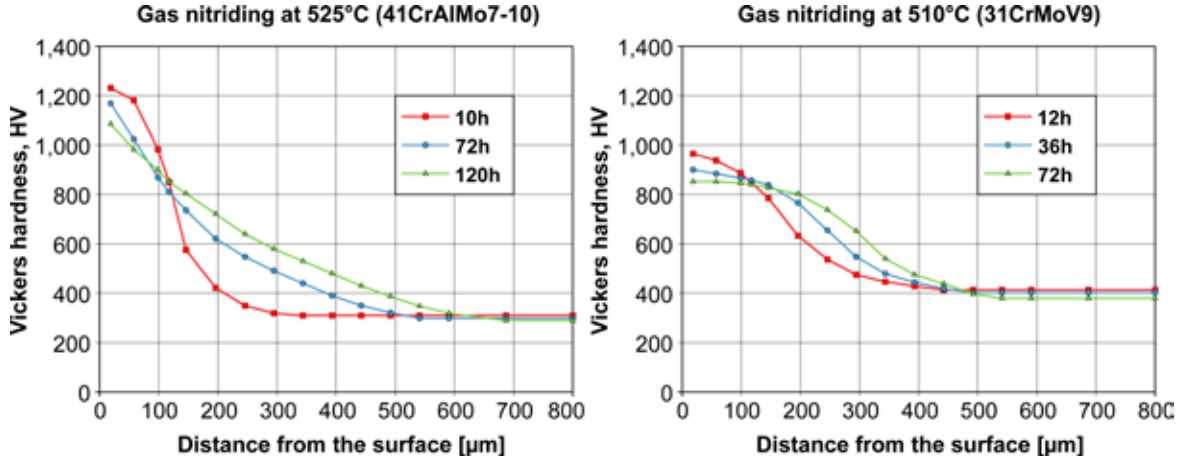

Figure 18.9 – Hardness profile trend after gas nitriding for EN 41CrAlMo7-10 steel, 525°C process temperature (on the left) and for EN 31CrMoV9 steel, 510°C process temperature (on the right) [Laboratories of the Department of Mechanical Engineering of Politecnico di Milano – Milan, Italy].

The hardness profile of the nitrided layer allows determining effective depth, d_e, i.e., the distance from the surface where you measure a hardness value that is 100 HV higher than steel core hardness. Effective depth d_e is obtained by means of the graphic construction suggested in the UNI 11153-2 standard[4] starting from the micro-hardness values measured at increasing distance from the surface (Figure 18.10).

[4] *UNI 11153-2: Misurazione dello spessore di strati superficiali induriti su elementi di lega ferrosa – Nitrurazione e nitrocarburazione ferritica (Measurement of thickness of hardened surface layers of ferrous parts - Nitriding and carbonitriding).*

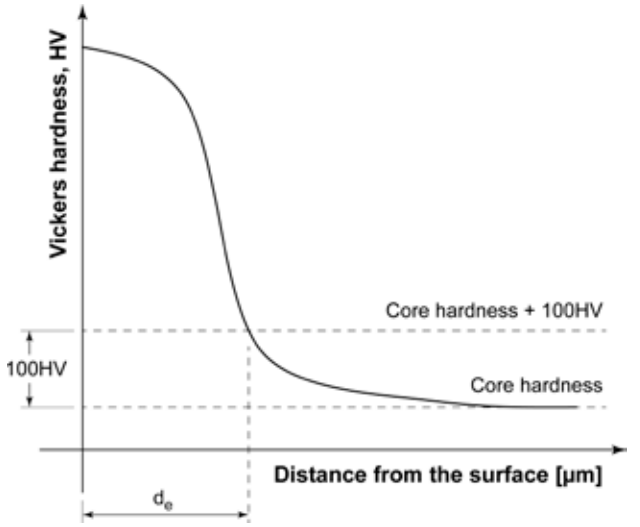

Figure 18.10 – Schematic to measure effective case depth, d_e , of a nitrided layer [from UNI 11153-2].

Thanks to its high hardness and low friction coefficient, the white layer guarantees optimum resistance to adhesion wear, seizure and contact fatigue.

For example, it has been observed that white layer thickness around 5 to 10 µm improves the operating behaviour of gears affected by pitting damages[5]; the same is true for components such as extruder screws or plastics moulds where high white layer thickness hampers deterioration from adhesion wear.

Negative effects connected to white layer brittleness affect parts subjected to abrasive wear (in the presence of hard particles that etch and scratch the surface) or components operating under dynamic stress or in bending/torsional fatigue conditions.

Effective depth d_e is the most relevant parameter when you are going to evaluate the overall behaviour of a nitrided layer. A considerable effective depth makes it easier to stand the local stresses and contact pressures imposed on the part during operation. As a general remark, you can say that, once obtained suitable surface hardness (800 to 1,000 HV, according to the steel grade[6]), resistance of a nitrided part mostly depends on nitriding effective depth.

[5] *See Chapter 17, Note 4.*

[6] *Remember that maximum surface hardness after nitriding depends not only on process effectiveness, but mainly on the types and amounts of alloying elements in steel. Therefore, with aluminium contents around 1%, you can reach hardness values of 1200 HV while in steels with no alloying elements you barely reach 600 HV.*

Another element not to be underrated is the field of compressive residual stresses that generates near the surface of a nitrided component (Figure 18.11). Compressive residual stresses are extremely beneficial in terms of fatigue resistance, given that they reduce the tensile stresses acting at the surface. As already said, this phenomenon is strictly connected with crystal lattice distortion and consequent localised increase of the metallic mass volume during the formation of nitrogen compounds.

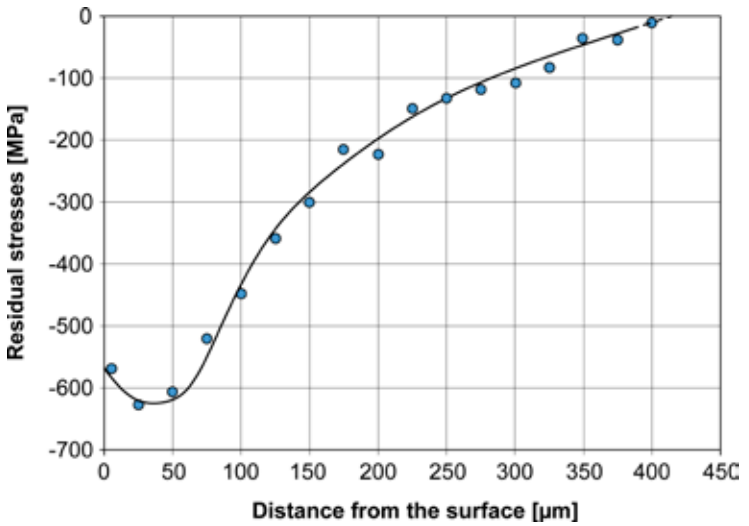

Figure 18.11 – Residual stress trend in a nitrided layer for EN 42CrMo4 steel (at 520°C for 50 hours), measured by means of X-ray difractometry [Laboratories of the Department of Mechanical Engineering of Politecnico di Milano – Milan, Italy].

18. 4 Gas Nitriding

In gas nitriding, the part to be treated is placed in contact with an atmosphere containing pure ammonia or diluted using nitrogen or nitrogen/hydrogen mixtures.

At process temperatures, due to the catalyst action of iron, ammonia tends to dissociate into atomic nitrogen and hydrogen in accordance with the reaction in [eq. 18.1]:

$$2NH_3 \rightarrow 2[N] + 3H_2 \qquad \text{[eq. 18.1]}$$

Its radius being much smaller than that of iron atoms, atomic state nitrogen [*N*] can easily "penetrate" and diffuse into the crystal lattice of the steel being nitrided. The amount of nitrogen that penetrates and diffuses into steel depends not only on process temperature and time, but also on the amount of ammonia, NH_3, that is present on the part surface. As the amount of ammonia increases, the amount of atomic state nitrogen, [*N*], available for steel nitriding purposes, also increases.

Nitrogen that forms from the reaction in [eq. 18.1] and does not manage to penetrate into steel, combines at molecular level following the traditional ammonia dissociation reaction in [eq. [eq. 18.2]:

$$2NH_3 \rightarrow N_2 + 3H_2 \qquad \text{[eq. 18.2]}$$

By measuring the amount of ammonia, NH_3, exiting the furnace, you can evaluate the ammonia dissociation degree. For example, if the amount of ammonia exiting the furnace is 75% of the total amount, the ammonia dissociation degree will be 25%. This means that approximately 25% of the ammonia let into the furnace dissociated as molecular nitrogen, N_2, and molecular hydrogen, H_2, while 75% remained non-dissociated. As the reaction in [eq. 18.2] takes place rather slowly[7], it suffices to guarantee a continuous flow of ammonia into the furnace to keep constant the NH_3 concentration in contact with the parts being treated, which results in a corresponding almost constant dissociation degree.

Figure 18.12 illustrates an approximate correlation between the amount of ammonia in contact with the parts being nitrided, ammonia dissociation degree and ammonia flow rate in the furnace (measured in terms of furnace volume change per hour). For example, using pure ammonia and taking care to set a flow rate that completely regenerates the furnace volume 4 times in an hour, you obtain a dissociation degree of 25%, which corresponds to an amount of ammonia constantly in contact with the parts of about 75%.

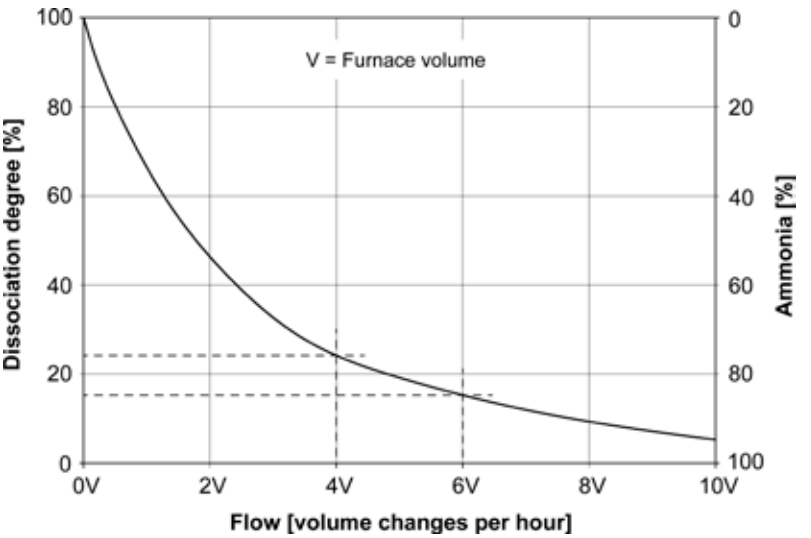

Figure 18.12 – Correlation of ammonia dissociation degree and flow rate in the process furnace in a 100% NH_3 atmosphere [from Herring 2011].

[7] *At usual nitriding temperatures, the reaction in [eq. 18.2] is considerably shifted to the product side, i.e., ammonia almost completely dissociates as molecular nitrogen and molecular hydrogen. Kinetics of the reaction in [eq. 18.2] is rather slow and this allows atomic nitrogen absorption into steel.*

If furnace volume change takes place more rapidly (6 times per hour), the dissociation degree drops to 15%, The two examples provided highlight that the nitriding ability of the atmosphere basically depends on the amount of dissociated/non-dissociated ammonia in the process furnace and interfacing with steel.
Knowing the characteristics of the nitriding atmosphere, especially ammonia dissociation degree, is of the utmost importance because it allows foreseeing nitrided layer micro-structure by means of Lehrer diagram (Figure 18.13).

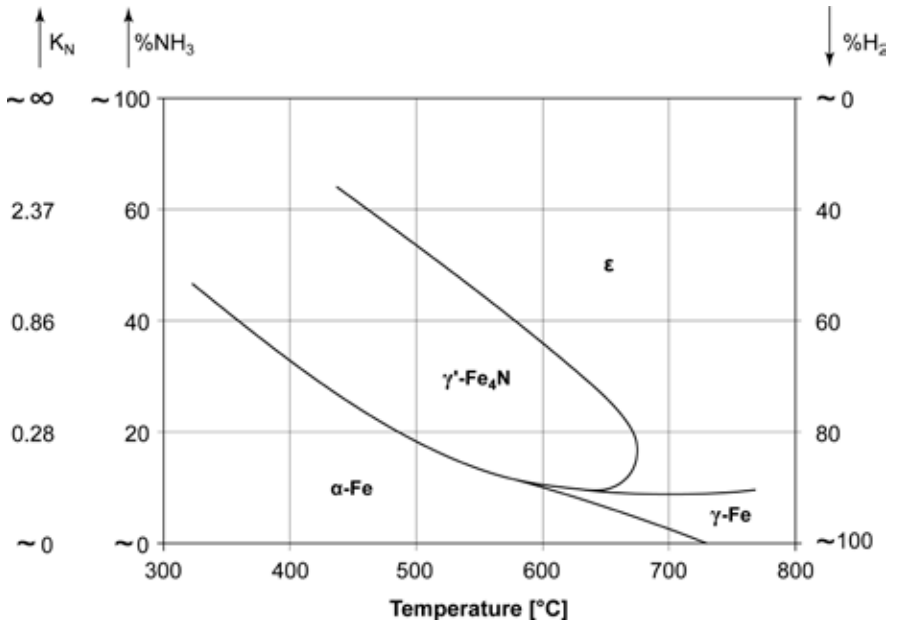

Figure 18.13 – Lehrer diagram for pure iron [from Lehrer 1930 and Maldzinski et al. 1999].

Even though it refers to pure iron, Lehrer diagram is widely used also for steels to determine which type of nitrides (ε or γ') will form depending on the characteristics of the nitriding environment.
In addition to the amount of ammonia, Lehrer diagram includes the parameter K_N (called "nitriding potential") plotted as ordinate. This parameter allows evaluating the ability of an atmosphere to give off atomic nitrogen to steel with greater accuracy[8].

[8] *The parameter K_N, called nitriding potential, derives from calculating the equilibrium constant K_{eq} of the reaction in [eq. 18.1]. Assuming the gases to be ideal gases and being a_N the nitrogen activity in the nitriding atmosphere, you obtain:*

$$K_{eq} = \frac{a_N \cdot {p_{H_2}}^{1,5}}{p_{NH_3}} \quad \rightarrow \quad a_N = K_{eq} \cdot \frac{p_{NH_3}}{{p_{H_2}}^{1,5}} \quad \rightarrow \quad a_N = K_{eq} \cdot K_N$$

The relation highlights that the nitrogen activity is proportional to the ratio between the partial pressures of ammonia and hydrogen raised to power of 1.5.

K_N is defined by the following formula [eq. 18.3]:

$$K_N = \frac{p_{NH_3}}{(p_{H_2})^{1,5}} \qquad \text{[eq. 18.3]}$$

where the numerator and the denominator are the partial pressures of ammonia and hydrogen that, in turn, are proportional to their respective amounts.

As the value K_N increases, the amount of ammonia in contact with the parts also increases (i.e., the ammonia dissociation degree decreases). Consequently, the nitriding ability of the atmosphere, i.e., its ability of giving off nitrogen to the part being treated, increases too.

The parameter K_N and the ammonia dissociation degree can be measured by determining the characteristics of the gas exiting the furnace or by analysing the nitriding atmosphere in-situ by means of probes opportunely installed in the process chamber.

Basically, you can perform gas nitriding either in a single-stage process or a double-stage process.

In the single-stage process you set the temperature and the atmosphere nitriding potential (i.e., ammonia dissociation degree) and keep them constant throughout the process. Typical operating temperatures are 500° to 525°C with a dissociation degree between 15% and 25% ($4 < K_N < 15$).

In the double-stage process, nitriding is obtained by changing both the temperature and the nitriding potential during the process. Initially, you implement the same modes as in the single-stage process but for shorter times; usually, this first phase lasts about 1/3 to 1/5 of total process time. The aim is to rapidly enrich the component surface in nitrogen, reach saturation and form a compact nitride layer. Subsequently, you slightly increase temperature (530° to 570°C) and bring the ammonia dissociation degree to 65 to 85% ($0.4 < K_N < 1$)[9] to support nitrogen diffusion towards the layers underneath.

The double-stage process (boost and diffusion) enables better control of the white layer characteristics (thickness and nitrogen content), thereby considerably reducing ammonia consumption. Table 18.1 shows a schematisation of the operating modes of both systems.

[9] *To guarantee a high ammonia dissociation degree, it is necessary to treat the gas mix using a pre-dissociator before letting it into the process furnace.*

Total time [hour]	Effective depth [μm]	First stage (*Boost*)		Second stage (*Diffusion*)	
		Time [hour]	Dissociation degree [%]	Time [hour]	Dissociation degree [%]
6	50-150	6	15-25	---	---
12	200-300	10	15-25	---	---
24	250-350	24	15-25	---	---
12	150-250	4	15-25	8	65-85
24	200-300	6	15-25	18	65-85
32	250-350	6	15-25	26	65-85
48	300-400	8	15-25	40	65-85
60	350-450	12	15-25	48	65-85
72	400-500	16	15-25	56	65-85
120	450-550	30	15-25	90	65-85

Table 18.1 – Characteristics of single-stage and double-stage nitriding processes. The extent of effective depth is indicative and depends on steel chemical composition.

18.5 Ion Nitriding

In ion nitriding (or plasma nitriding), the parts are placed into a chamber furnace where pressure below atmospheric pressure (130 Pa to 1,300 Pa) is implemented using vacuum pumps. Then, a nitrogen and hydrogen gas mix is let in and a constant potential differential (400 to 1,000 V) between the furnace chamber (with a positive potential) and the part being treated (with a negative potential) is applied. As a consequence, the process gas ionises and you obtain a violettish luminescent plasma composed of ionic nitrogen (N^+).

Due to the potential differential between the chamber and the components being nitrided, nitrogen ions are accelerated against the part surface, actually "bombing" it. The impact of these high kinetic energy particles causes the component to heat up to process temperatures between 480°C and 570°C.

This process, also called cathodic *sputtering*, produces two beneficial effects. Firstly, ions N^+ that hit the surface have the possibility to go through several layers of the crystal lattice, thereby nitriding the part in depth. Thus, in ion nitriding, nitrogen is provided also through this particular physical mechanism, called *ion implantation* , and not only by gas diffusion into a solid, as it is typical in gas nitriding.

Secondarily, ion repeated impacts cause the surface atoms (mainly *Fe*, *C* and *O* atoms) to detach from the metallic mass across a thickness of some nanometres. These atoms recombine with plasma nitrogen and deposit again evenly on the part surface. This improves white layer thickness control (below 3 µm) and the possibility to nitride stainless steels and titanium alloys, otherwise protected by their passive layer of oxides.
Pulsed arc plasma is a novel process recently introduced in the sector of ion nitriding. In these systems, voltage applied between the chamber and the parts being treated has a time frequency that varies between 3 µs and 2000 µs. The characteristic of pulsed arc plasma provides increased uniformity of the nitriding process both in terms of heating mode and hardness depth also in difficult to access areas, such as holes. Another specificity of this technology concerns furnace heating that is obtained by means of a set of electric resistors[10] in addition to ion impact on the components.
Another advantage of pulsed arc plasma systems is the possibility to perform nitriding processes at low temperature (300° to 400°C). This technique requires long process times, but seems to be suitable to both low-temperature tempered steels (spring or tool steels) and stainless steels as it reduces worsening of their mechanical and corrosion resistance.
From the metallurgical point of view, the hardened layer obtained through ion nitriding (by traditional arc or pulsed arc plasma processes) exhibits virtually the same mechanical and metallurgical properties as gas nitrided layers. Also in this case, you observe that the part cortical layers are enriched with nitrogen, with consequent increase of nitrided component hardness.
Process temperatures are not significantly different from gas nitriding while process times are often slightly shorter but obtain the same effective depth.
The process can be controlled either by regulating the system electrical parameters that change plasma energy properties and part temperatures or by changing the gas mix ratio. High nitrogen contents allow obtaining atmospheres with higher nitriding potential values.

18.6 Salt Bath Nitriding

Even though it is slowly being dismissed for ecological reasons, salt bath nitriding still is rather important at industrial level and is worth being dealt with.
The process is performed at 560° to 590°C in a molten salt bath consisting of potassium and sodium cyanides (*KCN* and *NaCN*).

[10] This process is called hot-wall ion nitriding in opposition to the traditional cold-wall process that relies exclusively on ion impact on the components.

The bath is activated by air insufflation, thereby producing cyanates (*KCNO* and *NaCNO*) that will subsequently decompose due to the catalyst action of iron according to the reactions in [eq. 18.4] and [eq. 18.5]:

$$8KCN + 4O_2 \rightarrow 8KCNO \rightarrow 4N + C + 2K_2CO_3 + 4KCN + CO_2 \quad \text{[eq. 18.4]}$$

$$8NaCN + 4O_2 \rightarrow 8NaCNO \rightarrow 4N + C + 2Na_2CO_3 + 4NaCN + CO_2 \quad \text{[eq. 18.5]}$$

Atomic nitrogen, N, and carbon, C, are released in the bath and diffuse in the steel surface layers. For these reasons, it would be more correct to talk of nitrocarburizing and not simply nitriding. Given that the reactions in [eq. 18.4] and [eq. 18.5] lead to the formation of carbonates (K_2CO_3 and Na_2CO_3) that gradually deplete the bath, specific regenerating organic substances should be added to preserve bath efficiency.

Salt bath nitriding processes currently used at industrial level have a very low content in cyanides (~1%) that are a highly polluting substance to be disposed of. Therefore, these "ecological" baths are composed of cyanates and sodium and potassium carbonates with additions of sodium and potassium chlorides[11].

The salt-bath nitriding process is much faster than gas nitriding as the effective depth desired is reached in 3 to 4 hours. The salt bath nitriding power is a function of cyanate content, but also time and temperature are important parameters to be kept under control during the process. Finally, the part is cooled down in an oil bath or in hot water.

Salt-bath nitrided layers exhibit high hardness, even if effective depth is more limited than in gas nitriding due to shorter process times.

A variant of salt bath nitriding is sulphur-nitriding, characterised by diffusion of sulphur in addition to nitrogen and carbon enrichment. Sulphur, generated by the sodium and potassium sulphites (Na_2SO_3 and K_2SO_3) that are present in the bath, forms a porous *white layer* that can be impregnated with lubricant oils. This peculiarity improves surface resistance to seizure, thereby making sulphur nitrided components less prone to suffer from adhesion wear.

18.7 Nitriding and Post-Oxidation

In recent years, the use has spread of performing post-oxidation after nitriding. In this manner, a thin layer of iron oxides, such as magnetite Fe_3O_4, is formed over the component surface, which considerably improves corrosion and oxidation resistance. The parts so treated take on the typical dark blue/blackish colouring similar to blackening.

Post-oxidation is performed on the nitride layer using gas mixtures composed of carbon dioxide (CO_2), nitrogen oxides (NO_x) or steam (H_2O) or in oxidizing molten salt baths.

[11] *It should be considered that cyanate toxicity is approximately one thousand times lower than that of cyanides. Waste baths are treated exactly in the aim of neutralising cyanides by adding chlorine (Cl_2) and caustic soda (NaOH).*

18.8 Nitriding Steels

Nitriding steels possess special characteristics as to their chemical composition. They are medium carbon content steels containing chromium, molybdenum, aluminium and vanadium. These elements have high chemical affinity with nitrogen and form a very hard nitrided layer. The most widespread nitriding steels include EN 31CrMo12, EN 41CrAlMo7-10 and EN 31CrMoV9.

Molybdenum is always present in nitriding steels, in contents ranging from 0.2 to 0.3%. This alloying element is essential to inhibit tempering brittleness, whose critical interval (500° to 550°C) exactly corresponds to nitriding temperatures.

Normally, nickel is not present in the chemical composition of nitriding steels because, due to its remarkable austenising effect, it tends to lower the temperature of eutectoid transformation $\gamma \rightarrow \alpha$ in the *Fe-N* phase diagram. However, if you want to nitride a steel alloyed with nickel (which is possible), you should decrease process temperature and increase process time relative to usual conditions. If, on one hand, this would be necessary to avoid braunite formation, on the other hand you would incur undesired higher costs[12].

Nitriding steels are covered by the EN ISO 683-5 standard[13] that specifies the technical delivery requirements for the semi-finished products (bars, wire rods, plates, strips, sheets and forgings) used to manufacture mechanical parts to be nitrided. In particular, the standard defines the chemical composition (Table 18.2) and the mechanical characteristics of the quenched and tempered material (Table 18.3).

Designation	%C	%Si	%Mn	%S	%P	%Al	%Cr	%Mo	%V
EN 31CrMo12	0.28-0.35	≤ 0.4	0.4-0.7	≤ 0.035	≤ 0.025	---	2.8-3.3	0.3-0.5	---
EN 31CrMoV9	0.27-0.34	≤ 0.4	0.4-0.7	≤ 0.035	≤ 0.025	---	2.3-2.7	0.15-0.25	0.1-0.2
EN 41CrAlMo7-10	0.38-0.45	≤ 0.4	0.4-0.7	≤ 0.035	≤ 0.025	0.8-1.2	1.5-1.8	0.2-0.35	---
EN 34CrAlMo5-10	0.30-0.37	≤ 0.4	0.4-0.7	≤ 0.035	≤ 0.025	0.8-1.2	1.0-1.3	0.15-0.25	---

Table 18.2 – Heat analysis for some nitriding steels [from EN ISO 683-5].

[12] *To avoid misunderstandings, it should be specified that also steels containing nickel can be nitrided. In these cases, it is necessary to slightly lower process temperature to prevent braunite formation. However, nitriding time should be prolonged to guarantee the same effective depth.*

[13] *EN ISO 683-5: Nitriding steels - Technical delivery requirements.*

Designation	16mm < Ø ≤ 40mm 8mm < tck. ≤ 20mm				40mm < Ø ≤ 100mm 20mm < tck. ≤ 60mm				100mm < Ø ≤ 160mm 60mm < tck. ≤ 100mm				160mm < Ø ≤ 250mm 100mm < tck. ≤ 160mm			
	YS [MPa]	UTS [MPa]	A%	KV [J]	YS [MPa]	UTS [MPa]	A%	KV [J]	YS [MPa]	UTS [MPa]	A%	KV [J]	YS [MPa]	UTS [MPa]	A%	KV [J]
EN 31CrMo12	≥ 835	1,030-1,230	≥ 10	≥ 25	≥ 785	980-1,180	≥ 11	≥ 30	≥ 735	930-1,130	≥ 12	≥ 30	≥ 675	880-1,080	≥ 12	≥ 30
EN 31CrMoV9	≥ 900	1,100-1,300	≥ 9	≥ 25	≥ 800	1,000-1,200	≥ 10	≥ 30	≥ 700	900-1,100	≥ 11	≥ 35	≥ 650	850-1,050	≥ 12	≥ 40
EN 41CrAlMo7-10	≥ 835	1,030-1,230	≥ 10	≥ 25	≥ 835	980-1,190	≥ 10	≥ 25	≥ 735	930-1,130	≥ 12	≥ 30	≥ 675	880-1,080	≥ 12	≥ 30
EN 34CrAlMo5-10	≥ 600	800-1,000	≥ 14	≥ 35	≥ 600	800-1,000	≥ 14	≥ 35	---	---	---	---	---	---	---	---

Table 18.3 – Mechanical properties of semi-finished products obtained from quenched and tempered nitriding steels; Ø: diameter, tck.: thickness [from EN ISO 683-5].

Figure 18.14 shows the manufacturing cycle used to manufacture a mechanical component to be nitrided.

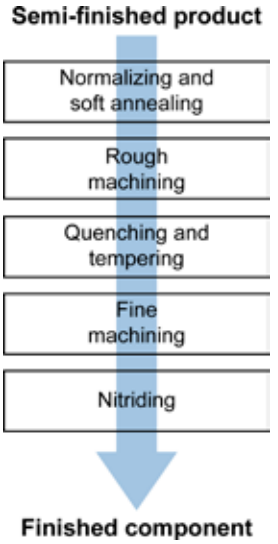

Figure 18.14 – Schematic of the manufacturing cycle used to manufacture a component from a nitriding steel.

After purchase, the semi-finished product (wire rod, round bar, forging, etc.) is subjected to normalizing and soft annealing heat treatments to induce the formation of very low-hardness homogeneous ferrite and pearlite in the metallic mass. This micro-structure facilitates rough machining after normalizing and soft annealing. After rough machining, the semi-finished product is quenched, cooled down in oil and then tempered at 600°C. The Q&T treatment generates the tempered martensite structure necessary to guarantee the high mechanical strength and fracture toughness values required in operation from this steel grade. The manufacturing cycle ends with the fine machining that gives the dimensions to the component, geometrical/dimensional tolerances and roughness requested by design.

Now the components are cleaned of all dirt, oxide or lubricant traces and nitrided. Normally, no other operations will be performed after the nitriding process.

Other machining would be detrimental because they would remove the hardened surface layer that has an extremely low thickness (0.2 to 0.4 mm). Also, the nitriding process does not cause noticeable deformation, thus the components do not require being remachined. If strictly necessary, you can consider whether to carry out final lapping[14].

[14] *Various opinions exist about the convenience to remove the white layer. Some authors deem that the white layer should always be lapped away because it is hard and brittle. Other authors recommend maintaining the white layer only if it is compact and low-thickness as it would produce beneficial effects in terms of mechanical strength. In any case, it is important to point out that the white layer should always be removed with great care to avoid inducing anomalous residual stresses resulting from uncontrolled lapping.*

If required, you can protect component areas not to be hardened by smearing them with anti-nitriding pastes or through the deposition of copper, nickel or tin.

18.9 Nitriding Other Steel Families

The nitriding process can be also performed on steels having a different chemical composition compared to that foreseen for nitriding steels.

Generally speaking, all Q&T steels can be nitride, provided that some cautionary measures are taken in the case of steels containing nickel. In any case, the manufacturing cycle should include the nitriding process as the last step in the manufacture of components.

Best results are obtained from chromium-molybdenum low-alloy steels, such as EN 25CrMo4 and EN 42CrMo4, even if surface hardness and hardening depth are lower than in nitriding steels at the same process temperatures and times. We wish to mention the possibility to successfully perform the nitriding process also on case hardening steels or spring steels, such as EN 20MnCr5 or EN 51CrV4, respectively. Hot work tool steels for, such as EN X40CrMoV5-1 (similar to AISI H13), can also be easily nitrided to increase their resistance to wear.

A separate approach should be devoted to nitriding stainless steels, where the nitriding process is hindered by the chromium oxide layer protecting the surface from corrosion. If you are to use gas nitriding, you should carry out chemical pickling to remove the passive film beforehand. A good alternative is ion nitriding, given that ion implantation destroys the oxide layer and nitrides the surface, without making recourse to chemical pickling.

Another option is salt-bath nitriding. The ability of the salt bath to activate stainless steel surface promotes oxide layer decomposition and allows nitrogen penetration into the components. Nonetheless, concurrent carbon diffusion, typical of salt bath processes, might induce the formation of chromium carbides and impair corrosion resistance.

In general, nitriding stainless steels is not recommended because their corrosion resistance considerably weakens when the passive chromium oxide film is removed. In case of need, martensitic stainless steels (AISI 410, AISI 420 and AISI 440) or precipitation hardening steels (17-4PH) are the most suitable for nitriding purposes.

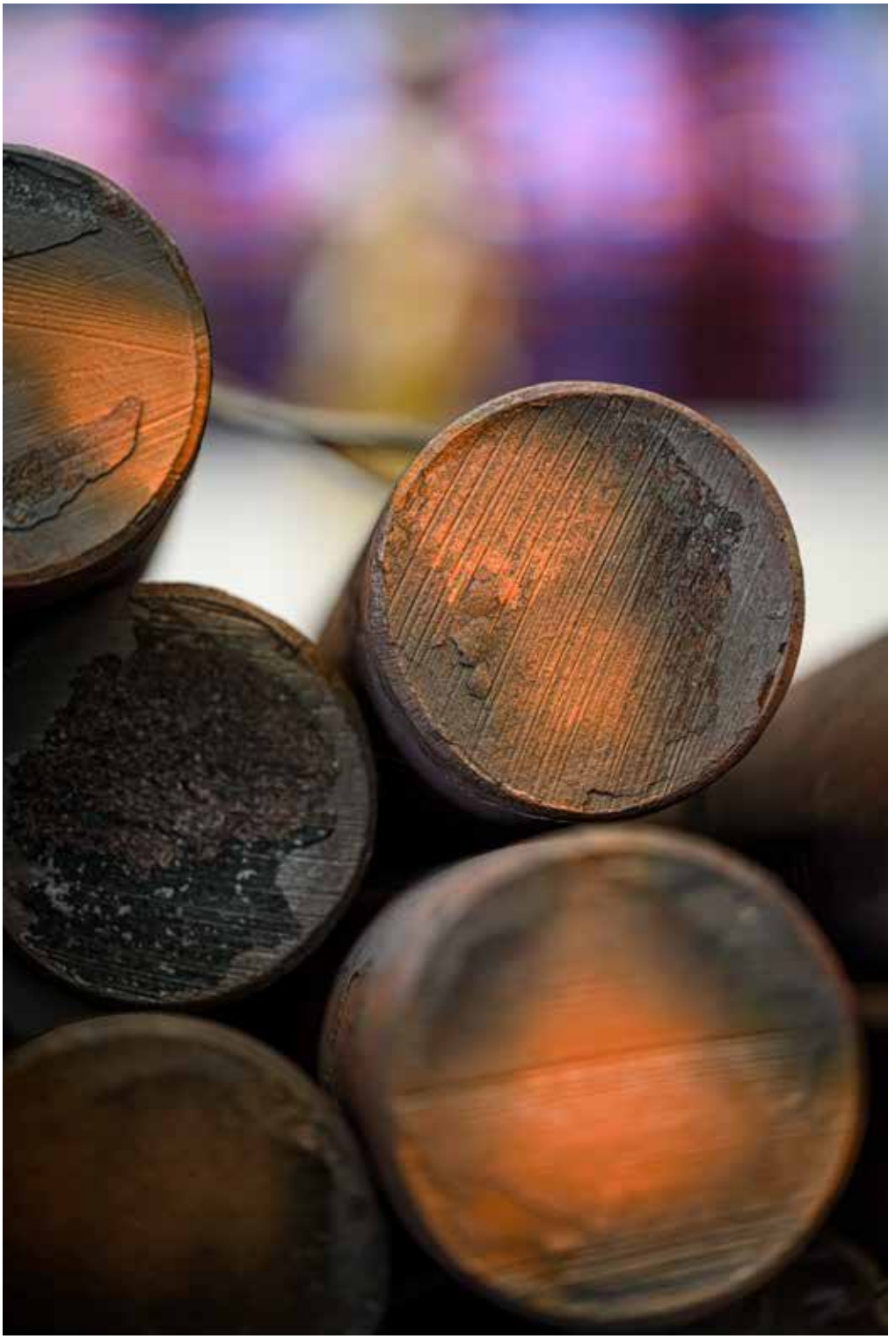

RECOMMENDED BIBLIOGRAPHY

Recommended bibliography in this volume cannot be much different from that given in Steel Metallurgy - Volume I. If you do not have that book, published in 2017, you can download it for free from our website *fa-fe.com* or from the Lucefin steel group website *lucefin.com*, together with the other book in this series titled Stainless Steels.

The two books by Prof. Walter Nicodemi Metallurgia - Principi generali and Acciai e leghe non ferrose, Zanichelli, Bologna, 2007 and 2008, are still valid. They are written in Italian.

If you speak English, you will find it very interesting reading the book Steel and its Heat Treatment by Karl Erich Thelning, Bofors Handbook, Butterworth, London (UK), 1975. Having been written fifty years ago, this book is hard to find in its original edition, but its contents are still up-to-date. Alternatively, about metallurgy of ferrous and non-ferrous alloys, we recommend the collection of texts published by Flake C. Campbell and titled Elements of Metallurgy and Engineering Alloys, ASM International, Metals Park Ohio (USA), 2008 or the book Steel Heat Treatment: Metallurgy and Technologies, cared by George Totten, CRCnet base, Taylor & Francis Group, Boca Raton, Florida (USA), 2006 or even the two books written by George Krauss, Principles of Heat Treatment of Steels, ASM International, Metals Park, Ohio (USA), 1980 and Steels: Processing, Structure, and Performance, ASM International, Metals Park, Ohio (USA), 2005.

If you are really interested in investigating all aspects of metallurgy in depth, we strongly recommend the volume by Anil Kumar Sihna, Physical Metallurgy Handbook, McGraw Hill, New York (USA), 2003. This book consists of more than 1,800 pages about physical metallurgy of iron-base alloys. In it you will find everything, including those very scientific details for which university professors go crazy. In our opinion, the book by Kumar Sihna is even better than the three volumes (more than 3000 pages) of the classic collection by Robert Cahn and Peter Haasen, Physical Metallurgy, 4th ed., North-Holland, Amsterdam (NL), 1996. Another book that is worth mentioning for the in-depth analyses it contains, is the one by Reza Abbaschian, Physical Metallurgy Principles, Cengage Learning, Stamford (USA), 2009.

Given that this second volume on steel metallurgy focusses also on mechanical tests, we deemed it necessary to include some specific bibliographic references. Even though all the books mentioned above also deal with steel mechanical behaviour (to which reference should be made), lab operators will find especially useful the text titled The Testing of Engineering Materials by Davis H. E., Troxell G. E. and Hauck G. F. W., 4th ed., McGraw Hill, Tokyo, Japan, 1984. Finally, as regards fatigue, which concerns both materials and mechanical engineering, we suggest the always valid book Metal Fatigue in Engineering by Stephens R.I., Fatemi A., Stephens R.R. and Fuchs H.O., 2nd ed., John Wiley & Sons, New York (USA), 2001.

BIBLIOGRAPHY

[AA.VV. 1955] Ministry of Transport and Civil Aviation, Cibvil Aircraft Accident, Report of the Court of Inquiry into the Accidents to Comet G-ALYP on 10th January 1954 and Comet G-ALYY on 8th April 1954, London (UK), 1955.

[Abbaschian et al. 2009] Abbaschian R., Abbaschian L., Reed-Hill R. E., Physical Metallurgy Principles, 4ª ed., Cengage Learning, Stamford (USA), 2009.

[Andrews 1965] Andrews K.W., "Empirical formulae for the calculation of some transformation temperatures", Journal of the Iron and Steel Institute, vol. 7, pp. 721-727, 1965.

[Askeland 2006] Askeland D. R., The Science of Engineering Materials, 5th ed., Nelson Engineering, Florence, Kentucky (USA), 2006.

[ASM-H.1 1991] ASM Handbook Committee, ASM Handbook, vol. 1 - Properties and Selection: Iron, Steels and High Performance Alloys, 10th ed., ASM International, Metals Park, Ohio (USA), 1991.

[ASM-H.3 1992] ASM Handbook Committee, ASM Handbook, vol. 3 - Alloy Phase Diagrams, 10th ed., ASM International, Metals Park, Ohio, USA, 1992.

[ASM-H.4 1991] ASM Handbook Committee, ASM Handbook, vol. 4 - Heat Treating, 10th ed., ASM International, Metals Park, Ohio (USA), 1991.

[ASM-H.4A 2013] ASM Handbook Committee, ASM Handbook, vol. 4A - Heat Treating Fundamentals and Processes, on-line ed., ASM International, Metals Park, Ohio (USA), 2013.

[ASM-H.14B 2006] ASM Handbook Committee, ASM Handbook, vol. 14B - Metalworking: Sheet Forming, on-line ed., ASM International, Metals Park, Ohio (USA), 2006.

[Bain e Paxton 1966] Bain E. C., Paxton H. P., Alloying Elements in Steel, 2nd ed., American Society for Metals, Metals Park, Ohio (USA), 1966.

[Brand et al 1991] Brand A., Flavenot J.P., Remy G., Données technologiques sur la fatigue, 3rd ed., CETIM, Senlis (F), 1991.

[Brandes e Brook 1992] E.A. Brandes e G.B. Brook, Smithell's Metal Reference Book, 7th ed., Butterworth-Heinemann, Oxford (UK), 1992.

[Briggs 1958] Briggs C. W., The Effect of Heat Treatment Variables on the Toughness of Cast Steel and Cast Armor, Steel Founders' Society of America, Cleveland, Ohio (USA), 1958.

[Burns e Pickering 1964] Burns K.W. e Pickering F.B., "Deformation and Fracture of Ferrite-Pearlite Structures", Journal of Iron and Steel Institute, vol. 202, n. 11, pp. 899-906, 1964.

[Callister 2007] Callister W. D., Material Science and Engineering: An Introduction, 7th ed., John Wiley & Sons, New York, USA, 2007 (trad. it., Caneva C. (a cura di), Scienza e ingeneria dei materiali - un'introduzione, 2a ed., Edises, Roma, 2007).

[Campbell 2008] Campbell F. C. (ed.), Elements of Metallurgy and Engineering Alloys, ASM International, Metals Park Ohio (USA), 2008.

[Campbell 2003] Campbell J., Castings, 2nd ed., Butterworth-Heinemann, Oxford (UK), 2003.

[Canale et al. 2008] Canale L.C.F., Mesquita R.A., Totten G., Failure Analysis of Heat Treated Steel Components, ASM International, Metals Park Ohio (USA), 2008.

[Capello 2008] Capello E., Le lavorazioni industriali mediante laser di potenza. La tecnologia, le applicazioni e i sistemi, Maggioli, Santarcangelo di Romagna - RN, 2008.

[Cheng et al. 1991] Cheng L., Van der Pers N.M., Böttger A.,De Keuser Th.H., Mittemeijer E.J., "Lattice Changes of Iron Carbon MartensiteAging at Room Temperature", Metallurgical Transaction A, vol. 22, pp. 1957-1967, 1991.

[Chipman 1972] Chipman J., "Thermodynamics and Phase Diagram of the Fe-C System", Metallurgical Transaction B, vol. 3, pp. 55-64, 1972.

[Chuvas et al. 2015] Chuvas T.C., Garcia P.S.P., Pardal J.M., Fonseca M.P.C., "Influence of Heat Treatment in Residual Stresses Generated in P91 Steel-pipe Weld", Materials Research, vol. 18, pp. 614-621, 2015.

[Clayton e Danks 1990] Clayton P., Danks D., "Effect of Interlamellar Spacing on the Wear Resistance of Eutectoid Steels under Rolling/Sliding Conditions", Wear, vol. 135, pp.369-387, 1990.

[Davies e Simpson 1979] Davies J., Simpson P., Induction Heating Handbook, McGraw-Hill Inc., New York (USA), 1979.

[Davis 2001] Davis J.R. (ed.), Alloying - Understanding the Basics, ASM International, Metals Park Ohio (USA), 2001.

[Davis 2002] Davis J.R. (ed.), Surface Hardening of Steels, ASM International, Metals Park Ohio (USA), 2002.

[Davoli et al 2003] Davoli P., Vergani L., Beretta S., Guagliano M., Baragetti S., Costruzione di Macchine 1, McGraw Hill, Milano, 2003.

[Díaz 2007] Díaz N.V., Nitriding of Iron-based Alloys; residual stresses and internal strain fields, Dissertation, Universität Stuttgart, Max-Planck-Institut für Metallforschung, Stuttgart (D), 2007.

[Dieter 1988] Dieter G. E., Mechanical Metallurgy, McGraw Hill, London (UK), 1988.

[Dossett 2020] Dossett J.L., Practical Heat Treating - Basic Principles, ASM International, Metals Park Ohio (USA), 2020.

[Endo e Miyao 1958] Endo K., Miyao Y., "Effects of Cycle Frequency on the Corrosion Fatigue Strength", International Journal of Mechanical Engineering, Series B - Fluids and Thermal Engineering, vol. 1, pp.374-380, 1958.

[Forrest 1962] Forrest P. G., Fatigue of Metals, Pergamon Press, London (UK), 1962.

[Gerold 1979] Gerold V., "Precipitation Hardening", Dislocations in Solids, vol. 4 - Dislocations in Metallurgy, North-Holland Publishing Company, Amsterdam (NL), 1979.

[Ginzburg 2005] Ginzburg V.B., Metallurgical Design of Flat Rolled Steels, Marcel Dekker, New York (USA), 2005.

[Grange e Baughman 1956] Grange R.A., Baughman R.W., "Hardness of tempered martensite in carbon and low alloy steels", ASM Transactions, vol. 48, pp.165-197, 1956.

[Grange et al. 1977] Grange R.A., Hribal C.R., Porter L.F., "Hardness of Tempered Martensite in Carbon and Low Alloy Steels", Metallurgical Transaction A, vol. 8, p.1775-1785, 1977.

[Hashimura 2007] M. Hashimura M., Miyanishi K., Mizuno A., "Development of Low-Carbon Lead-Free Free-Cutting Steel Friendly to Environment", Nippon Steel Technical Report, n.96, 2007.

[Herring 2011] Herring D., "Principles of Gas Nitriding - Part 1, 2 e 3", Industrial Heating, vol. 78, n. 4 (p.49), 5 (p. 53) e 9 (p. 61), 2011.

[Higgins 1993] Higgins R.A., Engineering Metallurgy - Part I: Applied Physical Metallurgy, 6th ed., Arnold, London (UK), 1993.

[Hollomon e Jaffe 1945] Hollomon J.H., Jaffe L.D., "Time-temperature relations in tempering steel", Transactions of AIME, Vol. 162, pp. 223-249 , 1945.

[Hosford 2005] Hosford W. F., Physical Metallurgy, Taylor & Francis Group, Boca Raton, Florida (USA), 2005.

[Hoyle 1988] Hoyle G., High Speed Steels, Butterworths, London (UK), 1988.

[Kalpakjian 1991] Kalpakjian S., Manufacturing Processes for Engineering Materials, 2nd ed., Addison-Wesley Publishing Company, Boston (USA), 1991.

[Keeler et al. 2017] Keeler S., Kimchi M., Mooney P.J., Advanced High Strength Steels - Application Guidelines Version 6.0, World Auto Steel, 2017.

[Kozasu 1992] Kozasu I., "Processing - Thermomechanical Controlled Processing", Constitution and properties of steels, Pickering F.B. ed., vol. 7 of Materials Science and Technology - A Comprehensive Treatment, Cahn R.W., Haasen P., Kramer E.J. eds., VCH, Weinheim (D), 1992.

[Krauss 1980] Krauss G., Principles of Heat Treatment of Steels, ASM International, Metals Park, Ohio (USA), 1980.

[Krauss 2005] Krauss G., Steels: Processing, Structure, and Performance, ASM International, Metals Park, Ohio (USA), 2005.

[Kurz e Fisher 1992] Kurz W., Fisher D.J., Fundamentals of Solidification, Trans Tech Publications (CH), 1992.

[Jost et al. 1976] Jost S., Langer H., Pietsch D., Uligh P., "Rechnerische Ermittlung der Erwärmdauer bei der Wärmebehandlung von Stahl", Fertigungstechnik und Betrieb, vol. 26, pp.298-301, 1976.

[Lamont 1943] Lamont J.L., "How to Estimate Hardening Depth in Bars", Iron Age, vol. 152, pp. 64-70, 1943.

[Lee et al. 2005] Lee Y.L., Pan J., Hathaway R., Bakway M., Fatigue Testing and Analysis, Butterworth Heinemann, Oxford (UK), 2005.

[Lee e Choi 1999] Lee D.L., Choi H.C., "Effect of Si and C on the mechanical property of SAE9254", POSCO Technical Report, 1999.

[Lehrer 1930] Lehrer E., "Ueber das Eisen-Wasserstoff-Ammonia-Gleichgewicht", Zeitschrift für Elektrochemie, vol. 36, p. 383-392, 1930.

[Liščič et al. 1992] Liščič B, Tensi H.M., Luty W. (eds.), Theory and Technology of Quenching, Springer Verlag, Berlin (D), 1992.

[Maldzinski et al. 1999] Maldzinski L., Liliental W., Tymowski G., Tacikowski J., "New possibilities for controlling gas nitriding process by simulation of growth kinetics of nitride layers", Surface Engineering, vol. 15, pp. 377-384, 1999.

[Massalski 1996] Massalski T. B. (ed.), Binary Alloy, ASM International, Metals Park Ohio (USA), 1996.

[Mittemeijer 2013] Mittemeijer E. J., "Fundamentals of Nitriding and Nitrocarburizing", in Dossett J., Totten G.E. (ed.), Steel Heat Treating Fundamentals and Processes, vol. 4A, ASM Handbook, ASM International, Metals Park Ohio (USA), 2013.

[Morcillo et al 2019] Morcillo M., Díaz I., Cano H., Chico B., de la Fuente D., "Atmospheric corrosion of weathering steels. Overview for engineers. Part I: Basic concepts", Construction and Building Materials, vol. 213, pp. 723-737, 2019.

[Morrison 1966] Morrison W.B., "The effect of grain size on the stress-strain relationship in low-carbon steel", Transaction of American Society of Metals, vol. 59, pp. 824-846, 1966.

[Nicodemi 2007] Nicodemi W., Metallurgia, 2ª ed., Zanichelli, Bologna, 2007.

[Nicodemi 2008] Nicodemi W., Acciai e leghe non ferrose, 2ª ed., Zanichelli, Bologna, 2008.

[Norton 1997] Norton R.L., Machine Design: An Integrated Approch, Prentice Hall, Hoboken, New Jersey (USA), 1997.

[Ohmori e Honeycombe 1971] Ohmori, Y. and Honeycombe, R. W. K., Ohmori, Y. and Honeycombe, R. W. K. Proceedings ICSTIS, "The Isothermal Transformation of Plain Carbon Austenite", Proceedings ICSTIS, Transactions of the Iron and Steel Institute of Japan, vol. 11, pp. 1160-1164, 1971.

[Onink et al. 1993] Onink M., Brakman C. M., Tichelaar F. D., Mittemeijer E. J., van der Zwaag S., Root J. H., Konyer N. B., "The Lattice Parameters of Austenite and Ferrite in Fe-C Alloys as functions of Carbon Concentration and Temperature", Scripta Metallurgica et Materialia, vol. 29, pp. 1011-1016, 1993.

[Ono et al 1982] Ono S., Nozoe O., Shimomura T., Matsudo K., "The effect of carbon on the mechanical properties of Continuous-Annealing Drawing-Quality Steels", Metallurgy of Continuous-Annealed Sheet Steel, Bramfitt B.L. e Mangonon P.L. eds., Warrendale, Pennsylvania (USA), 1982.

[Osawa et al 1984] Osawa K., Matsudo K., Kurihara K., Suzuki T., "Effetto del C e del Mn sulle caratteristiche di imbutibilità di nastri in acciaio laminati a freddo" (in giapponese), Tetsu-to-Hagane, vol. 70, pp.552-601, 1984.

[Pallarés-Santasmartas et al 2018] Pallarés-Santasmartas L., Albizuri J., Avilés A., Avilés R., "Mean Stress Effect on the Axial Fatigue Strength of DIN 34CrNiMo6 Quenched and Tempered Steel", Steel, vol. 8, n. 213, 2018.

[Phillips et al. 1964] Phillips R., Duckworth W.E., Copley F.E.L., "Effect of Niobium and Tantalium on the Tensile and Impact Properties of Mild Steel", Journal of Iron and Steel Institute, vol. 202, n. 7, pp. 593-600, 1964.

[Pilkey 1997] Pilkey W.D., Peterson's stress concentration factors, John Wiley & Sons, New York (USA), 1997.

[Puzak et al. 1952] Puzak P.P., Eschbacher E.W., Pellini W.S., "Iniziation and Propagation of Brittle Fracture in Structural Steels", The Welding Journal - Research Supplement, vol. 31, n. 12, pp. 561-581, 1952.

[Rineholt e Harris 1951] Rineholt J. A., Harris, W. J., "Effect of Alloying Elements on Notch Toughness of Pearlitic Steels", Transactions of American Society for Metals, vol. 43, pp. 1175-1214, 1951.

[Rocha et al 2012] Rocha A.S., Nunes R.M., Hirsch T., "Analysis by Design of Experiments of Distortion Potentials in Drawn and Induction Hardened Wire", Materials Research, vol. 15(2), pp. 266-276, 2012.

[Rudnev et al 2003] Rudnev V., Loveless D., Cook R., Black M., Handbook of Induction Heating, Marcel Dekker, Basel (CH), 2003.

[Sinha 2003] Sinha A.K., Physical Metallurgy Handbook, 3 voll., 1st ed., McGraw Hill, New York (USA), 2003.

[Singh 1999] Singh V., Physical Metallurgy, Standard Publishers Distributors, New Delhi (IN), 1999.

[Smith e Hashemi 2006] Smith W.F., Hashemi J., Foundations of Materials Science and Engineering, 4th ed., McGraw-Hill, New York (USA), 2006.

[Sprock et al 2008] Sprock A., Peretic M., Speer J.G., "Compact cooling as an alternative to alloying for production of DP/TRIP steel grades", in Speer J.G., Nelson B., Pradhan R. (eds), International Conference on New Developments in Advanced High-Strength Sheet Steels, AIST, Orlando, Florida (USA), pp.237-247.

[Spur e Stöferle 1980-1994] Spur G., Stöferle T. H. (ed.), Handbuch der Fertigungstechnik, 6 voll., Carl Hanser Verlag, Munich (D), 1980-1994.

[Steven e Haynes 1956] Steven W., Haynes A.G., "The Temperature Formation of Martensite and Bainite in Low Alloy Steels", Journal of the Iron and Steel Institute, vol. 183, pp. 349-359, 1956.

[Swift 1987] Swift T., "Damage tolerance in pressurized fuselages", 11th Plantema Memorial Lecture in New Materials and Fatigue Resistant Aircraft Design, Simpson D.L. (ed.), Engineering Materials Advisory Services, Warley (UK), pp. 1-77, 1987.

[Thelning 1975] Thelning K.E., Steel and its Heat Treatment, Bofors Handbook, Butterworth, London (UK), 1975.

[Thompson 1985] Thompson C.V., "Secondary grain growth in thin films of semiconductors: Theoretical aspects", Journal of Applied Physics, vol.58, pp.763-772, 1985.

[Tither 1990] Tither G., "The Development and Applications of Niobium-Containing HSLA Steels", Proceedings of the International Conference on HSLA Steels: Processing, Properties and Applications, Beijing (CN), pp. 61-80, 1990.

[Totten 2006] Totten G. (ed.), Steel Heat Treatment: Metallurgy and Technologies, CRCnet base, Taylor & Francis Group, Boca Raton, Florida (USA), 2006.

[Wannel et al. 1977] Wannel P.H., Blank J.R., Naylor D.J., Proceeding International Symposium on the Influence of Metallurgy on the Machinability of Steel, September, ISIJ/ASM, Tokyo (J), 1977.

[Wang et al. 2017] Wang M., Liu Z.Y., Li C.-G., "Correlations of Ni Contents, Formation of Reversed Austenite and Toughness for Ni-Containing Cryogenic Steels", Acta Metallurgica Sinica (English Letters), vol. 30, n. 3, pp. 238-237, 2017.

[Wells e Lherbier 1980] Wells M.G.H. e Lherbier L.W., Processing and Properties of High Speed Tool Steels, TMS-AIME, New York (USA), 1980.

[Wilson e Butler 1961-1962] Wilson D.V., Butler R.D., "The Role of Cup-Drawing Tests in Measuring Drawability", Journal of the Institute of Metals, vol. 90, pp. 473-483, 1961-1962.

Lucefin S.p.A.
I-25040 Esine - BS - Italy
www.lucefin.com

Graphics designed by: Lucefin
Photo by: Mino Martignano - Massimo Sperto
Printed by: Graphicscalve - Vilminore di Scalve - Bergamo - Italy
Translated by: Bianca Maria Curti - Andrea Casaroli

Photo by Fredi Marcarini

Marco V. Boniardi (Milano, 1964)

Full Professor of Metallurgy with the Department of Mechanical Engineering at Politecnico di Milano. For more than thirty years he has been involved in research and technological transfer activities in the sectors of Metallurgy and Materials Science. His main fields of interest are stainless steels, carbon and alloy steels, heat treatments and thermochemical treatments, fatigue, fracture mechanics, corrosion, steel production and transformation processes. In addition to standard issues in the sector of Metallurgy, his competence also includes fires, explosions and forensic ballistics. Author of more than 130 scientific publications, he cooperates with a number of Italian and international companies as regards forensic engineering, failure analysis and malfunctions during operation. He has also provided expert testimony in incidents widely covered by the media (such as the Viareggio train derailment and the Costa Concordia wreckage). He is the coordinator of the Failure Analysis & Forensic Engineering course that is held every two years.
Together with Andrea Casaroli he is the founder of the website **www.fa-fe.com.**

Andrea Casaroli (Piacenza, 1984)

Adjunct Professor of Metallurgy and Machine Design with the Department of Mechanical Engineering at Politecnico di Milano, and of Metallurgy at the University of Pavia. For more than ten years he has been involved in research activities in the metallurgical field as regards stainless steels, carbon and alloy steels, functional coatings and mechanical behaviour of materials. He also deals with failure analysis and industrial accidents and has acquired extensive expertise in fire investigations and fire resistance of materials. Author of more than 50 scientific publications, he cooperates with Italian and international companies in solving problems connected with mechanical failure, corrosion, fatigue and malfunctioning of industrial components and plants.
Together with Marco V. Boniardi he is the founder of the website **www.fa-fe.com.**

TRAFILIX
INDUSTRIES

Trafilix S.p.A.
I-25040 Esine - Brescia - Italia
www.trafilix.com